ΠΑΝΕΠΙΣΤΗΜΙΟ ΚΡΗΤΗΣ
UNIVERSITY OF CRETE

U.S. NAVAL RESEARCH LABORATORY

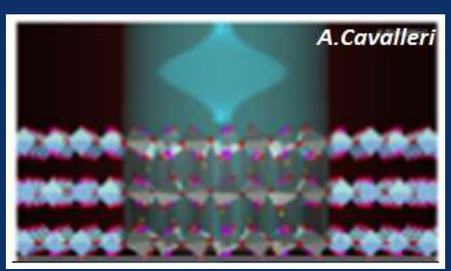

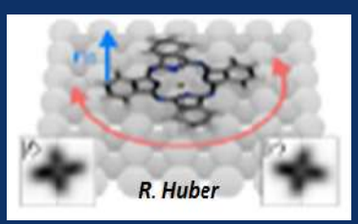

Abstract Proceedings

ULTRAFAST DYNAMICS & METASTABILITY

ULTRAFAST BANDGAP PHOTONICS

2022

VII International Symposium

n2 Photonics

ATI

Professor Ilias E Perakis
The Foundation Research & Technology – HELLAS
University of Alabama at Birmingham

Professor Michael K.Rafailov
University of Alberta

Doctor Jason M. Auxier
Advanced Technology Branch Head
Naval Research Laboratory

Abstract Proceedings comprising summaries of research papers prepared for two closely related Conferences – Ultrafast Bandgap Photonics and Ultrafast Dynamics and Metastability of Transient States, forming the Symposium. The Symposium is the seventh in a series of conferences on these topics. The motivation of the Symposium is to deal with the rapid evolution of Ultrafast Dynamics, Metastability, and Ultrafast Bandgap Photonics initiated in 2016 in response to a growing interest in athermal non-equilibrium induced by ultrashort stimuli in condensed matter, and rapidly expanding applications of matter in in electronic, magnetic, and optical transient states. The Symposium build a bridge between cutting edge modern physics and emerging applications which are desperately in need. Symposium is vertically integrated, covering the area of interaction of high intensity and relatively low energy pulses with condensed matter, from fundamental physics to practically applicable energy sources, devices and technologies.

The first five Conferences took place in the United States. In 2019 both Conferences were collocated at Georgetown University and formed a Workshop for the first time. The growing number of leading research groups in this field from outside the US makes it a right time to broaden the geography and to transform into International Symposium with location in the cradle of European Civilization. University of Crete and Foundation for Research and Technology - FORTH are hosting 7th Symposium on the island of Crete. Unfortunate and tragic circumstances of 2020 have affected the World and Symposium as well. The Symposium is re-scheduled for June 06-10 2022 at the same locations. In order to preserve the novelty of presented cutting-edge research results and to keep those all together in one place, we decided to publish the Abstract Proceeding ahead of the event. The Proceedings is actually a snapshot of most interesting and noticeable research results in Ultrafast Transient Phenomena and Ultrafast Bandgap Photonics which one can get in 2022.

Abstract Proceeding are divided by chapters that are focused either on research field or on phenomena. The division is pretty much conditional, while providing direct access to general topics of interest for the research community and Ultrafast Bandgap Photonics applications as well. Phenomenology topics, like phonon-assisted effects and spin-and orbital ultrafast phenomena may overlap areas of studies like photoinduced high temperature superconductivity and ultrafast magnetism, creating multiple entries into the proceedings based on specificity of research topics and therefore presented results. Each chapter begins with plenary papers, where results and considerations of most common interests are presented, while the rest of the chapter is compiled on author's name alphabetic order as it was submitted in author's list. Plus to Table of Contents the Abstract Prosceeding has list of authors where all authors of all submitted papers are listed with their papers associated page numbers. Chapters are not exacately reflecting Symposium sections and sessions as we are planning it for presentations in June 2022.

The Abstract Proceeding is a snapshot of up to date research results and progress in Ultrafast Dynamics and Metastability and the applications in Ultrafast Bandgap Photonics. It is an Encyclopedia of Ultrafast Dynamics, Metastability and Ultrafast Bandgap Photonics presenting the status quo in the disciplines ranging from Theoretical Physics to Applied Physics and covering practically all phenomena of interests in interaction of ultrashort high intensity-low energy interaction with condensed matter .

In Loving Memory of Elena

Contents

Lightwave quantum control at atomic length and time scales

R. Huber
University of Regensburg, Germany

Lightwave electronics has pushed the control of condensed matter to unprecedented time scales.
By harnessing the carrier wave of intense light pulses as an alternating voltage [1-13], electrons can be driven faster than a cycle of light, opening up a fascinating quantum world full of promise for future technologies.
I will first review prominent examples of lightwave-driven electron dynamics in solids, ranging from dynamical Bloch oscillations and high-harmonic generation [2-4] to quasiparticle collisions [5], lightwave valleytronics [6] and all-optical band structure reconstruction [7]. In the unique environment of topological insulators, electrons can be accelerated like relativistic particles to cover large distances without scattering, as directly visualized with the first subcycle band structure movie [8]. Intriguingly, this motion leads to a new quality of non-integer high-harmonic generation, whose frequencies can be continuously tuned by the carrier-envelope phase of the driving field. The anomalous Berry curvature warranted by the non-trivial topology enforces meandering ballistic trajectories of the Dirac fermions, causing a hallmark polarization pattern of the HH emission [9]. Thus, topological insulators form a unique playground to explore topology and relativistic effects in strong-field physics as well as non-dissipative topological electronics at infrared frequencies.
In the second part, lightwave electronics will be combined with the sub-angstrom resolution of scanning tunneling microscopy. Starting with the first atom-scale slow-motion movies of individual vibrating molecules [10], our concept is widely tunable to visualize structural and electronic dynamics in ultrafast videography. It also enables us to quantitatively sample atomic-scale waveforms inside the tunnelling junction [11].

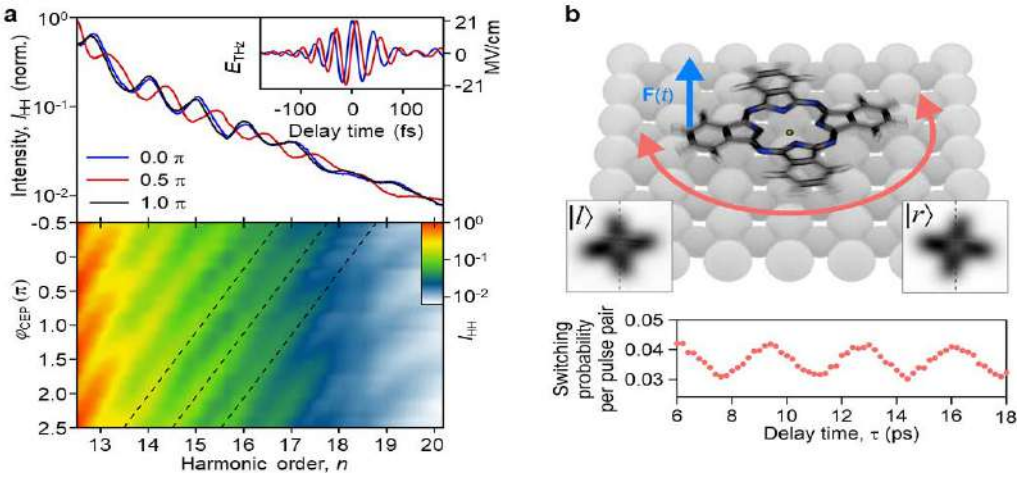

Fig. 1 a. *Topological lightwave electronics: High-harmonic spectra from the topological surface of Bi_2Te_3 depend sensitively on the CEP of the driving field, allowing for non-integer HHG;* ***b.*** *Atomic-scale lightwave electronics: Femtosecond atomic forces can prepare a structural wavepacket motion of a single-molecule switch (Mg phthalocyanine on NaCl).*

These fields can even be employed to directly exert femtosecond atomic forces, which selectively choreograph a coherent structural motion of a single-molecule switch in its electronic ground state [12].

References

[1] P. B. Corkum, F. Krausz, *Nature Physics* **3**, 381 (2007).
[2] O. Schubert, M. Hohenleutner, F. Langer, B. Urbanek, C. Lange, U. Huttner, D. Golde, T. Meier, M. Kira, S. W. Koch, R. Huber, *Nature Photonics* **8**, 119 (2014).
[3] M. Hohenleutner, F. Langer, O. Schubert, M. Knorr, U. Huttner, S.W. Koch, M. Kira, R. Huber, *Nature* **523,** 572 (2015).
[4] F. Langer, M. Hohenleutner, U. Huttner, S.W. Koch, M. Kira, R. Huber, *Nature Photonics* **11**, 227 (2017).
[5] F. Langer, M. Hohenleutner, C. P. Schmid, C.Poellmann, P. Nagler, T. Korn, C. Schüller,M. S.Sherwin, U.Huttner, J. T.Steiner, S. W Koch, M. Kira, R. Huber, *Nature* **533**, 225 (2016).
[6] F. Langer, C.P. Schmid, S. Schlauderer, M. Gmitra, J. Fabian, P. Nagler, C. Schuller, T. Korn, P.G. Hawkins, J.T. Steiner, U. Huttner, S.W. Koch. M.Kira. R. Huber. *Nature* **557**. 76 (2018).
[7] M. Borsch, C. P. Schmid, L. Weigl, S. Schlauderer, N. Hofmann, C. Lange, J. T. Steiner, S. W. Koch, R. Huber, M. Kira, *Science* **370**, 1204 (2020).
[8] J Reimann, S Schlauderer, C P Schmid, F Langer, S Baierl, K A Kokh, O E Tereshchenko, A Kimura, C Lange, J Güdde, U Höfer, R Huber, *Nature* **562**, 396 (2018).
[9] C. P. Schmid, L. Weigl, P. Grössing, V. Junk, C. Gorini, S. Schlauderer, S. Ito, M. Meierhofer, N. Hofmann, D. Afanasiev, J. Crewse, K. A. Kokh, O. E. Tereshchenko, J. Güdde, F. Evers, J. Wilhelm, K. Richter, U. Höfer, R. Huber. *Nature* **593**, 385 (2021).
[10] T. L Cocker, D. Peller, P. Yu, J. Repp, R. Huber, *Nature* **539**, 263 (2016).
[11] D. Peller, C. Roelcke , L. Z. Kastner , T. Buchner , A. Neef , J. Hayes , F. Bonafé , D. Sidler, M. Ruggenthaler, A. Rubio, R. Huber , J. Repp, *Nature Photonics* **15**, 143 (2021).
[12] D. Peller, L. Z. Kastner, T. Buchner, C. Roelcke, F. Albrecht, N. Moll, R. Huber, J. Repp, *Nature* **585**, 58 (2020).
[13] M. Plankl, P. E. Faria Junior, F. Mooshammer, T. Siday, M. Zizlsperger, F. Sandner, F. Schiegl, S. Maier, M. A. Huber, M. Gmitra, J. Fabian, J. L. Boland, T. L. Cocker, R. Huber, *Nature Photonics* **15**, 594 (2021).

Coherent Sensing and Quantum Control of Higgs Bosons in Unconventional Superconducting Materials

I. E. Perakis
University of Alabama at Birmingham, Birmingham, AL 119991, USA

The recent discovery of the Higgs boson created lots of excitement, recognized by the 2013 Nobel Prize in Physics. Celebrated as one of the most fundamental results in experimental physics, the observation of this amazing particle confirmed the existence of the associated Higgs field that plays a pivotal role in the Standard Model of particle physics. Because of the Higgs boson's large mass (about 125 GeV), it could only be detected so far in the world's most powerful accelerator—the multi-billion dollar Large Hadron Collider at CERN. The theoretical proposal of the Higgs mechanism, however, came from condensed matter physics ideas: the Higgs is a collective excited state of superconducting condensates with spontaneously-broken symmetry. While superconducting condensates are well-established in solid state, conclusive experimental evidence of their Higgs modes has been under debate, since symmetry does not allow them to couple linearly to electromagnetic fields and become observable with conventional spectroscopies. Furthermore, in conventional clean SC systems, it is hard to distinguish between Higgs collective modes and charge fluctuations. In this talk, I will discuss our theory-experiment-computation approach to identify and coherently control the Higgs Boson in iron-based unconventional superconductors by using multiple intense phase-locked Terahertz (THz) pulses. We attempt to do this relatively cheaply by simulating numerically and analyzing datasets of THz Two-Dimensional ultrafast nonlinear coherent spectroscopy. The concepts of "Terahertz Sudden Quantum Quench" and "Dynamical Symmetry Breaking via Sub-cycle Light-Wave Acceleration" and electromagnetic field propagation effects, to be discussed here, advance Light-Wave Quantum Electronics, Quantum Information Science and the U.S. National Quantum Initiative, by paving the way for a new quantum sensing and quantum tomography technique with extremely high sensitivity.

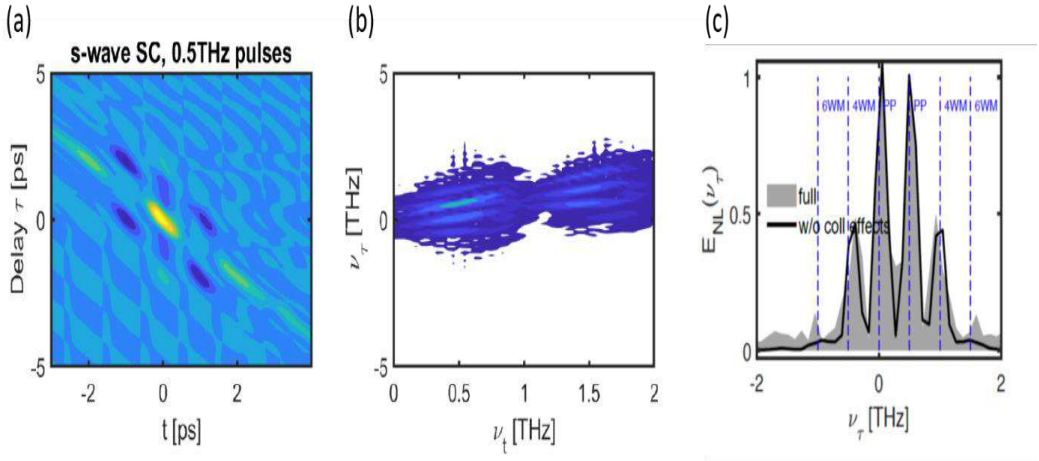

Fig. 1 (a) *Example of calculated signal measured in THz Multi-dimensional Coherent Spectroscopy experiments in Superconductors.* ***(b)*** *Fourier transform of the numerical data in (a) into the frequency domain.* ***(c)*** *A slice of the data in* ***(b)*** *along the y-axis. Black line shows our simulations without collective effects such as the Higgs mode in a one-band conventional BCS system.*

We strive to make significant progress in quantum materials science by coherently controlling quantum states very far from equilibrium, via numerical design of phase-coherent THz pulse sequences and by using Big Data analysis to optimize the weak signals and separate them from the background similar to CERN.

References

[1] X. Yang, C. Vaswani, C. Sundahl, M. Mootz, P. Gagel, L.Luo,J. Kang,P. Orth,I. E. Perakis, C.B. Eom,J.Wang, *Nature Materials***17**, 586 (2018).
[2] X. Yang, C.Vaswani, C.Sundahl, M.Mootz, P.Gagel, L. Luo, J. Kang, P.P.Orth,I. E. Perakis, C.Eom, J. Wang, *Nature Photonics* **13**, 707 (2019).
[3] C.Vaswani, C.Sundahl, M.Mootz, D.Mudiyanselage, J.Kang, et. al.. *arXiv* 1912.01676, (2019).

Exploring the Phase Diagram of Cuprates via Time- and Angle-resolved Photoemission Spectroscopy

F. Boschini[1,2,5] ,M. Zonno[1,2], E. Razzoli[1,2], R. P. Day[1,2], M. Michiardi[1,2], E. H. Da Silva Neto[3]
S. Zhadanovich[1,2], A. K. Mills[1,2], G. Levy[1,2], C. Giannetti[4], D. J. Jones[1,2], A. Damascelli[1,2]
[1]*University of British Columbia, Vancouver, BC V6T 1Z1 Canada*
[2]*Quantum Matter Institute, Vancouver, BC V6T 1Z1 Canada*
[3]*University of California, Davis, CA 95616, USA*
[4]*Universita Cattolica del Sacro Cuore, 25121 Brescia, Italy*
[5]*Institut National de la Recherche Scientifique-INRS, Québec City, G1K 9A9, Canada*

The phase diagram of cuprates is characterized by the emergence of exotic and/or ordered phases, from high-T_c superconductivity to charge- and magnetic-order. In the last decade, the development of time-resolved techniques has offered a novel perspective for investigating the dynamical/fluctuating properties of these quantum phases. In this regard, we recently demonstrated that time- and angle-resolved photoemission spectroscopy (TR-ARPES) can disentangle the dynamics of phase fluctuations and charge excitations, establishing the dominant role of phase coherence in the emergence of high-temperature superconductivity in Bi-based cuprates [1]. This was made possible via a careful analysis of the transient evolution of the one-electron removal spectral function (see Fig. 1a), which offers direct evidence for the filling of the superconducting gap via enhancement of phase fluctuations.We recently employed this same dynamical approach to reveal unambiguously the relation between the pseudogap and short-range antiferromagnetic correlations in the optimally-doped $Nd_{2-x}Ce_xCuO_4$ electron-doped cuprate [2]. This transient study provides clear evidence of the filling of the spin-fluctuations-induced pseudogap as a consequence of the reduction of the short-range spin-correlation length (see Fig. 1b).

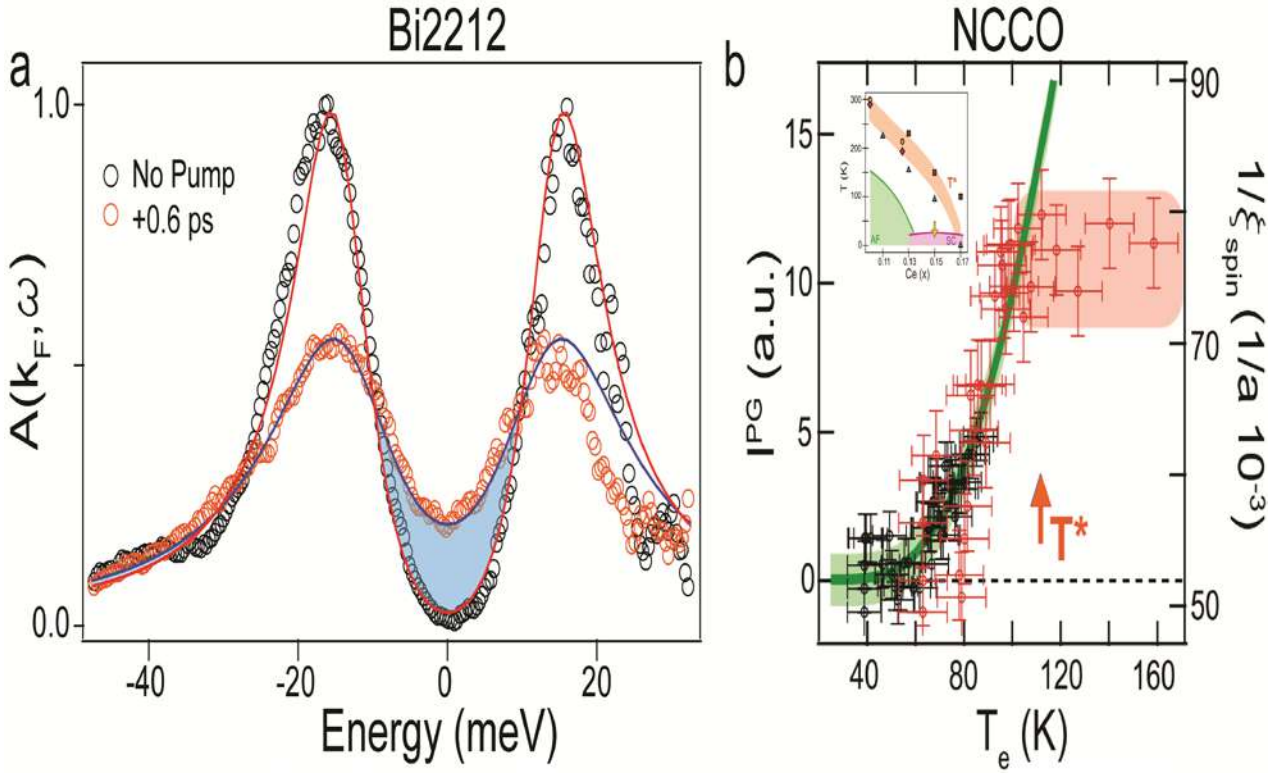

Fig.1. a*. Gap filling in $Bi_2Sr_2CaCu_2O_{8+x}$ (Bi2212), underdoped T_c≃82 K [1].*
b. *Temperature dependence of the pseudogap in $Nd_{2-x}Ce_xCuO_4$ (NCCO), optimally-doped x=0.15 [2]. The inset shows the phase-diagram of NCCO.*

Finally, we will present novel time-resolved resonant x-ray scattering results where we track the ultra-fast evolution of the charge-order upon the photoinduced melting of the phase-coherence of the su-perconducting condensate in Y-based cuprates.

References

[1] F. Boschini et al., *Nature Materials* **17**, 416 (2018).
[2] F. Boschini, M. Zonno et al., *npj Quantum Materials-Nature* **5**, 6 (2020).

Photo-Molecular High Temperature Superconductivity

M. Buzzi[1], D. Nicoletti[1], A. Cavalleri[1,2]
[1] *Max Planck Institute for the Structure and Dynamics of Matter, 22761 Hamburg, Germany*
[2] *University of Oxford, Oxford OX1 3PU, UK*

The non-equilibrium control of emergent phenomena in solids is an important research frontier, encompassing effects such as the optical enhancement of superconductivity. In high-T_c cuprates and alkali doped fullerides, resonant driving of specific phonon modes with mid-infrared pulses has been shown to induce transient optical properties reminiscent of superconductivity for temperatures far above the equilibrium T_c [1-3].Here, we discuss an analogous effect in the quasi two-dimensional organic superconductor κ-(BEDT-TTF)$_2$Cu[N(CN)$_2$]Br. At equilibrium, this material bears similarities to high-T_c cuprates, showing unconventional superconductivity that emerges from a correlated metallic state with a T_c of 11 K, in the vicinity of a Mott insulating phase [4]. In this experiment, we resonantly excited local vibrational modes of the BEDT-TTF molecule using mid-infrared pulses. Starting from the equilibrium metallic state at $T >> T_C$, we observed a photo-induced response compatible with that of a transient superconductor, which was strongly reduced when the pump wavelength was tuned away from the vibrational resonances [5].

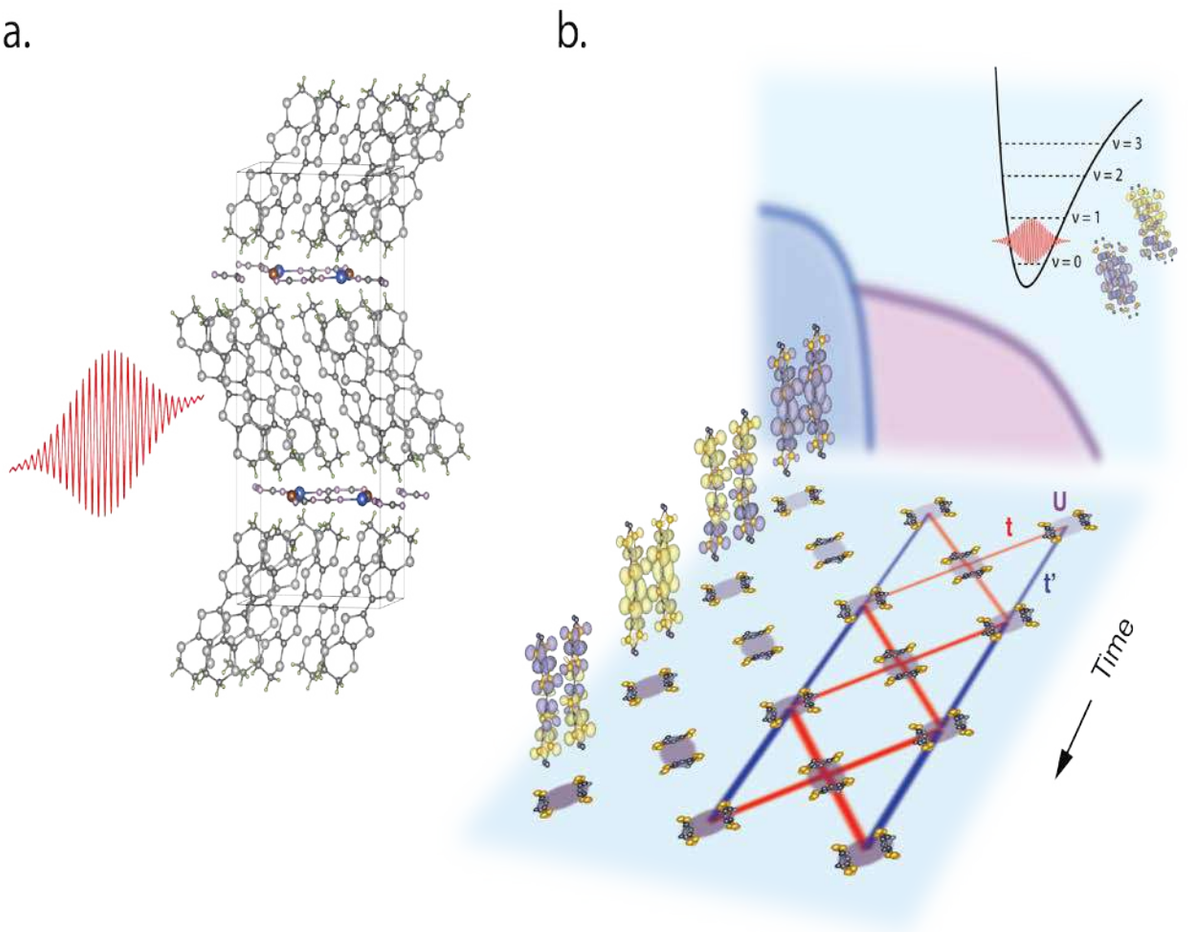

Fig 1. (a) *Crystal structure of κ-(BEDT-TTF)$_2$Cu[N(CN)$_2$]Br and excitation of a vibrational mode of the BEDT-TTF molecule with a mid-infrared pulse.*
(b) *Control of the electronic interaction parameters by molecular wavefunction engineering.*

Our results suggest that optically-enhanced superconductivity might be a far broader phenomenon than previously envisaged, thus opening new opportunities and challenges for both theoretical and experimental investigations.

References

[1] W. Hu et al., *Nature Materials* **13**, 705 (2014).
[2] M. Mitrano et al., *Nature* **530**, 461 (2016).
[3] A. Cantaluppi, M. Buzzi, et al. *Nature Physics* **14**, 837 (2018).
[4] A. Ardavan, et al. *Journal of the Physical Society of Japan*. **81**, 011004 (2011).
[5] M. Buzzi et al., *arXiv*:2001.05389 (2020).

Quench Dynamics and Pump-Induced Superconductivity of an Extended Hubbard Model

W.-C.Chen[1], Y.Wang[2], C.-C.Chen[1]
[1] *University of Alabama at Birmingham, Birmingham, AL 35294, USA*
[2] *Harvard University, Cambridge, MA 02138, USA*

Photo-induced phase transition is a promising approach to engineering material properties and has been demonstrated in several strongly correlated systems [1, 2]. Here, we study the equilibrium phases and nonequilibrium dynamics of a square-lattice extended Hubbard model using exact diagonalization. We show that quench dynamics and quantum fidelity computed on a finite-size cluster can accurately capture phase transition boundaries in excellent agreements with functional renormalization group studies [3]. On top of the equilibrium ground states, we then investigate the model's nonequilibrium dynamics with an oscillatory Gaussian pump pulse. We find that different order parameters can be selectively manipulated by pump frequency, amplitude, and polarization.

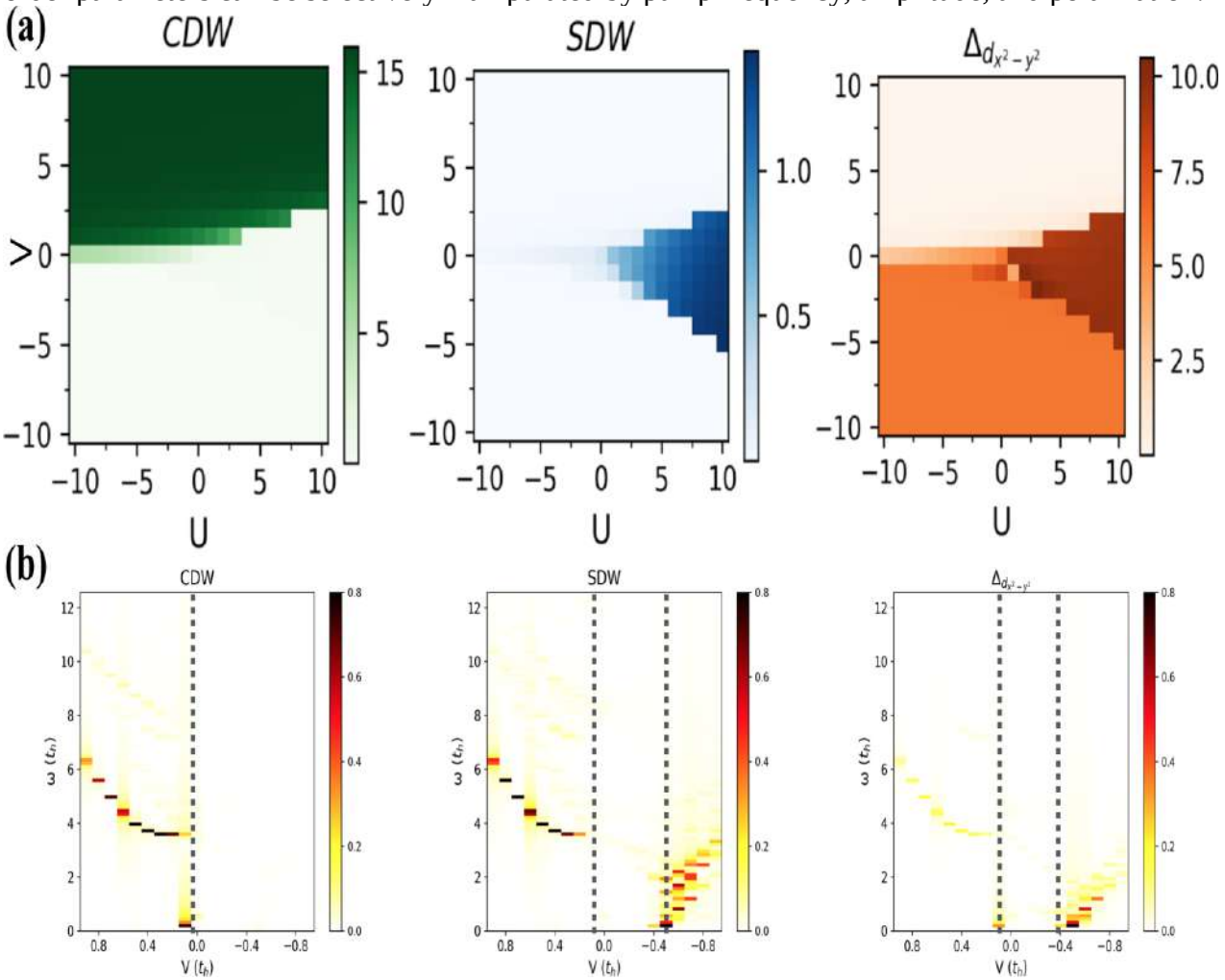

***Fig. 1**. **(a)** Correlation strength of different order parameters – charge density wave (CDW), spin density wave (SDW), and d-wave superconductivity – as functions of on-site (U) and nearest-neighbor (V) interactions in a square-lattice extended Hubbard model.*
***(b)** Characteristic excitations extracted from the Fourier spectra of quench dynamics for different order parameters. Phase transitions can be identified from the distinct behaviors of ultrafast response to an interaction quench.*

Our work demonstrates that using ultrafast light to control superconductivity of different pairing symmetries is possible.

References

[1] Y. Wang, C.-C. Chen, B. Moritz, T. P. Devereaux, *Physical Review Letters* **120**, 246402 (2018). [2] Y. Wang, T. P. Devereaux, C.-C. Chen, *Physical Review* B **98**, 245106 (2018).
[3] W.-M. Huang, C.-Y. Lai, C. Shi, S.-W. Tsai, *Physical Review* B **88**, 054504 (2013).

Collective Modes in Pumped Unconventional Superconductors with Competing Ground States

I. M. Eremin
Ruhr-Universität Bochum, 44801 Bochum, Germany

Motivated by the recent development of terahertz pump-probe experiments, we investigate the short-time dynamics in superconductors with multiple attractive pairing channels. Studying a single-band and multiband superconductors, we find the signatures of collective excitations of the pairing symmetries (known as Bardasis-Schrieffer modes) as well as the order parameter amplitude (Higgs mode) in the short-time dynamics of the spectral gap and quasiparticle distribution after an excitation by a pump pulse (Fig.1). We show that the polarization and intensity of the pulse can be used to control the symmetry of the non-equilibrium state as well as frequencies and relative intensities of the contributions of different collective modes. We find particularly strong signatures of the Bardasis-Schrieffer mode in the dynamics of the quasiparticle distribution function. In the multiband superconductors we particularly address the collective modes and the short time dynamics of the superconducting state with s + is-wave order parameter using an effective four-band model with two hole and two electron pockets. The amplitude and phase modes are coupled giving rise to a variety of collective modes and we further uncover a new coupled collective soft mode.

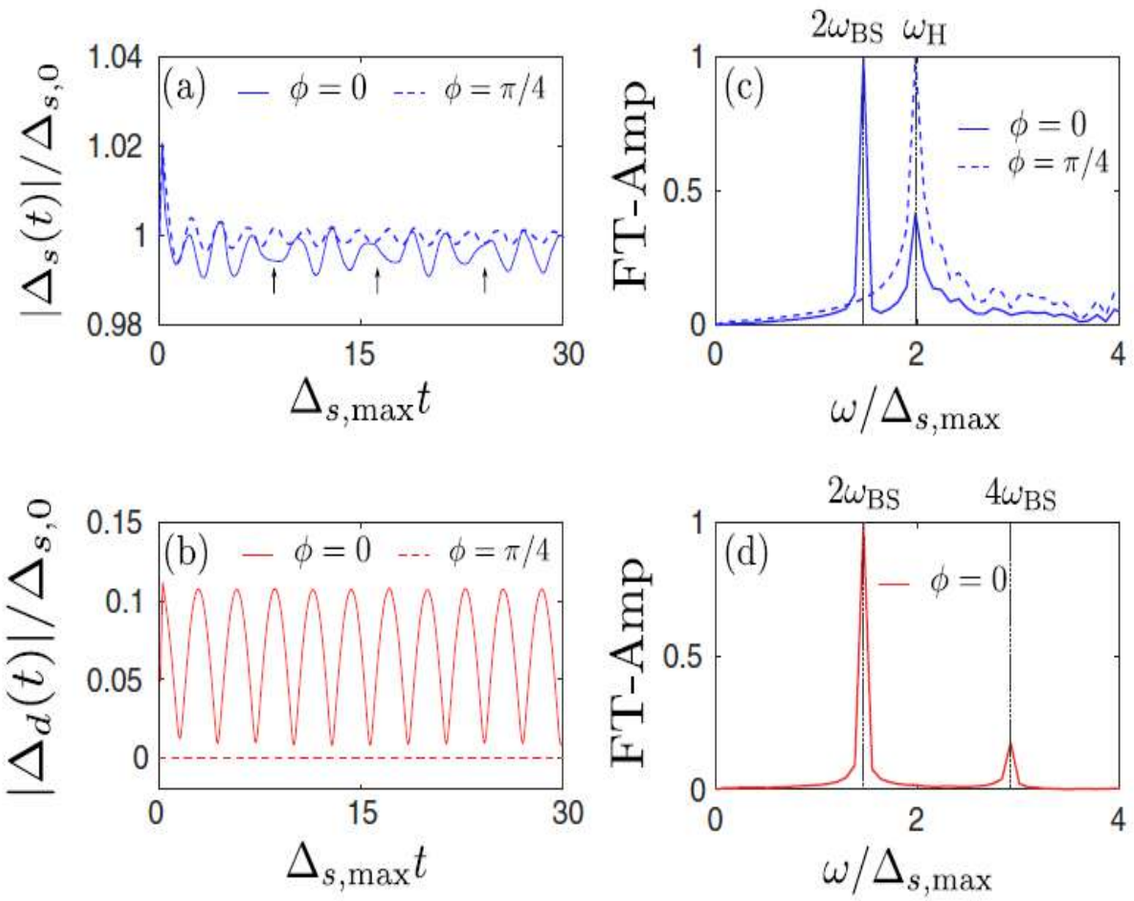

Fig.1 *Calculated evolution of the superconducting gap amplitudes for an s-wave ground state and an applied light pulse with polarization at an angle φ = 0 (solid line) and an angle φ = π/4 (dashed line) to the k_x axis.* ***(a)*** *and* ***(b)*** *show the short-time dynamics of the s- and dx2−y2-wave order parameter, respectively. To make the existence of a second frequency in* ***(a)*** *clear, arrows illustrate the beating pattern.* ***(c)*** *and* ***(d)*** *refer to the Fourier transform of $|\Delta_s|$ and $|\Delta_{dx2-y2}(t)|$, respectively.*

Our works shows the potential of modern ultrafast experiments to address the collective excitations in unconventional superconductors and highlights the importance of sub-dominant interactions for the non-equilibrium dynamics in these systems.

References

[1] M. A. Mueller, P. Shen, M. Dzero, I. M. Eremin, *Physical Review* B **98**, 024522 (2018).
[2] M. A. Müller, P. A. Volkov, I. Paul, I. M. Eremin, *Physical Review* B **100** , 140501(R) (2019).

Light-Induced Superconductivity: Insight from First-Principles Calculations

M. Fechner
Max Planck Institute for the Structure and Dynamics of Matter, 22761 Hamburg, Germany

Selective optical excitation of phonons in cuprates has been shown to induce transient superconducting correlations above the thermodynamic transition temperature [1]. Moreover, in $YBa_2Cu_3O_{6.5}$ it has been demonstrated that only phonon modes involving motions of the apical oxygen induce this effect [2, 3].

.

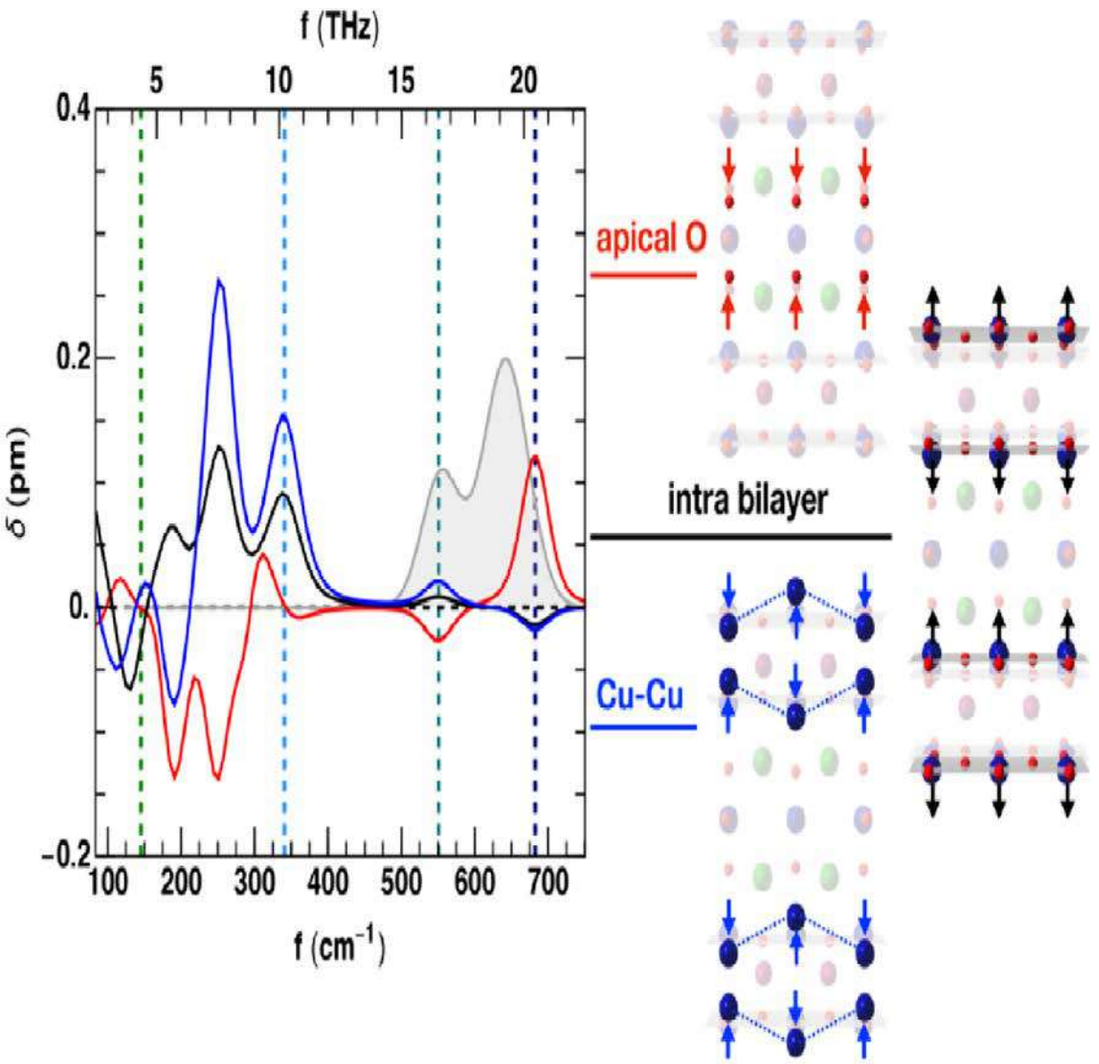

Fig.1 *- Transient average distortions of the apical oxygen positions* ***(red)****, the intra-bilayer distance* ***(black)*** *and the planar Cu buckling* ***(blue)*** *in $YBa_2Cu_3O_{6.5}$, derived from ab-initio calculations of nonlinear phonon-phonon interactions for different excitation frequencies. Arrows in the illustrations shown on the right correspond to positive displacements.*

Referring to these results, I will discuss how we can model phonon excitation processes in cuprates utilizing first principle calculations in combination with effective Hamiltonians. I will address the intense-excitation regime, in which both third and fourth-order phonon-phonon coupling terms dominate the dynamics. This approach allows to calulate the transient structural distortions created by driving the different phonons in $YBa_2Cu_3O_{6.5}$. Finally, I will discuss the electronic properties of these transient structures are from a density functional theory perspective and confer these results with the experimental findings

References

[1] W. Hu, et al, *Nature Mater*ials **13**, 705 (2014).
[2] B. Liu, M. Först, M. Fechner, D. Nicoletti, J. Porras, B. Keimer, A. Cavalleri, *ArXiv:*1905.08356 1 (2019).
[3] A. von Hoegen, M. Fechner, M. Först, J. Porras, B. Keimer, M. Michael, E. Demler, A. Cavalleri, *ArxXiv:*1905.08284 (2019).

Phase-Resolved Non-Linear THz Spectroscopy for Higgs Spectroscopy in Cuprate Superconductors

H. Chu[1], M.-J. Kim[1], K. Katsumi[2], S. Kovalev[3], R. D. Dawson[1], L. Schwarz[1], N. Yoshikawa[2], G. Kim[1], D. Putzky[1], G. Cristiani[1], G. Logvenov[1], Y. Gallais[5], B. Keimer[1], A. Schnyder[1], D. Manske[1], M. Gensch[3] Z. Wang[3], R. Shimano[2], S. Kaiser[4]

[1]*Max Planck Institute for Solid State Research, 70569 Stuttgart, Germany*
[2]*Department of Physics, University of Tokyo, Tokyo113-0033, Japan*
[3]*Helmholtz-Zentrum Dresden-Rossendorf, 01328 Dresden, Germany*
[4]*University of Stuttgart, 70569 Stuttgart, Germany*
[5]*Université Paris-Sud/Université Paris-Saclay, 91405 Orsay, France*

The Higgs mode of a superconductor is a collective excitation of the amplitude of the superconducting order parameter [1, 2, 3]. It can be coherently driven at a frequency 2ω by a multicycle terahertz pulse of frequency ω. This then leads to third harmonic generation (THG) as a result of sum frequency generation between the oscillating condensate and the terahertz driving pulse [4]. We applied such experimental scheme to different families of cuprate high-Tc superconductors. By phase-resolving the THG response with respect to the terahertz drive, we uncover the universal anti-resonance of the driven Higgs oscillation in all samples. This may be understood in terms of an additional collective mode coupled to the Higgs mode [5]. In extension to this work a careful analysis of the anti-resonance feature as a function of hole doping with the help of a coupled oscillators model as well as a magnetic field dependence suggests that the coupled mode could be the magnetic resonant mode.

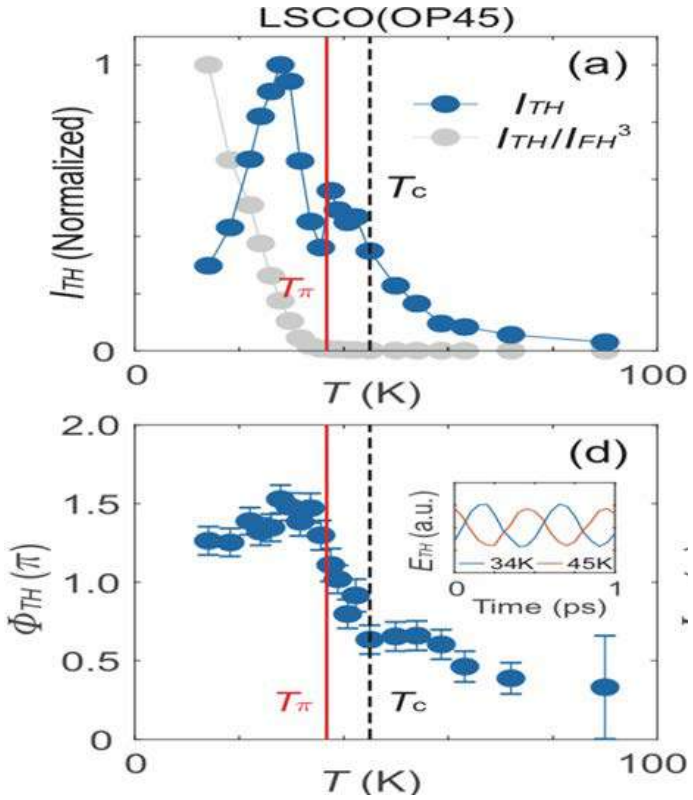

Fig. 1: *Amplitude (top) and phase (bottom) response of third harmonic generation in optimally doped LSCO*

Further we will report on the transient properties of the driven Higgs oscillations and driven supercurrents and potential competing orders. Our findings may shed light on the pairing mechanism in d-wave superconductors.

References

[1] D. Pekker, C. Varma, *Annual Review of Condensed Matter Physics* **6**, 269 (2015).
[2] R. Matsunaga et al., *Physical Review Letters* **111**, 057002 (2013).
[3] L. Schawrz et al., *Nature Communications* **11**, 287 (2020).
[4] R. Matsunaga et al., *Science* **345**, 1145 (2014).
[5] H. Chu et al. to appear (2020); *arxiv*:1901.06675 (2019).

Theory of Higgs Spectroscopy for Superconductors in Non-Equilibrium

D. Manske
Max Planck Institute for Solid State Research, 70569 Stuttgart, Germany

In conventional time-resolved pump-probe experiments on superconductors one measures the relaxation of an optical probe after the excitation by an ultra-short laser pulse. With the recent development of THz laser technology it is now possible to excite or quench collective excitation, such phonons or the superconducting condensate. In the past we have predicted characteristic Higgs oscillations after a quantum quench in superconductors that allows investigating the ground state directly that, indeed, has been confirmed experimentally for an s-wave superconductor. Furthermore, several predictions have been made for a 2-band superconductor in which two Higgs oscillations interact. During the last few years we have developed a classification scheme that allows to characterize Higgs oscillations of all possible symmetries [1]. Using polarized light in different directions, we predict that it is possible to map out the underlying gap symmetry of the superconducting ground state. We compare our analytical calculations with full (numerically exact) methods to get further insights into the nature of the Higgs mode. An alternative to a quench by THz laser is to measure the resonant third-harmonic generation (THG) signal; we have developed a theory for both cases. As an example, we have applied our theory to *d*-wave high-T_c superconductors: two Higgs modes are predicted. This, and other predictions, has been recently confirmed by experiment.

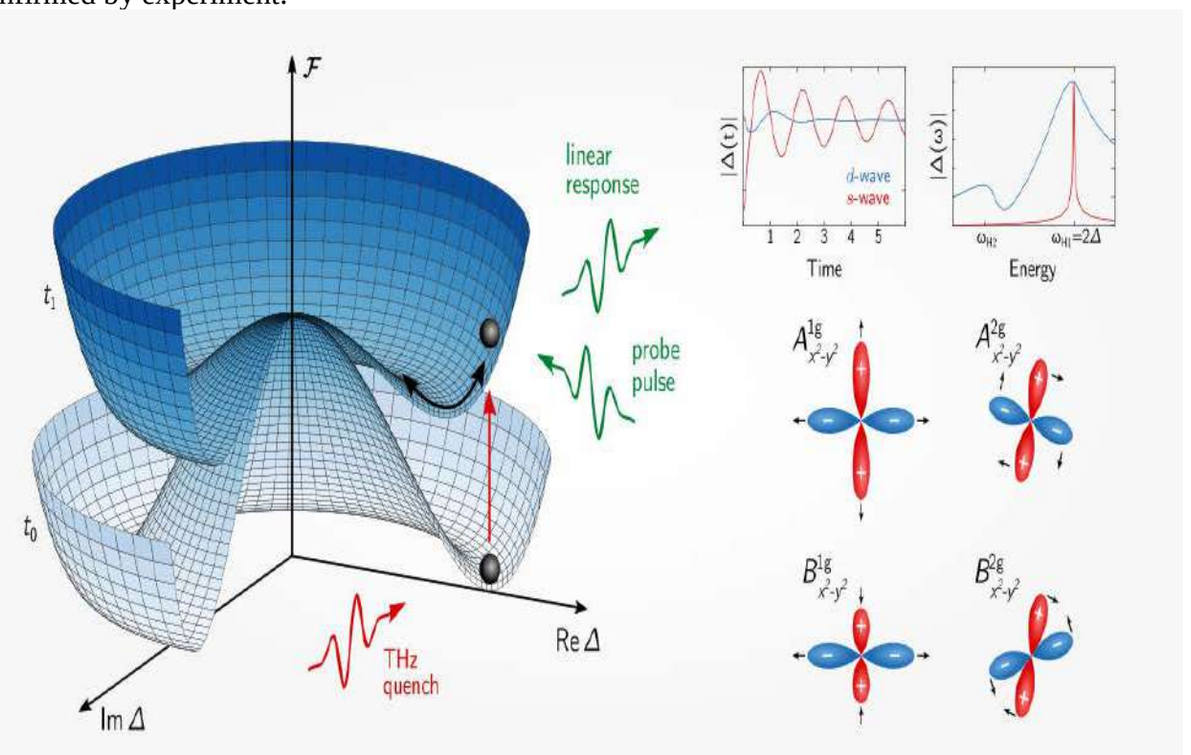

Fig.1. *Free Energy $\mathcal{F}$ of a superconductor as function of the order parameter Δ with the shape of a Mexian hat in equilibrium at $t=t_0$. In a THz pump-probe experiment, the pump pulse acts as a quench, which shrinks the Mexican hat at $t=t_1$. The order parameter, depicted as the black ball, is displaced in an out of equilibrium position, where it starts to oscillate with its characteristic frequency around the new minimum. This radial oscillation corresponds to the Higgs mode. The oscillation can be captured by a second probe pulse. The Fourier spectrum $|\Delta(\omega)|$ of the Higgs oscillations $|\Delta(t)|$ shows peaks at the energies of the Higgs modes ω_H. Depending on the gap symmetry, asymmetric oscillations of the condensate are possible, which can be classified according to group symmetry. These asymmetric oscillations for unconventional can lead to additional Higgs modes.*

Applying our theory of Higgs spectroscopy to THz tr-ARPES experiments would open a unique approach to distinguish between different symmetries of the condensate, even for new and unknown superconductors.

Reference

[1] L. Schwarz *et al.*, *Nature Communications* **11**, 287 (2020).

Ultrafast manipulation of Electronic Interactions in Quantum Materials

M. Mitrano
Harvard University, Cambridge, MA 02138, USA

Intense ultrashort electromagnetic fields are an increasingly important tool to realize and control novel emergent phases in quantum materials. Among a variety of nonthermal excitation pathways, a particularly intriguing route is represented by the direct light-engineering of effective many-body interactions, such as electron hopping amplitudes and electron-electron repulsion. Achieving a light-induced dynamical renormalization of the screened onsite Coulomb repulsion ("Hubbard *U*") would have far-reaching implications for high-harmonic generation, attosecond spectroscopy and ultrafast magnetism in the solid state. However, experimental evidence for a dynamically controlled Hubbard *U* remains scarce. In this talk, I will present a recent demonstration of light-induced renormalization of the Hubbard *U* in a high-temperature superconductor, $La_{2-x}Ba_xCuO_4$, [1] and discuss its implications for the control of superconductivity, magnetism, as well as to the realization of other long-range-ordered phases in light-driven quantum materials.

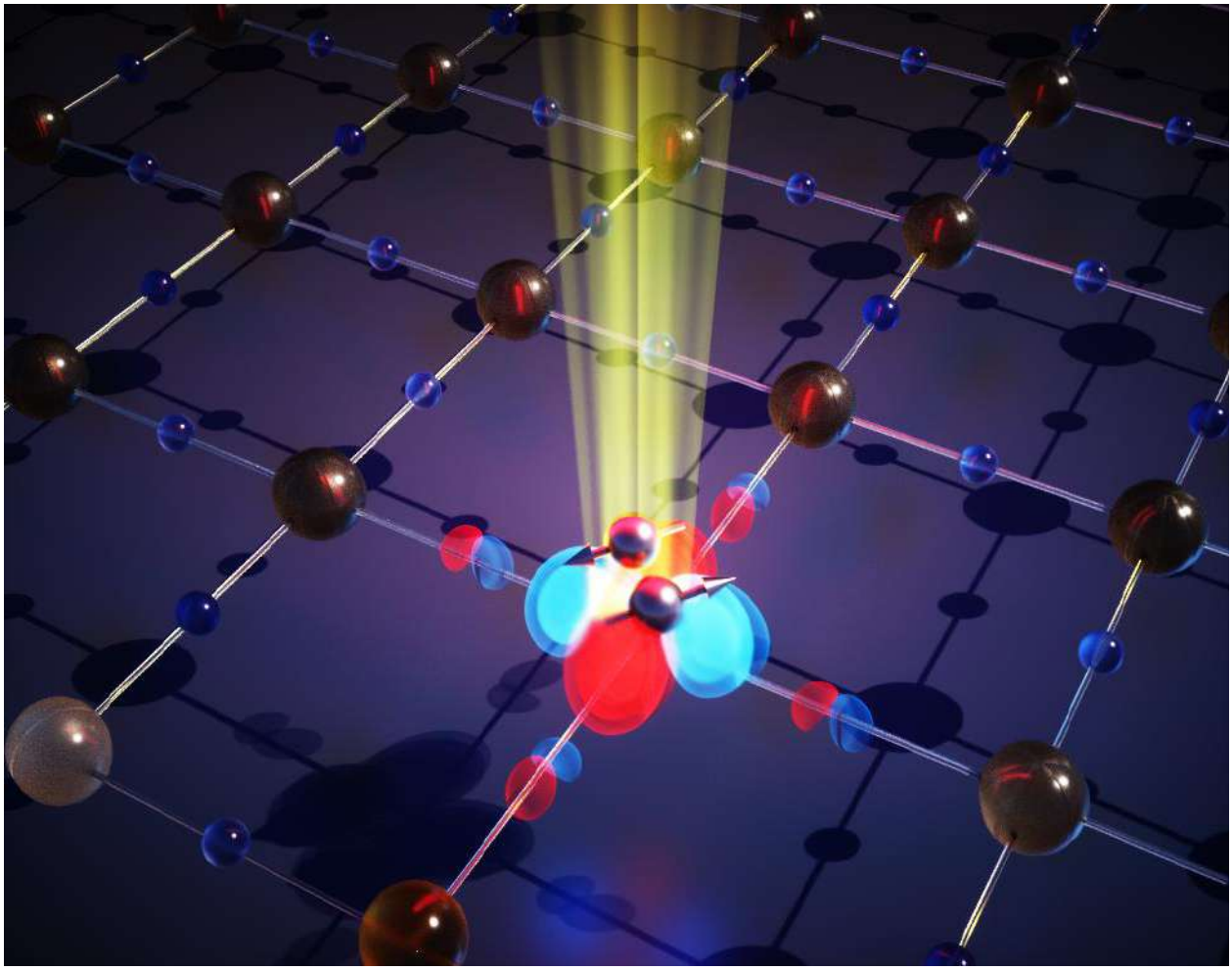

Fig. 1 *– Light-induced renormalization of the onsite Coulomb repulsion between electrons in the CuO_2 plane of the prototypical high-temperature superconductor $La_{2-x}Ba_xCuO_4$.*

Further, I will discuss the application of these methods to the control of quasi-1D correlated electron systems with long-ranged Coulomb interaction, such as Sr_2CuO_3.

References

[1] D. R. Baykusheva et al. *Physical Review* X **12**, 011013 (2022).

Photo-induced Metastable Superconductivity in K_3C_{60}: Recent Developments

E. Rowe, A. Cavalleri
Max Planck Institute for the Structure and Dynamics of Matter, 22761 Hamburg, Germany

Photoexcitation of the molecular superconductor K_3C_{60} with short mid-infrared pulses was shown to induce an exotic non-equilibrium state with superconducting-like optical properties at temperatures far above the equilibrium Tc. Interestingly, this phenomenon persists up to at least 100K which is five times higher than the equilibrium critical temperature [1,2]. Recently, we have shown that by photoexciting K_3C_{60} with more energetic mid-infrared pulses the same transient superconducting-like state emerges but instead of decaying over a few picoseconds, it remains metastable and persists for several nanoseconds. This discovery enabled us to go beyond time-resolved optical spectroscopy for the first time and perform GHz frequency transport measurements indicative of the onset of a non-equilibrium zero-resistance state [3]. New experiments highlight that by tuning the optical pump to be resonant with a T_{2u} phonon mode at ~10THz the efficiency with which the metastable state is generated is enhanced by up to 2 orders of magnitude. Strikingly, this giant increase in photo-susceptibility made it possible to observe the metastable superconducting-like state at room temperature.

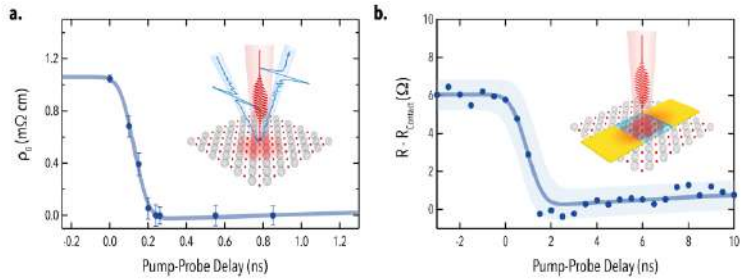

Fig. 1. (a) *Time evolution of the transient resistivity ρ_0 obtained from an extrapolation to zero frequency of a Drude–Lorentz fit to the transient optical conductivities.*
(b) *Resistance of a laser-irradiated K3C60 pellet that was embedded in a microstrip transmission line as a function of time after photoexcitation. The resistance value is obtained from a transient two-point transport measurement in which contributions from contact resistances are calibrated from a static four-point measurement.*

These observations constitute an important step forward not only towards the understanding of the underlying mechanisms for photo-induced superconductivity in K_3C_{60} but also towards the stabilization of this driven superconducting state using sustained drives and optical cavities.

References

[1] M. Mitrano et al, *Nature* **530**, 461(2016).
[2] A. Cantaluppi, M. Buzzi et al, *Nature Physics* **14**, 837-841 (2018).
[3] M. Budden, T. Gebert, et al, *Nature Physics* **17**, 611-618 (2021).

Controlling Crystal Structures with Light

A. Cavalleri
Max Planck Institute for the Structure and Dynamics of Matter, 22761 Hamburg, Germany

Coherent electromagnetic radiation at mid-infrared and terahertz frequencies can be used to drive low lying excitations of solids nonlinearly [1]. Here, I will especially focus on the response of phonons, which exhibit a wealth of interesting nonlinear phenomena [2] and open up new ways to control complex solids [3]. I will emphasize the role that nonlinear phonons play in driven superconductors and the enhanced electronic coherence observed in these materials [4]. Results in cuprates [5,6,7], doped fullerenes[8,9] and in organic salts will be highlighted[10].

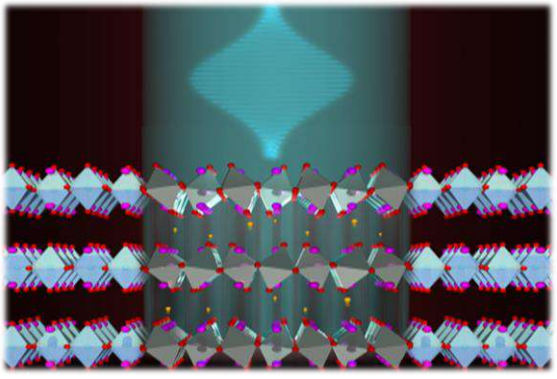

Fig.1. *Controlling crystal structures with light*

References

[1] D. Nicoletti, A. Cavalleri, *Advances in Optics and Photonics* **8**, 401 (2016).
[2] A. von Hoegen et al, *Nature* **555**, 79 (2018).
[3] M. Först et al. *Nature Physics* **7**, 854 (2011).
[4] R. Mankowsky et al, *Nature* **516**, 71 (2014).
[5] W. Hu et al, *Nature Materials* **13**,705 (2014).
[6] S. Kaiser, et al, *Physical Review B* **89**, 184516 (2014).
[7] B. Liu,et al, *Physical Review X* **10**, 011053 (2020).
[8] M Mitrano et al, *Nature* **530**, 461 (2016).
[9] A. Cantaluppi et al, *Nature Physics* **14,** 837 (2018).
[10] M. Buzzi et al, *Physical Review X* **10**, 031028 (2020).

Ultrafast Dynamics

The Emergent Quantum Critical Point of Electric Driven Charge Density Wave Materials

J. K. Freericks
Georgetown University, Washington, DC 20057, USA

Using a paradigmatic model for electrically driven charge-density-wave solids, we establish the existence of an "emergent quantum critical point." At T=0, the system remains an ordered insulator for all interaction strengths. But, for any nonzero temperature, the system becomes metallic at a critical interaction strength and remains metallic in the limit as the temperature approaches zero. The transition occurs via the development of metallic density of states at the Fermi level for any nonzero temperature. The resulting phase diagram resembles those of conventional quantum critical points, which is why we call this an emergent quantum critical point.

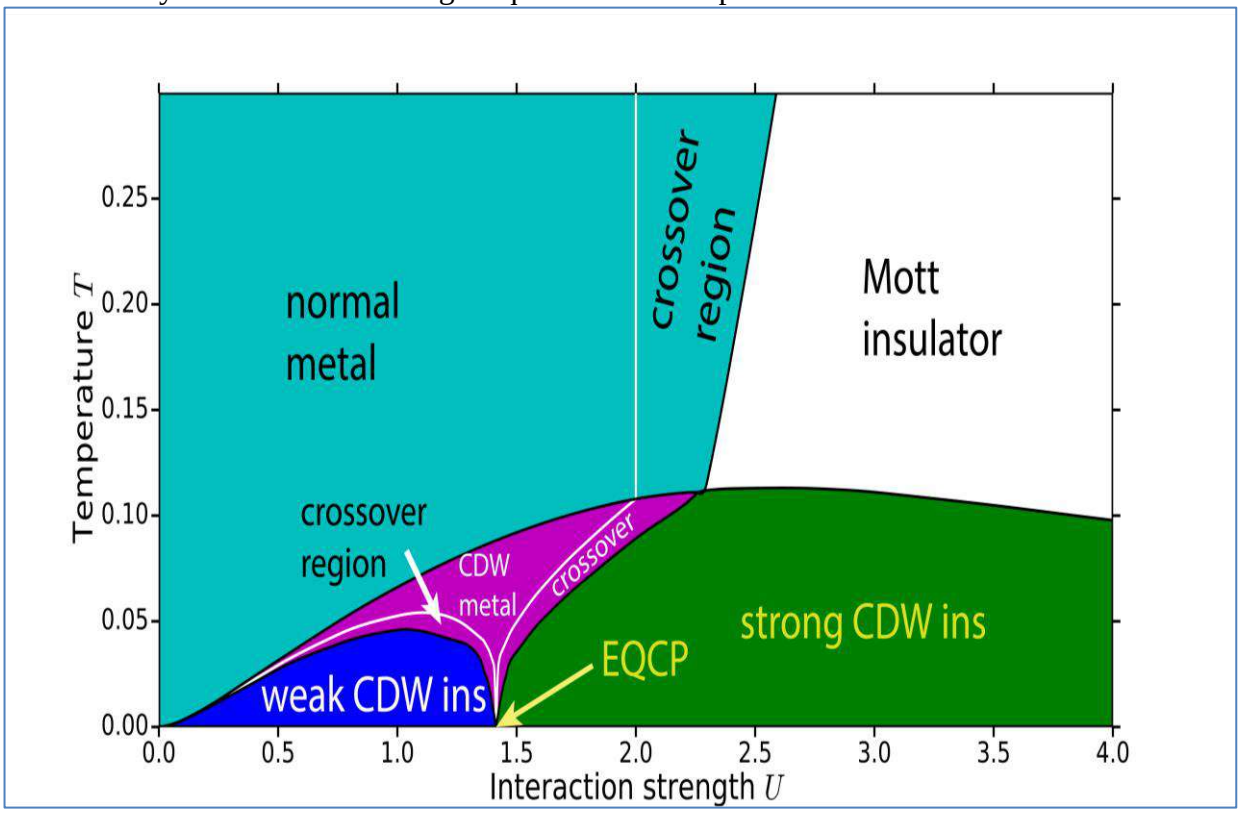

***Fig. 1**: Phase diagram for the emergent critical point (EQP) of the charge-density-wave order in the Falicov-Kimball model. The **blue** and **green** regions are charge-density-wave insulators with a gap in the density of states. The **magentia** region is a charge-density-wave metal. The **cyan** is the normal-metal, and tthe **white** region is the Mott insulator.*

Even though there is no transition for exactly zero temperature, the system behaves essentially like that of a traditional quantum critical point. We describe scaling relations and how one might be able to detect such a state experimentally.

References

This work was done in collaboration with Jakub Krawczyk and Romuald Lemanski. It is supported by the Department of Energy Basic Energy Sciences under grant number DE-FG02-08ER46542 and the McDevitt bequest at Georgetown University.

Ultrafast Spectroscopic Studies of Topological Quantum Matter

M. Z. Hasan, I. Belopolski, S.-Y. Xu, M. Neupane
Princeton University, Princeton, NJ 08544, USA

Over the last decade, ultrafast spectroscopic techniques have been crucial to gain fundamental insights into the topological properties of materials. We employed ultrafast time-resolved angle-resolved photoemission spectroscopy to probe and elucidate surface electronic structure and electron dynamics of Z_2 topological insulators, Dirac-Weyl semimetals and exotic spin-orbit superconductors [1, 2]. In this talk, I plan to present a few recent examples where ultrafast techniques have been crucial to discover the full topological behavior:

(1) In candidate Weyl semimetal class $TaIr(Te/Se)_4$, the Weyl points and Fermi arcs live entirely above the Fermi level, making them inaccessible to conventional ARPES. We utilized ultrafast pump-probe ARPES to directly access the electronic states above the Fermi level in $TaIrTe_4$. We observe signatures of Weyl nodes and correspondingly coupled spin textured Fermi arcs states. A full map reveals, for the first time, that $TaIrTe_4$ is a Weyl semimetal with the minimum number of four Weyl points [3].

(2) It was long been speculated that $Mo_xW_{1-x}Te_2$ materials may realize Lorentz violating topological Weyl fermions. In order to explore its quantum topology, we first showed theoretically that it is crucial to access the full electron dynamics to reveal a non-Lorentz Weyl state in $Mo_xW_{1-x}Te_2$. Then, we experimentally studied $Mo_xW_{1-x}Te_2$ materials by a suite of pump-probe ultrafast ARPES techniques. By comparing our pump-probe results with *ab initio* simulations, we concluded that the materials indeed features topological surface state associated with non-trivial Berry curvature field which is the generator of the non-Lorentz Weyl topology and non-trivial Chern number [4].

(3) The third example would be on the possibility of novel phenomena induced by light. Here, we used pump-probe photoemission spectroscopy to explore the optically excited Dirac surface states in the bulk-insulating topological insulator Bi_2Te_2Se. Our results revealed optical and ultrafast properties that are in sharp contrast to those of bulk-metallic topological insulators. We observed a gigantic optical lifetime exceeding 4 μs (1 μs=10−6 s) for the surface states in Bi_2Te_2Se, whereas the lifetime in most topological insulators, such as Bi_2Se_3, has been limited to a few picoseconds (1 ps=10−12 s). Moreover, we discovered a surface photovoltage, a shift of the chemical potential of the Dirac surface states, as large as 100 mV. Our results demonstrate a rare topological platform to explore charge excitation and relaxation in energy and momentum space in two-dimensional systems [5].

(4) Finally, (time permitting) I will talk about electronic structure and relaxation dynamics in a superconducting topological material. Topological superconductors host new states of quantum matter which show a pairing gap in the bulk and gapless surface states providing a platform to realize Majorana modes. Recently, alkaline-earth metal Sr intercalated Bi_2Se_3 has been reported to show superconductivity with a $T_c \sim 3$ K and a large shielding fraction. We report systematic electronic structure studies of $Sr_{0.06}Bi_2Se_3$ ($Tc \sim 2.5$ K). Using ARPES, we observed a quantum well confined two-dimensional state coexisting with a topological surface state in $Sr_{0.06}Bi_2Se_3$. Furthermore, our time-resolved ultrafast ARPES reveals the relaxation dynamics showing different decay mechanism between the excited topological surface states and the two-dimensional states.

Our experimental observation is understood by considering the intra-band scattering for topological surface states and an additional electron phonon scattering for the 2D states, which is likely responsible for the superconductivity [6].

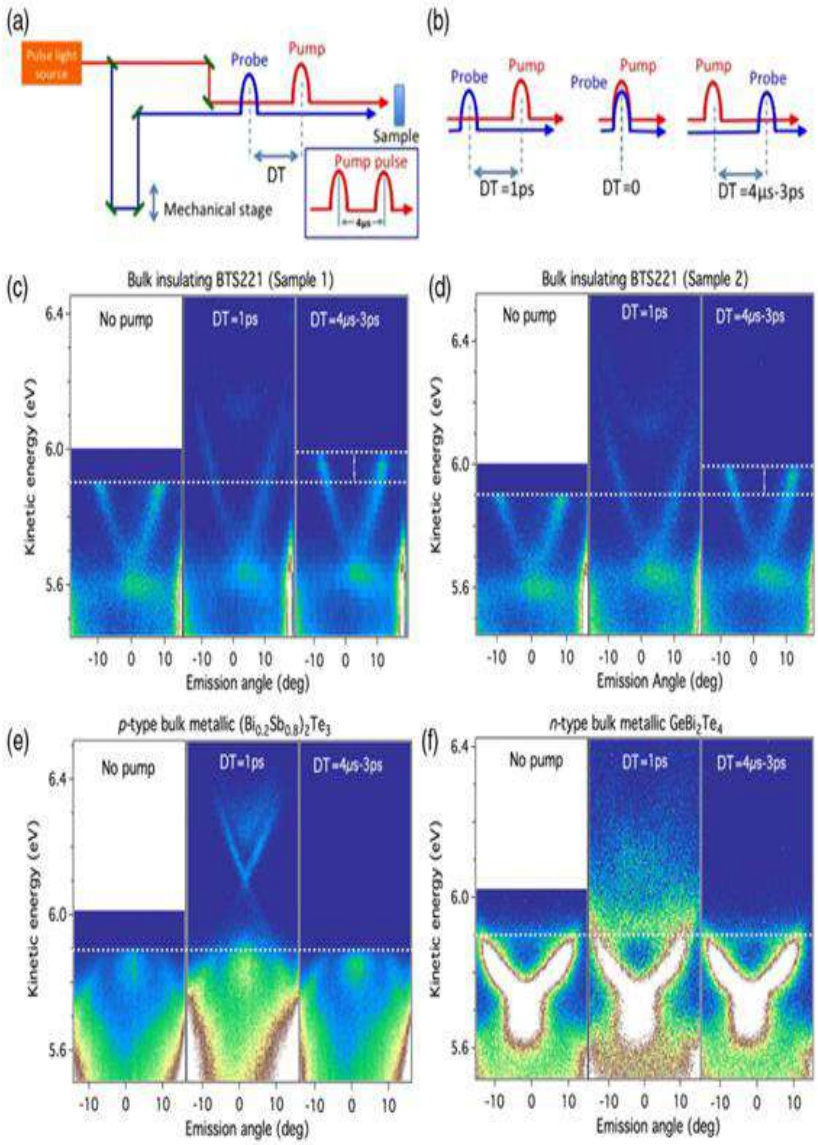

Fig.1 *Generation of photovoltage in a bulk insulating TI.*
(a), ***(b).*** *Schematic view of the pump-probe ARPES experimental setup. The delay line is defined in* ***(b).*** *The inset in* ***(a)*** *shows the frequency of the pump pulse.* ***(c)*** *ARPES band dispersion of bulk insulating Bi_2Te_2Se (sample1) near Γ point measured with no pump (**left-hand panel**), with pump (**middle** and **right-hand panel**).The delay time is noted on the spectra.*
(d). *Similar measurement in* ***(c)*** *for Bi_2Te_2Se (sample 2).*
From ***(c)*** *and* ***(d)*** *the generation of photovoltage (~100mV) is evident in the bulk insulating sample. Similar measurement as in* ***(d)*** *for* ***(e)*** *p-type bulk metallic ($Bi_{02}Sb_{08})_2Te_3$ TI and* ***(f)*** *n-type bulk metallic $GeBi_2Te_4$ TI. No generation of the photovoltage is obtained for the bulk metallic topological insulators [see* ***(e)*** *and* ***(f)****].*
The native Fermi level (Fermi level with the absence of pump pulse) is marked by the white dashed line in the spectra.

These ultrafast studies and their future extensions (that we plan to carry out) will be helpful in understanding low temperature superconducting states realized in these topological materials.

References

[1] M. Z. Hasan, C. L. Kane, *Review of . Modern Physics.* **82**, 3045 (2010).
[2] D. N. Basov, R. D. Averitt, D. Hsieh; *Nature Materials* **16**, 1077 (2017).
[3] I. Belopolski et.al., *Nature Communications* **8,** 942 (2017).
[4] I. Belopolski I, S.-Y. Xu, Y. Ishida *et al*., *Physical Review B* **94**(8): 085127 (2016)
[5] M. Neupane, S.-Y. Xu, Y. Ishida *et al*., *Physical Review Letters* **115**(11): 116801 (2015).
[6] M. Neupane *et.al.*, (unpublished: in preparation *Physical Review Letters*)

Dynamical Couplings in Laser-driven Quantum Materials: Towards the Quantum-Light Regime

M. A. Sentef
Max Planck Institute for the Structure and Dynamics of Matter, 22761 Hamburg, Germany

I will discuss recent progress in our understanding of control of microscopic couplings in quantum materials by light-matter interaction. Pump-probe experiments have demonstrated intriguing results, such as light-induced superconductivity in an organic kappa salt [1] or an ultrafast Lifshitz transition in the Weyl material Td-MoTe2 [2]. Both of these experiments have been linked to an effective dynamical Hubbard U triggering collective dynamics and novel non-equilibrium emergent phenomena. On the theory side, we have shown how laser driving can change the effective screening in the prototypical p-d charge transfer insulator NiO [3]. We have predicted that an analogous effect could allow for an ultrafast topological phase transition into the elusive Weyl semimetallic phase in pyrochlore iridates [4]. I will take these effects based on classical light as a starting point to discuss the crossover from classical to quantum light, which we comprehensively investigate for the paradigmatic spin-exchange interaction in the Hubbard model [5]. In this work we consider a correlated low-dimensional material placed inside a quantum electrodynamical cavity. We derive general expressions for the light-engineered spin-exchange coupling based on a Cavity-Schrieffer-Wolff transformation and discuss a time-resolved numerical study for a Hubbard dimer in a laser-driven cavity.

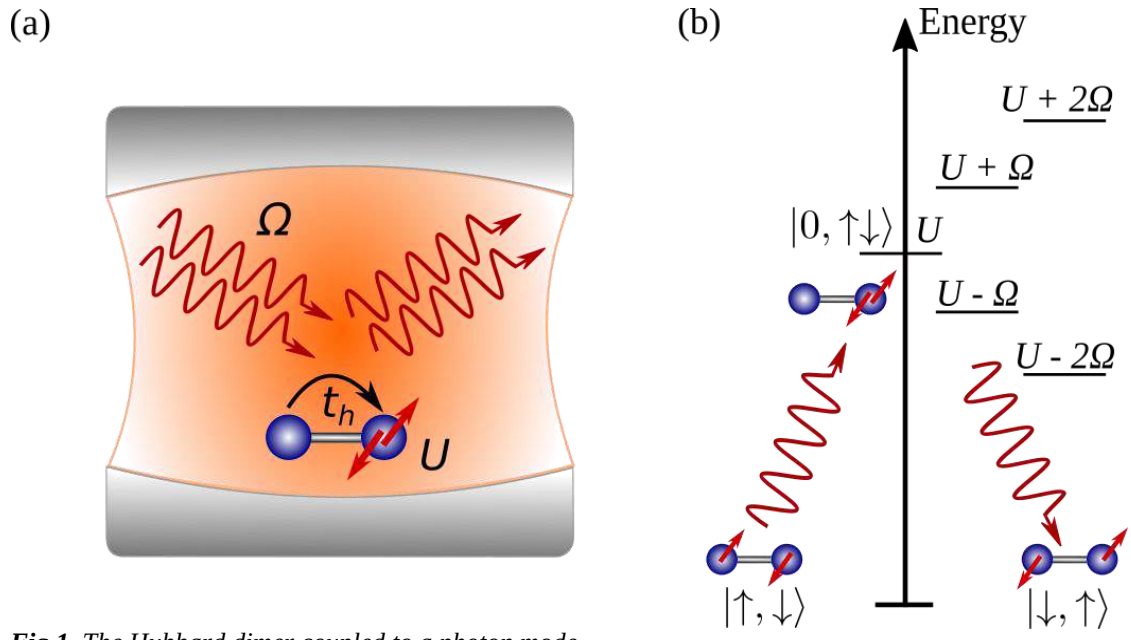

Fig 1. *The Hubbard dimer coupled to a photon mode.*
(a) *Sketch of a Hubbard dimer (Hubbard U, hopping t_h) coupled to the cavity photon mode at frequency Ω.*
b) *The energy structure of a cavity coupled Hubbard dimer at the strong coupling $U >> t_h$ limit. The two lattice sites exchange spins through virtual processes visiting different photon number sectors.*

As a key result, we show that the crossover from the extreme quantum limit to the classical Floquet limit does *not* require photon-field coherence but is equally achieved with photon-number eigenstates (and *vanishing* classical electromagnetic fields). In particular this Floquet-engineering limit happens for average photon numbers as low as *n=1* in the strong light-matter coupling regime, paving the way for novel light-matter materials design that avoids many of the complications of classical Floquet engineering in materials, such as heating and sample destruction.

References

[1] M. Buzzi et al., *arXiv*:2001.05389 (2020).
[2] S. Beaulieu et al., *arXiv*:2003.04059 (2020).
[3] N. Tancogne-Dejean, M. A. Sentef, A. Rubio, Physical Review Letters **121**, 097402 (2018).
[4] G. E. Topp et al., *Nature Communications* **9**, 4452 (2018).
[5] M. A. Sentef, J. Li, F. Künzel, M. Eckstein, *arXiv*:2002.12912 (2020).

Theoretical Understanding of Photon Spectroscopies in Correlated Materials In and Out of Equilibrium

T. P. Devereaux
Stanford University, Stanford, CA 94305, USA

Photon-based spectroscopies have had a significant impact on both fundamental science and applications by providing an efficient approach to investigate the microscopic physics of materials. Together with the development of synchrotron X-ray techniques, theoretical understanding of the spectroscopies themselves and the underlying physics that they reveal has progressed through advances in numerical methods and scientific computing. In this talk, I will provide an overview of theories for angle-resolved photoemission spectroscopy and resonant inelastic X-ray scattering applied to quantum materials, discussing methods for studying equilibrium spectroscopies and assessing the recent development of ultrafast techniques for out-of-equilibrium spectroscopies.

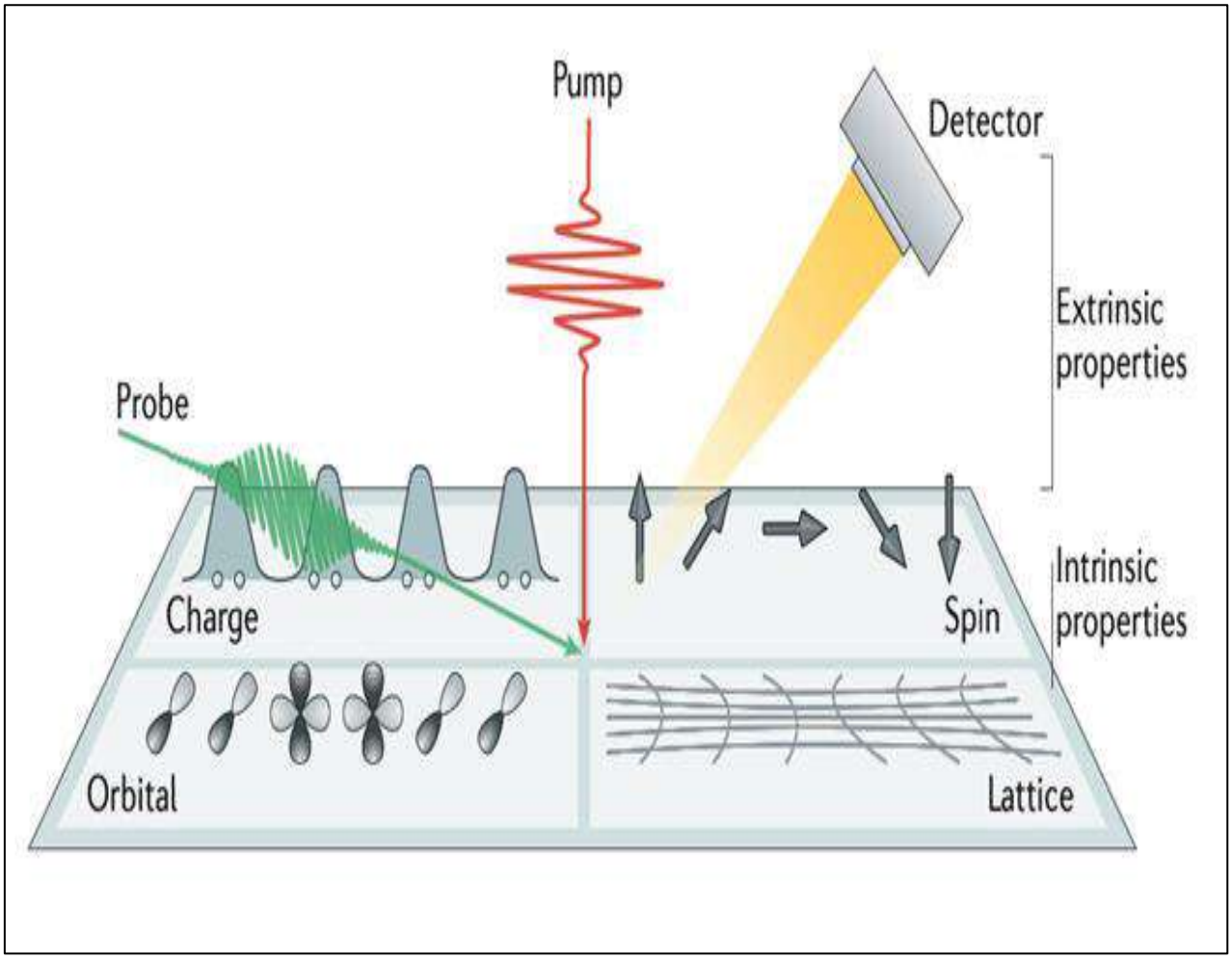

Fig.1. Theoretical evaluation of spectroscopies. *The schematic illustrates the two main factors required for the theoretical evaluation of spectroscopies:* ***first****, threatment of the extrinsic measurement details that describe the light-Fmatter interaction, and* ***second****, assessment of how the individual and collective degrees of freedom (including charge, spin, orbital and lattice) manifest in the intrinsic physical properties relevant to a specific probe.*

Finally, I will highlight some the main challenges and provide an outlook for the future direction of the field [1].

References

[1] Yao Wang, M. Claassen, C.D. Pemmeraju, C. Jia, B. Moritz, T. P. Devereaux, *Nature Review Materials* **3**, 312 (2018).

Charge Dynamics Electron Microscopy. Nanoscale Imaging of Femtosecond Plasma Dynamics

F. Barantani[1], I. Madan[1], E. J. C. Dias[2], S.Gargiulo[1], M. Yannai[3], G. Berruto[1], T. LaGrange[1]
L. Piazza[1], T. T. A. Lummen[4], R. Dahan[3], I. Kaminer[3], G. M. Vanacore[5],F. J. G. de Abajo[2]
F. Carbone[1]
[1]*Ècole Polytechnique Fèdèrale de Lausanne, 1015 Lausanne, Switzerland*
[2]*ICFO-Institut de Ciencies Fotoniques, 08860 Castelldefels, Spain*
[3]*Technion, Haifa 32000, Israel*
[4]*ETH Zurich, 4058 Basel, Switzerland*
[5]*University of Milano-Bicocca, 20126 Milano, Italy*

Controlling and probing the spatiotemporal dynamics of out-of-equilibrium electron clouds [1] is crucial for the design of electron and light sources as well as for novel ultrafast power electronic devices [2], and plasma-based applications. Nonetheless, following such dynamics on the nanometer and femtosecond scales has been proven challenging [3] and inaccessible to existent optical probes because of the intrinsic screening. Here, we investigate the evolution of electron clouds generated by a laser pulse impinging on metallic structures, by means of an ultrafast transmission electron microscope. We record -Fig.1, the charged plasma dynamics by measuring the electron-beam acceleration and spectral broadening with nanometer-femtosecond resolution. We combine the experimental results with a complete microscopic theory and thus we gain insights into the electron emission processes, screening phenomena, and cloud expansion dynamics.

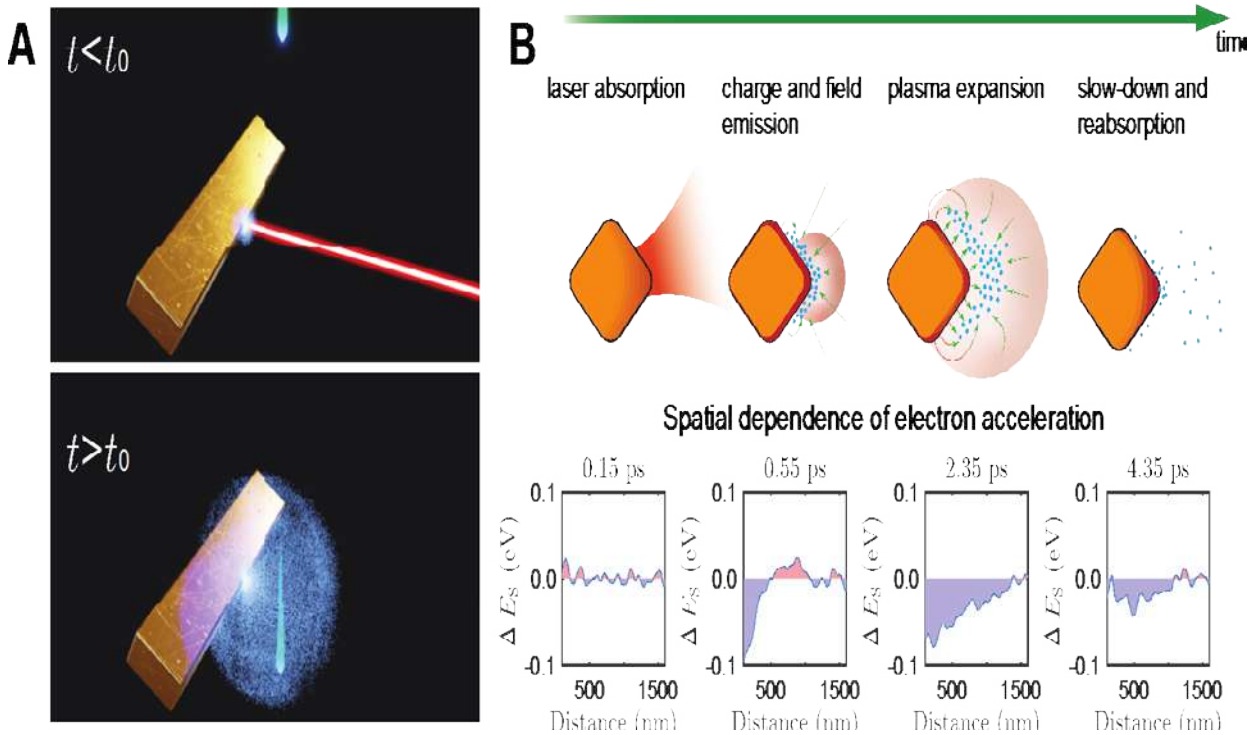

Fig.1, A) *Schematics of the experiment: a laser pulse (50 fs, 800 nm) generates a charged cloud that is probed by an electron pulse (200 keV, 600 fs) with a tunable delay time with respect to the laser pulse.* ***(B)*** *Dynamics of the generated electron cloud (upper schemes) and its impact on the probe electron spectral features (lower plots) at given delay times.*

Beyond these experimental observations, such technique, which we dubbed Charge Dynamics Electron Microscopy (CDEM), enables the exploration of various out-of-equilibrium electrodynamic phenomena which involve the ultrafast dynamics of bound and free charges at the nanometer length scale.

References

[1] P. Musumeci, et al. *Journal of Applied Physics* **108**, 114513 (2010).
[2] M. S. Nikoo et al. *Nature* **579**, 534 (2020).
[3] S. Schäfer, W. Liang, A. H. Zewail, *Chemical Physics Letters* **493**, 11 (2010).

Goldstone Modes and Soft Fluctuation Modes in Polariton Lasers

R. Binder, M. Spotnitz, N.H. Kwong
University of Arizona, Tucson, AZ 85721, USA

Semiconductor microcavities exhibit a wide range of optical phenomena and underlying physical processes. These properties can be probed and uncovered using linear response, but linear response poses different challenges in normal-state systems and condensed systems (i.e. systems with spontaneous symmetry breaking including lasing states). For a driven-dissipative quantum many-particle system prepared in a spontaneous broken-symmetry steady state, in addition to the Goldstone mode, the soft fluctuation modes provide important insight into the system's dynamics. An important example of such a system is a polariton laser, which combines effects of spontaneous symmetry breaking and many-particle effects due to the Coulomb interaction between the charge carriers (electrons and holes). Using a microscopic polariton laser theory, we have analyzed the system's linear response below and above lasing threshold and identified a rich transformation behavior of discrete and continuum soft modes in a two parameter (pump density and cavity dissipation rate) space.

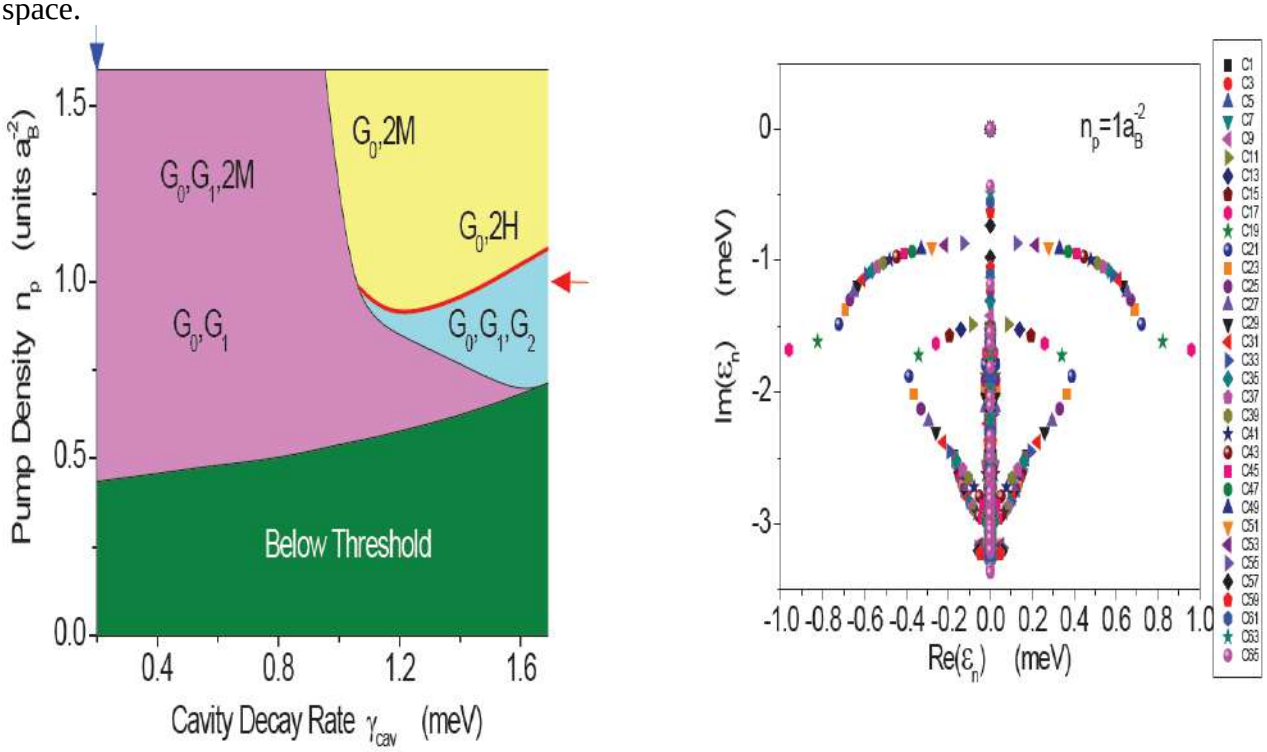

Fig.1. (Left) *A map of the discrete fluctuation modes (G_o -Goldstone mode, G_n -damped Goldstone companion mode). Each point on the red curve separating the blue and the yellow regions is an exceptional point.*
(Right) *Eigenenergies for equidistantly spaced cavity rates γ_{cav} from 0.9meV (C1) to 1.7meV (C65) at fixed pump density n_p. An example of an exceptional points is seen as annihilation of modes with non-zero frequency (i.e. non-zero Re(ε_v)) from C55 to C57 [1].*

In addition to finding exceptional-point Goldstone companion modes, our theory yields a unified picture of a variety of seemingly disconnected physical concepts including Mott transition, Mollow spectra or relaxation oscillations, and energy gaps in polaritonic Bardeen-Cooper-Schrieffer states [1, 2].

References

[1] R. Binder and N.H. Kwong, *Physical Review* B **103**, 085304 (2021).
[2] J. Hu *et al*., *Physical Review* X **11**, 011018 (2021).
[3] M. Spotniz, N.H. Kwong, R. Binder, *Physical Review* B **104**, 115305 (2021). [4]
M. Spotniz, N.H. Kwong, R. Binder, *Physical Review* B (to be published).
We gratefully acknowledge financial support from NSF under grant number DMR 1839570, and CPU time at HPC, University of Arizona.

Axial Higgs Mode Detected by Quantum Pathway Interference

K.S. Burch
Boston College, Chestnut Hill, MA 02467, USA

The observation of the Higgs boson solidified the standard model of particle physics. However, explanations of anomalies (e.g. dark matter) rely on further symmetry breaking[1] calling for an undiscovered axial Higgs model. In condensed matter, nonlinear optics has playd a key role in observing the Higgs in superconducting and charge density wave(CDW) systems[2, 3]. Uncovering a low energy mode's vector properties is challenging, requiring going beyond typical spectroscopic or scattering techniques. Here, we describe our discovery an axial Higgs mode in the CDW system RTe_3 using the interference of quantum pathways.[4] In RTe_3 (R=La,Gd), the electronic ordering couples bands of equal or different angular momenta[5–7]. As such, the Raman scattering tensor associated to the Higgs mode contains both symmetric and anti-symmetric components, which can be excited via two distinct, but degenerate pathways. This leads to constructive or destructive interference of these pathways, depending on the choice of the incident and Raman scattered light polarization. The qualitative behavior of the Raman spectra is well-captured by an appropriate tight-binding model including an axial Higgs mode. The elucidation of the antisymmetric component provides direct evidence that the Higgs mode contains an axial vector representation (i.e. a pseudo-angular momentum) and hints the CDW in RTe_3 is unconventional.

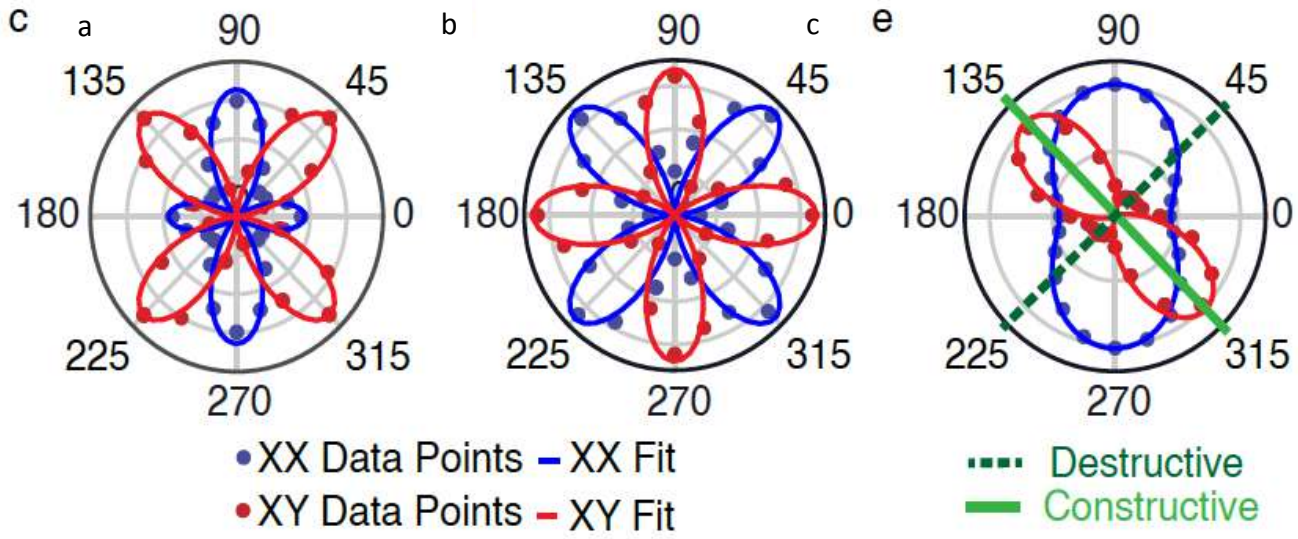

Fig. 1 *Angular resolved Raman intensities.* ***(a-c)*** *Angular dependence of the amplitudes of the Raman modes extracted from Voigt fits of the spectra in parallel* ***(blue dots)*** *and cross* ***(red dots)*** *linear polarization.* ***(a)*** *Ag mode of* $GdTe_3$. ***(b)*** *Bg mode of* $GdTe_3$. ***(e)*** *CDW mode of* $GdTe_3$ *revealing the constructive* ***(green a'b')*** *versus destructive* ***(dashed green b'a')*** *interference.*

Thus we provide a means for measuring collective modes quantum properties without resorting to extreme experimental conditions

References

[1] D.B. Franzosi, et al., *Journal of High Energy Physics* **2016**, 76 (2016).
[2] R. Shimano, N. Tsuji, *Annual Review of Condensed Matter Physics* **11**, 103 (2020).
[3] D. Pekker, C. Varma, *Annual Review of Condensed Matter Physics* **6**, 269 (2015).
[4] Y. Wang, et al, *Nature* (to be published).
[5] S. Klemenz, et al, *Journal of American Chemical Society* **142**, 6350 (2020).
[6] V. Brouet, et al, *Physical Review* B **77**, 235104 (2008).
[7] S. Lei, et al, *Science Advances* **6**, 6(2020).

Ultrafast Transmission Electron Microscopy of Charge-Density Waves

Th. Danz, T. Domröse, C. Ropers
University of Göttingen, 37077 Göttingen, Germany

Over the past decades, ultrafast optical techniques have considerably shaped our understanding of homogeneous materials, while transmission electron microscopy has greatly contributed to elucidating atomic structures and compositions on the sub-nanometer scale. Combining these concepts, ultrafast transmission electron microscopy allows for resolving femtosecond dynamics in heterogeneous materials using imaging, diffraction, and spectroscopy in a laser pump/electron probe scheme [1]. Here, we demonstrate the ultrafast real-space mapping of the order parameter for a charge-density wave (CDW) phase transition in the correlated material 1*T*-TaS_2 using the Göttingen Ultrafast Transmission Electron Microscope (UTEM) [2]. In the experiments, a free-standing, single-crystalline 1*T*-TaS_2 thin film [3] is pumped out of the nearly commensurate CDW phase at room temperature towards the high-temperature incommensurate CDW phase using a spatially structured laser field distribution (see Fig. 1A for a schematic of the experimental setup). Specifically, we employ ultrafast dark-field imaging to follow the formation, evolution, and relaxation of CDW domain patterns on their intrinsic femtosecond to nanosecond timescales, yielding nanoscale access to the order parameter of the structural phase transition (see Fig. 1B and C).

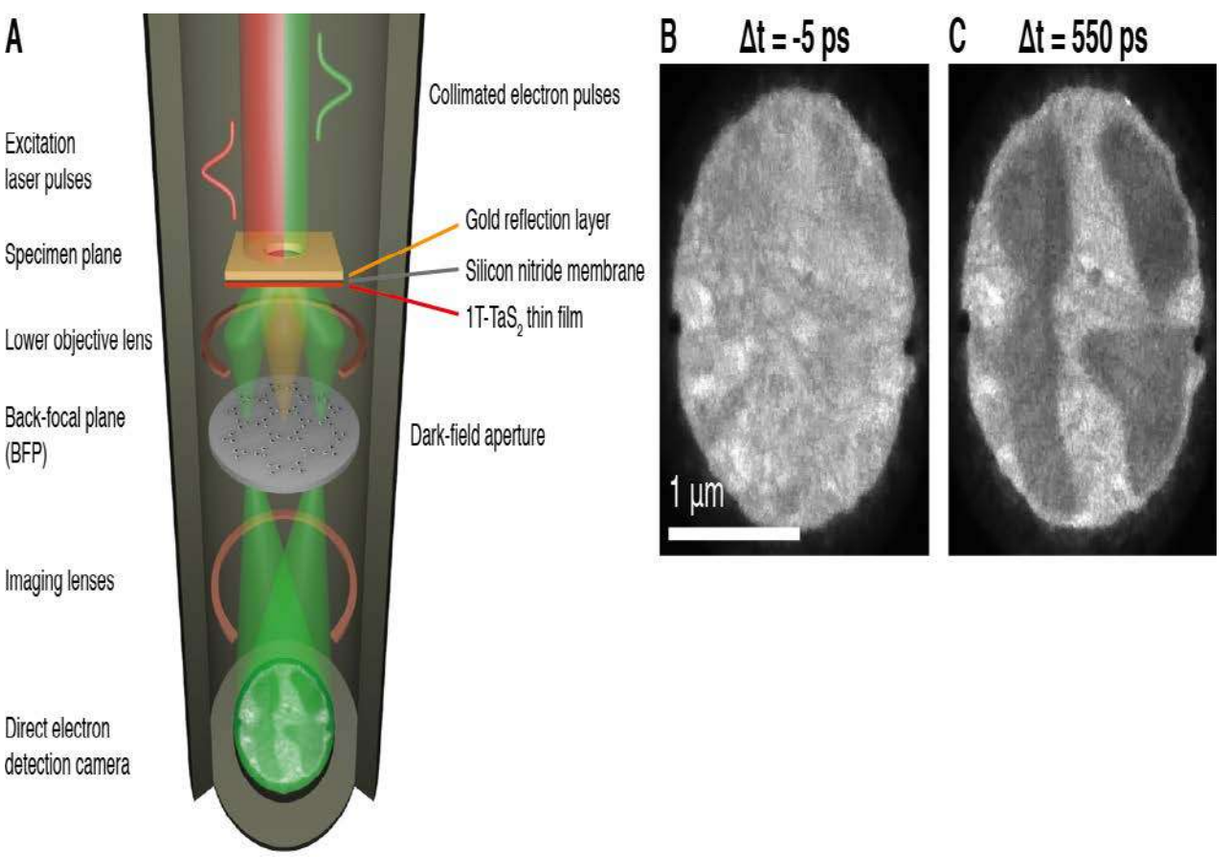

***Fig.1** (**A**) Simplified schematic of the experimental setup.*
*(**B** and **C**) Ultrafast electron micrographs of the specimen before and after time zero, showing CDW domains of the room- (bright) and the high-temperature phase (dark).*

Additionally, we show that prominent features in the spatio-temporal domain evolution can be modeled in a time-dependent Ginzburg-Landau approach, allowing us to distinguish different regimes of the observed dynamics [4].

References

[1] A.H. Zewail. *Science* **328**. 187 (2010).
[2] A. Feist. Th. Danz *et al.*. *Ultramicroscopy* **176**. 63 (2017).
[3] Th. Danz *et al.*. *Journal of Physics: Condensed Matter* **28**, 356002 (2016).
[4] Th. Danz *et al.*, *(in preparation).*

Ultrafast Transmission Electron Microscopy of Charge-Density Waves

Th. Danz, T. Domröse, C. Ropers
University of Göttingen, 37077 Göttingen, Germany

Over the past decades, ultrafast optical techniques have considerably shaped our understanding of homogeneous materials, while transmission electron microscopy has greatly contributed to elucidating atomic structures and compositions on the sub-nanometer scale. Combining these concepts, ultrafast transmission electron microscopy allows for resolving femtosecond dynamics in heterogeneous materials using imaging, diffraction, and spectroscopy in a laser pump/electron probe scheme [1]. Here, we demonstrate the ultrafast real-space mapping of the order parameter for a charge-density wave (CDW) phase transition in the correlated material 1*T*-TaS_2 using the Göttingen Ultrafast Transmission Electron Microscope (UTEM) [2]. In the experiments, a free-standing, single-crystalline 1*T*-TaS_2 thin film [3] is pumped out of the nearly commensurate CDW phase at room temperature towards the high-temperature incommensurate CDW phase using a spatially structured laser field distribution (see Fig. 1A for a schematic of the experimental setup). Specifically, we employ ultrafast dark-field imaging to follow the formation, evolution, and relaxation of CDW domain patterns on their intrinsic femtosecond to nanosecond timescales, yielding nanoscale access to the order parameter of the structural phase transition (see Fig. 1B and C).

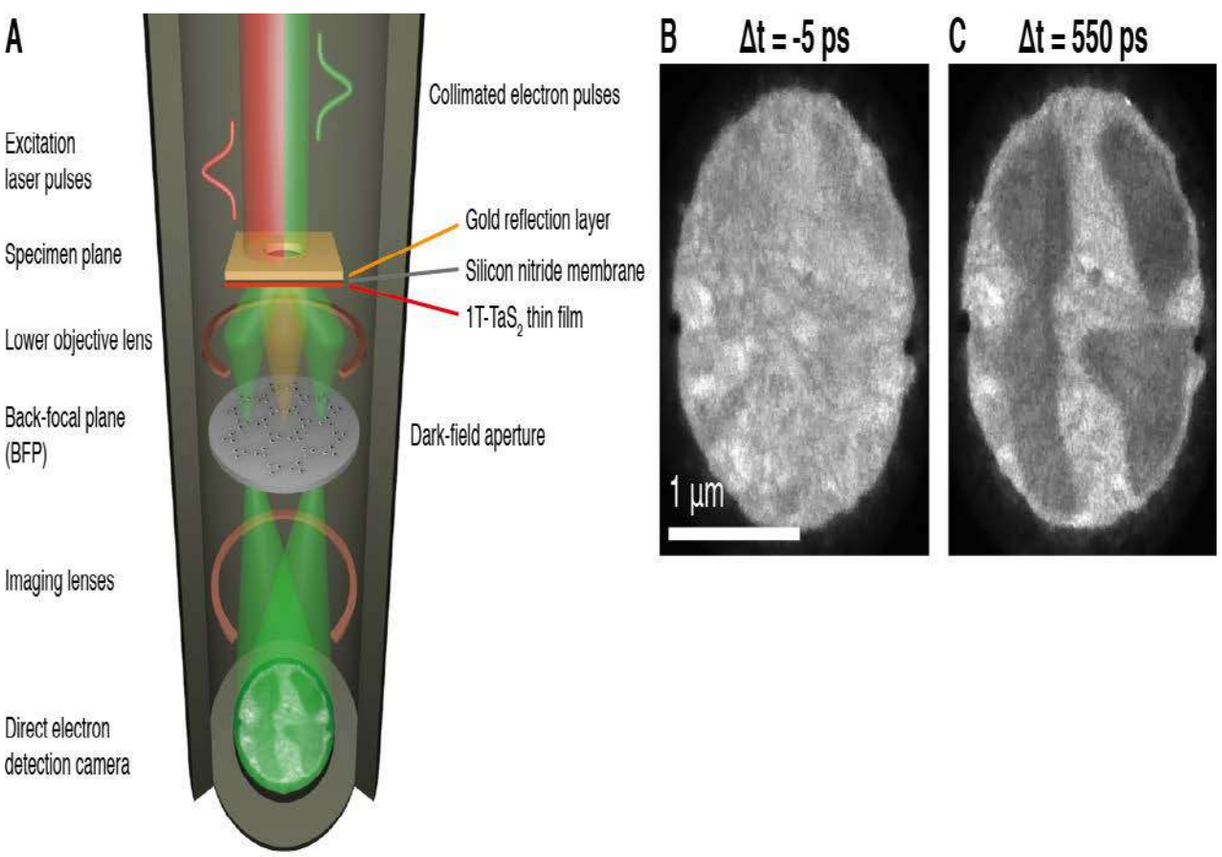

***Fig.1** (**A**) Simplified schematic of the experimental setup.*
*(**B** and **C**) Ultrafast electron micrographs of the specimen before and after time zero, showing CDW domains of the room- (bright) and the high-temperature phase (dark).*

Additionally, we show that prominent features in the spatio-temporal domain evolution can be modeled in a time-dependent Ginzburg-Landau approach, allowing us to distinguish different regimes of the observed dynamics [4].

References

[1] A.H. Zewail. *Science* **328**. 187 (2010).
[2] A. Feist. Th. Danz *et al.*. *Ultramicroscopy* **176**. 63 (2017).
[3] Th. Danz *et al.*. *Journal of Physics: Condensed Matter* **28**, 356002 (2016).
[4] Th. Danz *et al.*, *(in preparation).*

Non-Adiabatic Switch-off of Deep-Strong Light-Matter Coupling

J. Mornhinweg[1], M. Halbhuber[1], V. Zeller[1], C. Ciuti[2], D. Bougeard[1], R. Huber[1], C. Lange[1]
[1]*University of Regensburg, 93040 Regensburg, Germany*
[2]*Université de Paris, 75013 Paris, France*

Dressing electrons with the vacuum electromagnetic field of an optical microresonator can lead to fundamentally new states of matter. When the frequency of energy exchange between light and matter, the vacuum Rabi frequency, Ω_R, becomes comparable to the carrier frequency of light, ω_c, the regime of ultrastrong coupling is attained [1,2]. Here, anti-resonant interaction terms modify the dynamics and give rise to novel phenomena of cavity quantum electrodynamics (c-QED) such as the vacuum Bloch-Siegert shift [3]. In the yet more extreme setting of $\Omega_R \gtrapprox \omega_c$, deep-strong coupling [4] leads to a profoundly modified vacuum ground state. While the exploration of the equilibrium properties of deep-strong coupling has just begun, investigating the subcycle dynamics is expected to reveal qualitatively new quantum phenomena. Here, we explore the dynamics that arises when light-matter interaction of a deep-strongly coupled system is switched off quasi-instantaneously. We employ custom-tailored THz antennas coupled to cyclotron resonances of two-dimensional electron gases, resulting in a coupling strength of up to $\Omega_R/\omega_c = 1.3$. The switch-off is implemented by an $In_{0.55}Ga_{0.45}As$ semiconductor patch located in the central gap region of the resonator. Photoexcitation by near-infrared pulses of a duration of 70 fs forms a dense charge carrier plasma in this patch which screens the cavity mode, rapidly decoupling it from the electronic resonance more than an order of magnitude faster than the cycle duration of light. This quasi-instantaneous switch-off leads to characteristic oscillations of the transmission. Our quantum model including anti-resonant interaction terms verifies that these oscillations result from a strongly subcycle switch-off of deep-strong coupling within just 5% of the cycle duration of the lower polariton.

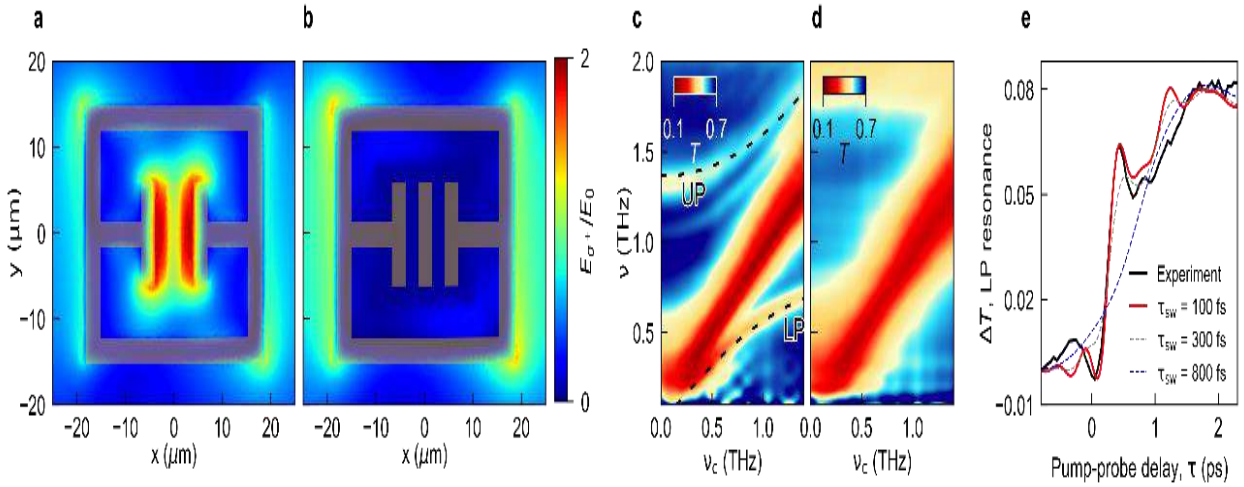

***Fig. 1 | a**, Near-field enhancement of the resonator calculated in the quantum well plane 200 nm below the resonator structure, at the resonance frequency. **b**, Near-field enhancement with an excited switch element. **c**, Steady-state transmission of an ultrastrongly coupled structure, as a function of the CR frequency, ν_c. The dashed lines tracing the lower polariton (LP) and upper polariton (UP) resonances correspond to a coupling strength of $\Omega_R/\omega_{LC} = 0.57$. **d**, Transmission measured after switching. **e**, Non-adiabatic deactivation dynamics of deep-strong coupling. The differential transmission ΔT of the LP (black solid curve) induced by the switching pulse as a function of pump probe delay τ, and calculation for various switching times (red and dashed curves).*

Our results blaze a trail towards exploring non-adiabatic settings of c-QED [5,6], transport modified by the vacuum field [7], cavity quantum chemistry [8], or light-induced superconductivity [9].

References

[1] A. Günter et al., *Nature* **458**, 178 (2009).
[2] G. Scalari et al., *Science* **335**, 1323 (2012).
[3] X. Li et al., *Nature Photonics* **12**, 324 (2018).
[4] A. Bayer, M. Pozimski, S. Schambeck, D. Schuh, R. Huber, D. Bougeard, C. Lange, *Nano Letters* **17**, 6340 (2017).
[5] C. Riek et al., *Science* **350**, 420 (2015).
[6] I. Benea-Chelmus. F.F.Settembrini. G. Scalari. J. Faist. *Nature* **568.** 202–206 (2019).
[7] G. L. Paravicini-Bagliani et al., *Nature Physics* **15**, 186 (2019).
[8] A. Thomas et al., *Science* **363**, 615 (2019).
[9] A. Thomas et al., *arXiv* 1911.01459v1 (2019).

Nonequilibrium Dynamics of Correlated Disordered Quantum Systems, a DMFT + CPA Effective Medium Approach

H. F. Fotso
University at Albany SUNY, Albany, NY 12222, USA

There is a pressing need to extend the treatment of quantum materials beyond typical models and simulations that assume idealized systems. In particular, it is important to properly incorporate the intrinsic complexity arising from disorder in the models describing real materials. One particular challenge in this context is understanding the interplay of disorder and strong electron-electron interactions which simultaneously contribute to the behavior of real systems. This interplay has intriguing consequences in equilibrium that are only enriched away from equilibrium. We present an effective medium approach to characterize the nonequilibrium dynamics of interacting disordered systems.

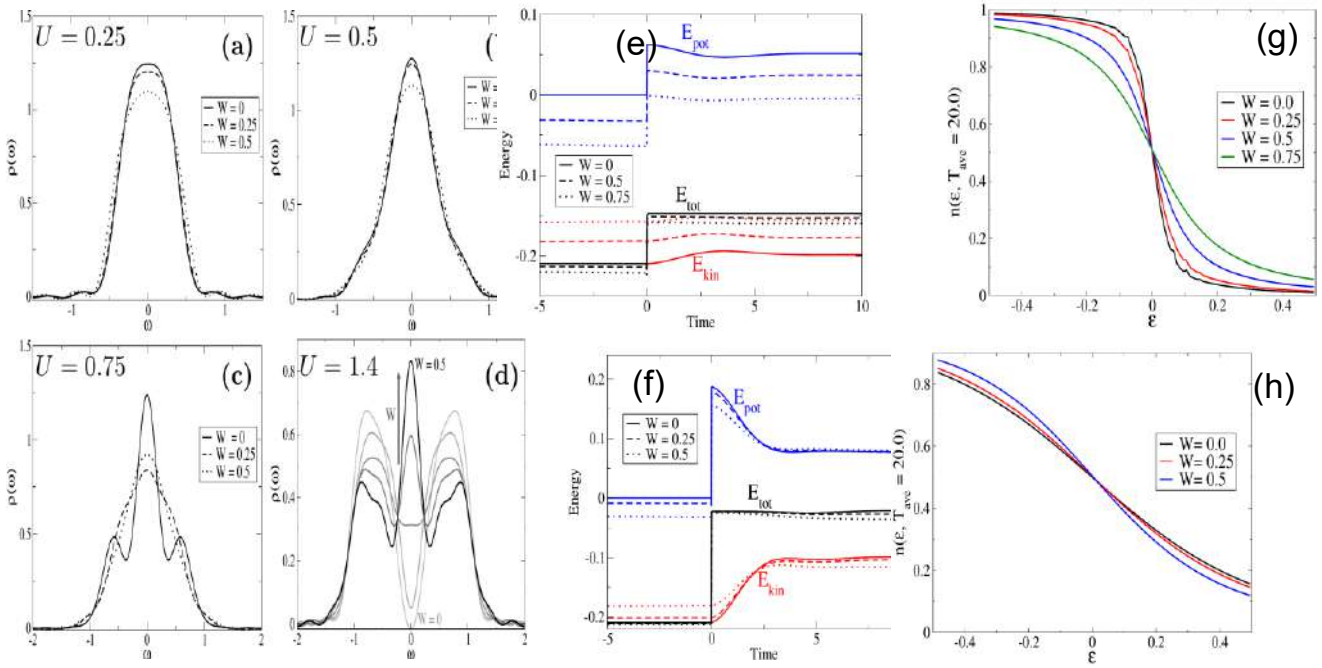

Fig 1. *Taken from Reference[1].* ***(a)-(d):*** *Equilibrium density of states for the Anderson-Hubbard model calculated with the time-domain DMFT+CPA approach. W is the disorder strength and W=0 corresponds to the clean system. For weak interactions, increasing the disorder strength broadens the density of states. As the interaction for the clean systems increases, it eventually opens a gap in the density of states. Panel* ***(d)*** *uses a gray scale with darker shades corresponding to stronger disorder. The Mott gap is closed by the presence of disorder at moderate interactions and we observe the insulator-to-metal transition previously identified in correlated disordered systems[2, 3].* ***(e)*** *and* ***(f):*** *Relaxation of the kinetic, potential and total energy when the interaction strength is changed from 0 to U=0.25* ***(e)****, and U=0.75 (f). Note the different comparative behaviors of the energies as a function of time between the two interaction strengths.* ***(g)*** *and* ***(h)****: Momentum distribution function as a function of disorder strengths for weak (U=0.25)* ***(g)*** *and for moderate (U=0.75)* ***(h)*** *interaction strengths. We can observe that the distribution function for weak interaction displays a behavior similar to that of an increasing temperature when the disorder strength is increased (g). The opposite effect occurs for moderate interaction strengths where the distribution function, when the disorder strength is increased, behaves as if the temperature were lowered* ***(h).***

Our solution adapts the combination of the equilibrium dynamical mean field theory (DMFT) and the equilibrium coherent potential approximation (CPA) methods to the nonequilibrium many-body formalism, using the Kadanoff-Baym-Keldysh complex time contour, for the dynamics of interacting disordered systems away from equilibrium. We use our time domain solution to calculate the density of states for an equilibrium disordered interacting system described by the Anderson-Hubbard model. The consistent results with the frequency domain calculation confirm the ability to recover spectral properties without resorting to analytical continuation. The approach is further applied to solve for the nonequilibrium dynamics of an interaction quench in the presence of disorder. Here, while keeping the disorder strength constant, the interaction strength is abruptly changed from one value (non-interacting system) to another constant (finite) value. The system displays different relaxation behaviors as the

disorder strength is tuned for different values of the final interaction strength. We study the Anderson-Hubbard on the infinite dimensional Bethe lattice. The bandwidth for the model is set equal to 1. This is used as the unit of energy and its inverse as the unit of time. The disorder is represented by a random on-site energy V_i at each lattice site i. We examine the case of "box" disorder where the V_i values are uniformly distributed between $-W$ and W. W is referred to as the disorder strength. The system is initially in equilibrium at temperature given by $\beta = 1/T = 40$. The nonequilibrium DMFT+CPA solution is formulated with contour ordered quantities following Ref[4, 5]. The equilibrium density of states for the clean system (Hubbard model) are in agreement with the frequency domain iterative perturbation theory (IPT) results[6] that are known to be accurate.
Similarly, we find agreement between our time domain simulations for the equilibrium Anderson model and the frequency domain CPA results. The nonequilibrium dynamics after the interaction quench shows different effects as a function of disorder strength for different interaction strengths. The approach will be valuable for studies of nonequilibrium properties of correlated systems in the presence of disorder.

References
[1] E. Dohner, H. Terletska, K.-M. Tam, J. Moreno, H. F. Fotso, *arXiv*:2111.11643 (2021).
[2] Z. Wang, et al, *Proceedings of. National Academy of Sciences USA* **115**, 11198 (2018).
[3] E. Lahoud, O. N. Meetei, K. B. Chaska, A. Kanigel, N. Trivedi, *Physical Review Letters* **112**, 206402 (2014).
[4] J. K. Freericks, V. M. Turkowski, V. Zlatic, *Physical Review Letters* **97**, 266408 (2006).
[5] J. K. Freericks, *Physical Review* B **77**, 075109 (2008).
[6] R. Bulla, *Physical Review. Letters* **83**, 136 (1999).

Ultrafast Thermometry with Pump-probe X-ray Photoemission Spectroscopy

A. M. Shvaika[1], O. P. Matveev[1,2], T. P. Devereaux[3], J. K. Freericks[2]
[1] *Institute for Condensed Matter Physics, Lviv, 79000 Ukraine*
[2] *Georgetown University, Washington, DC 20057, USA*
[3] *Stanford University, Stanford, CA 94305, USA*

We present results for time-resolved x-ray photoemission spectra (tr-XPS) for materials that undergo a metal-Mott-insulator transition. In such experiments, an intense light pulse pumps itinerant electrons to higher energies, and time-delayed high-energy x-ray probe pulse is used to emit an electron from a deep core-level state, creating a charged core hole. The itinerant electrons feel the core-hole potential and react by screening it and modifying its spectral function [1]. As an example, we study the Falicov-Kimball model which describes both metallic and Mott-insulator phases, and has an exact solution within nonequilibrium dynamical mean-field theory.

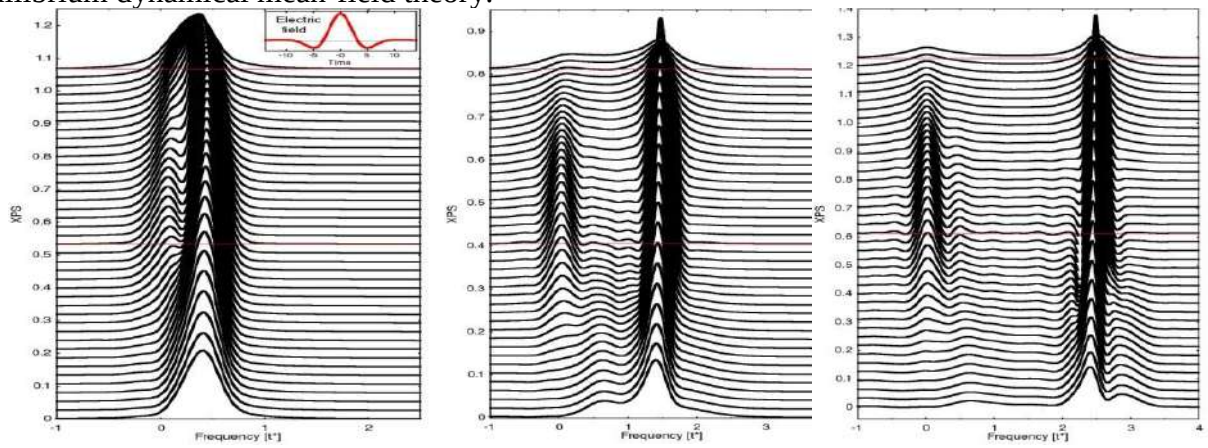

Fig. 1: *tr-XPS spectra for the case of dirty metal (U=1) and different core-hole potentials $Q_d = Q_f = 0.5, 1.5, 2.5$.*

We discuss the time evolution of the tr-XPS, in particular its shape at the Fermi level, and compare it with the tr-PES results [2], which allows us to estimate an effective temperature in the high-temperature regime introducing an ultrafast "thermometer," which can determine the energy content of the conduction electrons with a nondestructive *in situ* measurement on an ultrafast time scale. The obtained core-hole propagators can also be used to introduce the core-hole screening effects in the tr-RIXS spectra [3].

References
[1] N. Pakhira, A. M. Shvaika, J. K. Freericks, *Physical Review* B **99**, 125137 (2019).
[2] O. P. Matveev, A. M. Shvaika, T. P. Devereaux, J. K Freericks, *Physical Review Letters* **122**, 247402 (2019).
[3] Y. Chen, Y. Wang, C. Jia, B. Moritz, A. M. Shvaika, J. K. Freericks, T. P. Devereaux, *Physical Review* B **99**, 104306 (2019).

Ultrafast X-ray Hyperspectral Imaging of the light-induced Phase Transition in VO_2

A. S. Johnson
ICFO – The Institute of Photonic Sciences, 08860 Castelldefels, Spain

Optically driven quantum materials are believed to exhibit complex nanoscale phase dynamics, including domain nucleation, domain wall motion, and the emergence of non-equilibrium phases. Such transient phases are particularly challenging to study as they may have no equilibrium analogue, necessitating ultrafast probes which to date have been spatially integrating [1,2] despite photo-generated domain growth or the generation of topological defects leding to nanoscale inhomogeneity. Here we demonstrate femtosecond time-resolved hyperspectral X-ray nanoscale imaging of the prototypical photoinduced phase transition in vanadium dioxide. Using resonant coherent X-ray imaging [3] at the PAL X-ray free electron laser (Fig. 1), we map the insulator-to-metal transition with 50 nm spatial and 140 fs temporal resolution [4].

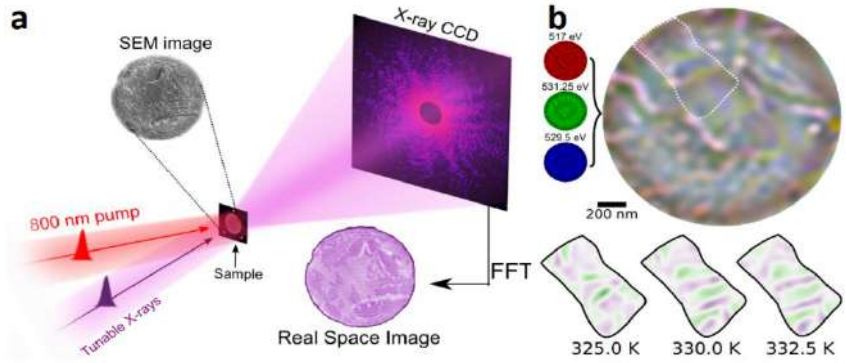

Fig. 1 a.) *Time resolved coherent X-ray imaging of the light-induced phase transition in VO_2.*
b).*Spectroscopic composite image of the initial domain structure showing sensitivity to the nanoscale phase separation.*

We find that the transition proceeds by a prompt, sub-140 fs switching followed by further few-picosecond dynamics across all domains, before the onset of inhomogeneous motion in the first few-hundred picoseconds (Fig 2a). The early time homogeneity suggests a step-like transition to the metallic phase which, due to a volume mismatch between the two phases, launches strain waves into the sample. Few-picosecond relaxation of the out-of-plane direction leads to a long-lived highly-strained transient orthorhombic phase, with a heterogeneous response only emerging after in-plane relaxation several hundred picoseconds later. This interpretation of the dynamics is corroborated by hyperspectral x-ray imaging spectroscopy [5] of the transient phase formed at 20 ps (Fig 2b).

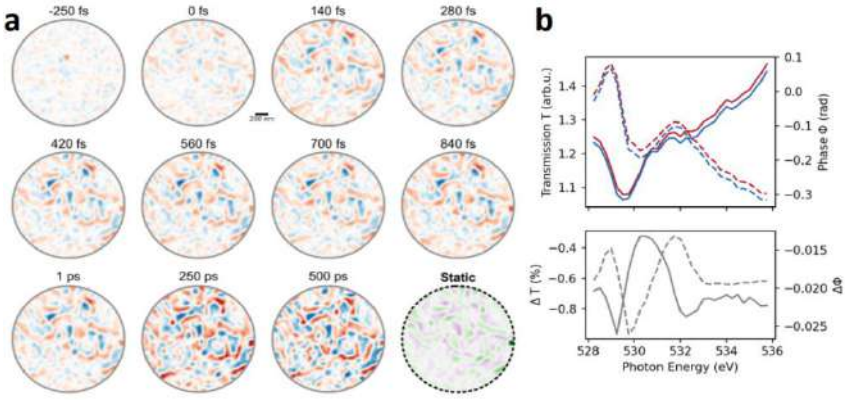

Fig. 2 a). *Time resolved difference images of the domain structure following photoexcitation through the insulator to metal phase transition. All domains switch promptly and show identical dynamics within the first 20 ps, with inhomogenous response only emerging after hundreds ps.*
b).*X-ray spectroscopy of regions beginning metallic* ***(red)*** *and switching to metallic* ***(blue).***

Our results demonstrate the necessity of true spatially, temporally, and spectrally resolved measurements for understanding the complex dynamics inside quantum materials, and pave the way for full characterization of ultrafast nanoscale dynamics in such systems.

References

[1] L. Vidas et al., *Physical Review X*, **10**, 031047 (2020).
[2] M.R. Otto et al., *Proceedings of the National Academy of Sciences of the United States of America* **116**, 450 (2019).
[3] L. Vidas *et al*., *Nano Letters* **18**, 3449(2018).
[4] A.S. Johnson et al., *arXiv*:2202.08585.
[5] A.S. Johnson *et al., Science Advances* **7**, eabf1386 (2021).

Pump-Probe Spectroscopy of Collective Modes

M. Udina[1], F. Gabriele[1], T. Cea[2], G. Seibold[3], C. Castellani[1], L. Benfatto[1]
[1] "Sapienza" University of Rome, 00185 Rome, Italy
[2] IMDEA Nanoscience, 28049 Madrid, Spain
[3] Institut für Physik, 03013 Cottbus, Germany

The latest advances in time-resolved spectroscopic techniques, based on the generation of intense ultra-short THz pulses, have paved new intriguing ways for the investigation of collective phenomena in many complex systems. As an example, recent experiments [1,2] showed the possibility to selectively excite electronic collective modes in superconductors, which lead to well-defined oscillation in the measured signal that strongly resemble the coherent excitation of Raman-active phonons in insulating and metallic compounds [3]. Despite the great interest and the huge experimental progress, a clear theoretical paradigm for the description of these experiments is still lacking. In this talk I will present a general scheme we recently developed [4] to describe step-by-step the processes behind the pump-probe detection of collective excitations, that can be equally well applied to ordinary phonons as well as to electronic excitation (Fig. 1).

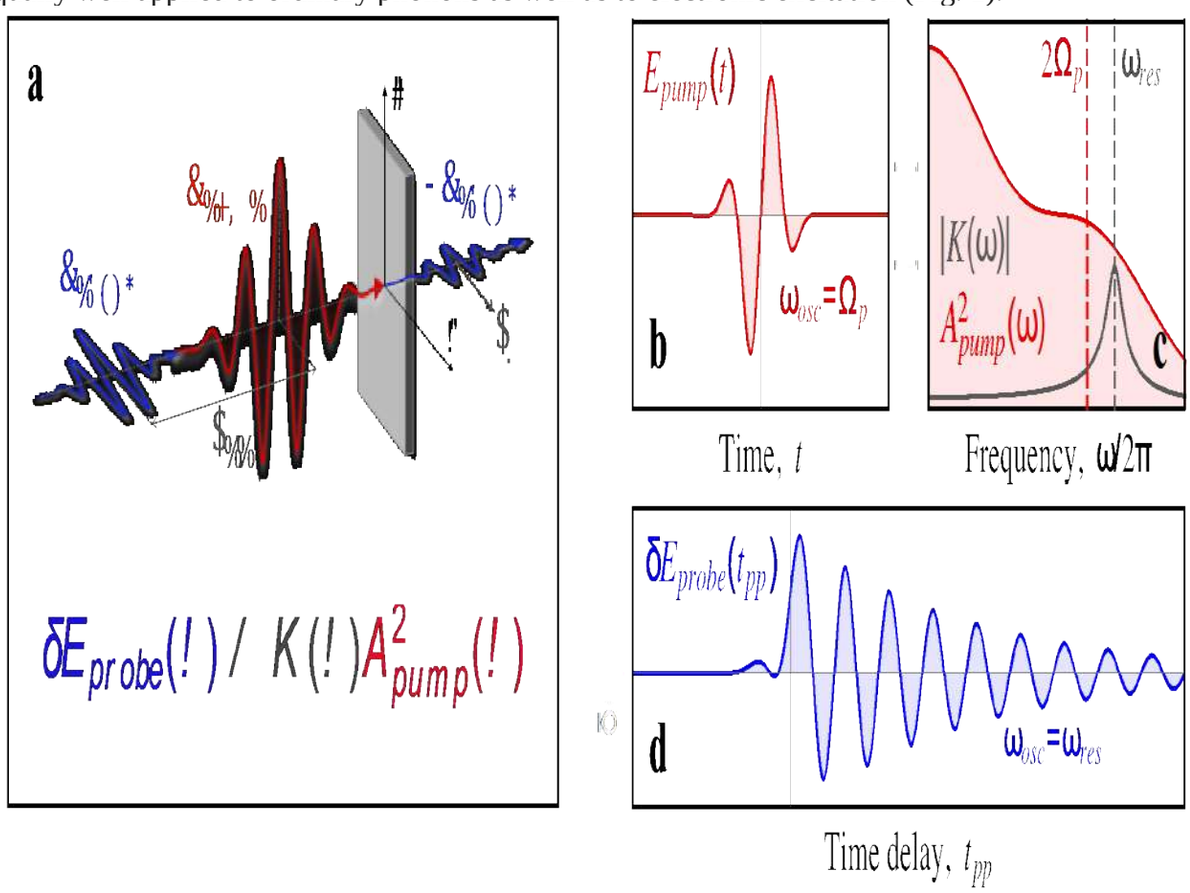

Fig. 1 (a) *Schematics of the experimental setup: an intense pump pulse* $\boldsymbol{E_{pump}}$ *hits the sample, variations in the transmitted (reflected) component of the probe field* $\boldsymbol{E_{probe}}$ *are measured as a function of the time delay* t_{pp} *between the two pulses at fixed observation time* $\boldsymbol{t_n}$*. The measured quantity* $\boldsymbol{\delta E_{probe}}$ *can be related to the product in the frequency domain between the Fourier transform of* $\boldsymbol{A_{pump}(t)}$ *squared, where* $\boldsymbol{E=-dA/dt}$*, and a Raman-like tensor* $\boldsymbol{K}$*, computed microscopically. As an example, for a broad-band (mono-cycle) THz pump* ***(b)****,* $\boldsymbol{A^2_{pump}(\omega)}$ *is a flat function in the frequency domain. If the nonlinear kernel* $\boldsymbol{K(\omega)}$ *has a well-defined divergence at* ω_{res} ***(c)****, associated e.g. with a Raman-active phonon, the measured quantity* $\delta E_{probe}(t_{pp})$ *is expected to oscillate at the frequency* $\omega_{osc}=\omega_{res}$ ***(d)****, reflecting the collective mode excitation.*

I will then discuss a direct application of our interpretative scheme to the light-induced excitation of superconducting collective modes, with applications ranging from low-energy plasma waves in cuprates [5] to the so-called Higgs (amplitude) mode in BCS superconductors, addressing the issue of its visibility both in the clean case as well as in the presence of disorder [6,7].

References

[1] R. Matsunaga, et al., *Physical Review Letters* **111**, 057002 (2013).
[2] F. Giorgianni, et al., *Nature Physics* **15**, 341 (2019).
[3] S. Maehrlein et al., *Physical Review Letters* **119**, 127402 (2017).
[4] M. Udina, T. Cea, L. Benfatto, *Physical Review* B **100**, 165131 (2019).
[5] F. Gabriele, M. Udina, L. Benfatto, *preprint* (2020).
[6] T. Cea, C. Castellani, L. Benfatto, *Physical Review* B **93**, 180507(R) (2016).
[7] G. Seibold, M. Udina, L. Benfatto, C. Castellani, *preprint* (2020).

Multimodal Studies of Photoinduced Metastable Phases: from THz to X-rays

S. W. Teitlebaum[1], J. Zhang[2], B. K. Ofori-Okai[3], V. Stoica[4], G. Zhang[5], G. De La Pena[3], Y.-H. Cheng[6]
M. Trigo[3], K. A. Nelson[6], F. Zhang[7], WB Wu[7], R. D. Averitt[5]
[1] *Arizona State University, Tempe, AZ85287, USA*
[2] *Hong Kong University of Science and Technology, Hong Kong, China*
[3] *SLAC National Accelerator Laboratory, Menlo Park, CA94025, USA*
[4] *Pennsylvania State University, University Park, PA 16802, USA*
[5] *University of California San Diego, La Jolla, CA 92093, USA*
[6] *Massachusetts Institute of Technology, Cambridge, MA02139, USA*
[7] *Hefei Institute of Physical Sciences, Hefei 230031, China*

Transition metal oxides offer a playground for condensed matter physics, where coupled lattice, orbital, and spin degrees of freedom exist on similar energy scales, resulting in a rich phase diagram, and susceptibility to external perturbation [1,2]. The interplay between these degrees of freedom results in competing metastable states that are nearly degenerate in energy. As one example, films of the perovskite manganite $La_{0.67}Ca_{0.33}MnO_3$ on $NdGaO_3$ (LCMO on NGO) form an insulating, antiferromagnetic charge-ordered state as strained thin films, while this material is ferromagnetic in bulk. These films can be driven to a metastable metallic phase by high fluence femtosecond laser excitation when cooled below 100 K [3,4]. Revealing the timescale of the evolution of intertwined electronic, magnetic, and structural order requires a concerted approach with multiple probes of each order. Experiments using optical, THz, and hard x-ray probes monitor the evolution of charge, orbital, structural and magnetic order throughout this phase transition. These experiments reveal how short-range structural distortions evolve after photoexcitation, and how structural distortions couple to ferromagnetism to stabilize the persistent ferromagnetic phase. Single-shot optical studies and time-resolved x-ray experiments reveal that charge order and structure (i.e. Jahn-teller distortions) are intertwined on ultrashort timescales. Conversely, the formation of the metastable conducing state occurs only after hundreds of picoseconds [5], as measured by single-shot THz spectroscopy. Time-resolved X-ray experiments conducted at LCLS are well-modeled at early times by the evolution of a time-dependent order parameter coupled to a cation mode (Fig. 1), but the switching dynamics at late times are described by complex stretched exponential dynamics characteristic of domain formation and a separation of length scales. In addition, we observe anomalously long photoinduced suppression of the structural order and persistent photoinduced broadening of the structural peak at higher temperatures, indicative of glassy charge-order dynamics above the magnetoelastic coupling temperature [6].

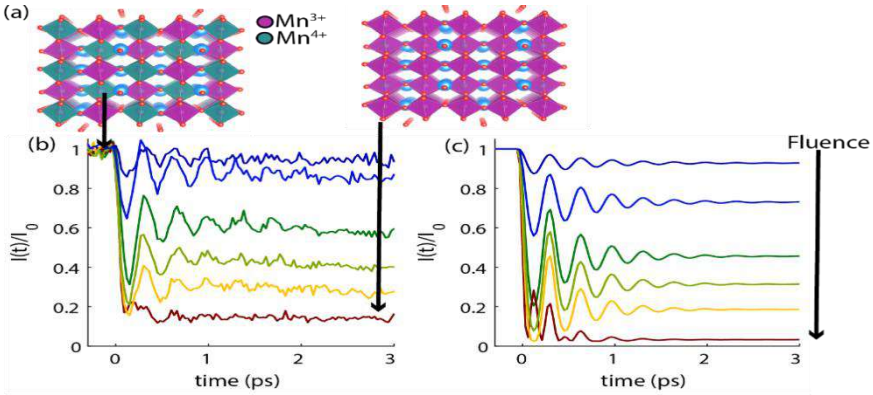

Fig, 1 (a). *Schematic structure of the monoclinic, charge-ordered* ***(left)*** *and metallic, orthorhombic* ***(right)*** *structures of strained LCMO* ***(b)*** *Time-resolved X-ray diffraction on the structural monoclinic peak, showing photoinduced suppression of the monoclinic phase.* ***(c)****Time-domain Ginzburg-Landau model of the suppression of structural order in a strained manganite.*

These effects demonstrate the key role nanoscale inhomogeneities play in the stabilization of metastable light-induced order, and the role that experiments spanning many decades of length and timescales with access to different degrees of freedom play in understanding how materials navigate complex energy landscapes.

References

[1] Y. Tokura, *Journal of the Physical Society of Japan* **75**, 1 (2006).
[2] Y. Tokura, *Reports on Progress in Physics* **69**, 797 (2006).
[3] J. Zhang, et al, *Nature Materials* **15**, 956 (2016).
[4] A. S. McLeod, et al, *Nature Materials* **19**, 397 (2020).
[5] S. W. Teitelbaum, et al, *Physical Review Letters* **123**, 267201 (2019).
[6] S. Y. Zhou, et al, *Scientific Reports* **4**, 4050 (2015).

Modelling of the Ultrafast Dynamics following irradiation of Solids with Mid-infrared Femtosecond Laser Pulses

G. D. Tsibidis [1], E. Stratakis [1,2]
[1] *Institute of Electronic Structure and Laser -FORTH, 70013 Heraklion, Greece*
[2] *University of Crete, 71003 Heraklion, Greece*

Irradiation of solids with ultrashort pulses in the mid-Infrared (mid-IR) spectral region is a yet unexplored field while it can set the basis for the development of new tools for non-linear optics and photonics for a large range of applications. We present a theoretical investigation of the yet unexplored ultrafast processes and dynamics of the produced excited carriers upon irradiation of Silicon with femtosecond pulsed lasers in the mid-IR spectral region. The role of induced Kerr effect is highlighted and it manifests a more pronounced influence at smaller wavelengths in the mid-IR range. A systematic analysis of the Surface plasmon (SP) dispersion relation for mid-IR and comparison with results upon excitation with λ_L=800 nm revealed that irradiation in the mid-IR region yielded SP that are weakly confined on the surface, exhibit longer lifetimes, and propagate on larger areas (Fig.1). These features can be potentially exploited to promote mid-IR-based technology to produce sensors, detectors or to present new capabilities in laser-based manufacturing.

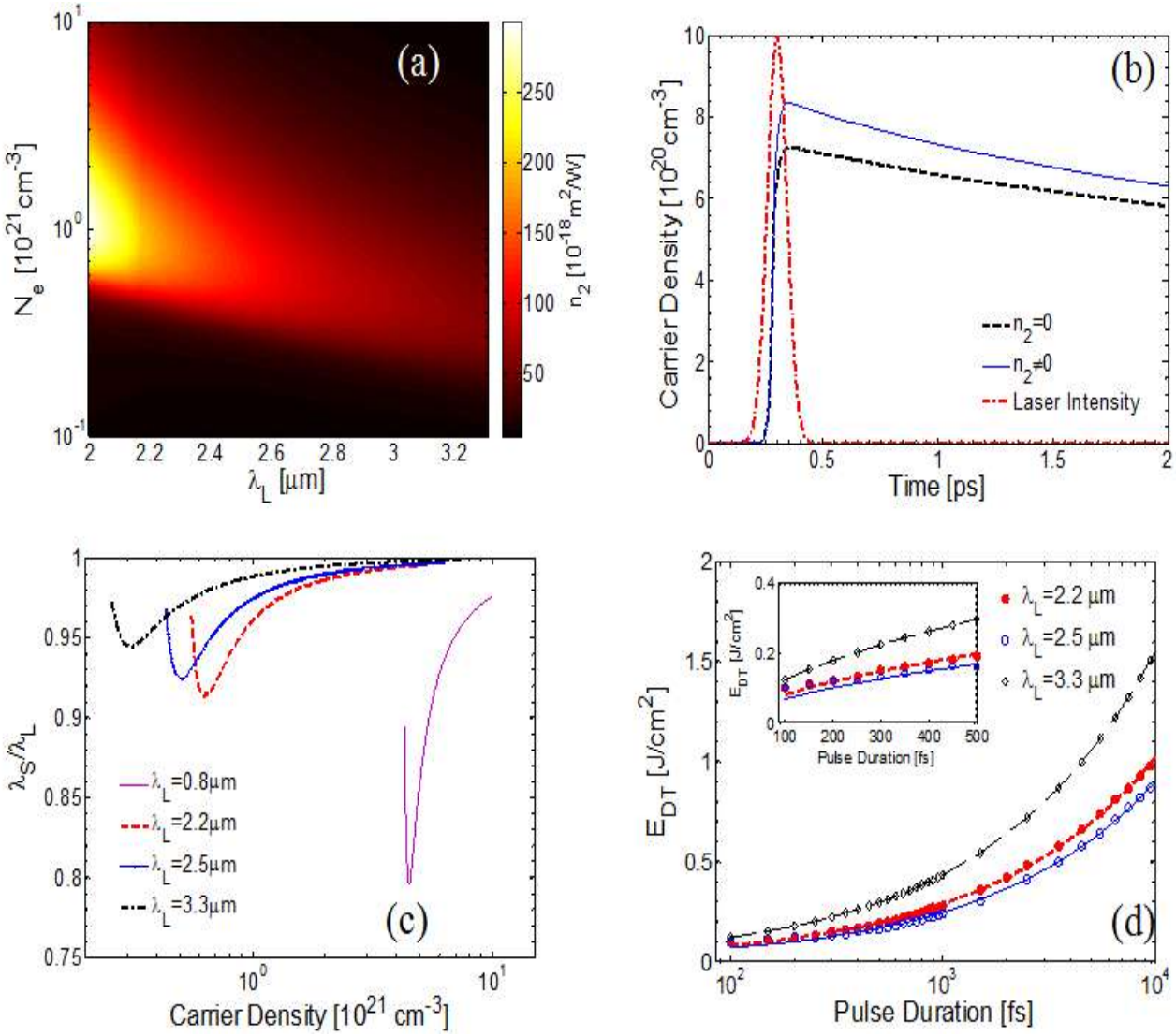

***Fig. 1**: **(a)** Carrier density vs laser wavelength, **(b)** Evolution oof carrier density, **(iii)** SP wavelength vs carrier density, **(iv)** Damage threshold vs pulse duration.*

A similar analysis has been performed to describe ultraafst dynamics folllowing irradiation of fused silica (SiO_2) with mid-IR femtosecond pulses pulses. One type of material, which is of paramount importance to the design of optics in high power laser systems, is fused silica (SiO_2). In this work, laser driven physical phenomena associated with processes following irradiation with ultrashort laser pulses in the mid-IR region, such as photoionization processes, electron excitation, and quantification of excitation levels are investigated in detail (Fig. 2). A multiscale modelling approach is performed that correlates conditions for formation of perpendicular (not previously explored in dielectrics) or parallel to the laser polarisation low spatial frequency periodic surface structures for low and high intensity mid-IR pulses, respectively.

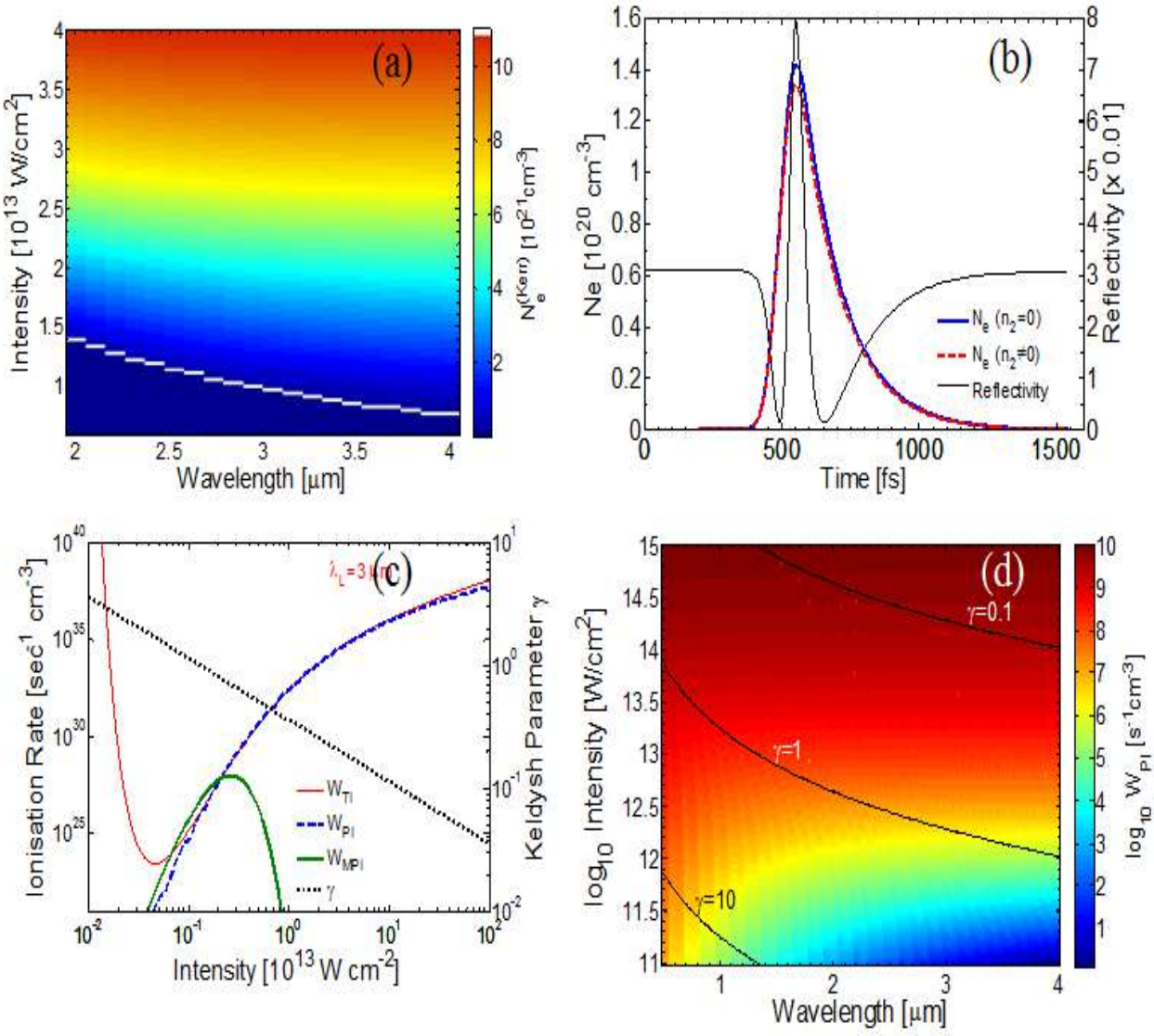

Fig. 2. ***(a)*** *Carrier density vs Laser Intensity,* ***(b)*** *Evolution oof carrier density,* ***(iii)*** *Ionisation rates vs laser intensity,* ***(iv)*** *Photoionisation rate vs laser wavelength.*

Results demonstrate a remarkable domination of tunnelling effects in the photoionization rates and a strong impact of avalanche ionization for long laser wavelengths. The methodology presented in this work is aimed to shed light on the fundamental mechanisms in a previously unexplored spectral area and allow a systematic novel surface engineering with strong mid-IR fields for advanced industrial laser applications.

References

[1] E. Petrakakis, G.D. Tsibidis, E. Stratakis, *Physical Review B* **99,** 195201 (2019).
[2] G.D. Tsibidis, E Stratakis, *Scientific Reports* **10,** 8675 (2020).

Spin and Orbitals

Inducing Quantum Disorder in a Kitaev Material

P. H.M. van Loosdrecht
University of Cologne, 50937 Cologne, Germany

One way to characterize quantum spin-liquids is through the fractionalization of spin excitations. A prime example of this is found in the exactly solvable Kitaev model of spin-1/2 moments with anisotropic exchange interactions on a tri-coordinated lattice [1]. To find examples of this kind of physics in nature turns out to be challenging. The currently best known examples of materials in which Kitaev-like physics plays a central role are the layered spin-orbit entangled J=1/2 systems Na_2IrO_3, α-Li_2IrO_3, and α-$RuCl_3$. However, these materials all possess additional interactions, which, among other, lead to a magnetically ordered state at low temperature preventing the formation of a pure Kitaev spin-liquid (KSL) state. Apart from the ongoing quest for materials showing a true KSL ground state, one can also destabilize the magnetic order in the existing materials, which potentially can induce the sought after KSL state. In this contribution I will discuss two methods to destabilize magnetic order in α-$RuCl_3$. The first one is through the application of an in-plane magnetic field. Though it has been shown by various authors that this indeed leads to suppression of the ordered state in α-$RuCl_3$, the nature of the field-induced state is not fully clear. The most intriguing suggestion comes from heat transport experiments showing the existence of a quantized thermal Hall conductivity [2] just above the critical field, which is a Hallmark of a KSL. Our spectroscopic Raman and THz experiments do not show evidence for a field induced Kitaev spin-liquid state, but rather, combined with exact diagonalization results, show the existence of a quantum disordered partially aligned high field phase characterized by a gapped continuum of magnetic excitations combined with single particle and bound state resonances. The second approach is a pump-probe method which creates holon and doublon excitations. These excitations are found to couple efficiently to magnetic excitations which in turn disorder the magnetically ordered state.

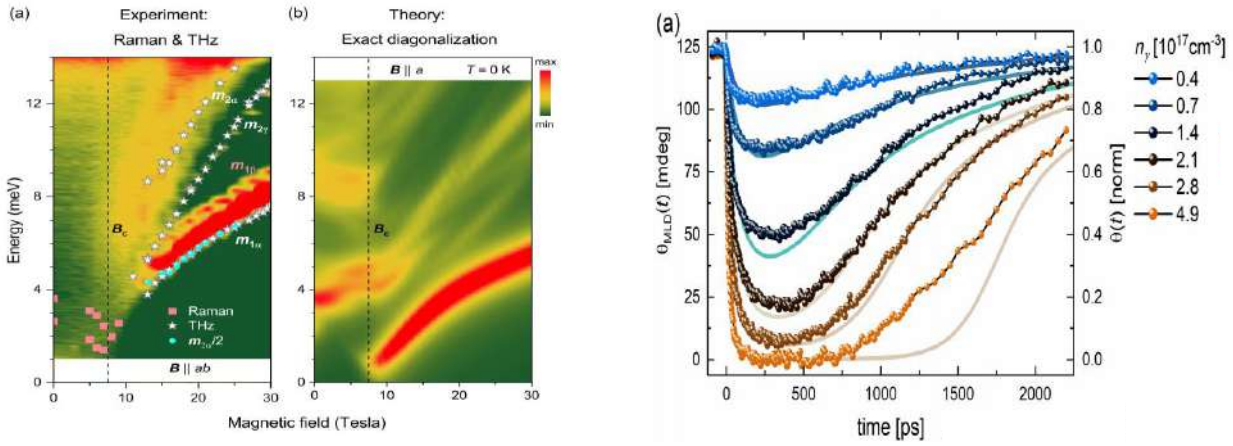

Fig. 1. *α-RuCl3* ***Left*** *Field dependent Raman spectra (with superimposed the position of sharp THz resonances) in false colour representation showing the opening of an excitation gap above 7T and the presence of single particle and bound state resonances. The right panel shows an exact diagonalization calculation of the field dependent Raman result [3].*
Right *pump-probe transients tracking the antiferromagnetic order parameter through magnetic linear dichroism after the creation of doublon-holon excitations. Above a doublon (holon) density of* 4.5×10^{17} cm^{-3} *the antiferromagnetic order is fully suppressed for a few hundred ps [4]*

.

For sufficiently high excitation densities the magnetic order is fully suppressed, leading to a quantum disordered magnetic state.

References

[1] A. Kitaev. *Annals of Physics* **321**. 2 (2006).
[2] Y. Kasahara, et al., *Nature* **559**, 227 (2018).
[3] A. Sahasrabudhe, et al., *arXiv*:1908.11617 (2019).
[4] R.B. Versteeg, et al., (unpublished, 2020)

Photoinduced Ultrafast Spin Dynamics in 2D Magnets and van der Walls Heterostructures

J. He[1,2], T. Frauenheim[2],
[1] *Charles University, Prague 12843, Czechia*
[2]*University of Bremen, Bremen 28359, Germany*

Two-dimensional (2D) magnets and van der Walls (vdW) heterostructures open unprecedented opportunities for discovering emergent phenomena and implementing device structures in all-2D spintronics. Although light is the fastest means to manipulate the magnetism, interfacial spininjection and magnetic proximity related quantum properties of 2D magnetic materials and vdW heterostructures, its potential remains mostly untapped. Using real-time density functional theory (rt-TDDFT) with non-collinear spin, we show demonstrate that laser pulses can directly induce ultrafast spin selective charge transfer between magnetic sublattices in a few femtoseconds and further generate dramatic changes in the magnetic structure of ferrimagnetic (FiM) MXenes, including a transition from FiM to transient ferromagnetism (FM).[1] On the other hand, using rt-TDDFT, we studied photoinduced interlayer spin transfer dynamics in 2D nonmagnetic-ferromagnetic (NM-FM) vdW heterostructures, including graphene-like materials interfaced Fe_3GeTe_2, $MoSe_2$ interfaced with ferromagnetic $MnSe_2$. We observed that laser pulses induce significant large spin injection from ferromagnetic layers to nonmagnetic (NM) layers within a few femtoseconds. [2,3]

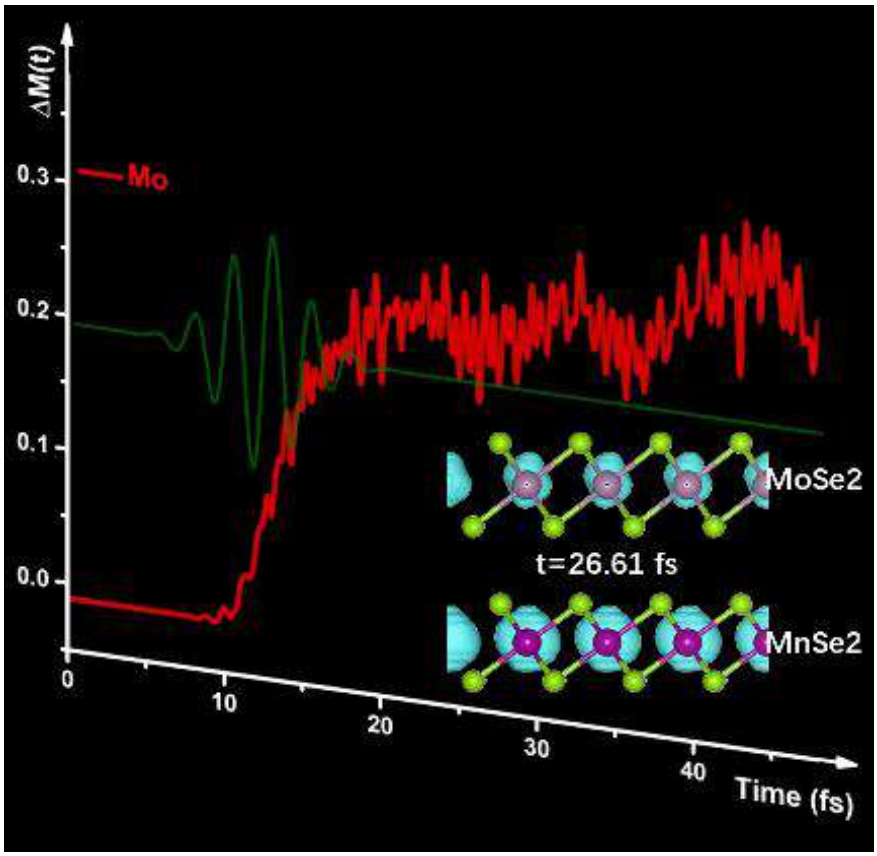

Fig.1: *Photoinduced ferromagnetic state in 2D $MoSe_2$ monolayer on $MnSe_2$ interface.*

The microscopic mechanism behind this ultrafast spin transfer in 2D magnets is governed by the optically induced intersite spin transfer (OISTR) effect. Our results provide the microscopic understanding for optically control intralayer and interlayer spin dynamics in 2D magnets and vdW heterostructures

References

[1] J. He, T. Frauenheim, *Journal of Physical Chemistry Letters* **11,** 6219 (2020).
[2] J. He, S. Li, A. Bandyopadhyay, T. Frauenheim, *Nano Letters* 21, 3237 (2021).
[3] J. He, S. Li, L. Zhou, T. Frauenheim, *Journal of Physical Chemistry Letters* **13**, 2765 (2022).

Spin Current Dynamics in Ferromagnetic/Non-Magnetic Bilayers Probed with GHz- and THz-Spectroscopy

E. Papaioannou
Martin-Luther University, 06120 Halle, Germany

Ultrafast spin-to-charge conversion in heterostructures composed of ferromagnetic (FM)/non-magnetic (NM) thin films can give rise to emission of THz electromagnetic waves [1,2]. The experimental scheme of the so-called field of THz spintronics involves the use of femtosecond (fs) laser pulses to trigger ultrafast spin and charge current dynamics in FM/NM bilayers, where the NM layer features a strong spin-orbit coupling [3], (Fig.1). The technological and scientific key-challenges of THz spintronic emitters are to increase their intensity and to shape the frequency bandwidth by controlling the source of the radiation, namely the transport of the ultrafast spin- and charge current [4-6]. In this presentation, I will address the transport properties of the spin currents and the subsequent THz emission at modified interfaces and nanostructures. The different factors that define the strength of the THz emission like the spin Hall angle, spin diffusion length, conductivity, interface transmission will be quantified and correlated with combined THz and GHz spectroscopic measurements. The physical mechanisms that give rise to the proportionality of GHz measured spin mixing conductance and THz emission will be discussed in samples in the form FM/X/NM where X= FePt, MgO, Au, Cu.It will be shown that the dusting of the FM/NM with a heavy metal like Au or with an insulator like MgO changes drastically the THz emission. Surprisingly the modification of the interface by inserting an alloy increases significantly the THz radiation. At specific growth conditions, an ordered $L1_0$-FePt interlayer appears at the Fe/Pt interface. The Fe/$L1_0$-FePt/Pt trilayer amplifies the THz emission by almost a factor of two compared to Fe/Pt bilayers [7], (Fig.1). This enhancement is correlated to the interface transmission which is probed with GHz spectroscopy and it accounts for the spin current transmission probability at the FM/NM interface.

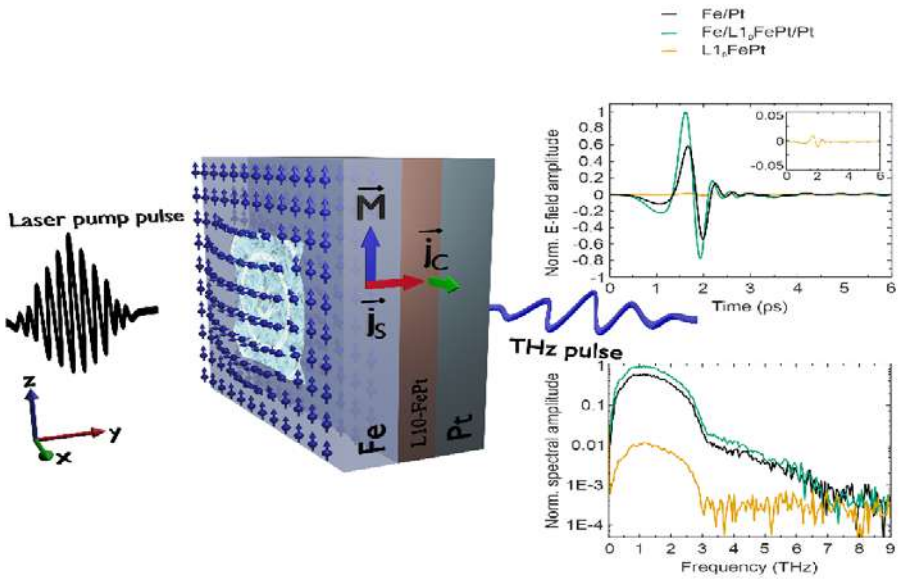

Fig. 1. ***(Left image)*** *Illustration of THz emission from spintronic emitters after fs-laser excitation.*
(Right image) *Comparison of THz emission of Fe/Pt bilayers with modified interface layers as indicated.*

The unique findings of the increased THz emission by alloying/modifying the interface opens new perspectives in the direction of application of spintronic THz emitters and can further stipulate theoretical and experimental studies.

References

[1] D. Yang et al, *Advanced Optical Materials* **4**, 12, 1944 (2016).
[2] T. Seifert et al, *Nature Photonics* **10**, 483 (2016).
[3] E. T. Papaioannou, R. Beigang, *Nanophotonics* **10**, 4, 1243 (2021).
[4]] G. Torosyan et al., *Scientific Reports* **8**, 1311 (2018).
[5] D. Nenno et al., *Scientific Reports* **9**, 13348 (2019).
[6] E. T. Papaioannou et al., *IEEE Transactions on Magnetics* **54**, 1 (2018).
[7] L. Scheuer et al., accepted in *iScience*, http://arxiv.org/abs/2204.00704, (2022).

Coherent Spin-wave Transport in an Antiferromagnet

D. Afanasiev[1], J.R. Hortensius[2], M. Matthiessen[2], R. Leenders[3], R. Citro[4], A. V. Kimel[1]
R.V. Mikhaylovskiy [3], B. A. Ivanov[5], A. D. Caviglia[1],
[1] *Radboud University,6525 Nijmegen, The Netherlands*
[2] *Technical University Deflt, 2628 CD Delft, The Netherlands*
[3] *Lancaster University, Lancaster LA1 4YW, UK*
[4] *Università di Salerno, 84084 Fisciano, Italy*
[5] *Institute of Magnetism, 03142 Kyiv, Ukraine*

Magnonics is a research field complementary to spintronics, in which quanta of spin waves (magnons) replace electrons as information carriers, promising lower dissipation [1,2]. The development of ultrafast nanoscale magnonic logic circuits calls for new tools and materials to generate coherent spin waves with frequencies as high, and wavelengths as short, as possible [3]. Antiferromagnets can host spin waves at terahertz (THz) frequencies and are therefore seen as a future platform for the fastest and the least dissipative transfer of information [4]. However, the generation of short-wavelength coherent propagating magnons in antiferromagnets has so far remained elusive. We report the efficient emission and detection of a nanometer-scale wavepacket of coherent propagating magnons in antiferromagnetic $DyFeO_3$ using ultrashort pulses of light [5]. The subwavelength confinement of the laser field due to large absorption creates a strongly non-uniform spin excitation profile, enabling the propagation of a broadband continuum of coherent THz spin waves (see Fig. 1). The wavepacket features magnons with detected wavelengths down to 125 nm that propagate with supersonic velocities V_0 of more than 13 km/s into the material.

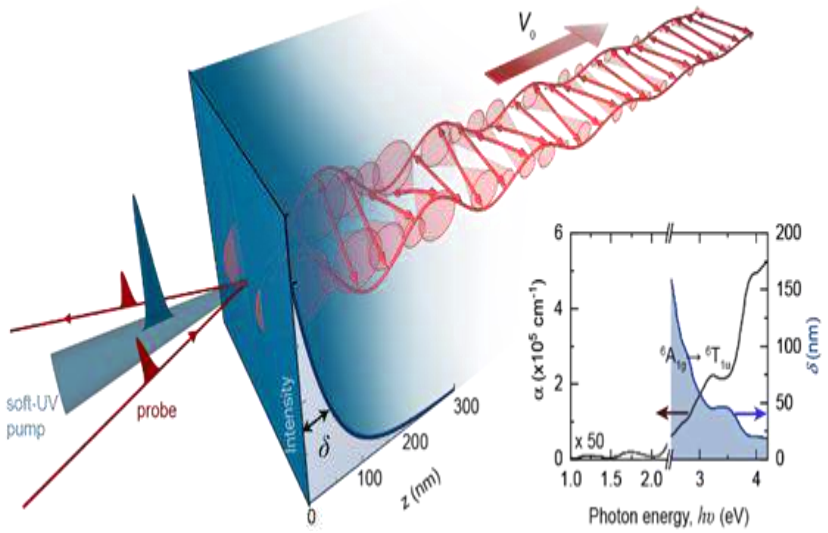

Fig.1. *Schematic of the generation of propagating AFM spin waves after above bandgap soft-UV photoexcitation. The optical penetration depth* ***δ*** *defines the excited region.*
Inset: *absorption coefficient* ***α*** ***(left axis)*** *and corresponding penetration depth* ***δ*** ***(right axis)*** *for the AFM* $DyFeO_3$ *as a function of photon energy.*

This long-sought source of coherent short-wavelength spin carriers opens up new prospects for THz antiferromagnetic magnonics and nanoscale coherence-mediated logic devices at THz frequencies.

References
[1] V.V. Kruglyak et al, *Journal of Physics D* **43,** 264001 (2010).
[2] B. Lenk et al, *Physics Reports* **507,** 107 (2011).
[3] A.V. Chumak et al, *Nature Physics* **11,** 453 (2015).
[4] T. Jungwirth et al, *Nature Nanotechnology* **11,** 231 (2016).
[5] J.R. Hortensius et al, *Nature Physics* **17,** 1001 (2021).

Extracting perfect Quantum Entangled Graph States from Imperfect 'Weighted' Graphs

R. Frantzeskakis[1], C. Liu[2], Z. Raissi[2], E. Barnes[2], S. Economou[2]
[1]*University of Crete, Heracleon 71003, Greece*
Virginia Tech, Blacksburg, VA 24061, USA

Photonic graph states serve as the central resource for important applications in quantum information science. Photon-emitter entangling gates based, e.g., on laser excitation and spontaneous emission are promising for creating these states. This approach sidesteps many of the difficulties associated with intrinsically probabilistic methods based on linear optics. However, the efficient creation of high-fidelity graph states of many photons remains an outstanding challenge due to both coherent and incoherent errors during the generation process. We propose an entanglement concentration protocol that can generate perfect GHZ states (which is a specific class of graph states) using only local gates and measurements on imperfect weighted graph states. We show that our protocol is both efficient and robust to incoherent noise errors.

The creation of nearly perfect photonic entangled states is demanding. One approach lies in the use of two-qubit measurements to probabilistically fuse smaller entangled states to create larger ones. On the other hand, a deterministic approach uses a nearly perfect photon emission in a spin-photon interface experiment to generate perfect entangling gates between the photons which may be technologically challenging. In our case, taking advantage of the nonlinearity induced by strongly coupled cavity-QED systems [1,2], a photon-photon controlled-phase (CZ) gate can be achieved between two incoming photons scattered by the cavity-QED system. However, the phase angle on photonic qubits induced by the nonlinearity from the cavity-QED system is not yet fully controllable [3-5]. CP gates are not maximally entangling gates when the phase is not π. When the CZ gates in the graph state generation procedure are replaced by CP gates, the resulting state is called a weighted graph state [6-8]. This then leads to the question of whether or not such states are still useful; in particular, is it possible to efficiently concentrate their entanglement [9,10] to obtain high-fidelity graph states?

In this talk, we propose an entanglement concentration protocol using local measurements to create highly entangled states. We present the detailed steps of the protocol to generate a perfect photonic GHZ state (Figure 1*)*.

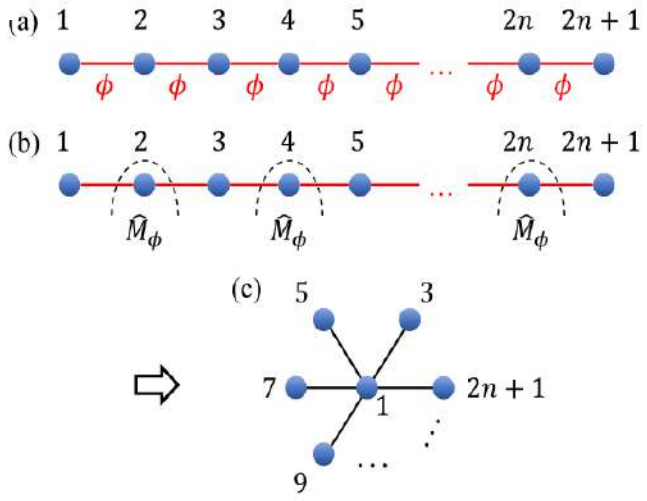

Fig. 1*: Sketch of entanglement concentration protocol for GHZ states*

Ideally, our entanglement protocol can extract GHZ states of any number of qubits. However, we may face additional errors that can affect our system in experiments. For ease of comparison, we focus on the case of the 3-qubit weighted graph state. We assume an additional coherent error in CP gates between neighboring qubits. We study how this two-qubit error affects our entanglement concentration after the middle qubit measurement on an optimized basis. We quantify the entanglement through concurrence after the middle-qubit measurement *(*Figure 2*)*.

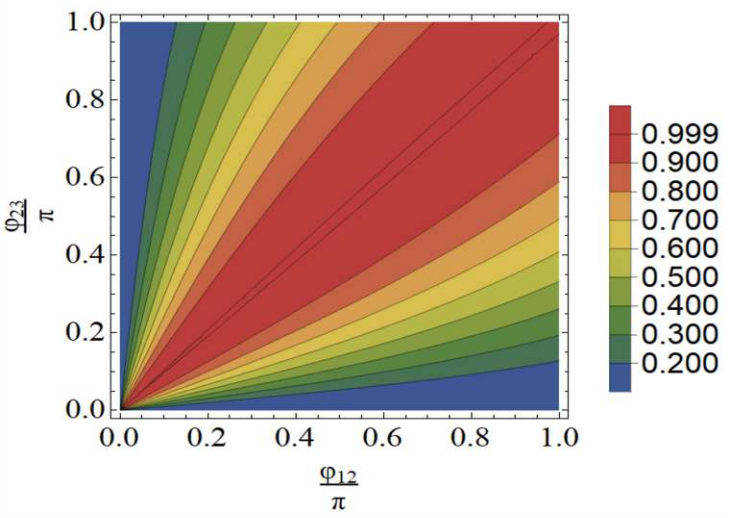

Fig. 2*: Concurrence for 3-qubit weighted graph state with different CP gates after middle qubit measurement.*

Finally, single-qubit errors are more than likely to occur. We study how a depolarizing channel in each photon can affect the entanglement concentration after the middle qubit measurement in the case of a 3-qubit weighted graph state. We calculated how much entanglement is concentrated after the local measurement in the presence of single-qubit depolarizing errors compared to the case of a two-qubit weighted graph state with depolarized photons *(*Figure 3*)*.

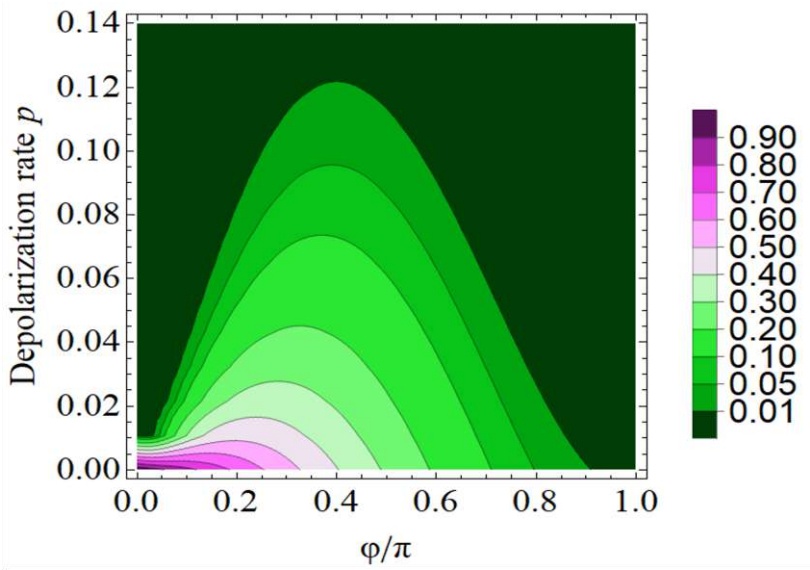

Fig.3*. Entanglement comparison with and w/o local measurement in the presence of depolarizing error*.

The measurement process and the initial structure of the imperfect weighted graph state affects the desired final entanglement concentrated structure. The protocol is focused on generating highly photonic entangled states with local photon measurements. This may open the road for the creation of perfect photon-photon interactions and generating complex photonic graph states. More information can be found in our recent arXiv preprint [11].

References

[1] L.-M. Duan, H. J. Kimble, *Physical Review Letters* **92**, 127902 (2004).
[2] A. Nysteen, D. PS McCutcheon, M. Heuck, J. Mørk, D. R Englund, *Physical Review* A **95**, 062304 (2017).
[3] H.Kim, R. Bose, T. C Shen, G. S Solomon, E. Waks, *Nature Photonics* **7**, 373 (2013).
[4] S. Sun, H. Kim, G. S. Solomon, E. Waks, *Nature Nanotechnology* **11**, 539 (2016).
[5] S. Sun, H. Kim, Z. Luo, G. S.Solomon, E. Waks, *Science* **361**, 57 (2018).
[6] L. Hartmann, J Calsamiglia, W Dur, HJ Briegel, *Journal of Physics* B **40**, S1 (2007).
[7] A D. K Plato, O.C Dahlsten,M. B Plenio, *Physical Review* A **78**, 042332 (2008).
[8] J. Ru Hu, Q. Lin, *The European Physical Journal* D **70**, 1 (2016).
[9] C. H Bennett, H. J Bernstein, S.Popescu, B. Schumacher, *Physical Review* A **53**, 2046 (1996).
[10] Z. Zhao, T. Yang, Y.-A. Chen, A.-N. Zhang,J.-W. Pan, *Physical Review Letters* **90,** 207901 (2003).
[11] R. Frantzeskakis, C.Liu, Z.Raissi, E. Barnes, S. *arXiv :* **2203.07210** (2022).

Quantum Control in the Era of Quantum Computing

A. B. Magann[1], M. D. Grace[3], H. A. Rabitz[2], M. Sarovar[3]
[1] *Sandia National Laboratories, Albuquerque, NM 87123, USA*
[2]*Princeton University, Princeton, NJ 08544, USA*
[3]*Sandia National Laboratories, Livermore, CA 94550, USA*

Laser fields tailored to interact with quantum systems on their natural, ultrafast time scales can provide an unprecedented degree of control over their dynamics. A longstanding dream has been to leverage these control capabilities towards high-value applications spanning physics, chemistry, materials science, and biology [1-3]. However, the pursuit of these goals continues to be challenged by the prohibitive cost of quantum dynamics simulations, which are needed to support and inform quantum control advances in the laboratory.

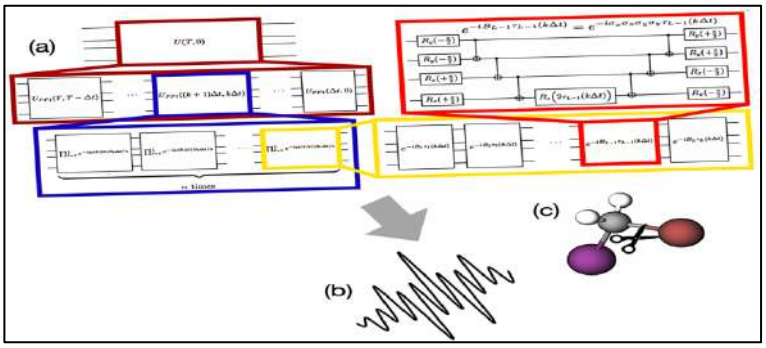

Fig. 1*: Quantum computers can be used to design quantum optimal control pulses. To this end,* ***(a)*** *shows a decomposition of a quantum circuit (adapted from [4]) for efficiently simulating the dynamics of a quantum system that is driven by an external laser field using a quantum computer. Then, by using a classical computer to optimize over the shape of the laser pulse, we obtain a hybrid quantum-classical algorithm for identifying* ***(b)*** *an optimally-shaped pulse for achieving a target transformation, such as the breakage of a selected chemical bond, as shown in* ***(c)****.*

Nevertheless, the future is bright. In this talk, I will discuss how quantum computing can alleviate these computational challenges and enable us to explore the principles and possibilities of quantum control in a scalable manner. To this end, I will introduce a hybrid quantum-classical algorithm that leverages quantum computing to facilitate simulation studies of quantum control [4]. I will outline the associated costs, discuss different application areas, and consider the feasibility of its implementation on quantum computing devices available today.

References

[1] C. Brif, R. Chakrabarti, H. Rabitz, *New Journal of Physics* **12**, 075008 (2010)
[2] S. J. Glaser, et. al., *The European Physical Journal D* **69**, 279 (2015)
[3] D. Keefer, R. de Vivie-Riedle, *Accounts of Chemical Research* **51**, 2279 (2018
[4] A. B. Magann, M. D. Grace, H. A. Rabitz, M. Sarovar, *Physical Review Research* **3**, 023165 (2021)
Sandia National Labs is managed and operated by NTESS under DOE NNSA contract DENA0003525. SAND2022-5541 A.

Speeding up Quantum Dynamics through Parametric Controls

C. Arenz
Arizona State University, Tempe, AZ 85287, USA

Speeding up the dynamics of quantum systems through external controls is of paramount importance for quantum technologies. However, for systems with finitely many states, such as qubits, it is easily shown to be impossible when details of the system are not known, or system access is limited. In contrast, here I show that this is no longer true for systems described by infinitely many states, such as quantum harmonic oscillators. For a large class of systems, I show that parametric controls that create squeezing operations allow for speeding up the system dynamics without knowing details of the underlying system model [1]. Consequently, the resultant procedure can be used to enhance unknown couplings or frequency components by locally squeezing individual modes along different axis. Finally, I report the experimental realization of the presented scheme in an ion trap system [2] to speed up Rabi oscillations, as shown in Fig. 1 below.

Fig. 1: *Probability as a function of the Jaynes-Cummings interaction duration without the amplification protocol r=0* ***(blue),*** *and with amplification* ***(red)*** *for a squeezing parameter r=1.1. An increase of the corresponding Rabi frequency by a factor 1.56 is obtained.*

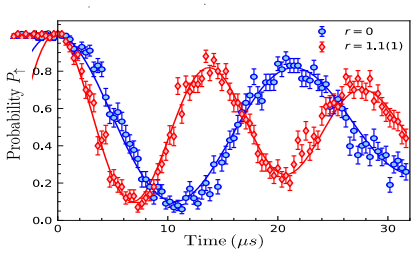

References

[1] C. Arenz, D. I. Bondar, D. Burgarth, C. Cormick, H. Rabitz, *Quantum* **4**, 271 (2020).
[2] S. C. Burd, et al, *Science* **364**, 1163 (2019).

Precision Measurements with a Multiplexed Strontium Optical Lattice Clock

S. Kolkowitz
University of Wisconsin-Madison. Madison, WI 53706, USA

The remarkable precision of optical atomic clocks offers sensitivity to new and exotic physics through novel tests of relativity, searches for dark matter, gravitational wave detection, and precision probes for beyond Standard Model particles and forces. While much of optical clock research has focused on improving absolute accuracy, many of the proposed searches for new physics can be performed with relative comparisons between two clocks. The use of correlated simultaneous differential clock comparisons relaxes the requirements on the clock laser linewidth, experimental duty cycle, and control over the systematic effects limiting absolute frequency uncertainty, offering orders of magnitude potential gains in sensitivity to new physics. In this talk we will present recent experimental results [1] in which we have demonstrated a "multiplexed" strontium optical lattice clock consisting of two or more clocks in one vacuum chamber (Fig. 1a). In inter-comparisons between two spatially separated atom ensembles in the same lattice we observe atom-atom coherence times exceeding 26 s using correlated Ramsey spectroscopy (Fig. 1b) and measure a fractional frequency shift at a precision below a part in 10^{19} (Fig. 1c). We also realize a miniaturized clock network consisting of 6 atom ensembles, corresponding to 15 unique pairwise clock comparisons performed simultaneously, each at a stability comparable to the previous record for clock comparisons.

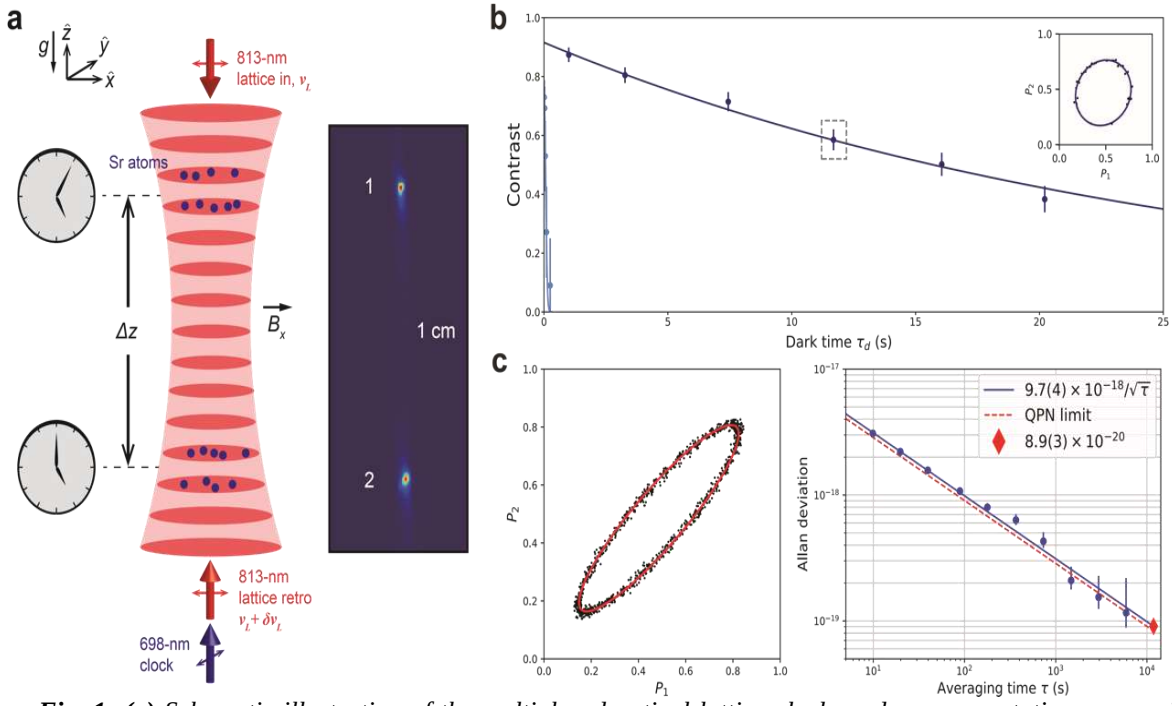

***Fig. 1**: **(a)** Schematic illustration of the multiplexed optical lattice clock, and a representative camera image of two clock ensembles.*
***(b)** Atom-atom coherence in differential comparisons between two ensembles (**dark blue**). The Ramsey contrast for a single ensemble is shown for comparison (**light blue**). **Inset:** representative parametric plot of excitation fraction P_2 versus P_1 illustrating synchronized Ramsey contrast at τ_d = 12 s.*
***(c) Left:** Parametric plot of a differential Ramsey comparison (**black points**) taken at a free precession time τ_d = 8.205 s and a dead time of 1.69 s with 1193 experimental runs for a total measurement time of 11800 s. **Right:** Corresponding Allan deviation (blue points) and anticipated quantum projection noise (QPN) limit (**dashed red line**.) Figure adapted from Ref. [1].*

We will discuss our ongoing campaign of evaluation of systematics for a test of the gravitational redshift at the sub-cm scale, and the prospects for future applications of the multiplexed optical lattice clock to searches for dark matter, novel tests of relativity, and precision isotope shift measurements to hunt for new forces.

Reference

[1] X. Zheng, J. Dolde, V. Lochab, B.N. Merriman, H. Li, S. Kolkowitz, *Nature* **602**, 425 (2022).

Non-equilibrium Modification of Quasiparticle Interactions in Magnetic Materials

H. A. Dürr
Uppsala University, Uppsala, Sweden

The idea to probe, change and control functional materials properties with the help of light has long intrigued researchers in materials science. Using fs laser pulses it is possible to control the magnetic order [1]. Such laser excitation of metalls creates out-of-equilibrium hot electrons that cool down by transferring their energy to other degrees of freedom and ultimately to lattice vibrations of the solid [2].The understanding of the resulting strongly non-equilibrium quasiparticle dynamics in solids is still very limited, in spite of its importance from a fundamental and applied science viewpoint. In this talk I will give an overview how modern ultrafast x-ray spectroscopy and scattering techniques allow us to determine, in an element- and momentum-resolved way, the influence of fs laser excitation on the non-equilibrium evolution of spin waves and phonons. Fig. 1 shows how ultrafast quenching of the ferromagnetic order in FePt nanoparticles results in a highly anisotropic lattice motion.

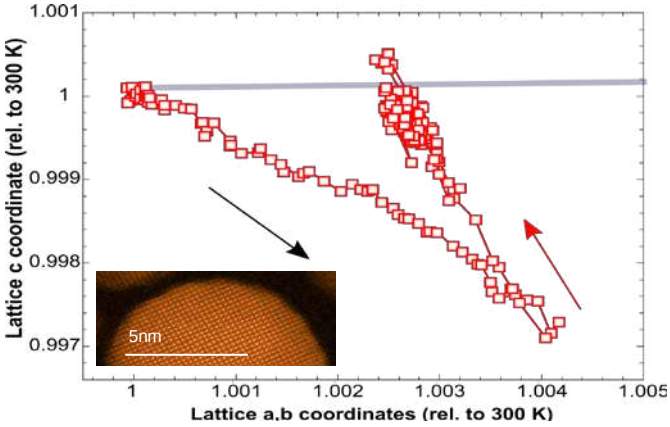

***Fig. 1**. Anisotropic ultrafast lattice expansion of FePt nanoparticles **(inset).** The first 3ps are characterized by a magnetism-induced c-axis contraction **(black arrow)** followed by an expansion (red arrow) moving the system towards the equilibrium **(blue line).** [3]*

The initial reduction of the c-axis lattice constant can be phenomenologically viewed as the result of a magnetic stress caused by a change of the magnetic order parameter [3]. More recent measurements indicate that this is accompanied by a significant hardening of acoustic phonons while the system is far from equilibrium. Fig.2 illustrates how the sub-ps magnetisation manipulation via fs optical pumping affects the spatial evolution of the magnetization. We find evidence of a universal rapid magnetic order recovery in ferrimagnets with perpendicular magnetic anisotropy via nonlinear magnon processes.

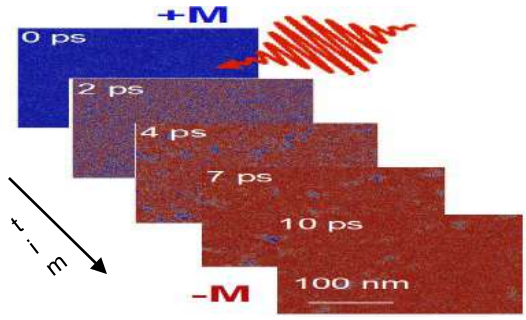

***Fig. 2.** Magnon condensation into transient magnon drops is observed for the non-equilibrium spin system following laser demagnetization of GdFeCo alloys. [4]*

We identify spin wave localization and coalescence processes, whereby localized magnetic textures nucleate and subsequently interact and grow as long as the spin system is still far from equilibrium.

References

[1] I. Radu, et al, *Nature* **472**, 205 (2011).
[2] P Maldonado, et al., *Physical Review* B, in press (2020); *arXiv*: 1906.08504.
[3] A. H. Reid, et al., *Nature Communications* **9**, 388 (2018).
[4] E. Iacocca, et al., *Nature Communications* **10**, 1756 (2019).

Link between Ultrafast Spin-Orientation and Insulator-Metal Transitions in Magnetite Fe_3O_4

I.O. Karpovsky,[1] D.L. Kazenwadel,[2] A.M. Balbashov,[3] R.V. Pisarev,[1] A.M. Kalashnikova[1]
[1] *Ioffe Institute, St. Petersburg 194121, Russia*
[2] *University of Konstanz, 78464 Konstanz, Germany*
[3] *Moscow Power Engineering Institute, Moscow 111250, Russia*

Ultrafast optically-driven switching of magnetization is an actively developing field in magnetism. In particular, experimental studies show that switching can be realized by using femtosecond laser pulses for heating the medium and inducing a spin-reorientation (SR) transition [1]. In this paper, we investigate the feasibility to trigger the ultrafast SR transition in a ferrimagnet – magnetite Fe_3O_4. SR transition takes place upon cooling Fe_3O_4 below T_{SR}=130 K when the cubic magnetic anisotropy changes to uniaxial, and the easy axis rotates from [111] to [001] direction. A distinct feature of Fe_3O_4, as compared to other materials possessing SR transitions, is that slightly below T_{SR}, at T_V=123 K, the Verwey metal-insulator and structural transitions.We examine whether the SR transitions in Fe_3O_4 can be triggered by the laser pulses and if it might have a non-thermal origin, similarly to the ultrafast Verwey transition [2]. For this purpose, we monitored the laser-driven magnetization dynamics in the single crystalline Fe_3O_4 using time-resolved polar magneto-optical Kerr effect (TRMOKE). The measurements were carried out in the temperature range 4.2–180 K with a magnetic field B= -500..500 mT applied in the (110) sample plane. We observed the laser-induced precession of magnetization at initial samples temperatures below and close to T_V and T_{SR} as shown in Figure 1.. The dependences of the precession amplitude, frequency and decay time on initial temperature and pump fluence showed that the excitation of magnetization precession is a manifestation of the laser-driven SR transition, which occurs on a time-scale shorter than ~10 ps.

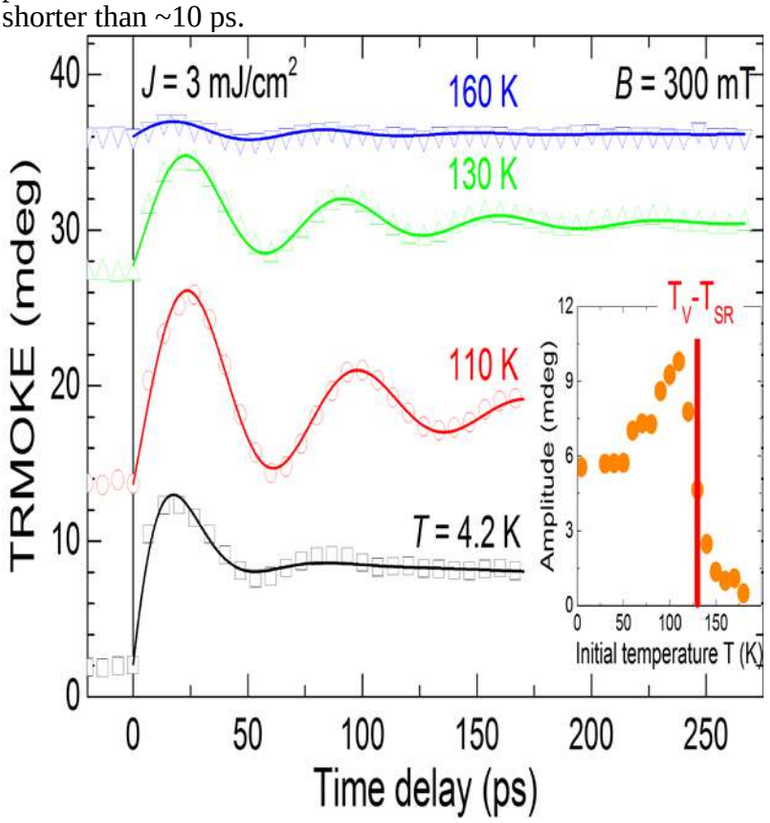

Fig 1. *Laser-induced polar Kerr rotation in magnetite Fe_3O_4, measured different initial sample temperatures T at the excitation fluence J = 3 mJ/cm^2. Measurements are performed at the applied magnetic field of B = 0.3 T.* ***Inset*** *shows the temperature dependence of the amplitude of the excited precession.*

The most intriguing result was that the precession could be excited even at very low temperatures and fluences where the laser-induced heating is not sufficient to drive the SR transition. This observation suggests that there is a non-thermal contribution to the SR transition, similarly to laser-driven non-thermal insulator-meta transition [2]. Our results suggest that the laser-driven SR transition is, at least in part, of non-thermal origin and occurs on the fast sub-picosecond scale, at difference to earlier reported laser-driven SR transitions in orthoferrites [1].

References

[1] S. de Jong et al., *Physical Review Letters* **108**, 157601 (2012).
[2] S. de Jong et al., *Nature Materials* **12**, 882 (2013).

This work was supported by RFBR grant 20-02-00938 and RSF grant 16-12-10456

Terahertz Electric-field driven Dynamical Multiferroicity in Paraelectric $SrTiO_3$

M. Basini[1], M. Pancaldi[2], B. Wehinger[3], M. Udina[3], T. Tadano[4], M. Hoffmann[5], A. Balatsky[6]
S. Bonetti[1]
[1]*Stockholm University, 10691 Stockholm, Sweden*
[2] *Elettra-Sincrotrone Trieste S.C.p.A., 34149 Basovizza, Italy*
[3] *Sapienza University of Rome, 00185, Rome, Italy*
[4]*National Institute for Materials Science, Tsukuba 305-0047, Japan*
[5]*SLAC National Accelerator Laboratory, Menlo Park, CA 94025, USA*
[6]*University of Connecticut, Storrs, CT 06268, United States*

The emergence of collective order in matter is among the most fundamental and intriguing phenomena in physics. In recent years, the ultrafast dynamical control and creation of novel ordered states of matter not accessible in thermodynamic equilibrium is receiving much attention. Among those, the theoretical concept of dynamical multiferroicity has been introduced to describe the emergence of magnetization by means of a time-dependent electric polarization in non-ferromagnetic materials [1,2]. In simple terms, a large amplitude coherent rotating motion of the ions in a crystal induces a magnetic moment along the axis of rotation. However, the experimental verification of this effect is still lacking. Here, we provide the first evidence of room temperature magnetization in the archetypal paraelectric perovskite SrTiO3 due to this mechanism. To achieve it, we resonantly drive the infrared-active soft phonon mode with intense circularly polarized terahertz electric field, and detect a large magneto-optical Kerr effect. A simple model, which includes two coupled nonlinear oscillators whose forces and couplings are derived with *ab-initio* calculations using self-consistent phonon theory at a finite temperature [3], reproduces qualitatively our experimental observations on the temporal and frequency domains. A quantitatively correct magnitude of the effect is obtained when one also considers the phonon analogue of the reciprocal of the Einsten – de Haas effect, also called the Barnett effect, where the total angular momentum is transferred from the coherent phonon motion to the electrons.

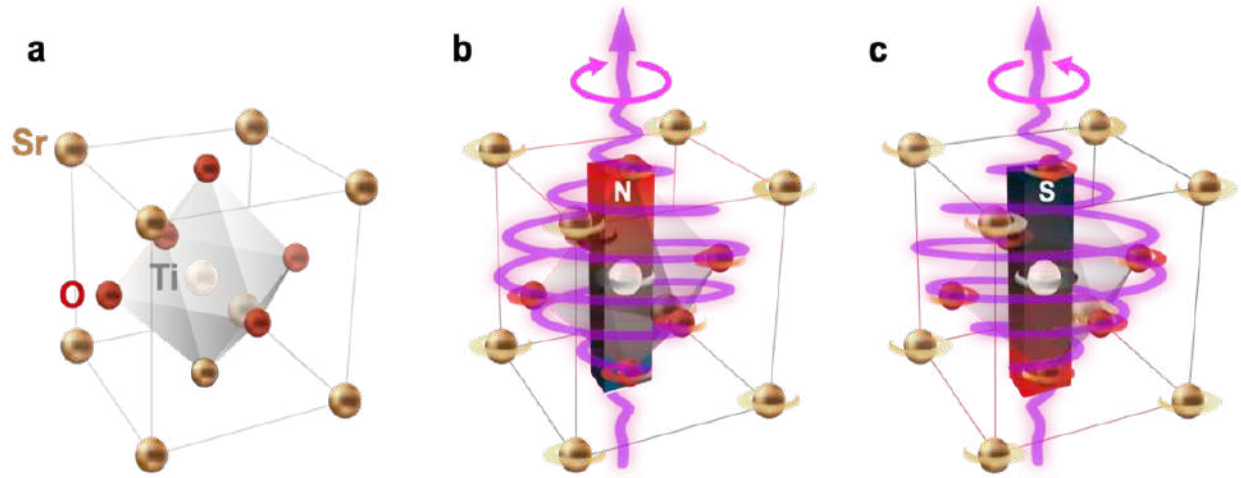

Fig. 1 *Schematic of the experimental realisation of dynamical multiferroicity.* ***(a)*** *$SrTiO_3$ unit cell in the absence of a terahertz electric field. When a circularly polarised terahertz field pulse drives a circular atomic motion, a net magnetic moment is created in the unit cell, which points;* ***(b)*** *north for a pulse with left-handed and* ***(c)*** *south for a pulse which is right-handed.*

Our findings show a new path for designing ultrafast magnetic switches by means of coherent control of lattice vibrations with light.

References:

[1] D.M. Juraschek, et al, *Physical Review Materials* **1**, 014401(2017).
[2] D. M. Juraschek, N. A. Spaldin, *Physical Review Materials* **3**, 064405(2019).
[3] Y. Oba, et al, *Physical Review Materials* **3**, 033601(2019).

Trapped Transient Magnons in the Gapped Antiferromagnet $Sr_3Ir_2O_7$

D. G. Mazzone[1], D. Meyers[1,2], Y. Cao[3], J. G. Vale[4], C. D. Dashwood[4], I. K. Robinson[1], J. P. Hill[4]
D. F. McMorrow[4], M. Först[5], S. Wall[6], X. Liu[7], M. P. M. Dean[1]

[1] *Brookhaven National Laboratory, Upton, NY 11973, USA*
[2] *Oklahoma State University, Stillwater, OK 74078, USA*
[3] *Argonne National Laboratory, Lemont, Il 60439, USA*
[4] *University College London, London WC1E 6BT, United Kingdom*
[5] *Max Planck Institute for the Structure and Dynamics of Matter, 22761 Hamburg, Germany*
[6] *ICFO - The Institute of Photonic Sciences, 08860 Castelldefels, Spain*
[7] *ShanghaiTech University, Shanghai, 201210 China*

Although ultrafast manipulation of magnetism holds great promise for new physical phenomena and applications, targeting specific states is held back by our limited understanding of how magnetic correlations evolve on ultrafast timescales. We have used ultrafast resonant elastic and inelastic x-ray scattering techniques, as illustrated in Fig. 1, to investigate the transient magnetic correlations in the gapped antiferromagnet $Sr_3Ir_2O_7$ after ultra-fast excitation by an optical pump tuned to excite carriers across the bandgap. The magnetic order parameter is found to be suppressed for several ps after photo-excitation with high fluence. We then used RIXS to examine the Q dependence of the short range magnetic correlations as shown in Figure 2. We find that transient magnetic fluctuations are trapped throughout the entire Brillouin zone, opposite to the behavior in a nearly gapless Sr_2IrO_4 [1].

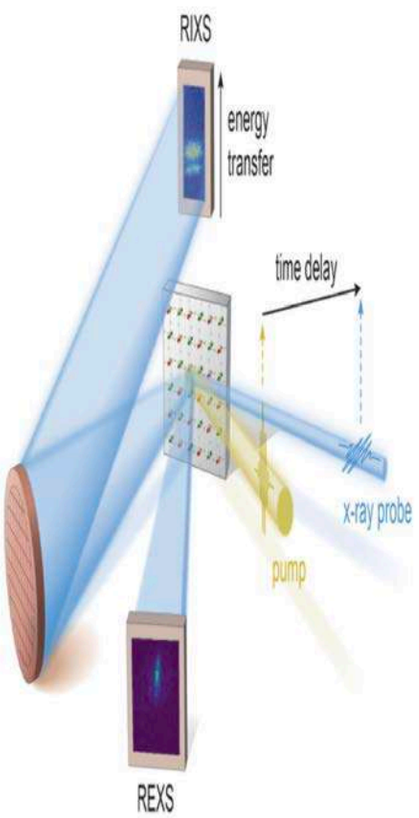

Fig. 1*: An illustration of the time resolved x-ray technique used here [1, 2].*

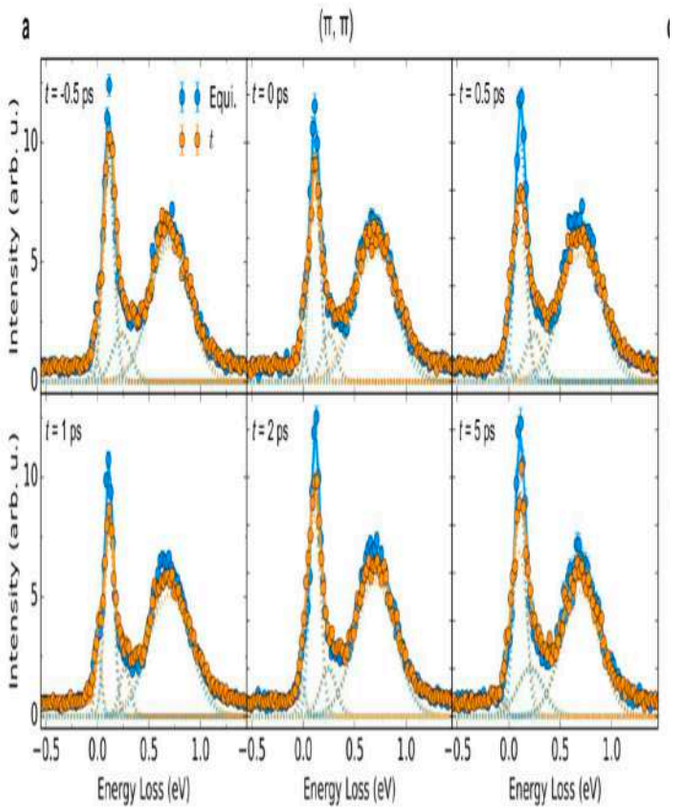

Fig. 2*: Static and transient magnetic correlations of $Sr_3Ir_2O_7$. A suppressed magnetic intensity around 100 meV is observed in the transient state (orange points). Data at the other high symmetry point is available in Ref. [3].*

The result is interpreted in a spin-bottleneck scenario, in which the full recovery of magnetism is delayed by the exitance of a large magnon gap. Our results suggest that materials featuring isotropic magnetic interactions are preferred to achieve rapid manipulation of magnetic order.

References

[1] M. P. M. Dean et al., *Nature Materials* **15**, 601 (2016).
[2] Y. Cao, D.G.Mazzone, D Meyers, JP Hill, X Liu, S Wall, M. Dean, *Philosophical Transactions of the Royal Society A* **377**, 20170480 (2019).
[3] D.G. Mazzone, D. Meyers, M. P. M. Dean *arXiv*:2002.07301 (2020).

Giant effective Magnetic Fields from Optically driven Chiral Phonons in 4*f* Paramagnets

D. M. Juraschek
Tel Aviv University, Tel Aviv 6997801, Israel

Light-induced control of magnetic order is conventionally achieved through opto-magnetic effects, such as the inverse Faraday effect, in which the light from a laser interacts with the electronic states of a magnetic material. Here, we theoretically describe a vibrational analog of the inverse Faraday effect, in which coherently excited infrared-active chiral phonons replace circularly polarized photons in the scattering process, and which is mediated through spin-phonon interaction [1,2,3]. In particular, we show that optically driven chiral phonons in the rare-earth trihalide $CeCl_3$ (Fig. 1a, b) produce giant effective magnetic fields that couple to the paramagnetic cerium 4*f* spins [3]. Microscopically, the chiral phonons induce transitions between the crystal-field states of the cerium 4*f* electrons, as shown in Fig. 1c.We compute the coherent chiral phonon dynamics in response to the excitation by a circularly polarized terahertz pulse using a combination of phenomenological modeling and density functional theory calculations. We then feed these dynamical calculations into a rate-equation model to simulate the population and magnetization dynamics of the cerium 4*f* spins in response to the chiral phonon dynamics. We find that effective magnetic fields of up to 100 tesla can possibly be generated that polarize the spins to near saturation for experimentally accessible pulse energies. The direction of induced magnetization can be reversed by changing the handedness of phonon chirality, which in turn can be controlled through the circular polarization of the laser pulse.

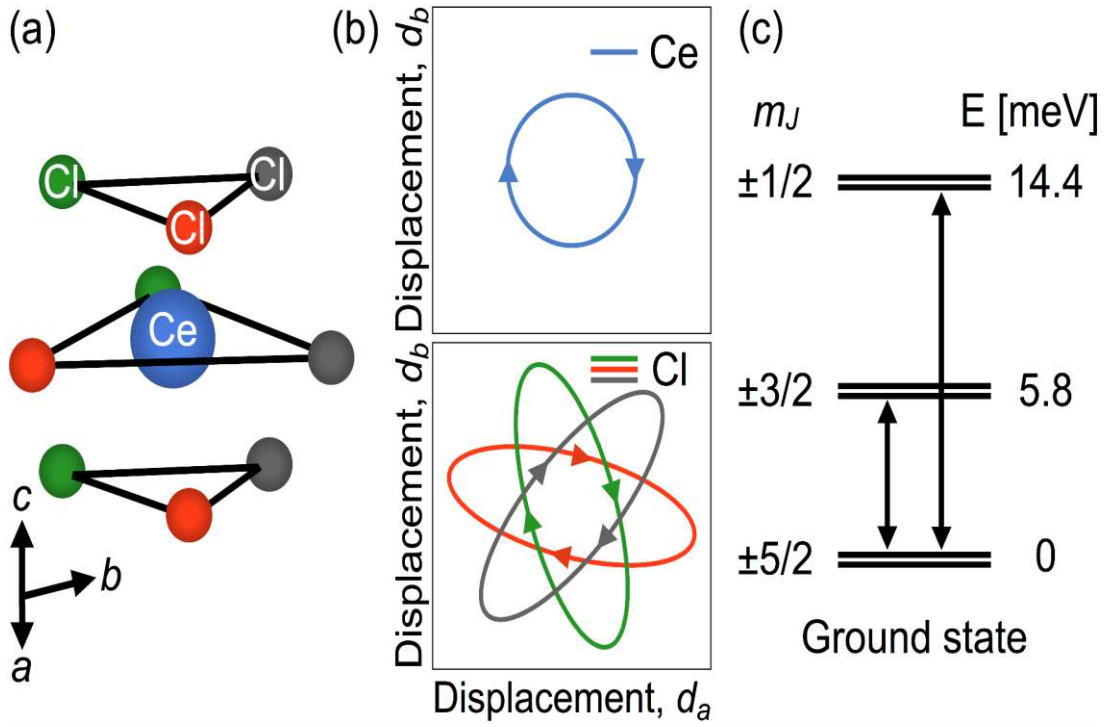

Fig. 1: *Chiral phonons in $CeCl_3$.*
(a) *Crystal-field environment of a paramagnetic cerium ion.* ***(b)*** *Motion patterns of the cerium and chloride ions in the ab crystal plane relative to their equilibrium positions, induced by chiral phonons.*
(c) *Chiral phonons induce transitions between crystal-field states that act as an effective magnetic field on the paramagnetic cerium 4f electrons.*

This *phonon inverse Faraday effect* offers a new route to achieving control over and switching of magnetic order at terahertz frequencies.

References

[1] D. M. Juraschek, P. Narang, N. A. Spaldin, *Physical Reie. Research* **2**, 043035 (2020).
[2] D. M. Juraschek, D. S. Wang, P. Narang, *Physical Review* B **103**, 094407 (2021).
[3] D. M. Juraschek, T. Neuman, P. Narang, *Physical Review Research* **4**, 013129 (2022).

Real Space Dynamics in Topological Magnets in Time-Resolved Lorentz TEM

I. Madan[1], G. Berruto[1], Y. Murooka[1], R. Lamb[2], Y. Togawa[3], D. McGrouther[2], F. Carbone[1]

[1]*École Polytechnique Fédérale de Lausanne (EPFL), CH-1015 Lausanne, Switzerland*
[2] *University of Glasgow, Glasgow G12 8QQ, United Kingdom*
[3] *Osaka Prefecture University, Osaka 599-8531, Japan*

Fast and high-resolution imaging techniques are crucial for progress in application-oriented field of modern magnetism. In-detail investigation of topological defects, such as domain walls, solitons or skyrmions and their dynamics is crucial for practical nanoengineering as well as for the explanation of macroscopic observables field dependence such as magnetization, Hall conductivity etc. A widely used technique with one of the highest resolution capabilities is transmission electron microscopy.It has various configurations that allow to extract magnetic information either through material properties EMCD[1] or directly through the effect of magnetic field on electrons trajectory (DPC[2], Lorentz-TEM[3]), in some cases reaching atomic-scale resolution. Here we describe a modification of such instrument for ultrafast and in-situ laser experiment [4]. We demonstrate writing and erasing of skyrmion clusters with individual laser pulses in itinerant helimagnet FeGe (Fig 1). By analyzing temperature, field, wavelength and pulse duration dependence of this phenomenon we conclude that observed skyrmions are metastable.

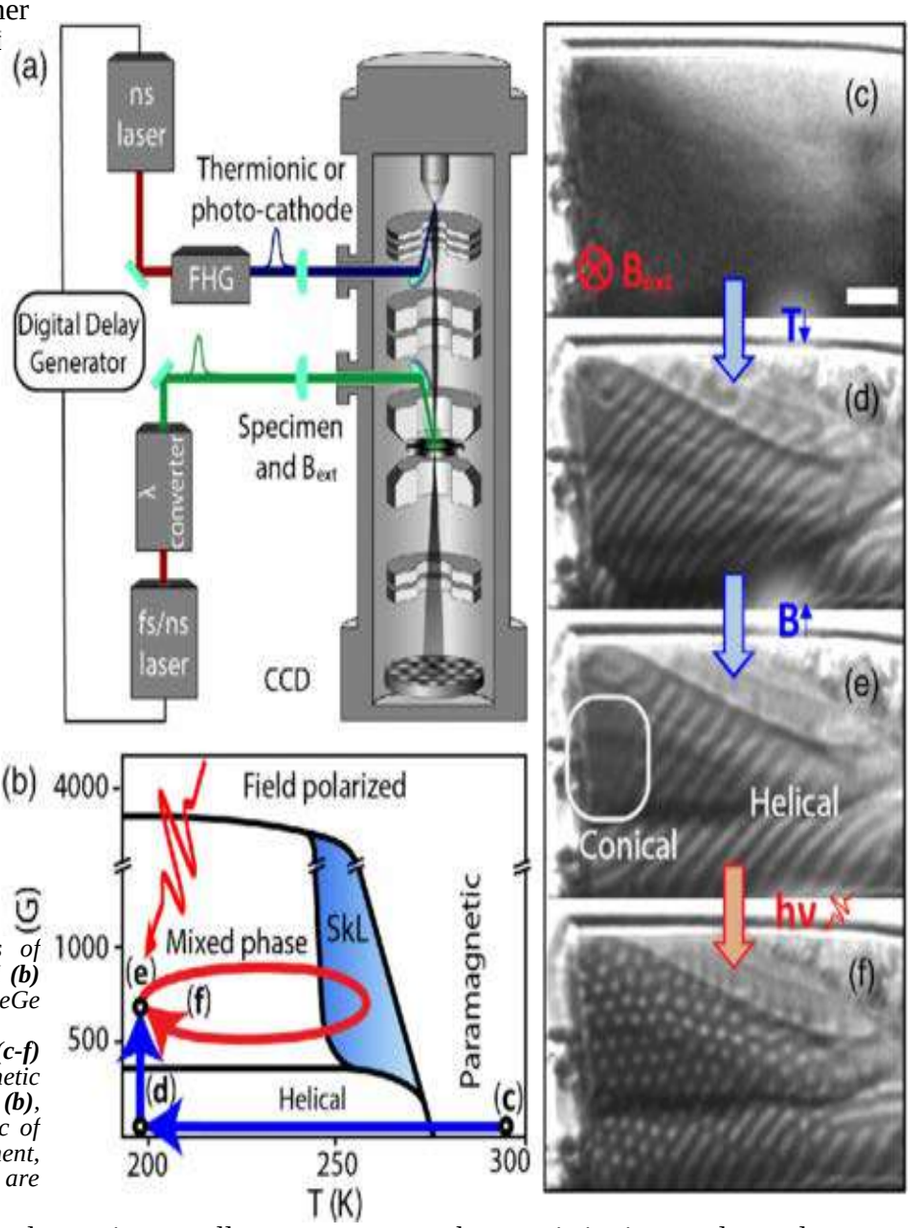

Fig.1 (a) *Schematics of ultrafast Lorentz-TEM* ***(b)*** *phase-diagram of FeGe and skyrmion photocreation path* ***(c-f)*** *Snapshots of magnetic contrast along the in* ***(b)****, lines are characteristic of helical spin arrangement, while white dots are skyrmions*

Time-resolved nanosecond experiments allow us to extract characteristic time-scales and propose a memorydevice based on the pulse duration control of writing/erasing processes.

References

[1] Z. Wang et al., *Nature Materials* **17**, 221, (2018).
[2] N. Shibata, S. D. Findlay, Y. Kohno, H. Sawada, Y. Kondo, Y. Ikuhara, *Nature Physics* **8**, 611, (2012).
[3] S. McVitie, M. Cushley, *ePrints* **106**, 423, (2006).
[4] G. Berruto, I. Madan et al., *Physical Review Letters* **120**, 117201, (2018).

Ultrafast Magnetic switching by Resonant Excitation of Optical Phonons

A.I. Kirilyuk
Radboud University, 6525 ED Nijmegen, The Netherlands

Identifying an efficient pathway to change the order parameter via a subtle excitation of the coupled high-frequency mode is the ultimate goal of the field of ultrafast phase transitions [1,2]. This is an especially interesting research direction in magnetism, where the coupling between spin and lattice excitations is required for switching [3]. Control of the crystal environment arguably represents the most universal mechanism to act on magnetization, as it is present in all materials regardless of their magnetic structure. One interesting approach to manipulate crystal lattice is via the anharmonic interaction of different phonon modes, which transfers the high-frequency excitation of an infrared-active mode into a rectified coordinate shift along a coupled Raman-active coordinate. Despite several attempts [4,5] however, the switching between magnetic states via resonant pumping of phonon modes has not yet been demonstrated. To provide resonant excitation of the optical phonon modes, we use pulses from FELIX (Free Electron Lasers for Infrared eXperiments, Nijmegen, The Netherlands). Single pulses of IR/THz light with photon energy ranging between 25-124 meV (wavelength 10-50 μm) are typically used. The pulses of FELIX have been shown to be Fourier-transform limited [6], with their bandwidth experimentally tunable in the range of 0.5-2.0%, corresponding to the typical pulse width of 1-10 ps, depending on the wavelength range.And thus we show how an ultrafast resonant excitation of the longitudinal optical phonon modes in magnetic garnet films switches magnetization into a peculiar quadrupolar magnetic domain pattern, unambiguously revealing the magneto-elastic mechanism of the switching [7]. In contrast, the excitation of strongly absorbing transverse phonon modes results in thermal demagnetization effect only. The mechanism appears to be very universal, and is shown to work in samples with different crystallographic symmetry and magnetic properties, including antiferromagnets [8], but also in ferroelectrics.

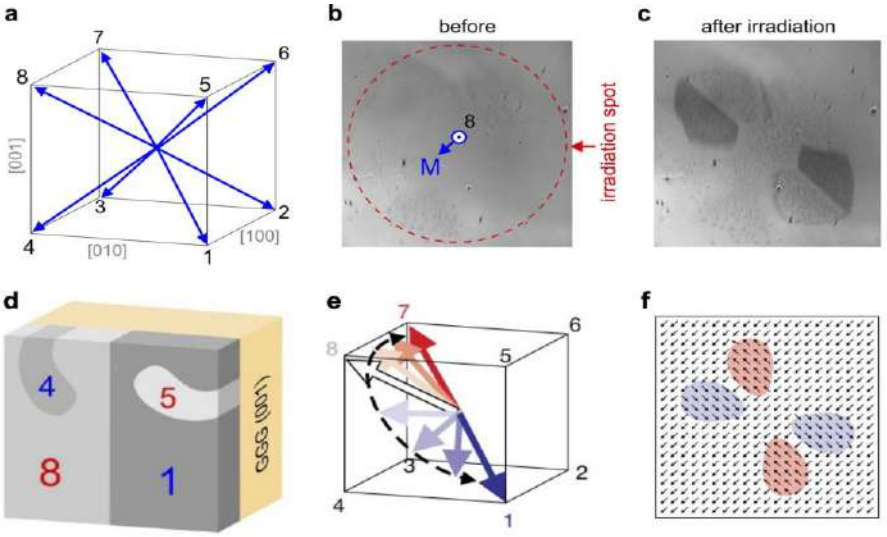

Fig.1. a. *Four easy axes of magnetization in relation to the cubic crystal symmetry.*
b. *Image of the initial state of the magnetic domain structure.* ***c.*** *Image of the magnetic domain structure after radial strain is generated by a pump pulse.*
d. *Typical equilibrium domain structure in Co:YIG.*
e. *Pathway of switching between the different magnetic phases.*
f. *Micromagnetic simulations of switching.*

Using single-shot time resolved microscopy, we demonstrate that the dynamics of the domain formation proceeds via a strongly inhomogeneous magnetic state [9], arguably related to the spin-wave instabilities [10].

References

[1] T. Kubacka et al, *Science* **343**, 1333 (2014).
[2] A. Kirilyuk, A.V. Kimel, T. Rasing, *Review Modern Physics* **82**, 2731 (2010).
[3] N. Li et al, *Review Modern Physics* **84**, 1045 (2012).
[4] T.F. Nova et al, *Nature Physics* **13**, 132 (2017).
[5] S.F. Maehrlein et al, *Science Advances* **4**, 5164 (2018).
[6] G.M.H. Knippels et al., *Physical Review Letters* **83**, 1578 (1999).
[7] A. Stupakiewicz et al., *Nature Physics* **17**, 489 (2021).
[8] P. Stremoukhov et al., *New Journal of Physics* **24**, 023009 (2022).
[9] M. Gidding et al., to be published
[10] A. Kashuba, Physical Review Letters **96**, 047601 (2006).

Ultrafast Switching of Ferroelectric Polarization by Infrared Laser Pulses

M.Kwaaitaal, D.B. Lourens, C.S. Davies, A. Kirilyuk
Radboud University, 6525 XZ Nijmegen, The Netherlands

The perovskite barium titanate ($BaTiO_3$) is a ferroelectric crystal with a spontaneous electric polarization at room temperature. Switching of such polarization is typically controlled with static or pulsed electric fields, which results in a slow and incoherent process. As an alternative, it has been suggested that a resonant excitation of anharmonic phonon modes can provide the mechanism for ultrafast coherent switching [1,2].Therefore we applied short intense tunable infrared pulses from the FELIX free electron laser onto single crystals of $BaTiO_3$ and followed the induced changes via optical birefringence. We discovered that these laser pulses can leads to the appearance of switched ferroelectric domains (Fig.1), with lifetimes ranging from hundreds of ms to infinity, unlike ultrafast transient in previous study [2].We also prove that the appearance of the domains is not related to temperature,the latter is being directly deduced from temperature dependent birefringence data from [3].

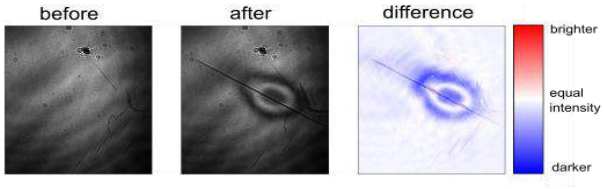

Fig 1. *Images before* ***(left)*** *and shortly after* ***(middle)*** *the FELIX pulse arrived. The difference in intensity ($I_{after} - I_{before}$) of these two Pictures is shown in the* ***right*** *image*

Our discovery thus opens a new avenue in the manipulation of ferroelectrics on an ultrafast time scale.

References
[1] S. Fahy, R. Merlin, *Physical Review Letters* **73**,1122 (1994).
[2] R. Mankowsky, M. Först, A. Cavalleri, *Reports on Progress in Physics* **79**, 064503 (2016).
[3] K. Buse, S. Riehemann, S. Loheide, H. Hesse, F. Mersch, E. Krätzig, *Physica Status Solidi a* **135**, K87(1993).

Supermagnonic of Quantum Spin Correlations in 2D Antiferromagnets

G. Fabiani, M.D. Bouman, J.H. Mentink
Radboud University, 6525 EDNijmegen, The Netherlands

Magnons, the collective excitations of magnetically ordered materials can oscillate up to 100 THz over a distance of less than one nanometer. With intrinsically small energy loss, such magnons have great potential for smaller, faster and more energy-efficient data processing. However, understanding the magnon spectrum at such short wavelengths has been challenging even for the simplest model: the antiferromagnetic Heisenberg model in 2D [1]. Furthermore, studying the space-time dynamics of this model defines an intricate quantum many-body problem out of equilibrium, for which until recently no accurate methods were available. Beyond the limitations of existing methods, we adopt a machine learning inspired ansatz [2] to simulate the dynamics of the 2D Heisenberg model [3-4]. In this approach, the wavefunction of the system is approximated with a restricted Boltzmann machine, which allows us to simulate systems up to 24x24 spins. We show that quench-like perturbations of the exchange interaction excite dynamics of spin correlations, which spread highly anisotropically in space. Interestingly, we find that magnon-magnon interactions enhance the spreading speed up to 40% above the highest magnon velocity. Furthermore, opposed to well-known results in one dimension, we find that the dynamics of entanglement is not determined by the highest magnon velocity, but changes much faster on the time scale determined by the oscillation frequency of zone-edge magnon pairs [5].

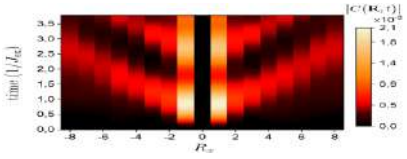

Fig.1*. Snapshots of spin correlations* $C_i(\boldsymbol{R}, t) = \langle \psi(t) | \hat{S}(\boldsymbol{R}_i) \cdot \hat{S}(\boldsymbol{R}_i + \boldsymbol{R}) | \psi(t) \rangle$ *in the Heisenberg model on a 20x20 lattice. Following small impulsive perturbations of the exchange interaction leads to spreading of correlations with a speed that is transiently higher than the highest magnon velocity.*

We believe that our results are fundamental for understanding magnetism on the shortest length and timescale and may have high impact on the future development of faster and smaller magnon-based information processing.

References
[1] H. Shao et al, *Physical Review* X **7**, 041072(2017).
[2] G. Carleo, M. Troyer, *Science* **355**, 602(2017).
[3] G. Fabiani & J.H. Mentink, *SciPost Physics* **7**, 004(2019).
[4] G. Fabiani, M.D. Bouman and J.H. Mentink, *Physical Review Letters* **127**, 097202 (2021).
[5] G. Fabiani & J.H. Mentink, *Physical Review* B **105**, 094438 (2022).

Ultrafast all-Optical Switching of Ferromagnets: A 2-Step Process

T. Rasing
Radboud University, 6525AJ Nijmegen, The Netherlands

Since the demonstration of All-Optical Switching (AOS) of magnetization by a single 40 femtosecond laser pulse more than a decade ago [1, see Fig.1], the manipulation of spins by ultra-short laser pulses has become a fundamentally challenging topic with a potentially high impact for future spintronics and data storage, as it provides an alternative and energy efficient approach to manipulate and record magnetic information [2]. Originally, AOS was demonstrated, and later also understood, in ferrimagnetic materials, where the exchange interaction between the anti-ferromagnetically coupled sub-lattices appeared to play a crucial role[3-5]. However, recently, Helicity Dependent AOS (HD-AOS) in ferromagnetic materials like Co/Pt and Fe/Pt was successfully demonstrated, giving an enormous boost to the field, though this switching required hundreds of laser pulses [6]. By studying the dynamics of this switching process, we have discovered that this switching is a 2-step process [7] and that highly efficient HD-AOS can be achieved by using pairs of femto/pico-second laser pulses.

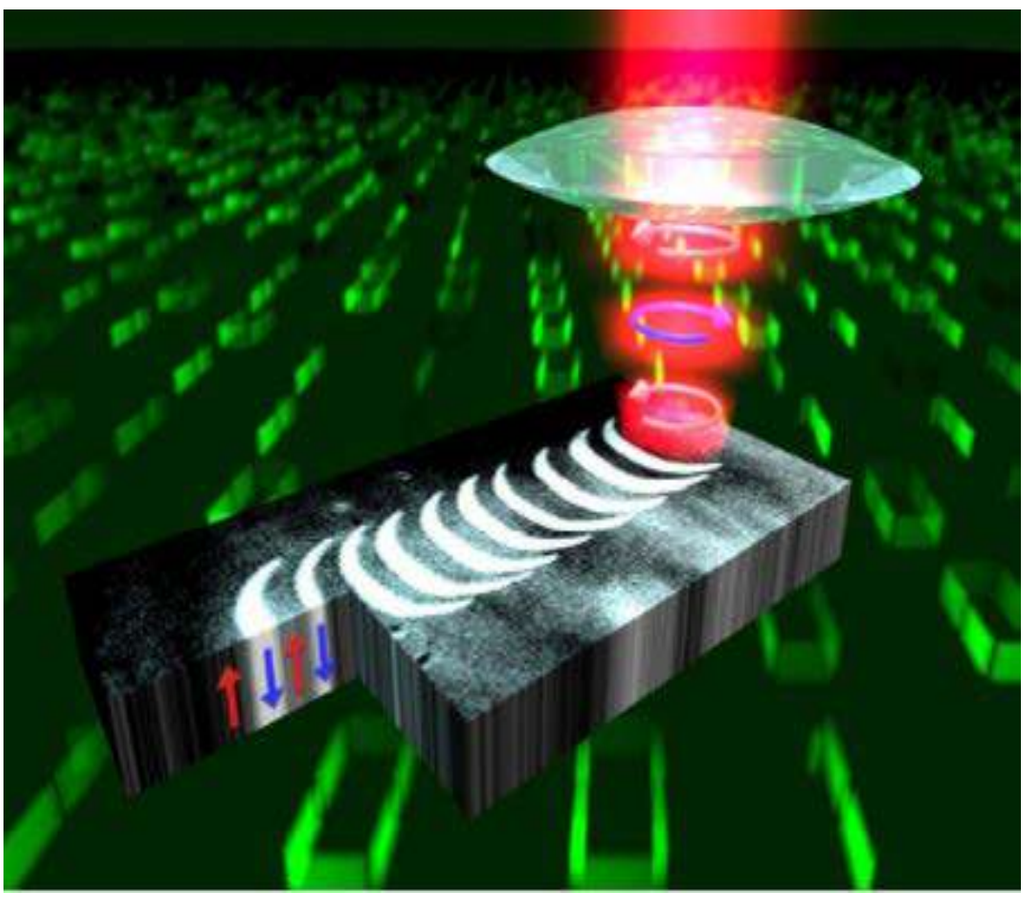

Fig.1: *All-Optical Switching of magnetization, by moving 40fs, circularly polarized, laser beam over thin FeGdCo film while switching the helicity between successive pulses (from [1]).*

Here we show that the most efficient switching is realized when the first, femtosecond pulse of the pair brings the ferromagnet into a strongly nonequilibrium, nearly demagnetized state, while the second, circularly polarized picosecond pulse controls picosecond relaxation from this state in a helicity-dependent deterministic way.

References

[1] D. Stanciu et al, *Physical Review Letters* **99**, 047601 (2007).
[2] A. Kirilyuk, et al, *Review of Modern Physics* **82**, 2731 (2010).
[3] I. Radu et al, *Nature* **472**, 205 (2011).
[4] T. Ostler et al, *Nature Communications* **3**, 666 (2012).
[5] J. Mentink et al, *Physical Review Letters* **108,** 057502 (2012).
[6] C-H. Lambert, et al, *Science* **345**, 1337 (2014).
[7] R. Medapalli et al, *Physical Review* B **96**, 224421 (2017).

Coherent Driving of Magnons by Optically Excited Phonons in Metallic Ferromagnets

A. V. Scherbakov
Technische Universität Dortmund, 44221 Dortmund, Germany

Phonons generated in a metallic ferromagnet by ultrashort light pulses are effective mediators, which convert the energy of optical excitation to the precessional response of the spin system, i.e., coherent magnons. The energy transfer is provided by modulation of the magnetocrystalline anisotropy: a tilt of the anisotropy field induces torque and launches the spin precession. There are two mechanisms of modulation [1]: (i) the lattice strain induced by coherent phonons acts via the magneto-elastic interaction, (ii) non-coherent thermal phonons modify the anisotropy by its temperature dependence. Typically, the interaction occurs between nonequilibrium phonons with a broad spectrum and a bunch of spectrally close magnon modes. Our experiments are designed to make this interaction more precise. We couple optically excited phonons of specific frequencies with selected magnon modes by their spectral and spatial matching in surface-patterned ferromagnets [2,3] and ferromagnetic layers of several nanometer thicknesses [4,5]. The observed effects include the formation of a magnon polaron, i.e., a hybridized state of strongly coupled phonons and magnons, multimode mixing of magnons and phonons in a propagating coherent phonon wavepacket, and driving a single magnon mode by resonant thermal modulation. Fig. 1 illustrates the experiments with surface-patterned ferromagnets [3,6].

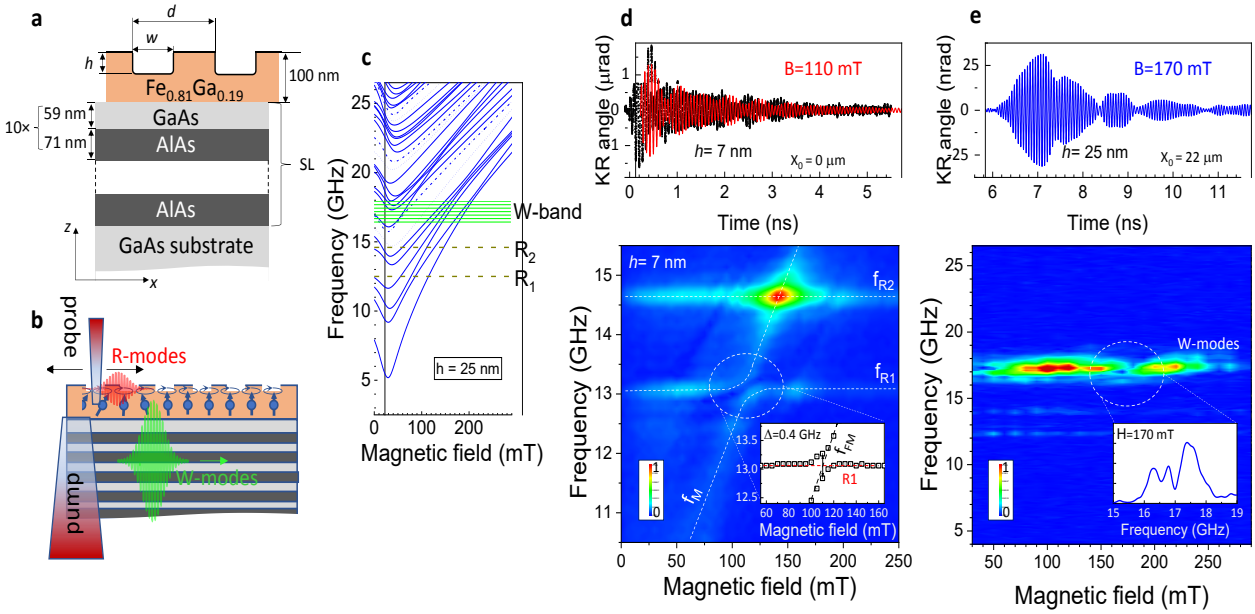

***Fig. 1**. Resonant phonon driving of magnons in surface-patterned ferromagnetic layers [3,6]. **a**. Schematic of the studied structure. **b** Experimental scheme with optical excitation of the NG by the near-infrared pump pulses through the substrate and detection of the transient response of the lattice and spin system by the probe pulses in the optically-excited area and at a distance up to 100 μm along the reciprocal vector of the NG. **c** Calculated field dependence of the magnon spectra (blue lines) in the NG with d = 200 nm, w = 100 nm, and h = 7 nm. Horizontal lines show the calculated spectral position of the two lowest pseudo-Rayleigh modes (R-modes) and 22 guided modes localized in the SL (W- modes). **d**. Transient Kerr rotation (KR) signal measured in the shallow NG at the overlap of the pump and probe beams at resonant conditions for the fundamental magnon mode and the lowest R-mode. The lower panel shows the field dependence of the fast Fourier transform (FFT) of the transient KR signal. The inset zooms the avoided crossing of the magnon and phonon modes. **e**. Transient KR signal measured in the deep NG at the distance X_0=22 μm between the probe and pump beams. The external magnetic field corresponds to the intersection of the W-modes and the six lowest magnon modes of the NG. The lower panel shows the field dependence of the FFT of the transient KR signal in this structure. The inset shows the FFT of the signal shown in the upper panel.*

The ferromagnetic structure is a nanograting (NGs) formed by parallel grooves milled in 105-nm Galfenol ($Fe_{0.81}Ga_{0.19}$) layer grown on GaAs/AlAs superlattice (SL). In a pump-probe experiment, the 100-fs pump pulse focused to the spot of ~1 μm diameter excites the coherent response of the lattice

and the spin system. In the optically-excited phonon and magnon transients detected using the linearly polarized probe pulse, the dominating contribution is provided by the Eigen phonon modes of the structure. There are two main mode types: pseudo-Rayleigh modes (R-modes) localized at the surface and the modes guided by the SL along the surface (W-modes) [6]. An external magnetic field applied in the layer plane serves for tuning the magnon frequencies relative to the phonon modes of NG. The manifestation of the magnon-phonon interaction depends on the structural design, which sets the phonon and magnon mode lifetimes and their spatial profiles. In the shallow NG (h = 7 nm), both the first R-mode and the fundamental magnon mode possess long lifetimes and are perfectly spatially matched. They form a hybridized state, clearly manifested by avoiding crossing at the resonant conditions [3]. The most exciting effect in the deep NG (h =25 nm) is the resonant driving of the six lowest magnon modes by the 22 propagating W-modes. The waveform of this coherent magnon-phonon mixture continuously modifies during the propagation along the surface and demonstrates ultimate spatial-time volatility. The experiments on resonant thermal modulation of magnons in Galfenol nanolayers [5] are summarized in Fig. 2.

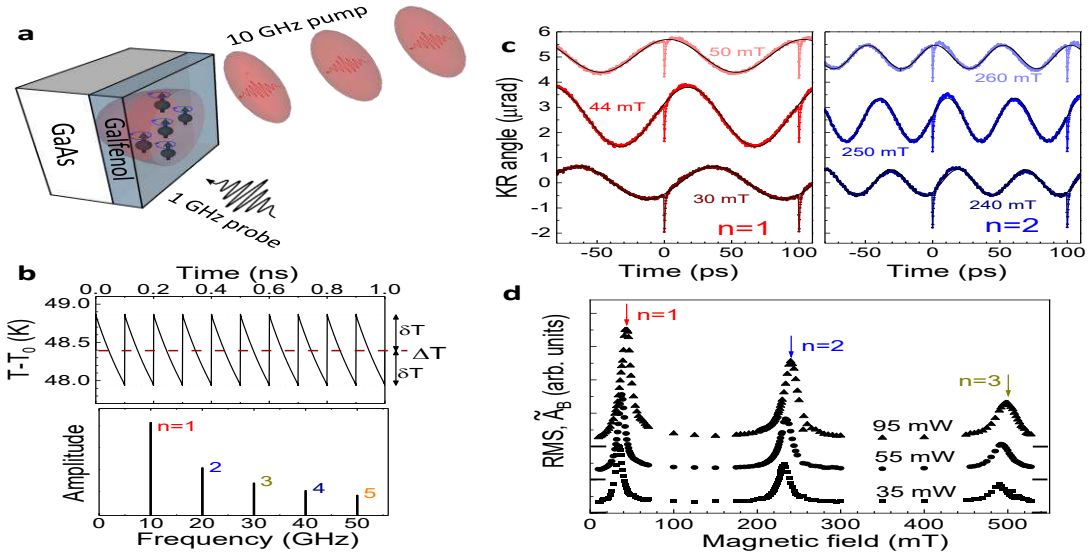

***Fig. 2**. Resonant thermal driving of magnons in ferromagnetic nanolayers [5].*
***a**. Scheme of the experiment. **b** Calculated temporal evolution of the $Fe_{0.81}Ga_{0.19}$ lattice temperature, T, over the room-temperature background, T_0=293 K, induced by the 10-GHz optical excitation of a 5-nm $Fe_{0.81}Ga_{0.19}$ layer at the pump excitation power W = 95 mW (**upper panel**) and its FFT spectrum (**lower panel**). **c**. Transient Kerr rotation signals measured in the vicinity of the resonance of the magnon mode and the first (**left panel**) and second (right panel) harmonics of the thermal modulation. **d.** Measured magnetic field dependences of the root mean square (RMS) amplitude of the Kerr rotation signal for three values of pump excitation power. The vertical arrows indicate the magnetic fields at which the corresponding resonance conditions is fulfilled.*

A $Fe_{0.81}Ga_{0.19}$ layer of 5-nm thickness is excited by the pump laser pulses with a repetition rate of 10-GHz. In the experimental geometry with the in-plane external magnetic field, the energy transfer to the spin system is provided exclusively by non-coherent phonons. However, the temperature modulation at the laser repetition rate can resonantly excite the fundamental magnon mode. The amplitude of non-decaying spin precession achieves maximum at the resonant conditions when the magnon mode frequency is a multiply of the laser repetition rate.The main experimental results described above are supported by comprehensive theoretical modeling, which allows visualizing the transient processes and gives a clear explanation of the experimental observations. Because all the experiments were carried out under ambient conditions at room temperatures, we consider exciting application perspectives in non-conventional computing, generation of spin currents, and nanoscale energy harvesting. They will also be discussed in the talk.

References

[1] V. N Kats et al, *Physical Review* B **93**, 214422 (2016).
[2] S. Salasyuk et al, *Physical Review* B **97**, 060404(R) (2018).
[3] F. Godejohann et al, *Physical Review* B **102**, 144438 (2020).
[4] A. V. Scherbakov et al, *Physical Review Applied* **11**, 031003 (2019).
[5] M. Kobecki et al, *Nature Communications* **11**, 4130 (2020).
[6] D. Yaremkevich et al, *ACS Nano* **15**, 4802 (2021).

Mode-selective Ballistic Control of the Transition pathway between Structural Phases in Atomic Indium Wires

Hannes Böckmann[1], Jan Gerrit Horstmann[1], Abdus Samad Razzaq[2], Stefan Wippermann[2]
Claus Ropers[1]
[1]*University of Göttingen, Göttingen 37077, Germany*
[2]*Max-Planck-Institut für Eisenforschung GmbH, Düsseldorf 40237, Germany*

Exploiting vibrational coherence for the dynamic selection of material properties is an attractive goal with wide-ranging technological potential [1, 2]. The metal-to-insulator transition in charge-density-wave systems is mediated by few structural modes and thus represents a promising target for selective excitation towards a desired electronic phase [3]. However, such active steering across a generally multi-dimensional potential energy landscape requires microscopic insight into the non-equilibrium reaction pathway. In this talk, I will outline our findings about the mode-selective coherent control over the metal-to-insulator structural phase transition in atomic indium wires on the Si(111) surface. By using ultrafast low-energy electron diffraction (ULEED) in combination with sequential optical excitation, we harness vibrational coherence in key structural modes to govern the transition. We control the vibrational amplitudes and thereby steer the collective atomic motion from the insulting to the metallic state within the potential energy surface (PES), underlying the transition. In combination with *ab initio* simulations, we elucidate the two-dimensional PES, spanned by the Peierls amplitude modes and demonstrate the ballistic evolution of the transformation along the deformation vectors. We have developed ULEED to explore non-equilibrium structural dynamics at surfaces in the time-domain, combining the superior surface sensitivity of LEED with ultrafast optical excitation [4]. For this, we employ low-energy electron pulses in a laser-pump/electron-probe scheme (Fig. 1a, left). To investigate the role of vibrational coherences in the In/Si(111) system, a femtosecond multi-pulse optical excitation scheme is used to switch the surface from the insulating to a metastable metallic state, and the corresponding structural changes are monitored by ULEED [5]. We generate sequences of NIR pump pulses with adjustable mutual delays and intensities. In the experiments, the coherent control of the phase transition is demonstrated by using one “preparation pulse” and a subsequent “switch pulse”, while we gain access to the vibrational amplitude via interference of induced atomic motion from two preparation pulses.

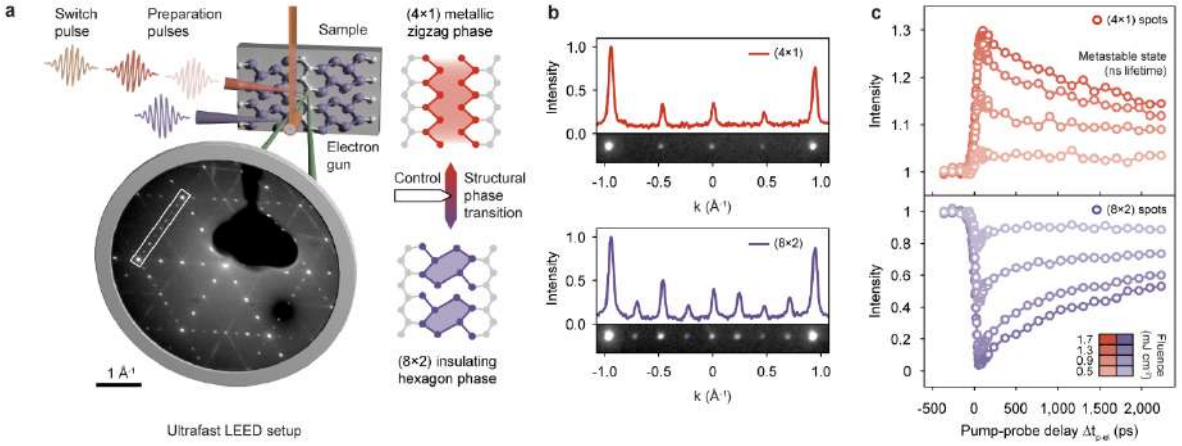

***Fig. 1. a**, Sketch of the ULEED set-up and structure models for the metallic and insulating phase of atomic indium wires on Si(111). **b**, Selected regions and line profiles of the metallic (4×1) and insulating (8×2) phase (see white frame in a). **c**, Integrated intensities of the (4×1) and (8×2) diffraction spots as a function of the pump-probe delay $\Delta t_{p\text{-}el}$.*

In a first step, we study the structural dynamics induced by the Peierls transition after excitation with a single preparation pulse and the subsequent switch pulse. Specifically, we map the laser-driven transformation from the (8×2) insulating hexagon structure to the (4×1) metallic zigzag structure (Fig. 1a, right and Fig. 1b). We observe a rapid increase/decrease of the (4×1)/(8×2) diffraction spot intensity directly after optical excitation and subsequent relaxation to a level persisting over nanoseconds (Fig. 1c), indicating the metastability of the (4×1) structure.

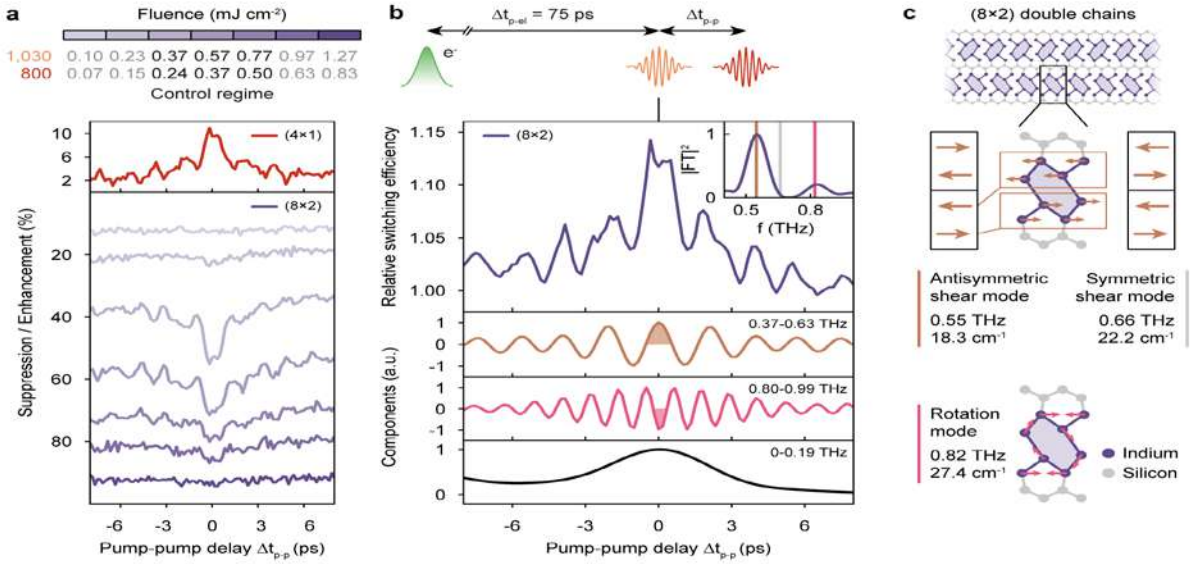

***Fig. 2**. **a**, Suppression or enhancement of the integrated (8 × 2) and (4 × 1) diffraction spot intensity as a function of the double-pulse delay Δt_{p-p} and incident fluence F. **b,** Relative switching efficiency for the (8×2) to (4×1) transition. Inset, spectral density of the switching efficiency. Bottom, Fourier-filtered contributions of different frequency components. **c**, Structural modes of the (8×2) phase in the relevant frequency regime. Note the only the anti-symmetric shear and the rotation mode are linked to the transition.*

Next, in analogy with control schemes in femtochemistry, we excite the surface by a pair of optical pump pulses with variable delay Δt_{p-p} to manipulate the transition efficiency and probe the resulting structure by ULEED at a later time of Δt_{p-el} = 75 ps, well after the excitation. Pronounced oscillations as a function of Δt_{p-p}, demonstrate a coherent response of the signal at intermediate fluences (Fig. 2a). The extracted modulation frequencies (Fig.2b inset) point to shear and rotation phonon modes linked to the metal–insulator phase transition (Fig.2c)[6].Fourier-filtered traces of the two observed frequency bands exhibit opposite phases at time zero, suggesting distinct roles of the corresponding phonons in controlling the transition (Fig. 2b bottom). Mode-selective steering of the transition pathway [7]: for sequential subthreshold excitations with one preparation pulse preceding the switch pulse, vibrational coherences shear and rotation modes was demonstrated to significantly influence the transition efficiency (Fig. 3a). This observation strongly suggests that the light-induced structural transformation can be described in a configuration space spanned by these select collective modes (Fig. 3b left).Two preceding preparation pulses, adapted to the vibrational periods, induce a well-defined vibrational state (Fig. 1b), followed by the switch pulse completing the transition (Fig. 1b right). This excitation scheme allows the steering of the trajectory along the individual modes towards the (4x1) structure.

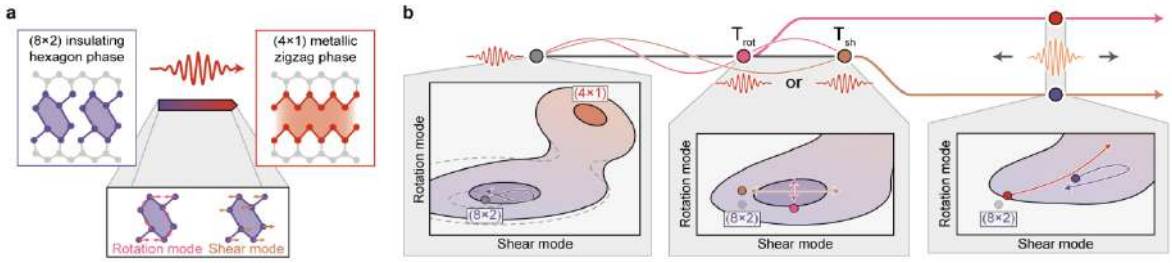

***Fig. 3**: **a**, Photo-induced structural phase transition of atomic indium wires, mediated by shear and rotational motion. **b**, Sketch of the experimental scheme. Dynamic control of ultrafast pathways via displacive excitation of coherent phonons. The momentary vibrational state critically influences the phase transition probability.*

We retrieve a characteristic vibrational response which we can link to the ultrafast motion within the underlying PES. Based on density functional theory calculations we reveal the two-dimensional PES and the location of the transition state. Using ab initio molecular dynamics simulations, we demonstrate the decisive role of kinetic energy in traversing an off-diagonal transition state and overcoming the potential barrier.

References

[1] M. Rini *et al*, *Nature* **449**, 72-74 (2007)
[2] M. Mitrano *et al*., *Nature*. **530**, 461-464 (2016)
[3] T. Huber *et al*., *Physical Review. Letters* **113**, 026401 (2014)
[4] S. Vogelgesang *et al*., *Nature Physics* **14,** 184 (2018)
[5] J. G. Horstmann, H. Böckmann *et al*., *Nature* **583**, 232 (2020).
[6] S. Wippermann *et al*., *Physical Review Letters* **105**, 126102 (2010).
[7] H. Böckmann *et al*., submitted

Dynamics of Propagating and Localized Electronic Excitations Analyzed by Femtosecond Solid State Spectroscopy

U. Bovensiepen
University of Duisburg-Essen, 47057 Duisburg, Germany

An excited electron in condensed matter propagates with its momentum **k** at an energy $E(\mathbf{k})$ and experiences elastic and inelastic scattering processes, which lead to relaxation. Experiments employing femtosecond time-resolved photoelectron spectroscopy exploited so far very successfully the surface sensitivity of photoelectron spectroscopy and probed such scattering processes locally at the surface or the surface near region in the time domain [1]. Here, we report on first experimental results which analyze the non-local dynamics of excited electrons in two-photon photoemission (2PPE) [2]. In these experiments one photon excites in a Au/Fe/MgO(001) heterostructure electrons in Fe. Electron propagation through the layer stack to the Au surface is detected in 2PPE in back side pump front-probe experiments, similar to pioneering pump-probe experiments in condensed matter, which revealed time- dependent changes in the linear optical reflectivity of free standing Au films [3]. Electrons which propagate through the layer stack in the intermediate state are detected in a time-of- flight like scheme. We observe pronounced differences between front and back side pumping the heterostructure which are attributed to electron transport contributions through the layer stack. Given the investigated Au film thickness $5\ \text{nm} \leq d_{\text{Au}} \leq 30\ \text{nm}$, the Fermi velocity of Au of v_{F}=1.4 nm/fs, and the 2PPE cross correlation width on the Au surface of 70 fs we are setup to distinguish ballistic and superdiffusive transport contributions. We identify scattered electrons which propagate in a superdiffusive regime [4]. Furthermore, competition of e-e scattering with e-ph coupling will be discussed in $[\text{Fe/MgO}]_n$ heterostructures.

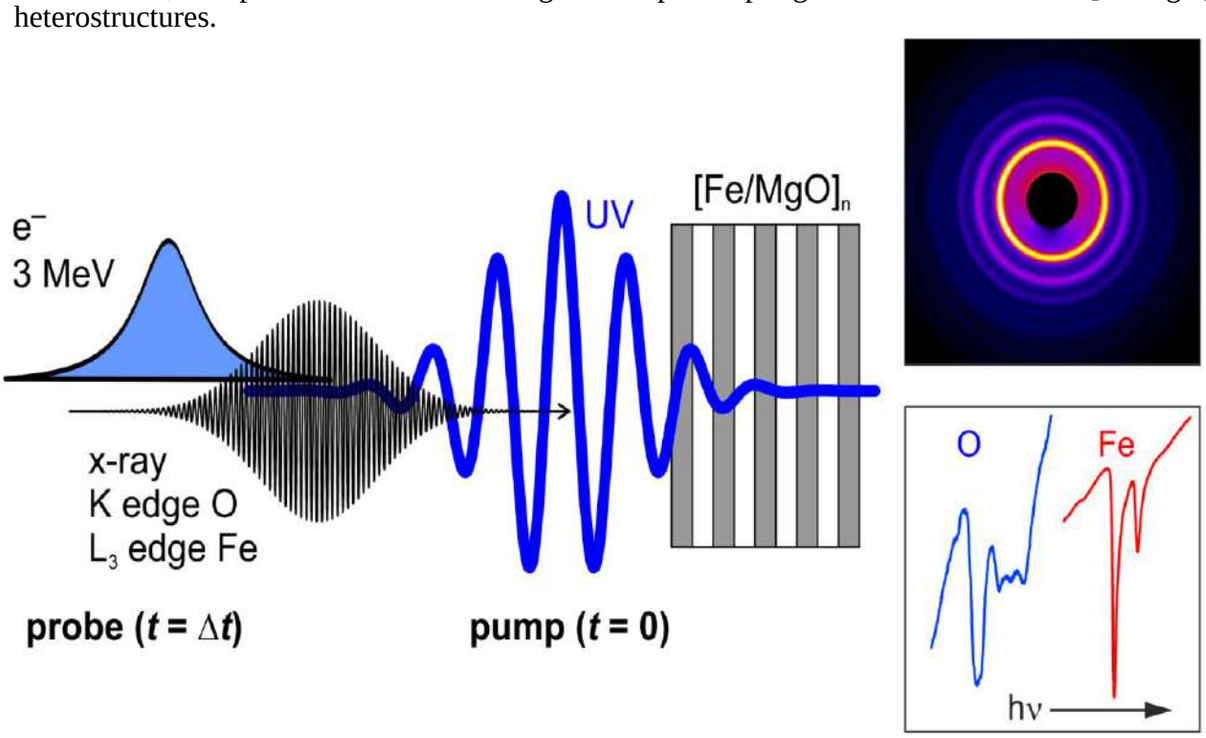

Fig.1. *Schematic of UV pump, electron diffraction, and soft x-ray probe experiment. In both cases, the signal transmitted through a Fe/MgO]$_n$ heterostructure is analyzed, see [5].*

Pump-probe experiments of element specific spectroscopy in combination with electron diffraction provide here unprecedented insights regardi the mechanism of energy transfer across interfaces and emphasize the importance of coupling of electrons with interface phonons [5].

References
[1] U. Bovensiepen, H. Petek, M. Wolf, *Dynamics at Solid State Surface and Interfaces*, Vol. **1**, Wiley-VCH, 2010.
[2] Y. Beyazit J. Beckord, P. Zhou, J. Meyburg, D. Diesing, M. Ligges, U. Bovensiepen, *arXiv*: 1910.14309.
[3] S. D. Brorson, J. G. Fujimoto, E. P. Ippen, *Physial Review. Letters* **59**, 1962 (1987).
[4] M. Battiato, K. Carva, P. M. Oppeneer, *Physical. Review* B **86**, 024404 (2012).
[5] N. Rothenbach, et al, Physical Review B 100, 174301 (2019).
This work was funded by the Deutsche Forschungsgemeinschaft through the Collaborative Research Center CRC 1242.

Low Dimentional

Crystal Electrons in Elementary Dimensions of Time and Space

A. Leitenstorfer
University of Konstanz, D-78457 Konstanz, Germany

Studies of the quantum dynamics of electrons which are confined to intrinsic spatio-temporal scales are presented. Single electrons excited in individual semiconductor quantum dots constitute the first part (Fig. 1), aiming at single-photon amplification for the ultimate control of the quantum statistics in ultrashort light pulses [1]. In these systems, the ultrafast dynamics of electrons and holes is dominated by fundamental aspects such as Coulomb correlations and the Pauli principle [2,3]. Based on a pump-probe system optimized for single-electron sensitivity at low temperatures and high magnetic fields [4], we present specimens with extremely asymmetric relaxation channels in valence and conduction bands, where femtosecond quantum kinetics of hole-phonon coupling and persistent intraband coherence of hot electrons coexist [5]. The second part introduces the concept of transient Wannier-Stark localization [6]. Here we induce a two-dimensional character in the electronic system of a bulk semiconductor by lifting the chemical bonds in the direction of subcycle electric fields of intramolecular strength, adiabatically shifting the bandgap (Fig. 2). Finally, we control the transport of single electrons in plasmonic nanoantennas with phase-locked single-cycle pulses in the near infrared-Fig. 3. The attosecond dynamics of electronic currents in a few-nanometer gap between metallic contacts is investigated both in experiment and theory [7-10].

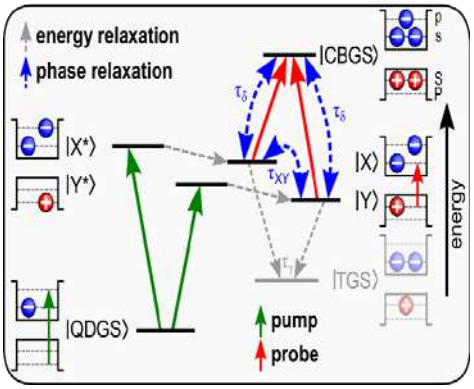

Fig.1. *Scheme of energy levels of ground-state, hot trionic and charged bi-excitonic configurations of a singly-charged CdSe/ZnSe quantum dot, including Coulomb exchange interactions between carriers. Transitions induced by broadband pump and probe pulses are indicated by green and red arrows, respectively.*

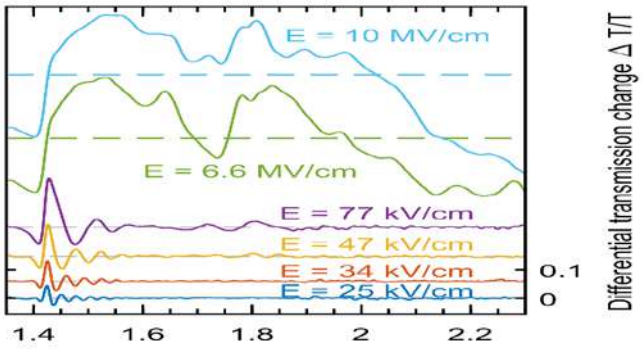

Fig.2. *Differential transmission change of GaAs under biasing with mid-infrared phaselocked waveforms, as recorded with a few-femtosecond broadband probe during the most intense half-cycle of peak electric field E. Franz-Keldysh oscillations at the fundamental absorption edge appear at low fields while beyond 5 MV/cm, an instantaneous increase of the bandgap by 0.7 eV is due to the onset of Wannier-Stark localization.*

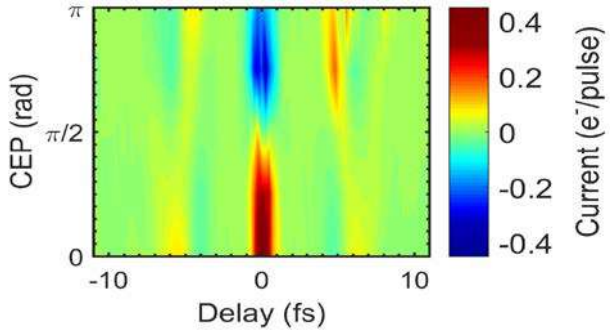

Fig.3. *Electronic current induced by biasing a gold tical antenna with a gap of 6 nm with a pair of ıgle-cycle phaselocked near-infrared pulses rived from a broadband dispersion-balanced ach-Zehnder interferometer. The duration of a ıgle pulse is 4.2 fs, covering a spectrum from 800 ı to 2200 nm. The current per double pulse is lor-coded as a function of interpulse time delay d carrier-envelope phase CEP.*

An outlook will be given, summarizing the status of our efforts to access quantum transport phenomena at truly atomic scales of space and time.

References

[1] F. Sotier et al., *Nature Physics* **5**, 352 (2009).
[2] J. Huneke et al., *Physical Review* B **84**, 115320 (2011).
[3] C. Hinz et al., *Physical Review* B **97**, 045302 (2018).
[4] C. Traum et al., *Review of Scientific Instruments* **90**, 123003 (2019).
[5] P. Henzler et al., submitted.
[6] C. Schmidt et al., *Nature Communications* **9**, 2890 (2018).
[7] T. Rybka et al., *Nature Photonics* **10**, 667 (2016).
[8] G. Aguirregabiria et al., *Faraday Discussions* **214**, 147 (2019).
[9] M. Ludwig et al., *Nature Physics* **16**, 341 (2020).
[10] M. Ludwig et al., *Physical Review* **B 101**, 241412(R) (2020).

Hot Carriers and Screening Effects in a Two Dimensional Electron Gas on InSe

L. Perfetti
Ecole Polytechnique, 91120 Palaiseau, France

The van der Waals chalcogenides display a variety of different specifics that depend on their composition and number of layers. Weak mechanical binding of atoms along the stacking direction facilitates the realization of heterostructures with different functionalities. Some recent achievements have been the fine tuning of the band gap, the control of valley polarization, and the realization of devices with high mobility. In this context, InSe is one of the building blocks with the highest potentials. On one hand, the mobility of charge carriers rivals the one measured in graphene. On the other hand, the bulk band gap of 1.26 eV is ideally suited for optoelectronic devices. In the first part of the talk I will discuss the dynamics of hot carriers in InSe on the femtosecond regime. The electrons excited by photons of 3.12 eV experience a manifold relaxation. First, they thermalize to electronic states degenerate with the M valley. Subsequently, the electronic cooling is dictated by Fröhlich coupling with phonons of small momentum transfer. Ab initio calculations predict cooling rates that are in good agreement with the observed dynamics.

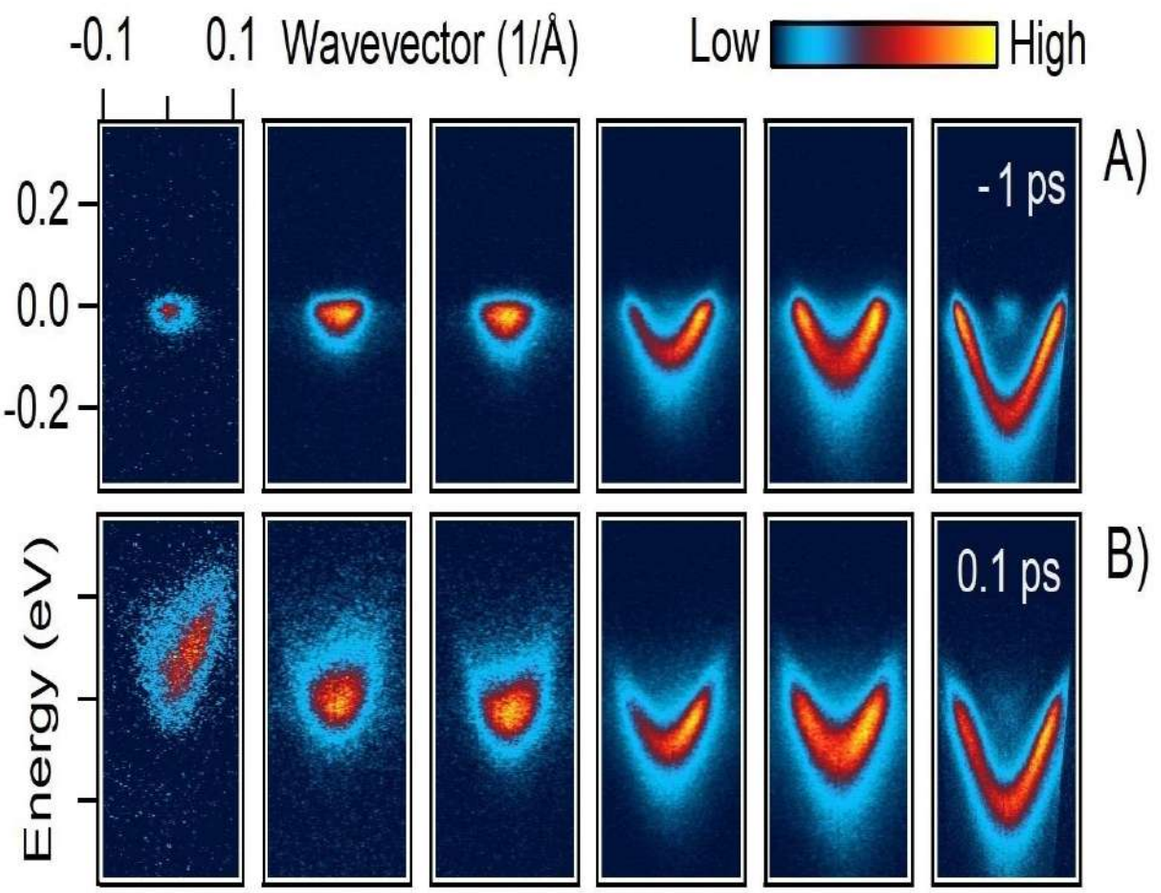

***Fig. 1**. Electrons in the accumulation layer of InSe just before **(line A)** and just after photoexcitation **(line B)**.*

We argue that electrons accumulating in states degenerate with the M valley could travel through a multilayer flake of InSe with a lateral size of 1 μm. In the second part of the talk I will discuss hot carriers cooling in a two dimensional electron gas on InSe. We show that the cooling rate can be correctly reproduced by first principle calculations accounting for the Pauli blocking of intraband transition and many-body screening of the Froehlich coupling.

References

[1] Z. Chen. et al.. *Physical Review* B **97** (24). 241201 (2018).
[2] J. Sjakste.et al.. *Journal of Physics: Condensed Matter* **30**, 353001 (2018).
[3] Z. Chen, et al., *Nano Letters* **19**, 488 (2019).

Heterostructures

Ultrafast Charge Transfer in Heterostructures of Two-Dimensional Materials

C. Trovatello, Z. Wang, V. Policht, S. Dal Conte, G. Cerullo
Politecnico di Milano, 20133 Milano, Italy

Heterostructures (HS) of two-dimensional materials offer unlimited possibilities to design new materials for applications to optoelectronics and photonics. In such HS the electronic structure of the individual layers is well retained because of the weak interlayer van der Waals coupling. Nevertheless, new physical properties and functionalities arise beyond those of their constituent blocks, depending on the type and the stacking sequence of layers. In this presentation we use high time resolution ultrafast transient absorption (TA) and two-dimensional (2D) spectroscopy to resolve the interlayer charge scattering processes in HS [1, 2]. We first study a $WSe_2/MoSe_2$ HS (Fig. 1(a)), which displays type II band alignment with a staggered gap, where the valence band maximum and the conduction band minimum are in the same layer. By two-colour pump-probe spectroscopy, we selectively photogenerate intralayer excitons in $MoSe_2$ and observe hole injection into WSe_2 on the sub-picosecond timescale, leading to the formation of interlayer excitons (Fig. 1(b)). The temperature dependence of the build-up and decay of interlayer excitons provide insights into the layer coupling mechanisms. We also employ 2D electronic spectroscopy, which guarantees simultaneously high temporal and spectral resolution, to time resolve the sub-50-fs interlayer exciton formation in a MoS_2/WS_2 HS by monitoring the dynamics at the cross peak between A excitons in MoS_2 and WS_2. Finally, we investigate a graphene/WS_2 HS where, for excitation well below the bandgap of WS_2, we observe the characteristic signal of the A and B excitons of WS_2, indicating ultrafast charge transfer from graphene to the semiconductor.

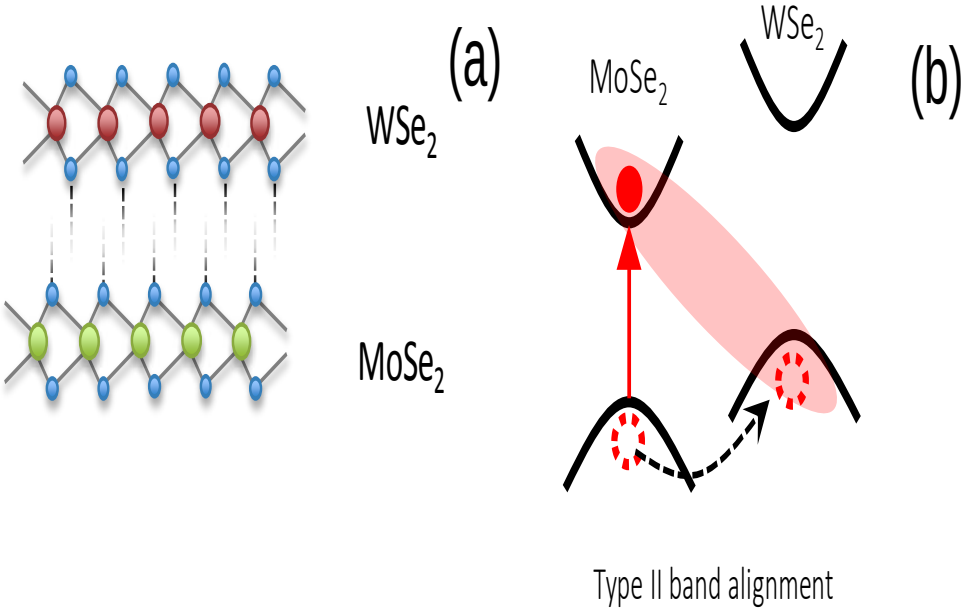

Fig. 1. ***(a)*** *A heterostructure of single-layer transition metal dichalcogenides.*
(b) *Scheme of the ultrafast hole transfer process leading to the formation of interlayer excitons.*

The nonlinear excitation fluence dependence of the TA signal reveals that the underlying mechanism is hot electron/hole transfer, whereby a tail the hot Fermi-Dirac carrier distribution in graphene tunnels through the Schottky barrier. Hot electron transfer is promising for the development of broadband and efficient low-dimensional photodetectors.

References

[1] C. Jin, E.Y. Ma, O. Karni, E.C. Regan, F. Wang, T.F. Heinz, *Nature Nanotechnology* **13**, 994 (2018).
[2] S. Dal Conte, C. Trovatello, Ch. Gadermaier, G. Cerullo, *Trends in Chemistry* **2**, 28 (2020).

Multidimensional Coherent Spectroscopy and Imaging of Transition Metal Dichalcogenides

S. T. Cundiff
University of Michigan, Ann Arbor, MI 48109 USA

Transition metal dichalcogenides (TMDs) are regarded as a prime materials platform for applications ranging from solar-energy to quantum light-emitting diodes. The rapid charge transfer [1], coherent coupling [2], and interlayer excitons (ILEs) [3,4] have been characterized for their device applications potential. Depending on the proposed application and materials system, different physical parameters matter for the feasibility and performance of a device. Dephasing times, charge transfer times and efficiency, ILE lifetimes, and coherent coupling strengths are quantities of interest. Multi-dimensional coherent spectroscopy (MDCS) [2] can show the existence of coherent coupling between excitons in $MoSe_2$ and WSe_2 monolayers stacked together to form a heterostructure, despite the presence of notable incoherent coupling in the form of charge transfer between the materials. By combining MDCS with imaging [5], we visualize complex local strain changes and map the robustness of charge transfer, coherent coupling, and ILE lifetimes across monolayers and heterostructures.

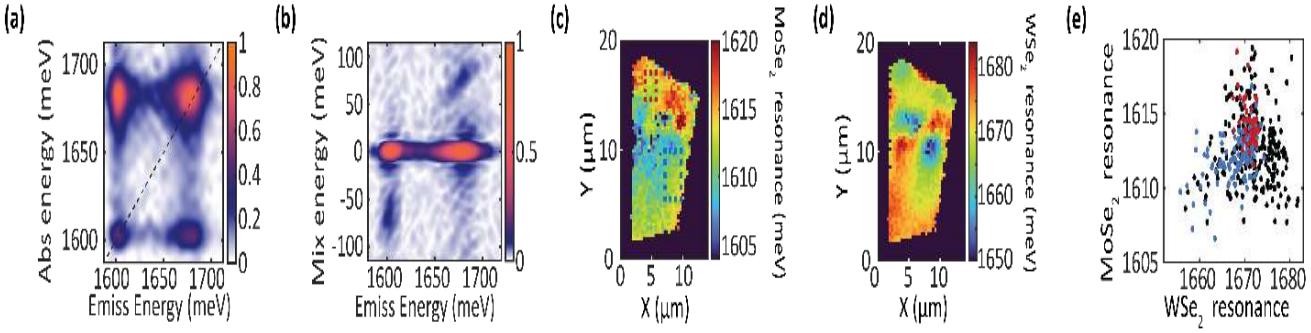

Fig. 1 (a) *Low-power MDCS spectrum of a $MoSe_2/WSe_2$ heterostructure.* ***(b)*** *Zero-quantum spectrum showing evidence for coherent coupling between $MoSe_2$ and WSe_2 excitons.* ***(c)*** *$MoSe_2$ resonance energy map* ***(d)*** *WSe_2 resonance energy map* ***(e)*** *$MoSe_2$ vs. WSe_2 resonance energy, visualizing (anti-)correlation for the areas marked by (red)blue rectangles in* ***(c)***.

A typical low-power MDCS spectrum for a heterostructure sample is shown in Fig. 1(a). The two on-diagonal peaks (dashed line) correspond to the $MoSe_2$ and WSe_2 A-excitons. The off-diagonal coupling peaks can be caused by either coherent coupling or incoherent electron and hole (charge) transfer or by both. We distinguish between coherent and incoherent coupling by performing zero-quantum spectroscopy [2], where instead of the absorption energy, the mixing energy between the two resonances is resolved. The zero-quantum spectrum shown in Fig. 1(b) clearly shows two peaks at mixing energies of ±72 meV. This value equals the energy difference between $MoSe_2$ and WSe_2 resonances and is thus a clear indication of coherent coupling. This coupling between the excitons can be caused by static dipole-dipole, exchange interactions, or transition dipole (Förster) coupling [2], among other things. We have also previously resolved the incoherent charge transfer dynamics in this sample using MDCS [2].

Robust coupling properties are critical for device applications, but not a given due to the complex strain environments common in TMD heterostructures. Demonstration of such a complex environment can be seen in Figs. 1(c-e). Fig. 1(c) and (d) are maps of the resonance energy of the $MoSe_2$ and WSe_2 exciton, respectively. Broad resonance shifts occur for both intralayer excitons. Noticeably, the resonance shifts are globally uncorrelated - with a Pearson correlation coefficient of ρ = 0.10 for all data points in Fig. 1(e), but locally strongly (anti)-correlated. This lack of correlation is evident from the resonance energies for the red (blue) rectangle in Fig. 1(c), which are plotted in red (blue) in Fig. 1(e). For the blue rectangle, there is a strong correlation (ρ = 0.54). For the red rectangle, there is a strong anti-correlation (ρ = -0.43). Since encapsulation, heterostructure formation, and strain commonly shift the resonances in both monolayers in the same direction, these observations point to complex local strain dynamics where the two materials experience different strain. The assignment to strain is further supported by the spatially inhomogeneous interlayer exciton photoluminescence (PL) shown in Fig. 2(a).

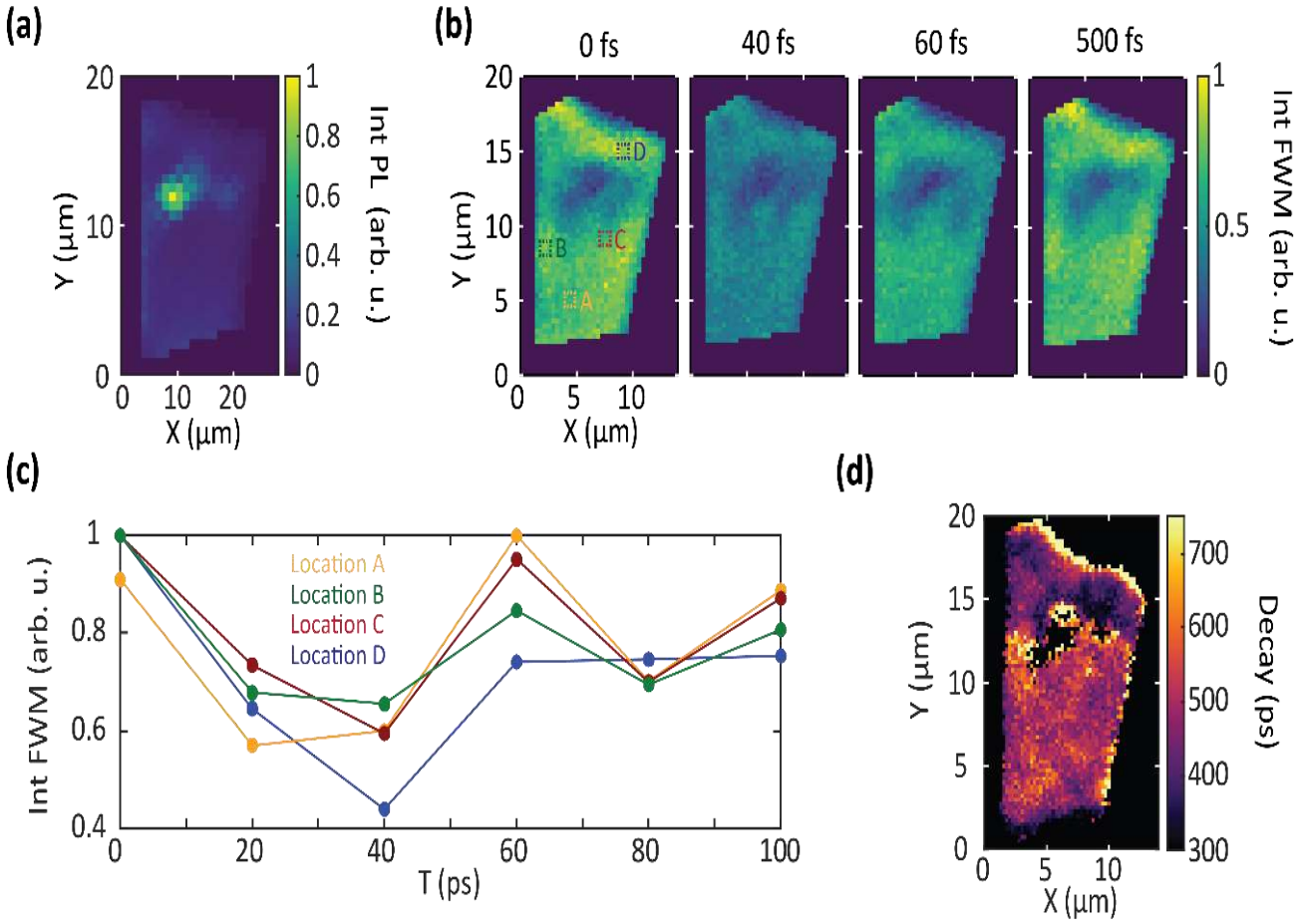

Fig. 2. ***(a)*** *Integrated PL map of the ILE.* ***(b)*** *Integrated FWM signal map for the $MoSe_2/WSe_2$ coupling peak for varying T delay.* ***(c)*** *T-dependent integrated FWM signal for the $MoSe_2/WSe_2$ coupling peak for four sample points marked in* ***(b)*** *indicated by the corresponding color.* ***(d)*** *Four-wave mixing decay map, an indirect measure of interlayer exciton lifetime.*

Despite these strain-induced changes to the sample properties, imaging MDCS experiments show a mostly uniform four-wave mixing (FWM) strength across the sample, apart from the high strain area of maximum PL emission. Fig. 2(b) shows the integrated FWM amplitude of the $MoSe_2/WSe_2$ coupling peak (lower right in Fig. 1(a)) as a function of pump-probe delay *T*. The *T*-dependence visualizes the uniformity of coherent coupling and charge transfer. The initial decay between $T = 0$ fs and 40 fs and partial recovery for 60 fs suggests coherent coupling oscillations. The rise between 100 fs and 500 fs occurs due to hole transfer from the $MoSe_2$ to the WSe_2. Given that the strength of the signal changes, but not the spatial profile, these measurements establish robustness of coherent coupling and charge transfer. This conclusion is corroborated by the full *T*-dependent data plotted in Fig. 2 (c), where the upper area of the sample shows slightly weaker coupling. Further support evidence is provided by the FWM decay map plotted in Fig. 2(d), an indirect measure of the ILE lifetime. The map shows on average lower decay times at the top of the sample, which we associate with increased layer spacing. Nonetheless, the robustness of the sample properties is surprising given the sensitivity of the couplings and ILEs to sample parameters, including twist angle and layer separation, the latter should be affected by the complex strain dynamics.

The potential of TMDs in device applications depends on the scalability and quality of fabricated devices. These results shows reproducibility of crucial physical properties across the sample, laying the groundwork for TMDs as a next-generation materials platform.

References

[1] V. R. Policht, M. Russo, F. Liu, C. Trovatello, M. Maiuri, Y. Bai, X. Zhu, S. Dal Conte, G. Cerullo, *Nano Letters* **21**, 4738 (2021).
[2] T. L. Purz, E. W. Martin, P. Rivera, W. G. Holtzmann, X. Xu, S. T. Cundiff, *Physical Review.* B **104**, L241302 (2021).
[3] P. Rivera, et al, *Nature Communications* 6, 6242 (2015).
[4] A. Ciarrocchi, D. Unuchek, A. Avsar, K. Watanabe, T. Taniguchi, A. Kis, *Nature Photonics* **13**, 131 (2019).
[5] T. L. Purz, S. T. Cundiff, E. W. Martin, *Optics Letters* **46**, 4813 (2021).
[6] B. Kasprzak, J.Patton, V. Savona, W. Langbein, *Nature Photonics* **5,** 57 (2011).

Correlation Effects in the Dynamics of Molecular Excitons

M. Aeschlimann
University of Kaiserslautern, 67663 Kaiserslautern, Germany

In the last decade, organic semiconductors have emerged as a novel class of functional materials with the potential to complement inorganic semiconductors for future electronic and spintronic applications. Most importantly, the optical and transport properties of molecular materials can be actively controlled by tuning the molecular structure and composition using chemical synthesis. This creates the opportunity to design and optimize the light absorption spectrum of molecular materials for light harvesting or photonic applications. One of the great challenges in this field is to advance todays' understanding of the light-to-charge conversion process in molecular materials. In contrast to inorganic semiconductors, optical excitation of molecular thin films with visible light does not directly result in free charge carriers, but in bound electron-hole pairs called excitons. These excitons can exhibit different degrees of localization and spatial charge distributions and are typically described in the limit of Frenkel or charge transfer (CT) excitons. The latter are particularly interesting since they can act as precursor for the generation of free charge carriers from excitons. In this contribution, we focus on the ultrafast dynamics of CT and Frenkel excitons in fullerene thin films grown on the Ag(111) surface. Using time- and momentum-resolved photoemission with fs-XUV radiation, we uncovered a transient renormalization of the local molecular valence band structure after optical excitation with visible light [1,2]. This renormalization is the result of the electronic correlations and the dielectric screening in molecular materials as shown in Fig. 1. It results in a transient linewidth broadening of the entire valence band structure which was identified by theoretical simulations as the transient spectroscopic signature of CT excitons in the molecular film. Taking advantage of this correlation, we uncovered stepwise transitions between charge transfer and Frenkel excitons with different charge character and spatial distributions.

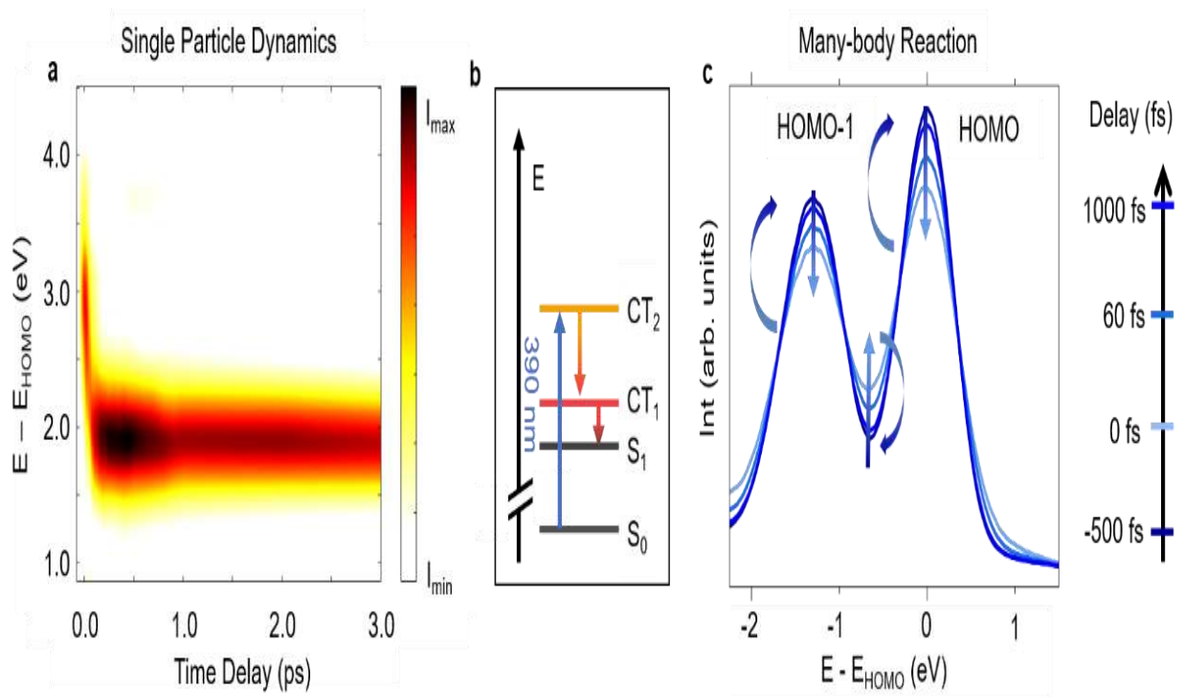

Fig. 1 (a, b.) *Single particle (exciton) dynamics, induced by our 3.2eV pump pulse. The optically generated population of CT_2 decays into CT_1 and then condenses in S_1.*
(c). *Simultaneous transient broadening of valence orbital linewidth, interpreted as many-body reaction of molecules in vicinity of a charge-transfer exciton. By comparing time scales of single particle dynamics* ***(a)*** *and many-body reaction* ***(c)****, the charge distribution of the excitonic states can be deduced.*

Our comprehensive study of the exciton dynamics of fullerene thin films provides a clear view onto transient changes of the charge character and the spatial distribution of optically excited excitons during their decay process in molecular films.

References

[1] B. Stadtmüller et al., *Nature Communications* **10,** 1470 (2019).
[2] S. Emmerich et al., Ultrafast charge-transfer exciton dynamics in C_{60} thin films, *arXiv:* 2002.04297 (2020).

THz Studies of Conductive Metal-Organic Frameworks

B. Pattengale[1], R. Okabe[2], Jr., S. Ostresh[1], C. A. Schmuttenmaer[1]
[1]*Yale University and Energy Sciences Institute, New Haven, CT 06520 USA*
[2]*Tokyo Institute of Technology, Yokohama 226-8501 Japan*

We report on the development of a light harvesting architecture based on a conductive metal organic framework (MOF) photosensitizer. The Zn_2TTFTB (TTFTB = tetrathiafulvalene tetrabenzoate) MOF was deposited directly onto the metal oxide TiO_2 and its structure was confirmed via pXRD and EXAFS measurements. Interfacial charge transfer dynamics were investigated using time-resolved THz spectroscopy. Sub-600 fs injection was observed for both the Zn_2TTFTB-TiO_2 and the TTFTB ligand-sensitized analog that lacks the extended MOF architecture. Rapid injection of a photo-generated electron is accompanied by facile migration of the corresponding hole away from the interfacial region leading to much longer recombination times in the Zn_2TTFTB-TiO_2 sample. Photocatalytic reactions, such as those related to artificial photosynthesis, involve light harvesting followed by efficient charge separation. One widely used charge separation mechanism is interfacial charge transfer, wherein a carrier transfers from one component to another in a hybrid system resulting in a state that is spatially charge-separated. However, a persistent issue with such systems is recombination of the electron in the conduction band with the surface-localized hole. Even for single-electron transfers that mediate the function of solar energy harvesting devices such as dye-sensitized solar cells (DSSCs), recombination can be prohibitively fast. Optical pump/THz probe spectroscopy was performed on Zn_2TTFTB-TiO_2 and TTFTB-sensitized TiO_2 [1]. The samples were photoexcited at 400 nm using various pump fluences as shown in Fig. 1. Zn_2TTFTB-TiO_2 shows an onset of THz attenuation that is due to electron injection into mobile conduction band states of TiO_2. It is followed by a decay that is the result of trapping and recombination processes that depopulate the conductive states.

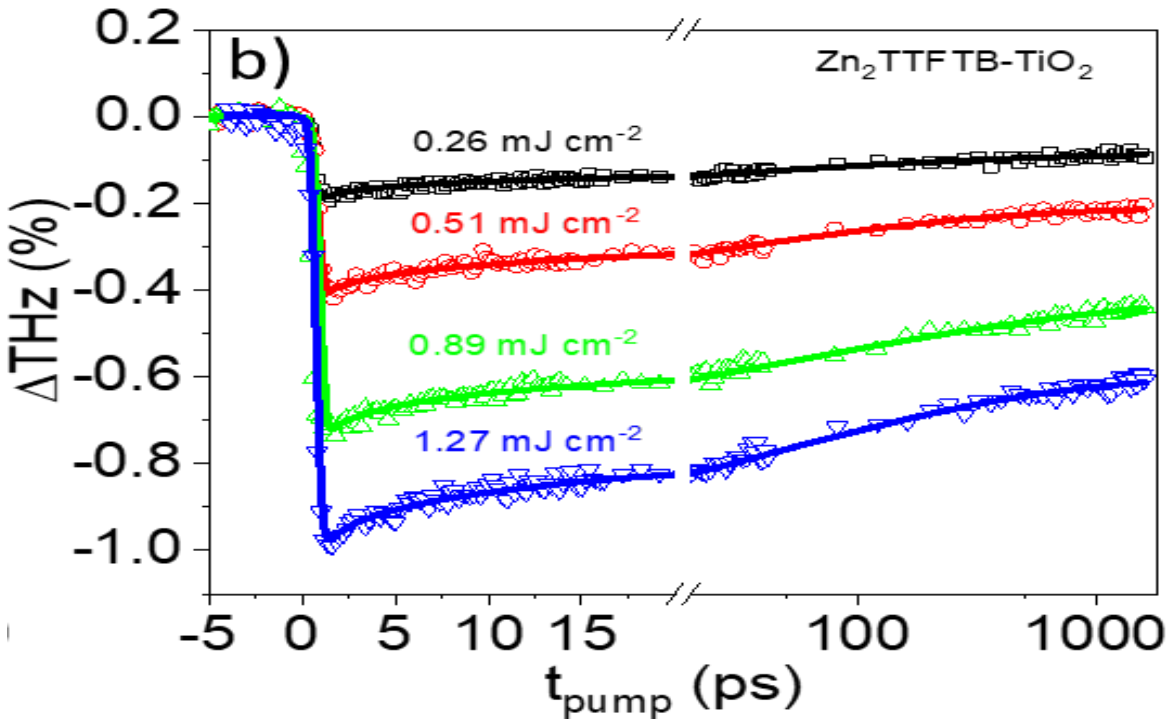

Fig. 1. *OPTP traces for Zn_2TTFTB-sensitized TiO_2 at four excitation fluences.*

A plot of the peak THz attenuation as a function of pump fluence shows that the THz attenuation scales linearly with pump fluence. The decay dynamics decrease with increasing pump fluence due to trap filling.

References

[1] B. Pattengale, J. Freeze, M. J. Guberman-Pfeffer, R. Okabe, S. Ostresh, S. Chaudhuri, V. Batista, C. Schmuttenmaer, *Chemical Science* **35**, (2020).

Anisotropic Carrier Dynamics in a Laser-excited Fe/(MgO)(001) Heterostructure from Real-time Time-dependent DFT

M. E. Gruner, E. Shomali, R. Pentcheva
University of Duisburg-Essen, 47057 Duisburg, Germany

The interaction of a femtosecond optical pulse with a metal/oxide interface is addressed in the framework of time-dependent density functional theory (TDDFT) in the real-time domain using the Elk code. In particular, we systematically investigate the layer-resolved dynamics of the electronic excitations in a $Fe_1/(MgO)_3(001)$ heterostructure as a function of laser frequency, peak power density and polarization direction [1,2]. We find a marked anisotropy in the response to in- and out-of-plane polarized light, which changes its character qualitatively depending on the excitation energy: the Fe-layer is efficiently addressed at low frequencies by in-plane polarized light, whereas for frequencies higher than the MgO band gap, we find a particularly large response of the MgO-layers for cross-plane polarized light-see Fig. 1.

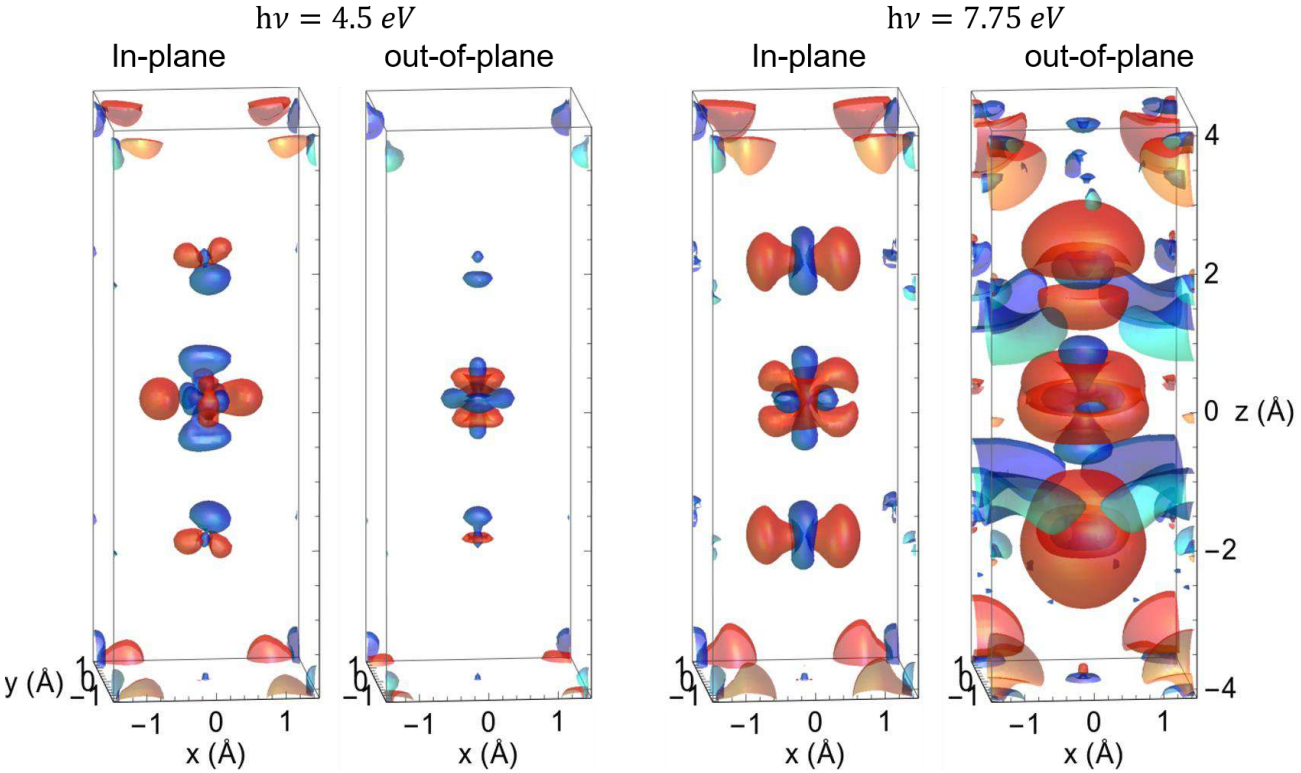

Fig. 1. *Electron density redistribution in a $Fe_1/(MgO)_3(001)$ heterostructure at t=20.2 fs with respect to t=0 upon excitation with a laser pulse with frequency of 4.50 and 7.75 eV and in- and out-of-plane polarization of the electric field (**blue**=accumulation, **red**=depletion of electronic charge). Adapted from [2].*

This points towards a path to selectively manipulate the excitation dynamics pattern in anisotropic systems. Moreover, the hybridized states at the interface play an essential role, as they mediate transitions from the valence band of MgO into the 3d states of Fe closely above the Fermi-level and transitions from the Fe-states below the Fermi level into the conduction band of MgO. As these transitions can occur simultaneously without altering charge balance of the layers, they could potentially lead to an efficient transfer of excited carriers into the MgO part.

References

[1] M. E. Gruner, R. Pentcheva, *Physical Review* B **99**, 195104 (2019).
[2] E. Shomali, M. E. Gruner, R. Pentcheva, *Physical Review* B (in press).

Funding by the German Research Foundation (DFG) within CRC 1242, project C02, and computing time at the MagnitUDE supercomputer are gratefully acknowledged.

Ultrafast Generation and Decay of a Surface Metal

L. Gierster[1], S. Vempati[2], J. Stähler[3]
[1] *Fritz-Haber-Institut der Max-Planck-Gesellschaft, 14195 Berlin, Germany*
[2] *Indian Institute of Technology Bhilai, Raipur 492015, India*
[3] *Humboldt University, 10117 Berlin, Germany*

The control of material properties upon laser excitation on ultrafast timescales is a central topic in modern physics. In many strongly correlated materials, light can trigger a photoinduced phase transition (PIPT) [1,2]. In conventional semiconductors, however, the only PIPT is ultrafast melting with intense laser pulses [3,4]. Here, we show that ZnO undergoes a semiconductor-to-metal transition (SMT) at its surface upon excitation with orders of magnitude lower laser fluence. Generation and decay of the metal phase occur on femto- and picosecond timescales, respectively. The mechanism is based on the strong surface charge induced by photodepletion of deep surface defects, different from intrinsic renormalization effects of the band structure of semiconductors in the high excitation regime. We confirm the PIPT up to near room temperature. As ZnO is transparent and one of the best oxides for nanostructuring porposes, our discovery will likely trigger new device designs based on ultrafast photoswitches. Further, the concept is likely applicable to induce PIPTs in a wide range of semiconductors.

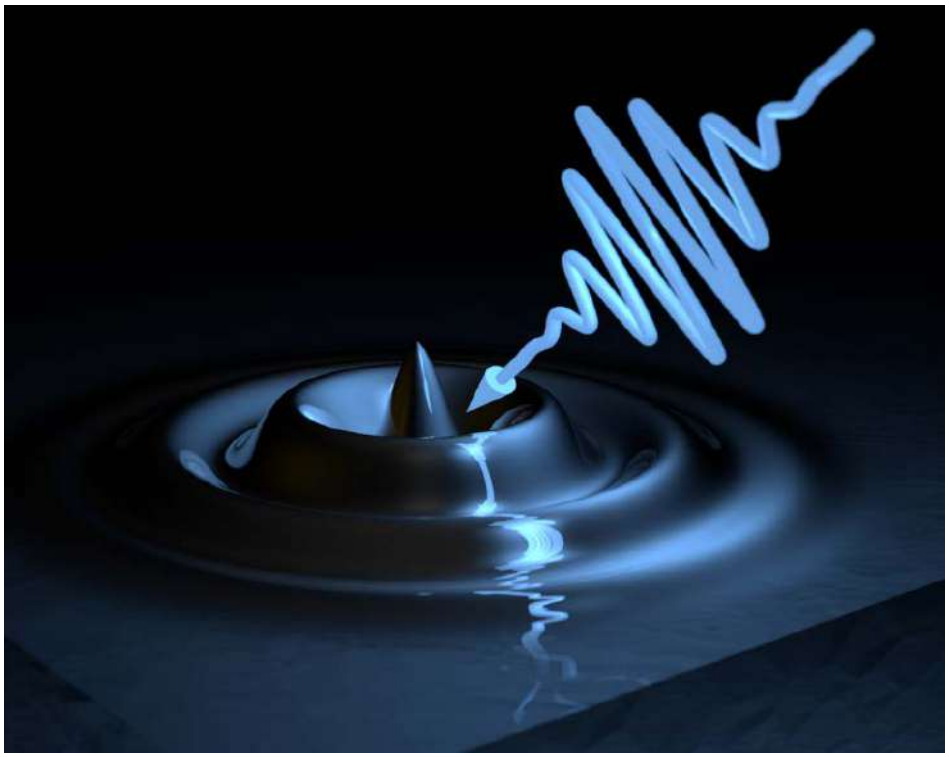

Fig.1. *Optical excitation of ZnO in the $\mu J/cm^2$ range surfaces generates a transient surface metal within only 20 fs through surface photovoltage inversion by photodoping.*

We confirm the PIPT up to near room temperature. As ZnO is transparent and one of the best oxides for nanostructuring porposes, our discovery will likely trigger new device designs based on ultrafast photoswitches. Further, the concept is likely applicable to induce PIPTs in a wide range of semiconductors.

References

[1] Y. Tokura, *Journal of The Physical Society of. Japan* **75**, 6 (2006).
[2] C. Giannetti, et al, *Advances in Physics* **65**, 58 (2016).
[3] A. Rousse, D. Hulin, *Nature* **410**, 65 (2001).
[4] L.Huang, et al., *Physical Review Letters* **1**, 185 (1998).

Intraband Transition

Carrier Dynamics in Wide Band Gap Materials: New Insights from Double Pulse Experiments

S. Guizard
Laboratoire Interactions Dynamique Lasers- CEA Saclay, 91191 Gif Sur Yvette, France

When an intense ultrashort light pulse – in the visible domain- interacts with a wide band gap dielectric, plasma can be generated by non-linear photoexcitation of carrier from the valence band to the initially empty conduction band. These carriers can be further excited in the conduction band, leading to an increase of their energy distribution, and thus of the amount of energy transferred to the material. If this deposited energy exceeds some critical threshold, permanent modification, damage or ablation may take place. The two key parameters determining the energy deposition are the density and the temperature of the plasma. In this presentation, we wish to demonstrate that a sequence of double pulse can be used to better control these two parameters, and thus to optimize energy deposition and facilitate for instance ablation of insulators and semi-conductors in the VUV domain. First, in the visible domain, using the second harmonic and the fundamental of a Ti-Sa laser, we show that time resolved double pump- and probe experiment allows to directly observe the sequence of events carrier excitation/ carrier heating, provided the parameters (energy, duration, delay) are appropriately chosen. Then, the ablation threshold (due to the first pulse) is dramatically reduced by the presence of the second pulse, while the characteristic of ablation are still determined by the first pulse [1]. Finally, new information regarding the excitation mechanisms, in particular impact ionization and avalanche are obtained [2]. For instance, a result obtained on Silica is displayed on Figure 1.

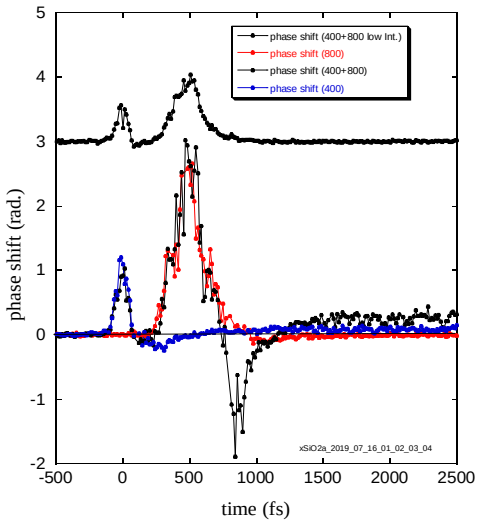

Fig.1*: Phase shift measured by time resolved interferometry in a silica (a-SiO_2) sample excited by a single pulse at 400nm* ***(blue line)*** *a single pulse at 800nm* ***(red line)*** *and when both pulses together (****black lines).*
Upper curve *-shifted by 3 rad.- at low intensity, only positive phase shift due to Kerr effect is observed.*
Lower curve*: at higher intensity,after positive phase shift due to Kerr effect, negative phase shift due to free carriers appears. The strong increase of – negative -signal when both pulse are applied is due to laser induced electronic avalanche (to be published).*

In the second part, we show that this double pulse technique can be extended in the VUV domain. Using high order harmonics of a Ti-Sa laser (harmonic 25, i.e. wavelength of 32 nm), whose intensity of far too low to damage any material, we could observe direct ablation of a dielectric, namely quartz, a-SiO_2, when the VUV pulse if followed by an IR pulse with appropriate characteristics, paving the way to direct laser machining in the VUV domain.

References

[1] S. Guizard; S. Klimentov; A. Mouskeftaras; N. Fedorov, G. Geoffroy; G. Vilmart, *Applied Surface Science* **336**, 206 (2015)..
[2] A Mouskeftaras, S Guizard, N. Fedorov, S. Klimentov, *Applied Physics A* **110** (3), 709 (2013).

Terahertz Generation in Semiconductor Quantum Dots, Incorporated in Nonlinear Matrix

O.M. Fedotova[1], O.K. Khasanov[1], G.A. Rusetsky[1], T.V.Smirnova[3], A.V. Husakou[4], A.S. Fedotov[2], U.K Usmanov[5]
[1]*Scientific-Practical Materials Research Centre, Minsk 220030, Belarus*
[2]*Belarusian State University, Minsk 220030, Belarus*
[3]*International Sakharov Environmental Institute, Minsk 220070, Belarus*
[4]*Max Born Institute, 12489 Berlin, Germany*
[5]*Tashkent State Technical University, Tashkent 100097, Uzbekistan*

We study broadband terahertz (THz) generation in nanocomposites with semiconductor quantum dots (QD) [1] incorporated into transparent dielectric matrix with quadratic nonlinearity in the field of chirped high-intensity femtosecond pulse. Distinguishing features of such media are large values of transition dipole moments (DM) between exciton states and permanent DM exceeding hundreds of Debye'-s. We propose semiconductor metal-oxide QDs (ZnO) as the most suitable material, with DM an order of magnitude greater than in CdS. The pump pulse is supposed to be in resonance with a transition between excitonic levels. Numerical code allowing to model resonant and non-resonant mechanisms of down frequency conversion in nanocomposite has been developed. We account for resonant contribution to THz generation from QDs as well as for non-resonant contribution (optical rectification) from the matrix. According to our preliminary simulations under conditions of Zakharov-Benny resonance between high- and low- frequency harmonics [2], THz generation efficiency in such materials may reach 17%. This generation originates from two-photon transitions due to impact of permanent dipole moment. Additional increase of the efficiency can be obtained using the pump phase modulation. According to our results, even in the case of THz radiation absorption by the matrix, its generation efficiency in above media (Fig.1) is η=5.82%, which is higher than that in $LiNbO_3$.

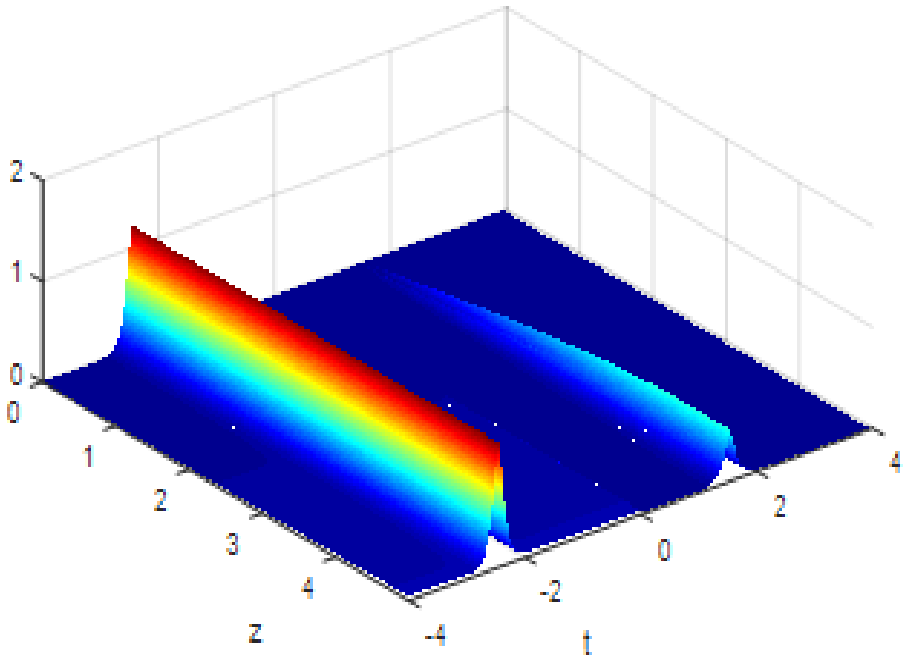

Fig. 1*: Numerical simulations of the THz generation during propagation of pump pulse with initial area* $\theta_1=4\pi$ *in KDP matrix with dissipation* $\delta=0.1$ *(propagation length* $z=4/\alpha$*,* α *is resonant absorption coefficient)*

We suggest that down-frequency conversion can be more effective in nanocomposites due to plasma formation by photoionization. In addition, one can tailor the exciton states of nanocomposite by choice of dielectric susceptibilities of the QD and the matrix material.

References

[1] D.D Awschalom, D. Loss, N.Samarth, Semiconductor Spintronics and Quantum Computation. Springer-Verlag, Berlin, Heidelberg, 2002.
[2] O Khasanov, T Smirnova, O Fedotova et.al.. *Ultrafast Bandgap Photonics III, Proc. SPIE* **10638,** 106381E1-E10, (2018).

Ultrafast Intra-Band Laser-driven Electron Dynamics and Generation of Bias-free Photocurrent Pulses in Wide-Band-Gap Semiconductors

V. Gruzdev[1], O. Sergaeva[2]
[1]*University of New Mexico, Albuquerque, NM 87106, USA*
[2]*ITMO University, St. Petersburg, 197101 Russia*

Recently, it was reported generation of electric current and charges on metal electrodes metal-dielectric-metal [1,2] of metal-semiconductor-metal [3,4] nanostructures by 1.5-cycle laser pulse without external bias via ultrafast light-to-current conversion. Theoretical interpretation of those results is a significant challenge since a broad family of potential mechanisms can be involved, e. g., Wannier-Stark localization in wide-band-gap dielectrics, quantum interference of multiphoton inter-band transitions of different orders, laser-driven intra-band Bloch oscillations of electrons, and generation of virtual carriers [1-4]. Although those results suggest breakthrough developments in many areas of ultrafast science [1-4], absence of a reliable theoretical model with good predictive capabilities substantially blocks progress in that area. Published models dominantly predict cosine-type scaling with carrier-envelope phase (CEP) and power scaling with peak intensity [1-4]. However, better understanding of physics and development of applications require scaling with pulse width, wavelength or spectral width that are not available from the published models [1-4]. In this talk, we hypothesize that the ultrafast bias-free light-to-current conversion is driven by a universal mechanism in all wide-band-gap solids. It is attributed to intra-band laser-driven oscillations of the free carriers generated by a few-cycle laser pulse via inter-band electron excitation (photo-ionization). Utilizing a recently proposed cycle-averaged approach [5], we report a simple qualitative model and analytical relations for scaling of laser-induced current (or charge) with peak irradiance, CEP, central wavelength of a few-cycle laser pulse, and material parameters. The model considers time variations of cycle-averaged electron momentum driven by pulse envelope (Fig. 1) and combined with ionization.

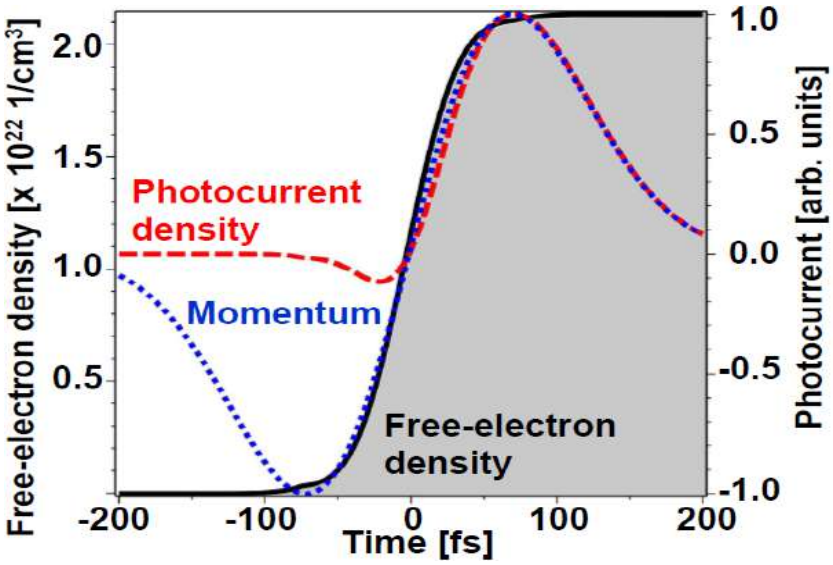

***Fig.1**. Free-electron momentum **(blue),** laser-generated conduction-band density **(black)**, and photocurrent **(red)** modeled for 90-fs laser pulse (1/e level of peak electric field) in AlN (central wavelength 2400 nm; carrier-envelope phase = 0; peak flux is 10 TW/cm^2).*

The photoionization produces monotonous increase of free-electron population that violates the temporal symmetry of the slow momentum variations within a laser pulse (Fig. 1). Since amplitude of the momentum variations reduces as inverse pulse duration, we predict power scaling of the effect with pulse duration and feasibility of detecting it even for pulses carrying as many as 10 cycles. Reported analytical relations perfectly fit the measured scaling with peak field and CEP of laser pulses [1-4] and explain some specific non-trivial features of the CEP scaling of the laser-induced electric charge.

References

[1] A. Schiffrin, T. Paasch-Colberg, N. Karpowicz et al, *Nature* **493**, 70 (2013).
[2] A. Schiffrin, T. Paasch-Colberg, N. Karpowicz, et al, *Nature* **507**, 186 (2014).
[3] T. Paasch-Colberg, A. Schiffrin, N. Karpowicz, S. Kruchinin, et al, *Nature Photonics* **8**, 214 (2014).
[4] T. Paasch-Colberg, S. Yu. Kruchinin, Ö. Saglam, et al, *Optica* **3** , 1358 (2016).
[5] V. Gruzdev, O. Sergaeva, *Physical. Review* B **98**, 11, 115202 (2018).
This work is partly supported by the Office of Naval Research via award No. N00014-21-1-2395.

Injection Current and its Role in Harmonic Generation in Amorphous Dielectrics

A. Husakou[1], P. Jürgens[1], B. Liewehr[2], B. Kruse[2], C. Peltz[2], D. Engel[1], T. Witting[1], M. Ivanov[1], M. J. J. Vrakking[1], T. Fennel[1,2], A. Mermillod-Blondin[1]
[1] *Max-Born-Institute for Nonlinear Optics, 12489 Berlin, Germany*
[2] *University of Rostock, 18059 Rostock, Germany*

Inter- and intraband electron dynamics cause Kerr-type optical nonlinearities in condensed matter; these nonlinearities not only form the basis for understanding of nonlinear optical phenomena, such as self-focusing and wave mixing, but also provide insights into the electronic properties of the solid state materials. In strong fields, Kerr nonlinearities are complemented by higher-order nonlinearities that are responsible for harmonic generation, which is currently understood as the interplay of light-driven intraband charge dynamics and interband recombination, as shown in Fig. 1(a). Remarkably, the nonlinear response originating from the associated sub-cycle ionization dynamics of emerging electrons into the conduction band has been almost completely overlooked in solids and only partially taken into account in the gas phase by the so-called Brunel term [1]. Here we investigate this strong-field-induced nonlinearity in a-SiO2 and show that close to the material damage threshold the so far unexplored injection current dominates the material response. In this contribution, we have experimentally characterized the sideband harmonic generation in fused silica by two-color pump-probe time-resolved experiment with polarization control. An extensive series of experiments allowed us to exclude Kerr-type harmonics, recombination harmonics, and intraband harmonics - see Fig. 1(a), as the origin of the observed effect. This leaves us with the two terms in ionization-induced harmonics: Brunel term and the novel term related to injection current. Simulations of light propagation and corresponding effective nonlinearity order [see curves in Fig. 1(b)] and comparison to the experimental data (circles) clearly indicate that the previously unknown injection current in fact provides dominant contribution to the optical nonlinearity of the amorphous wide-bandgap dielectrics [2].

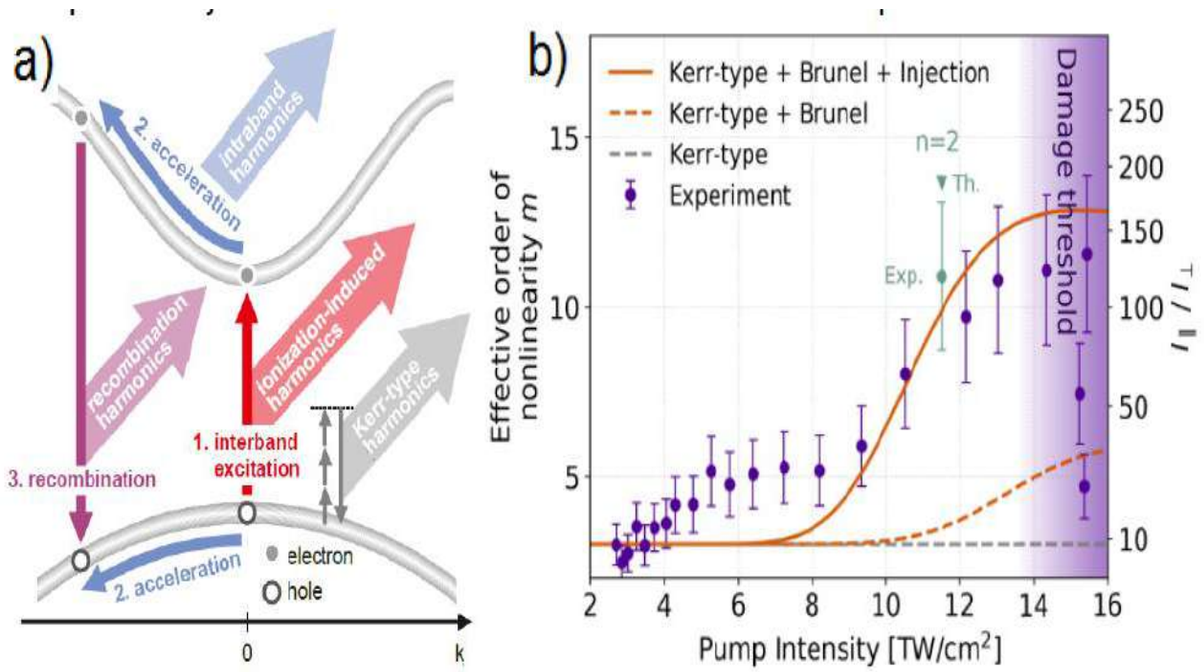

***Fig. 1**: **a)** Scheme of the relevant electron dynamics. The up to now unexplored injection current is (along with Brunel contribution) part of interband excitation, denoted by red.*
b)** Simulated effective nonlinearity order of different mechanism, along with experimental data **(circles).

Further experimental and numerical investigation provided deeper insights into the relative contribution of the two terms and into the transient dynamics of the electron ionization and motion. These findings have important implications for the studies of the optical properties of dielectrics, in particular, they provide the means to characterize and investigate the interband dynamics under the conditions of strong-field excitation.

References

[1] F. Brunel, *Journal of Optical Society of America. B* **7**.521–526 (1990).
[2] P. Jürgens et al., *https://arxiv.org/abs/*1905.05126,

Light induced Harmonic Oscillations

M. K. Rafailov
University of Alberta, Edmonton, Alberta, Canada T6G 1H9

Response to ultrashort pulse provides a glimpse into core of energy-matter interaction. Nonintuitive photovoltaic (pv) response-so called negative photoresponse or the NPR observed in earlier experiments with ultrashort - below few hundred fs, laser pulses demonstrated few peculiarities [1,2] that may not be clearly explained by any conventional models, while may open new advances in applications and not only pv ones but generally in ultrafast bandgap photonics. The most interesting is that athermal non-equilibrium induced by energies<nJ/cm^2 lasting up to ms, and while amplitude of the negative response max is strongly depends on intensity reaching up to 50% of overall max pv response, the life time is always the same-Fig. 1, a,b. Classic harmonic oscillator may not explain the effect of observed deeply "underdumped oscillations" when elastic deformations is simulated - NPR electric LRC HO simulacra is depicted in Fig.1,c

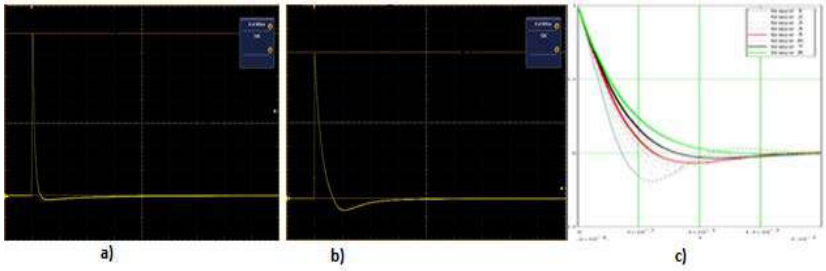

Fig. 1.*Negative photoresponse- NPR as a harmonic oscillator:*
a) *and* ***b)****-while USP intensity different in order of magnitude the NPR having the same life time; while simulacra of harmonic oscillations* ***c)*** *is not reaching even comparable lasting time in underdumped oscillation mode.*

Taking into account that "flight distance" of 10fs pulse in refractive media, say in Ge with n~4, is less than 1μm- the layer has different than bulk material transient electronic and optical ("bleached") phases as well as mechanical characteristics due to the strain -not to mention strain-induced bandgap changes [3] that leading to appeared photoluminescence that may be considered also as an energy dissipation way. Therefore transient heterostructure appears at an area of pulse entering the material and with the depth of pulse "flight distance". It is actually two different materials co-existing in one bulk for short period of time. Then timing is the key. Coherent optical phonons-CAPs generated upon USP excitation differently progressing in longitudinal and shear modes [4], they may create acoustic resonance cavities especially in "bleached" layer. That may create a resonant effect inside of that bleached layer which lasting much longer than any simple harmonic oscillations can do. There is alternative but pretty much same nature paradigm explaining of USP induced long lasting athermal nonequlibrium. Bleaching, i.e. an ultimate concentration of excited electrons in the conduction band in irradiation-affected layer creates strong electric field. The field may lead to electrostriction effect, which in its turn mechanically deforms lattice up to a point when electro-mechanic oscillations may initially formed [5] and resonate in the transient bleached layer leading to such long lasting NPR. When the majority of excited by ultrashort pulse electrons recombined and already available for another transition cycle in ps-time frame the irradiation by non-ultrafast modulated irradiance generate a conventional positive response [1].Therefore, USP and longer pulses can be combined to support metastability -effect very similar to one used in light-emitting diodes [6]. Finally, the bleached layer is an ideal "playground" where even low probability of multi-photon absorption- MPA may lead to creation of significant pool of actually free electrons and holes, that eventually may form cold electron-hole plasma-EHP [7]. The latest is not only affecting metastability with its long lasted lifetime but opens a path to new exciting applications in electronic, magnetic and optical fields. Finally few words about the tool that can be used to study such pv response in USP-material interactions: that is conventional and available on the market p-i-n photodiodes which also easy to reproduce and which is consisting of intrinsic indirect semiconductor part thatt is as a matter of fact convenient for such studies - due to its high level of CAPs generations from one side and separation of charge generation and purification (junctions) zones from each other-from another.

References

1. I.K. Zak. M.K. Rafailov. *Proceedinas SPIE* **9467**. 946726 1-7 (2015).
2. X.A. Dou, X. Sun, H. Li, X. Chen, *Optik* **126**, 3267 (2015).
4. V. Juvé, et al, *Physical Review B* **102**, 220303(R) (2020).
5. A.A. Gunjian, *IEEE Transaction on Electron Devices* **13,** 866(1966).
6. M.K. Rafailov, US Patent 10242618, *US Patent ad Trademark Office* (2019).
7. A.W. Bataller, R.A. Younts, A. Rustagi, Y. Yu, H. Ardekani, A. Kemper, L. Cao, K. Gundogdu, NanoLetters **19,** 1104 (2019).
Acknowledgment for: very interesting and productive discussions on the nature of the effect with Dr. Jason Auxier of the NRL.

Strain

Transient Strain as a Measure of Magnetic Order in Non-Equilibria Following Ultrafast Photoexcitation

A. von Reppert, J. Pudell, S. Zeuschner, M. Mattern, M. Herzog, M. Bargheer
[1]*University of Potsdam, 14467 Potsdam, Germany*

Ultrafast X-ray diffraction (UXRD) experiments provide a unique access to coherent longitudinal acoustic phonons (coherent strain wave packets) [1-3] and heat transport at the nanoscale (flow of incoherent excitations) [4-6]. Bragg-peak shifts are especially useful experimental observables in nano-layered heterostructures [2-9], and contemporary laser-based sources of hard x-rays with femtosecond pulse duration have sufficient x-ray flux and stability to analyze the dynamics of films with single-digit nanometer thickness [4]. We show examples of heterostructures composed of noble metals, transition metals or rare earths including Au, Cu, Pt, Ni, Gd, Dy, Ho, Y, Nb, $TbFe_2$, FePt, etc. This presentation will show that strain measured by UXRD is an excellent proxy for following spin-excitation both in ferromagnets and antiferromagnets [5-9]. Ultrafast changes of spin-entropy - often discussed as (sublattice-)demagnetization triggers hypersound-waves that can be analyzed in a dedicated adjacent detection layer [8-9]. Persistent spin excitations and heat flow into the spin system can be identified by a characteristic negative thermal expansion [5-9].

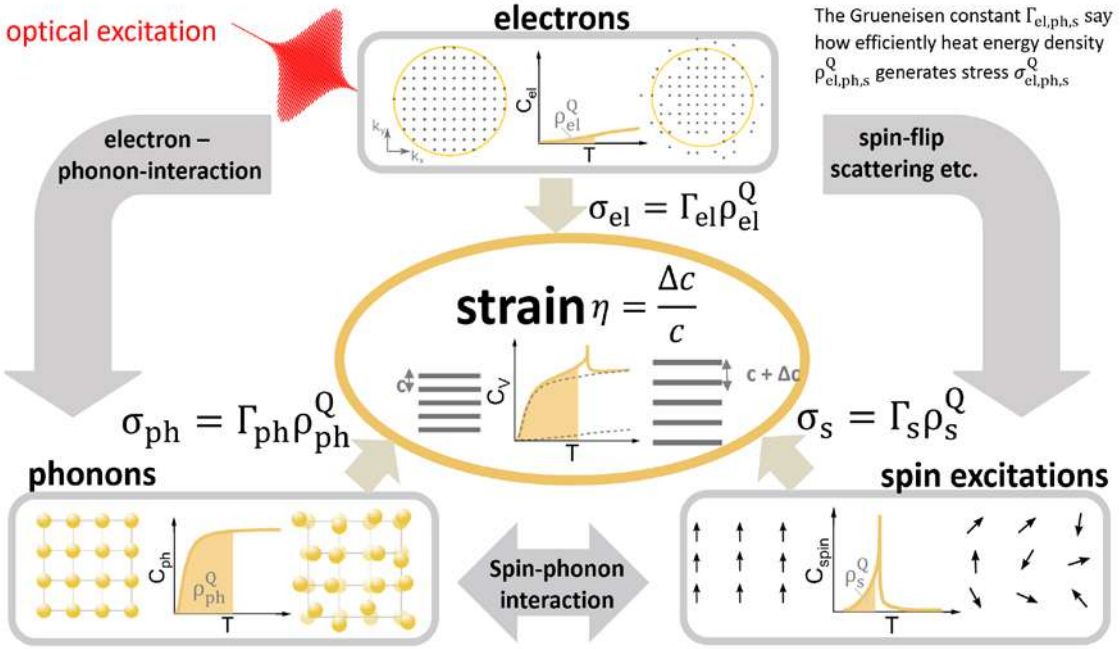

Fig. 1: *Schematic of the strain actuation by excitation various quasiparticles*

As a basis of our analysis of ultrafast (non-)thermal expansion, we discuss the concept of macroscopic Grüneisen-parameters for the electronic, magnetic, and phononic system and a thermodynamic framework of thermal expansion. In UXRD experiments with double-pump excitation we can distinguish different contributions to the thermal expansion by saturating the excitation of one of the contributing quasiparticles.

References

[1] A. Bojahr et al, *Physical Review Letters*, **115**, 195502 (2015).
[2] S. Zeuschner et al., *Structural Dynamics* **6**, 024302 (2019).
[3] A. von Reppert et al., *Applied Physics Letters* **113**, 123101 (2018).
[4] J. Pudell et al., *Nature Communications*, **9**, 3335 (2018) .
[5] A. Koc et al., *Journal of Physics: Condensed Matter* **29**, 264001 (2017).
[6] A. von Reppert et al., *Structural Dynamics* **3**, 5 (2016).
[7] A. Koc et al., *Physical Review B* **96**, 014306 (2017).
[8] J. Pudell et al., *Physical Review B* **99**, 094304 (2019).
[9] A. von Reppert et al., *Structural Dynamics*, doi: 10.1063/1.5145315 (2020).

Induced Inhomogeneous Structural Transitions in Strain Engineered Ca_2RuO_4

O. Gorobtsov, A. Lnu, J. Gollwitzer, Z. Shao, A. Singer
Cornell University, Ithaca, NY 14853, USA

The origins of a Mott metal-insulator transition (MIT) lie in an interplay of structural, electrical, and magnetic effects. The multitude of degrees of freedom opens a wide variety of technologically relevant control possibilities but complicates the physical interpretation. Strain engineering of thin coherent films is a powerful MIT control mechanism in materials with structurally driven MIT, such as the layered perovskites series Ca_2-xSrxRuO$_4$. However, nanoscale structural processes in a strain-engineered MIT and their effect on macroscopic properties, as well as ultrafast behavior, remain poorly understood. We have observed in-situ the intrinsic nanoscale domain superstructure during the MIT in an epitaxial thin film of Ca_2RuO_4 and connected it to anisotropic resistivity changes [1,2]. We have achieved this by combining X-ray nanodiffraction and macrodiffraction methods. We have observed intrinsic domains of the low temperature (LT) phases of a 100-300 nm width growing and orienting along a single direction at lower temperatures, containing a smaller (30 nm) domain structure within. Remarkably, we observed a differently oriented spatial structure in the high-temperature (HT) phase. We correlate the domain pattern orientation with the anisotropic conductivity of the material above and during the MIT.

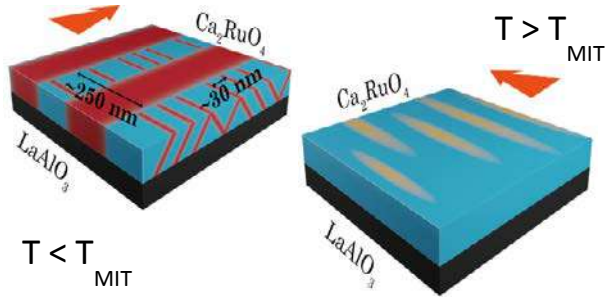

Fig.1 *Experiment-based superstructure model calcium ruthenate films below and above transition temperature.*

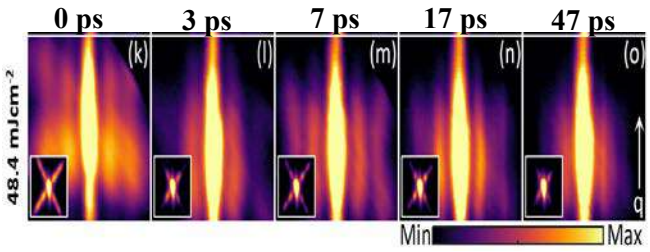

Fig.2*. Evolution and reappearance of superstructure after photoexcitation, visible in diffraction.*

Ultrafast time-resolved x-ray diffraction at X-ray free-electron lasers (XFELs) enables investigating the dynamics of photoinduced structural phase transitions. Unlike transition caused by slow temperature change, ultrafast, photoexcited transition takes different pathways. We excited the strained film with optical pulses and interrogated the structural dynamics with ultrafast time-resolved x-ray diffraction at X-FELs SACLA and LCLS. Upon photoexcitation of the predominantly low-temperature phase, we observed a one picosecond rise in normalized scattering intensity corresponding to the high-temperature phase [3]. Additionally, the Bragg peak associated with the high-temperature phase shifts in the reciprocal space, suggesting a unit cell volume expansion within one ps. Our results reveal a photoinduced volume modifying phase transition with a transition time rivaling much longer timescales observed in bulk systems. The ultrafast nature of phase transition suggests that the structural transition is non-thermal, potentially enabling the tuning of quantum material properties in ways not possible by other methods.

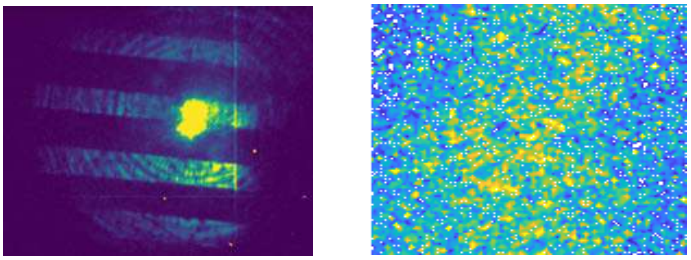

Fig.3. Examples of diffraction patterns from Ca_2RuO_4 for novel ultrafast spatial measurements: dark field microscopy image **(left)** and speckle pattern (**right)** measured at an FEL LCLS.

Furthermore, to resolve the spatial differences in the transition pathways, we have been developing methods such as ultrafast dark field microscopy [4] and speckle metrology [5] at FELs. These approaches will provide tools for understanding sub picosecond scale differences in structural transitions not just on an averaged basis, but with statistical or direct imaging of the spatial contribution.

References

[1] - [5] O. Gorobtsov, O.. Shao.Z., A. Lnu,. J Gollwitzer, A. Singer, *in preparations.*

Twisted Tessellations: Coherent Translational and Rotational Symmetry Control in Crystalline Materials with Light

G. Khalsa, J. Kaaret, N. A. Benedek
Cornell University, Ithaca, NY 14853, USA

Advances in mid and far-infrared THz sources have created a new paradigm in condensed matter physics: ultrafast structural and functional control through direct lattice excitation. Striking changes in magnetism[1], metallicity[2], ferroelectricity[3], and superconductivity[4] observed experimentally on ultrafast timescales have been tied to the *anharmonic* coupling between pumped infrared-active (IR) phonons and Raman active phonons via the *nonlinear phononics effect*. This nonlinear phononics pathway elevates coupling between two zero-wavevector phonons – the IR and Raman phonons – above the vast scattering phase space allowed in the Brillouin zone of crystalline materials.

In our theoretical exploration of coherent energy transfer from large amplitude excitations of IR phonons we have found that strong coupling to non-zero wavevector phonons is common and can dominate the lattice response, even condensing to form new nonequilibrium phases periodically modulated on extended length scales. This scenario represents coherent control of not only rotational symmetry, but also translational symmetry via the increase in the crystalline unit-cell size. We find that this coupling to non-zero wavevector phonons can be unified with the conventional nonlinear phononics pathway and several known concepts from the study of dynamical systems (Figure 1).

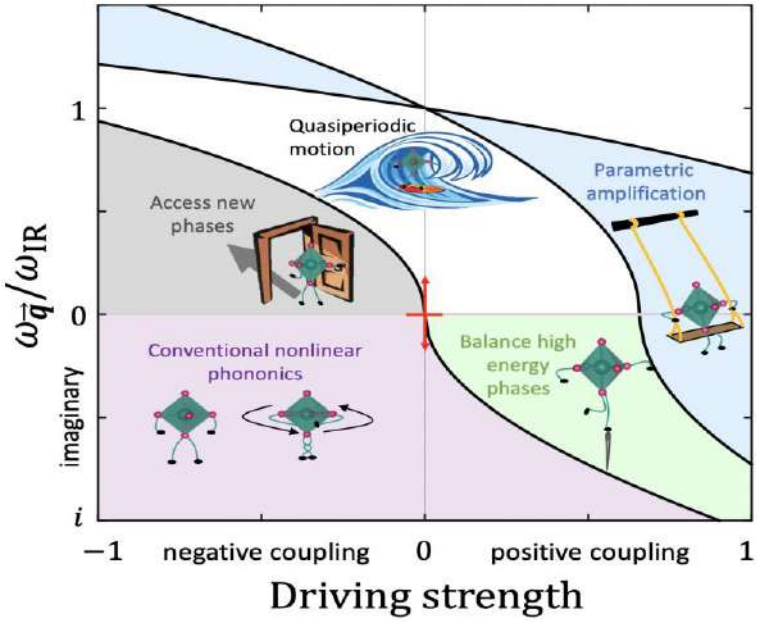

Fig. 1. Expanded nonlinear phononics phase diagram as a function of the driving strength (pump characteristics and intrinsic anharmonic coupling) and the frequency ratio of $\omega_{\vec{q}}$, where $(\omega_{\vec{q}})$ is the angular frequency of the IR (anharmonically driven) phonon. For small $\vec{q}$, driven quasiperiodic motion (**white**) -- harmonic motion weakly perturbed by the anharmonic coupling -- transitions to parametric amplification (**blue** – positive coupling) or to condensation (**gray** – negative coupling) of the non-zero wavevector phonon. For imaginary $\omega_{\vec{q}}/\omega_{IR}$, when the zone-edge mode is already condensed in the equilibrium structure, the conventional nonlinear phononics response (**purple**) is present in most of parameter space. For large positive coupling, this transitions to a new regime that selectively increases the symmetry of the crystal (**green**), before again reach a parametrically amplified response (**blue**).

In this talk, I will show that in ABO_3 perovskites (e.g. $SrTiO_3$) this coupling to non-zero wavevectors can condense zone-edge octahedral rotations above the structural phase transition temperature, in the high-symmetry cubic phase where no Raman phonons exist. Finally, I will show how selective access to new structural phases, not found in any equilibrium perovskite, is garnered and discuss strategies for theoretical and experimental identification of materials well-suited for this approach.

References

[1] M. Först et al, *Physical Review* B **84**, 241104(R) (2011).
[2] M. Rini, et al, *Nature* **449**, 72 (2007).
[3] R. Mankowsky, A. Hoegen, M. Först, A. Cavalleri, *Physical Review Letters* **118**, 197601 (2017).
[4] R. Mankowsky, et al, *Nature* **516**, 71 (2014).

Invisible Electrons: Light Producing Strain in Semiconductor Devices

E. C. Landahl
DePaul University, Chicago, IL60604, USA

Deformation potential theory was originally developed by Bardeen and Shockley [1] to describe the interactions between thermal electrons and acoustic vibrational modes in non-polar crystals. It was initially used to explain the dependence of electrical conductivity on pressure. The theory also predicts a dependence of the energy band gap upon dilation; changes in energy band structure consequently result in changes in carrier concentration. The deformation potential effect can be inverted to explain the generation of electronic strain [2]. The deformation potential can be either negative or positive. In crystal Silicon the deformation potential is negative (contractile), whereas in crystal Gallium Arsenide the deformation potential is positive (tensile) and therefore also results in expansion similar to thermal strain. In the past two decades, it has become recognized that the deformation potential often plays a dominant role in the lattice dynamics of semiconductor materials following ultrafast laser excitation [3]. In many of these studies, such as the one presented here, small transient changes in lattice spacing can be resolved by high-resolution synchrotron x-ray diffraction, and the logarithmic range of timescales probed can be exploited along with depth or material sensitivity to disentangle the transport of heat, sound, and charge in bulk or heterostructure crystals. Although both the direction and magnitude of the deformation potential has been calculated and measured in many materials of interest, it is generally assumed that the charge carriers are electron-hole pairs and exist locally in equal concentrations. To the best of our knowledge, the contributions of the individual species (electrons or holes) to electronic strain have never been directly distinguished.

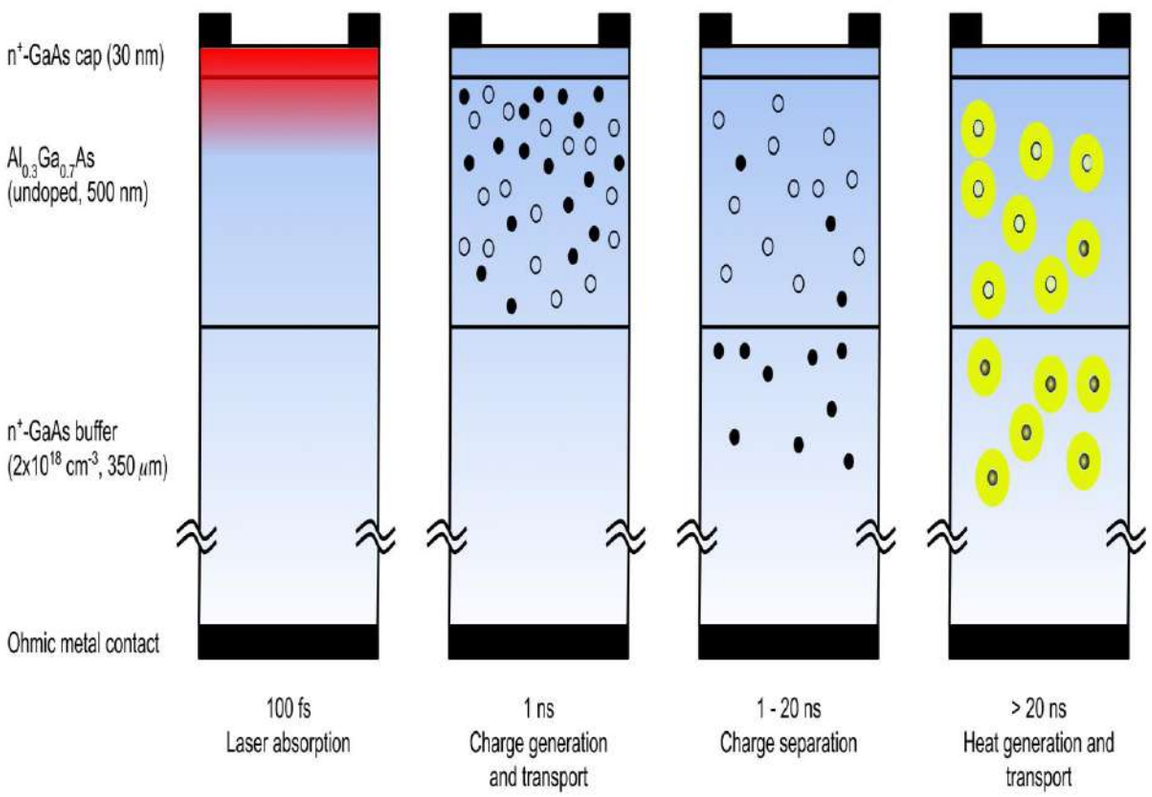

Fig. 1. *Light Producing Strain in Semiconductor Devices*

We present time-resolved x-ray measurements of strain propagating across a laser-excited intrinsic AlGaAs / n-doped GaAs interface which imply that electronic strain is produced only by holes – and that the electrons are invisible by strain measurements.

References

[1] J. Bardeen. W. Shocklev. *Phvsical Review* **80**. 72 (1950).
[2] T. Figielski, *Physica Status Solidi B* **1**, 306 (1961).
[3] G.J. Williams, S. Lee, D.A. Walko, M.A. Watson, W. Jo, D.R. Lee, E.C. Landahl, *Scientific Reports* **6**, 39506 (2016)..

Ultrafast Lasers

Recent Progress in Infrared Ultrafast Lasers and Combs based on Transition Metal Doped Chalcogenides

S.Vasilyev[1], V. Smolski[1], I. Moskalev[1], J. Peppers[1], M. Mirov[1], K. Vodopyanov[3], S. Mirov[2]
[1]*IPG Photonics Southeast Technology Center, Birmingham, AL 35211, USA*
[2]*University of Alabama at Birmingham, Birmingham AL 35294, USA*
[3]*University of Central Florida, Orlando, FL 32816, USA*

Ultrafast sources based on Cr:ZnS and Cr:ZnSe polycrystals enable direct generation and amplification of few-cycle pulses over the 2–3 μm spectral range [1]. We report ultra-broadband optical frequency comb based on Cr:ZnS fs laser platform. The laser design represents an extension of the approach that was introduced in [2]. We couple a 3-cycle Cr:ZnS oscillator to a single-pass bulk polycrystalline Cr:ZnS amplifier at a full repetition rate of f_R = 80 MHz. The amplifier is optimized for simultaneous amplification of input pulses, nonlinear pulse compression to 2-cycle regime, broadening of pulses' spectrum to an octave, and the generation of optical harmonics from second (2f) to fourth (4f) orders. Here the chain of intrapulse three-wave-mixings occurs in polycrystalline Cr:ZnS via random quasi phase matching process [3]. The spectra of adjacent optical harmonics merge in a continuum that spans 3.4 octaves from 0.4 to 4.5 μm. Thus, the spectral components used for the measurement of the comb's carrier envelope offset frequency (f_0) are obtained directly inside the laser medium. The laser architecture of the ultrafast source/comb further spectral extension to VIS-LWIR spectral range is based on a tandem arrangement of few-cycle mode-locked Cr:ZnS laser and ZGP crystal. Figure 1 compares the brilliance of obtained continuum with the brilliance of a synchrotron: we used the definition of the brilliance provided in [4] and also used the same reference spectrum. This combination enabled intrapulse difference frequency generation with unprecedented 9% efficiency, which corresponds to 1.5% conversion from off-the-shelf cw EDFL to offset-free LWIR transients. Further, the chain of three-wave mixings in ZGP significantly enhances the spectral bandwidth of the frequency comb and fundamental wavelength.

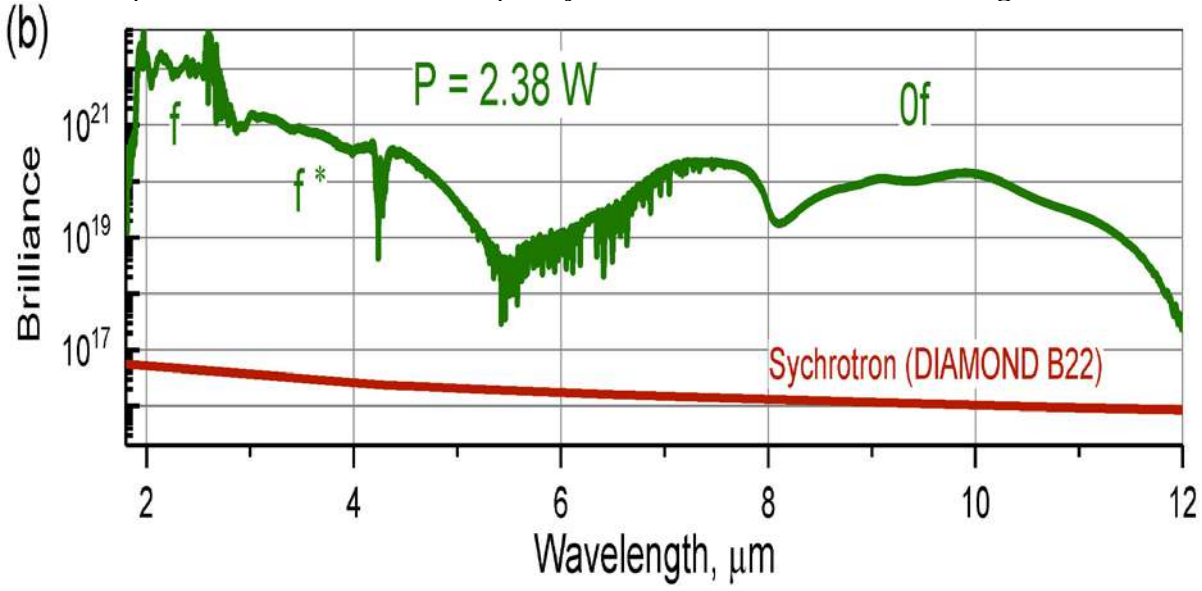

Fig. 1 *Estimated brilliance of the source in photons (s·mm^2·sr·0.1% BW)$^{-1}$, presented in log scale.*

High temporal and spatial coherence Cr:ZnS–ZGP tandems together with their compactness anaa relatively low cost opens new avenues in molecular spectroscopy.

References
[1] S. Mirov, et al., *IEEE Jornual of Selected Topics in Quantum Electronics* **24**, 1601829 (2018).
[2] S.Vasilyev, et al., *Optics Express* **27**, 35079-35087 (2019).
[3] S. Vasilyev, et al., *Proceedings of SPIE*, **9731**, Mar. 2016, Art. no. 97310B.
[4] T. P. Butler, et al., *Journal of Physics: Photonics* **1**, 044066 (2019).

Recent Advances in Ultrafast Mid-Infrared Fiber Lasers

M. Bernier, P. Paradis, V. Fortin, J.-C. Gauthier, S. Duval, M. Olivier, R. Vallée
Université Laval, Québec, G1V 0A6 Canada

Ultrafast lasers emitting in the mid-infrared (mid-IR), particularly within the 3-5 microns atmospheric window, are nowadays in strong demand, namely for spectroscopy and remote sensing in this portion of the molecular fingerprint region. Such sources are also quite promising for new applications where a strong interaction with molecules are required, for instance in biological (O-H bonds) and polymer (C-H bonds) laser processing at respectively 2.9 and 3.4 microns. Direct mid-IR femtosecond laser emission from fiber-based sources was recently reported at 2.8 and 3.1 microns [1,2] by modelocking rare-earth doped fluoride fiber gain media using the nonlinear polarization evolution mechanism. In this report, in addition to review these modelocked fiber lasers based on erbium and dysprosium in fluoride fibers, we will also discuss a promising scheme for generating new frequencies further in the mid-infrared through nonlinear amplification in a fiber-based system as illustrated in Fig 1.

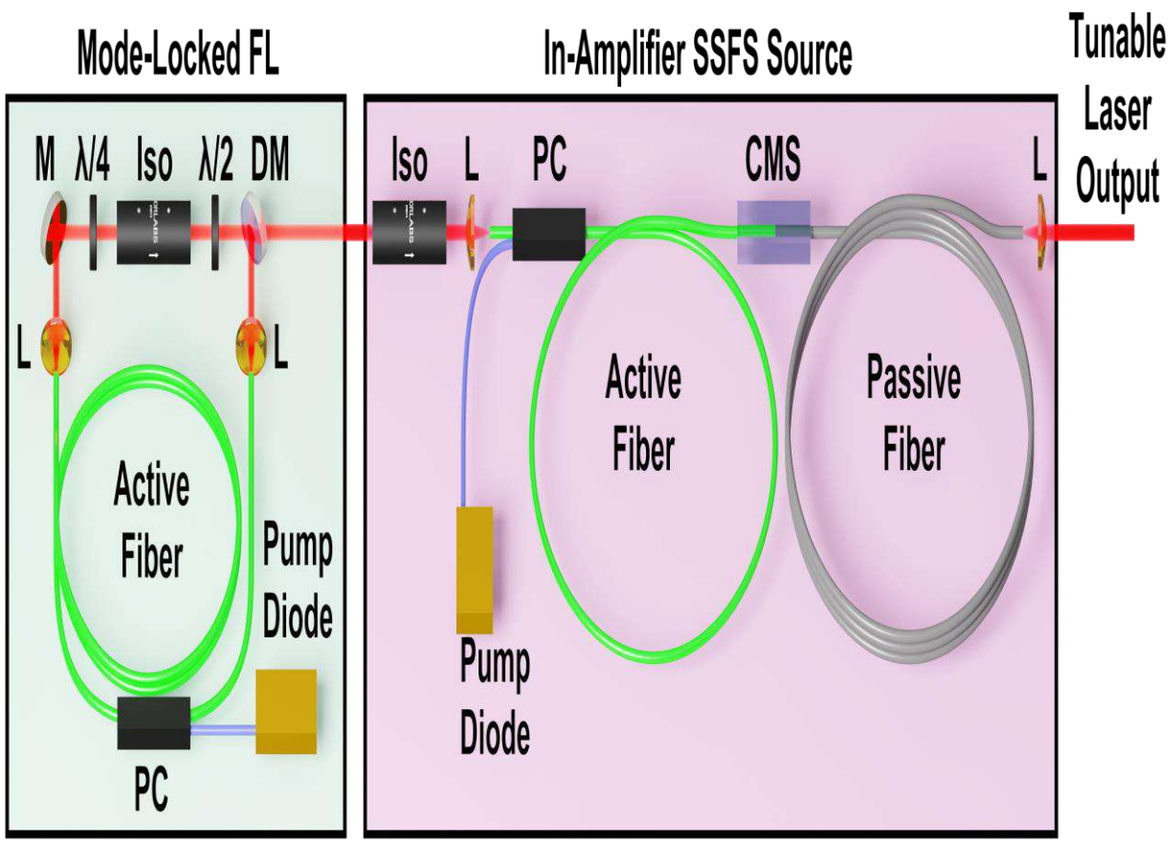

Fig. 1. *Experimental setup implementing in-amplifier nonlinear frequency conversion of a modelocked fiber laser through soliton self-frequency shift (SSFS).*
M*: Mirror,* ***λ/2****: half-wave plate,* ***λ/4****: quarter-wave plate,* ***L****: lens,* ***PC****: pump combiner,* ***ISO****: isolator,* ***DM****: dichroic mirror,* ***CMS****: cladding mode stripper*

Based on this in-amplifier approach and by seeding with picosecond pulses, we reported a few years ago on efficient supercontinuum generation in the mid-infrared, limited by the transparency of the fiber host, i.e. up to 4 microns in ZrF_4-based fibers [3] and up to 5.4 microns in InF_3-based fibers [4]. Using the same architecture but replacing the picosecond seed laser by a modelocked mid-IR femtosecond fiber laser allows for the generation of a tunable femtosecond source operating at watt-level average power based on in-amplifier soliton self-frequency shift [5]. This source is currently used to investigate promising applications, particularly for nonlinear pumping of coherent mid-IR supercontinua [6] and directed infrared countermeasures.

References

[1] S. Duval, M. Bernier, V. Fortin, J. Genest, M. Piché, R. Vallée, *Optica* **2**, 623 (2015).
[2] Y. Wang, F. Jobin, S. Duval, V. Fortin, P. Laporta, M. Bernier, G. Galzerano, R. Vallée, *Optics Letters* **44**, 395 (2019)
[3] J.-C. Gauthier, V. Fortin, S. Duval, R. Vallée, and M. Bernier, *Optics Letters* **40**, 5247 (2015)
[4] S. Duval, J.-C. Gauthier, L.-R. Robichaud, P. Paradis, M. Olivier, V. Fortin, M. Bernier, M. Piché, R. Vallée, *Optics Letters* **41**, 5294 (2016).
[5] J.-C. Gauthier, V. Fortin, J.-Y. Carrée, S. Poulain, M. Poulain, R. Vallée, M. Bernier, *Optics Letters* **41**, 1756 (2016)
[6] L.-R. Robichaud, S. Duval, L.-P. Pleau, V. Fortin, S.T. Bah, S. Châtigny, R. Vallée, M. Bernier, *Optics Express* **28**, 107 (2020).

Optical Parametric Oscillators: Recent Advances and Future Prospects

M. Ebrahim-Zadeh
ICFO-Institut de Ciencies Fotoniques, 08860 Castelldefels, Spain

The advent of novel nonlinear optical materials over the past decade, together with progress in solid-state and fiber laser technology, have had a major impact on frequency conversion sources, enabling their advancement to new spectral and temporal domains. The developments have led to the realization of a new generation of advanced solid-state sources of tunable coherent radiation, now providing formidable performance capabilities with regard to wavelength coverage, output power and efficiency, spatial, spectral and temporal quality, and in all time-scales from the continuous-wave (cw) to the ultrafast few-cycle pulses. In particular, optical parametric oscillators (OPOs) are now firmly established as truly versatile and practical sources of broadly tunable coherent radiation capable of accessing extended spectral regions from the ultraviolet (UV) to the deep-infrared (deep-IR), not available to conventional solid-state lasers. Harnessing the superior linear and nonlinear optical properties of new birefringent and quasi-phase-matched (QPM) crystals combined with advanced laser pump sources, together with the application of innovative design concepts, OPOs have transformed solid-state laser technology in new directions and towards new frontiers. The exploitation of birefringent crystals such as BiB_3O_6 (BIBO) and $CdSiP_2$ (CSP), and QPM materials such as MgO-doped periodically-poled $LiNbO_3$ (MgO:PPLN), stoichiometric $LiTaO_3$ (MgO:sPPLT), $KTiOPO_4$ (PPKTP), orientation-patterned GaAs (OP-GaAs) and GaP (OP-GaP), combined with cw and ultrafast solid-state and fiber pump lasers, have enabled the generation of tunable coherent radiation across vast spectral regions from ~250 nm in the UV up to ~12 μm in the deep-IR, and in all temporal domains from cw to few-cycle femtosecond time-scales[1-3].In the ultrafast time-scale, operation of femtosecond OPOs into deep-IR at wavelengths as long as ~8 μm has been realized by exploiting internal cascaded parametric generation based on MgO:PPLN and CSP using the KLM Ti:sapphire laser as pump source [4] or by external cascaded pumping[5] using a commercial near-IR femtosecond OPOs as the intermediate stage, as shown in Fig. 1. At the same time, by employing ultrashort pump pulses of ~20 fs duration, with careful control of dispersion, operation of femtosecond OPOs has been extended to new temporal limits, providing broadband mid-IR pulses with as few as 3.7 optical cycles and bandwidths spaning over ~500 nm [6].

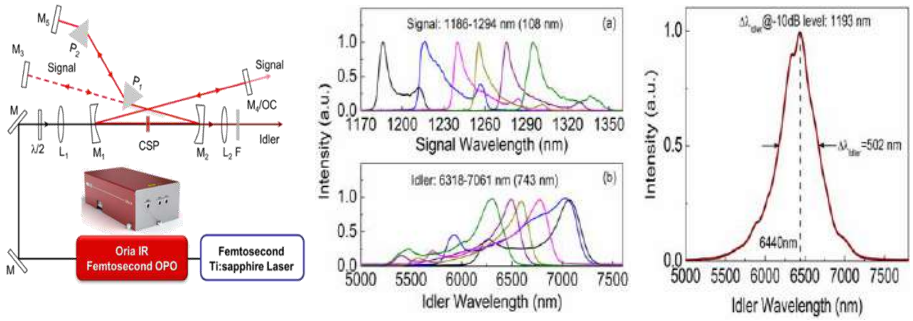

Fig.1. *Schematic of the cascaded CSP femtosecond OPO tunable in the deep-IR; Corresponding* ***(a)*** *signal, and* ***(b)*** *idler spectra across the tuning range; Representative idler spectrum centred at 6440 nm [5].*

More recently, operation of ultrafast femtosecond OPOs has been achieved at wavelength beyond 8 μm in the deep-IR by direct pumping with the KLM Ti:sapphire laser, and without the need for intermediate cascaded step[7,8]. The configuration of the OPO is shown in Fig. 2. By exploiting type-I (*e*→*oo*) critical phase-matching in combination with angle-tuning in CSP, the high-repetition-rate femtosecond OPO can provide continuous wavelength coverage across 7306–8329 nm (1201–1369 cm^{-1}) in the deep-IR. The oscillator delivers up to 18 mW of idler average power at 7306 nm and >7 mW beyond 8000 nm at 80.5 MHz pulse repetition rate, with the spectra exhibiting bandwidths of >150 nm across the tuning range. Moreover, the signal is tunable across 1128–1150 nm in the near-IR, providing up to 35 mW of average power in ~266 fs pulses at 1150 nm. Both beams exhibit single-peak Gaussian distribution in TEM_{00} spatial profile. With an equivalent spectral brightness of ~5.6×10^{20} photons s^{-1} mm^{-2} sr^{-1} 0.1% BW^{-1}, this OPO represents a viable alternative to synchrotron and supercontinuum sources for deep-infrared applications in spectroscopy, metrology and medical diagnostics. The development of high-repetition-rate ultrafast OPOs in the picosecond time-scale has also recently become possible into the deep-IR spectral range by direct pumping using Yb-fiber lasers at 1.064 μm.The major improvements in the optical quality of the CSP crystal with low

transmission loss over long interaction lengths have made it possible to overcome the low nonlinear gains under low pumping intesities, thus enabling the realization of high- repetition-rate ps picosecond OPOs at wavelegnths out to 6.7μm [9].

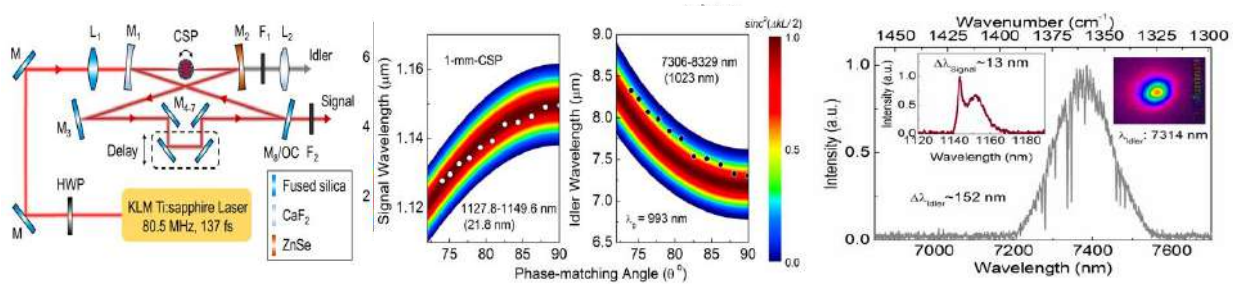

Fig. 2. *Schematic of the experimental setup for the Ti:sapphire-pumped CSP femtosecond OPO; Idler and signal tuning as a function of the internal phase-matching angle in the CSP crystal, for a pump wavelength of 993 nm, superimposed on the parametric gain map; Deep-IR idler spectrum centered on 7387 nm with a FWHM bandwidth of 152 nm.* ***Insets****: Corresponding signal spectrum centered at ~1150 nm with FWHM bandwidth of 13 nm, TEM_{00} beam profile at 7314 nm.*

The configuration of such an OPO is shown in Fig. 3. The OPO is based on a 16.3-mm-long CPS crystal at θ=90º (ϕ=45º) for type-I ($e \rightarrow oo$) noncritical phase-matching and symchorously pumped by synchronously pumped by ~20 ps pulses from a mode-locked Yb-fiber laser 79.5 MHz repetition rate. The OPO is tunable across 6205-6710 nm in the idler, providing as much as 105 mW of average power at 6205 nm, with >55 mW over nearly the entire tuning range. The deep-IR idler output exhibits a passive power stability better than 2.3% rms over 12 hours in high beam quality. With the extended wavelength coverage, practical average powers, high beam quality, and good passive stability, this OPO represents an attractive source of high- repetition-rate picosecond pulses in the deep-IR for many applications including spectroscopy and imaging. With the rapid progress in new QPM materials, such as OP-GaP, and advances in the reliable fabrication of more traditional MgO:PPLN, the development of novel OPO sources as well as more simplified single-pass OPG/ OPA across the entire mid-IR to deep-IR spectral range is now also a practical reality[10-12].

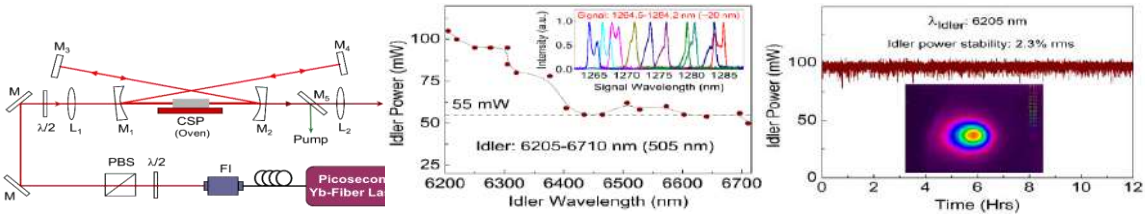

Fig. 3*. Schematic of the experimental setup for the Yb-fiber laser pumped high-average-power deep-IR picosecond OPO; Power across the idler tuning range of the picosecond CSP OPO.* ***Inset****: Signal spectra across the temperature tuning range; Long-term power stability of the deep-IR idler from the picosecond CSP OPO. Inset: Deep-IR idler beam profile at an operating wavelength of 6205 nm.*

In this talk, I will provide an overview of the latest progress at the forefront of OPO technology, enabled by new nonlinear materials, advanced solid-state and fiber laser pump sources, and novel desing concepts. I will also disucss future prospects for the advancement of OPO sources in new directions in cw and ultrafast picosecond time domain. Some emerging applications of OPO sources in optical microscopy, imaging and spectroscopy will also be highlighted.

References

[1] M. Ebrahim-Zadeh, *Solid-State Mid-Infrared Laser Sources*, *Topics in Applied Physics* Springer-Verlag **89**,184 (2003).
[2] M. Ebrahim-Zadeh, "Continuous-wave optical parametric oscillators", in *Handbook of Optics*, McGraw-Hill, 1-33 (2010).
[3] S. Chaitanya Kumar, P. G. Schunemann, K. T. Zawilski, M. Ebrahim-Zadeh, *JOSA* B **33**, D44 (2016).
[4] V. R. Badarla, et al, *Optics Letters* **41**, 1708 (2016).
[5] S. Chaitanya.Kumar, et al, *Optics Letters* **41**, 3355 (2016).
[6] S. Chaitanya. Kumar, et al, *Laser and Photonics Review* **8**, 86 (2014).
[7] C. F. O'Donnell, S. Chaitanya Kumar, K. T. Zawilski, P. G. Schunemann, M. Ebrahim-Zadeh, *Optics Letters* **43**, 1507 (2018).
[8] C. F. O'Donnell, et al, *IEEE Journal of Selected Topics in Quantum Electronics* **24**, 1 (2018).
[9] S. Chaitanya Kumar, K. T. Zawilski, P. G. Schunemann, M. Ebrahim-Zadeh, *Optics Letters* **42**, 3606 (2017).
[10] C. F. O'Donnell, S. C. Kumar, P. G. Schunemann, M. Ebrahim-Zadeh, *Optics Letters* **44**, 4570 (2019).
[11] B. Nandy, S. Chaitanya Kumar, M. Ebrahim-Zadeh, *Optics Letters* **45**, 3981 (2020).
[12] B. Nandy, S. Chaitanya Kumar, M. Ebrahim-Zadeh, *Optics Letters* **45**, 6126 (2020).

Generation of Strong Field THz Pulses and Application for Electro-absorption Modulation in Heterostructure Quantum Dots

C. Gollner[1], R. Jutas[1], D. Kreil[2], D. N. Dirin[3], S. C. Boehme[3], M. Shalaby[4], C. Brodeur[5]
M. V. Kovalenko[3], A. Baltuška[1], Audrius Pugžlys[1]
[1] *TU Wien, A-1040 Vienna, Austria*
[2] *Johannes Kepler University, A-4040 Linz, Austria*
[3] *ETH Zürich, CH-8093 Zürich, Switzerland*
[4] *EMPA, Dübendorf CH-8600, Switzerland*
[5] *Swiss Terahertz Research-Zurich, Techpark, CH-5234 Villigen, Switzerland*

Due to numerous unique properties, such as the capability of resonantly exciting crystal lattice vibrations, molecular rotations and other low energy transitions in solids, liquids and gases, terahertz (THz) radiation belongs to one of the most interesting but yet least explored spectral regions. Despite the rapid development of THz science during the last few decades, both with respect to applications and sources, the interactions of THz radiation with matter are mostly limited in the realm of linear optics. In turn, development of strong THz sources pave the way for additional interesting applications, such as control of matter by coherent lattice excitations, triggering of transient phase transitions, THz-enhanced superconductivity, polarization switching in ferroelectric materials, or THz driven Stark effect, to name only a few [1,2]. Recently, a considerable progress has been demonstrated in THz generation by optical rectification (OR) in organic crystals, such as DAST (4-N, N dimethylamino-4'-N' methyl-stilbazolium tosylate)andDSTMS(4-N,N-dimethylamino-4′-N′-methyl-stilbazolium2,4,6-trimethylbenzenesulfonate), conventionally driven by near-IR fs-pulses centered at the telecommunication wavelength of 1.5μm. Although high optical- to THz conversion efficiencies of 1-3% with pulse energies of up to 0.9 mJ [3] can be achieved, the conversion efficiency is nevertheless deteriorated by multiphoton absorption (MPA) and is fundamentally limited by the damage threshold of the crystal. This restricts the applicable pump fluence to nothing more than 20 mJ/cm^2. Therefore, the extraordinarily high THz energy of 0.9 mJ could only be achieved with a large-size partitioned crystal, wherein multiple pieces of uncoated DSTMS crystals are fixed on a host substrate in a mosaic-like structure, resulting in a crystal surface area of 4 cm^2. In this work, we report on efficient THz generation in DAST when the crystal is pumped with mid-IR sub 100-fs pulses centered at 3.9 μm [4]. With the resulting intense THz pulse, we demonstrate a direct all optical encoding of the free-space, ultrafast, high-bandwidth THz signal onto an optical signal probing the absorption of a film consisting of CdSe/CdS quantum dots (QDs) [5].

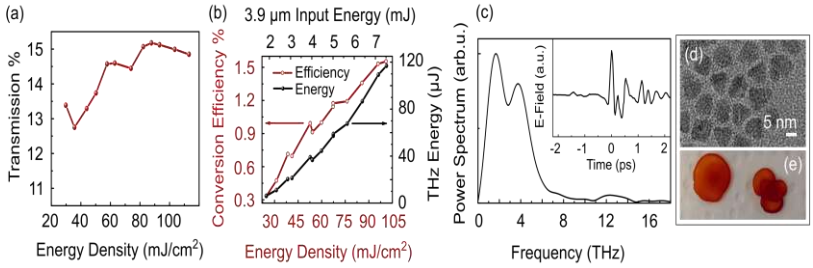

***Fig.1**. Results on optical rectification of the 3.9 μm pump pulses in a DAST crystal. Dependencies of the transmission **(a)** and optical to THz conversion efficiency **(b)** on the pump energy density. THz spectrum recorded with EOS(**c**). Transmission electron microscopy (TEM) image (**d**) and thin films of colloidal CdSe/CdS QDs drop casted on a glass substrate (**e**).*

To generate THz radiation by OR in a ~ 170 μm thick DAST crystal (Swiss Terahertz LLC), we use a high power mid-IR optical parametric chirped pulse amplifier (OPCPA), operating at a repetition rate of 20 Hz, generating up to 30 mJ of pulse energy [6]. In order to observe a possible onset of MPA, we measure the crystal transmission with respect to the pump energy density, as shown in Fig. 1 (a). The presents of MPA would be noticeable by a sudden drop in transmission, which is not detected even for a pump fluence of more than 100 mJ/cm^2, being almost one order of magnitude higher as compared to near-IR pump sources. Despite strong linear absorption at 3.9 μm, a high mid-IR to THz conversion efficiency of 1.5% can be achieved (Fig. 1 (b)), which we attribute to advantageous matching between the THz phase velocity and group velocity of the driving pulse, as well as to a resonantly-enhanced nonlinearity. Moreover, no saturation of the conversion efficiency can be distinctively identified even for pump fluence of more than 100 mJ/cm^2. The peak THz electric field strengths of 40 MV/cm is obtained by measuring the THz pulse energy, spot size and temporal field evolution with electro optic sampling (EOS). The Fourier transform of the sampled waveform reveals a multiple octave-spanning spectrum with a maximum at 2.1 THz (see Fig. 1 (c)). The measured central frequency is similar to that reported for 1.5 μm driving pulses [7], but the spectral bandwidth of 4.2 THz at

FWHM in this work is twice as broad.The resulting strong THz field is used to drive electro-absorption modulation in a drop casted film consisting of colloidal QDs, shown in Fig. 1 (d) and (e), with a CdSe core diameter of 4.1 nm, and CdS shell thickness of 2.4 nm. When an external electric field is applied to such a quantum structure, it bends the energy levels and shifts the absorption edge to smaller energies. In addition, the overlap between electron and hole wave functions decreases, which diminishes the amount of absorption, as described by the quantum confined stark effect (QCSE) [8]. The time evolution of a measured THz pulse is depicted in Fig. 2 (a) with the corresponding power spectrum in the inset. The probe pulse is provided by a wavelength tune-able optical parametric amplifier (OPA). A change in absorption in the QD film of the visible sub 50-fs probe pulse with respect to the time delay of the THz pulse is measured in a balanced detection scheme. The blue area in Fig. 2 (b) represents the THz intensity, given by the square of the THz field amplitude shown in Fig. 2 (a)

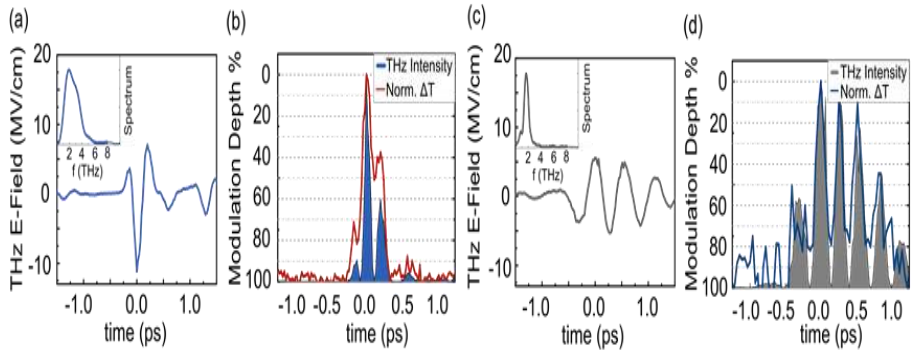

***Fig.2**. **(a)** THz waveform measured with EOS and corresponding spectrum (inset). **(b)** Normalized change in transmission of the QD sample at 622 nm **(red line)** and THz intensity **(blue area)**, obtained by taking the square of the field transient shown in **(a)**. The y-axis indicates the modulation depth. **(c)** and **(d)** present the same as **(a)** and **(b)** for a modulated THz transient.*

The relative change in transmission (red line) for a visible probe pulse centered at 622 nm (with a photon energy larger than the band gap of the hetero structure QDs) evidently follows the THz electric field. Measurements with an applied THz field strength of 13.3 MV/cm at the focal position reveal an absolute change in transmission of groundbreaking 15.8%, which is to the best of our knowledge, the highest value of electro-absorption modulation ever reported for solution processed materials at room temperature. Nevertheless, the modulation depth of the signal is limited by the pulse duration and spectral width of the probe pulse, as well as the short THz field period. The modulation time can be elongated by inserting a long pass filter with a cut-of frequency of 2 THz into the THz beam path, as shown in Fig. 2 (c). The contrast between the THz periods is thereby substantially increased, leading to an extinction ratio of 6.8 dB of the probe signal (see Fig. 2 (d)), which is on a par with conventional quantum-well electro-absorption modulators operating in the GHz range [9], demonstrating the feasibility to manipulate the electronic structure of QDs by direct THz excitation.In order to investigate the origin of the observed outstanding performance, we conduct Stark spectroscopy measurements by tuning the central wavelength of the probe pulse across the band gap of the QD film, as illustrated in Fig. 3 (a), while keeping the delay between the THz-pump and visible-probe at the position when the induced changes in absorption are the largest. The results of two separate measurements with different field strengths are presented in Fig. 3 (b) by blue and red dots. The solid lines show the results of a straightforward theoretical model, strongly supporting our experimental findings. By solving Schrödinger's equation with an envelope based ansatz numerically, we get access to the wave functions and are able to conclude fundamental physical properties from this. Note that the electric field experienced by the excitons of the QDs can be up to an order of magnitude smaller compared to the field amplitude propagating in dry air, due to screening effects of the QD film. With the electric field strength as the final and only fitting parameter, the simulation reproduces the experimental data surprisingly well and justifies further discussion on the energy band alignment of the CdSe/CdS hetero structure QDs. In general, the energy band alignment of core/shell QDs can be categorized in *type-I, quasi-type II*, and *type-II*, depending on the energy band offsets between the core and shell material and probability density of electron and hole wavefunctions. In this work, the energy band structure exhibits a quasi-type II alignment, wherein the holes are located in the core material while the electrons are delocalised across the entire QD. Figure 3 (c) shows the calculated relative change in overlap integral of the electron and hole wavefunction (top) and Stark energy shift (bottom) with respect to an applied electric field strength for three different energy band alignments. As it follows from the simulations, the strongest change of the overlap integral and the largest Stark shift, especially at small and moderate electric field strengths, is expected for type-II and quasi type-II band structures.

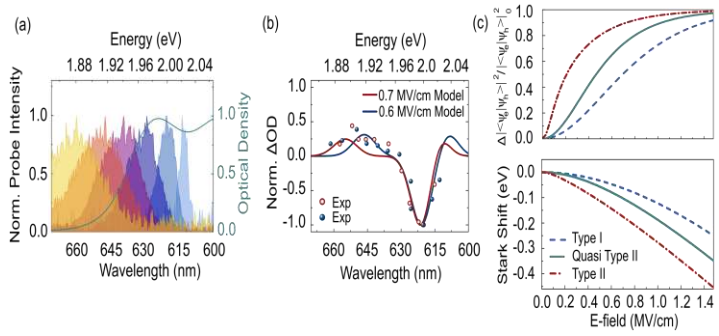

Fig.3. a) *Optical density (green line) and normalised probe spectra (**areas**) tuned across the band edge. (**b**) Measured Stark spectra (dots) for two different field strengths experienced by the excitons of the QDs, and simulated changes in optical density (**lines**) for 0.7 MV/cm (**red**) and 0.6 MV/cm (**blue**). (**c**) Relative change of the squared overlap integral of the electron and hole wavefunction (**top**) as well as Stark energy shift (**bottom**) with respect to an applied electric field for three types of energy band alignments (**see legend**). The electron and hole wavefunctions are denoted as Ψ_e and Ψ_h, respectively.*

We therefore suggest that type-II QDs are promising materials for electro-absorption modulators with extremely high modulation signals. The fact that CdSe/CdS QDs can be tuned between the type-I and type-II regime by varying the core radius and shell thickness [10], makes it possible to precisely adjust the energy band structure and optimize the performance as well as tune the operation wavelength for future high-speed optical communication systems.

References

[1] P. Salén, M. Basini, S. Bonetti, *et al*, *Physics Reports* **836-837**, 1 (2019).
[2] B. C.Pein, W.Chang, H. Y.Hwang, J.Scherer, I.Coropceanu, X.Zhao, X.Zhang, V.Bulović, M.Bawendi, K. A.Nelson, *Nano Letters* **17**,5375 (2017).
[3] A. C. Vicario, A. V. Ovchinnikov, S. I. Ashitkov, M. B. Agranat, V. E. Fortov, C. P. Hauri, *Optics Letters* **39**, 6632 (2014).
[4] C. Gollner, M. Shalaby, C. Brodeur, I. Astrauskas, R. Jutas, E. Constable, L. Bergen, A. Baltuška, A. Pugžlys, *APL Photonics* **6**, 046105 (2021).
[5] C. Gollner, R. Jutas, D. Kreil, D. N. Dirin, S. C. Boehme, A. Baltuška, M. V. Kovalenko, and A. Pugžlys, *Adv. Optical Mater*. 2102407 (2022)
[6] G.Andriukaitis,T.Balčiūnas,S.Ališauskas,A.Pugžlys,A.Baltuška,T.Popmintchev,M.-C.Chen,M.Murnane,H.Kapteyn,*Optics Letters* **36**, 2755 (2011).
[7] C. P. Hauri, C. Ruchert, C. Vicario, F. Ardana, *Applied Physics Letters* **99**, 161116 (2011).
[8] D. A. B. Miller, D. S. Chemla, T. C. Damen, A. C. Gossard, W. Wiegmann, T. H. Wood, C. A. Burrus, *Physical Review Letters* **53**, 2173 (1984).
[9] H. Fukano, T. Yamanaka, M. Tamura, *Journal of Lightwave Technolology* **25**, 1961(2007).
[10] L. Dong, A. Sugunan, J. Hu, S. Zhou, S. Li, S. Popov, M. S. Toprak, A. T. Friberg, M. Muhammed, *Applied Optics* **52**, 105 (2013).

Continuous-Wave and Pulsed Operation of Tm^{3+}-doped Fluoride Lasers near 2.3 µm

A Sennaroglu[1], A. Muti[1], Y. Morova[1], F. Canbaz[1], I. Yorulmaz[1], I. Baylam[1], M. Tonelli[2], J. E. Bae[3]
F. Rotermund[3], V. Petrov[4]
[1]*Koç University, Istanbul 34450, Turkey*
[2]*Università di Pisa, 56127 Pisa Italy*
[3]*Korea Advanced Institute of Science and Technology (KAIST), 34141 Daejeon, Republic of Korea*
[4]*Max Born Institute for Nonlinear Optics and Short Pulse Spectroscopy, 12489 Berlin, Germany*

In addition to the widely explored 2-µm laser transition to the ground level of the Tm^{3+} ion, another long-known important laser emission occurs near 2.3 µm between the $^3H_4$ and $^3H_5$ levels. The presentation will focus on some of our recent studies aimed at the investigation of tunable, continuous-wave and/or pulsed operation of Tm^{3+} ion-doped KY_3F_{10}, BaY_2F_8, and $YLiF_4$ lasers near 2.3 mm. In the continuous-wave regime, broadly tunable laser output could be obtained with Tm^{3+}:KY_3F_{10} and Tm^{3+}:BaY_2F_8 lasers in the wavelength ranges of 2260-2385 nm and 2233-2385 nm[1,2]. Graphene mode locking was employed in an extended cavity configuration to generate pulses as short as 740 fs pulses at 2340 nm from a Tm^{3+}:KY_3F_{10} laser[3]. Passive Q switching of Tm^{3+}:YLF laser was demonstrated near 2.3 µm with a Cr:ZnSe saturable absorber to generate microsecond pulses[4]. Up-conversion pumping at 1064 nm was further demonstrated as an alternative and efficient excitation scheme for the Tm^{3+}-doped KY_3F_{10} laser host [5].

References

[1] A. Muti, M. Tonelli, V. Petrov, A. Sennaroglu, *Optics Letters* **44**, 3242 (2019).
[2] A. Muti, I. Baylam, M. Tonelli, A. Sennaroglu, *Optics Letters* **45**, 4104-4107 (2020).
[3] A. Muti, F. Canbaz, M. Tonelli, J. E. Bae, F. Rotermund, V. Petrov, A.Sennaroglu, *Optics Letters* **45**, 656(2020).
[4] F. Canbaz, I. Yorulmaz, A. Sennaroglu, *Optics Letters* **42**, 1656(2017).
[5] Y. Mor**ova, M. Tonelli, V. Petrov,** A. Sennaroglu, *Opt**ics** Lett**ers*** 45**, 931**(2020).

2-µm Chirped Pulse Amplifier System Emitting >10 GW Peak Power at kHz Repetition Rate

U. Griebner, L. von Grafenstein, M. Bock, T. Elsaesser
Max Born Institute for Nonlinear Optics & Short Pulse Spectroscopy, 12489 Berlin, Germany

High performance pump sources operating at wavelengths beyond 2 µm are a key component to generate high-energy ultrashort pulses in the midwave- and longwave-infrared spectral range via parametric down-conversion. Today, such 2-µm ultrashort pulse sources, required to deliver tens of mJ pulse energy, rely on chirped pulse amplification (CPA) in holmium-doped active materials [1,2]. Here, we report on a picosecond Ho:YLF CPA at kHz repetition rate, delivering more than 10 GW of peak power. The Ho:YLF amplifier chain is composed of a regenerative amplifier (RA) and two single-pass booster amplifiers. All laser crystals are water cooled and in-band pumped at 1940 nm by continuous-wave Tm:fiber lasers. The 2-µm seed for the CPA is provided by a 40 MHz femtosecond Er:fiber laser based supercontinuum source. These pulses are stretched by two chirped volume Bragg gratings to 1 ns and pre-amplified by a single Tm:fiber amplifier to an energy of ~0.5 nJ [2].

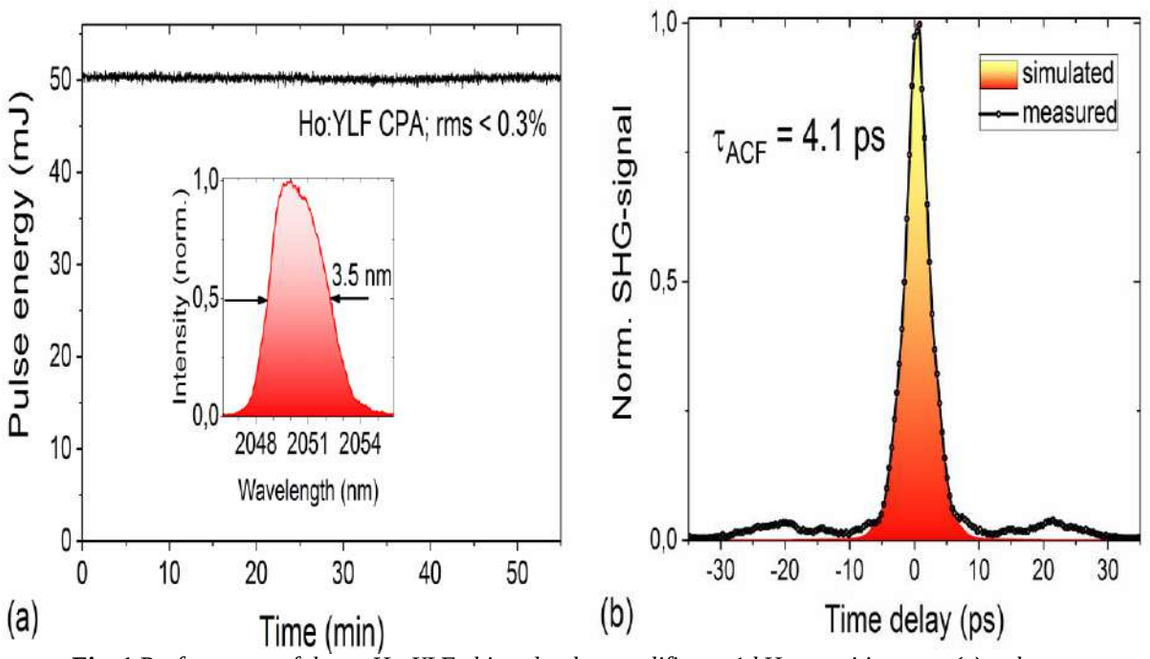

Fig. 1 *Performance of the ps Ho:YLF chirped pulse amplifier at 1 kHz repetition rate**:(a)** pulse energy and long-term stability, Inset: optical spectrum; **(b)** measured and simulated autocorrelation trace (ACF).*

The RA is carefully designed to mitigate the common issue of pulse energy bifurcation in such high-repetition rate RAs [3], and emits 11 mJ pulses at a 1 kHz repetition rate with <0.3% rms stability. The two subsequent amplifiers boost the pulse energy further to 55 mJ. With a bandwidth of 3.5 nm (FWHM), centered at 2050 nm, the spectrum supports a Fourier-transform limited (FTL) pulse duration of 1.8 ps (Inset Fig. 1a). After amplification, the pulses are compressed using a Treacy-type grating arrangement, characterized by an efficiency of 90%. The recorded autocorrelation trace (ACF) exhibits a FWHM of 4.1 ps (Fig. 1b). Applying an accumulated nonlinear phase of ~1 rad to the spectral phase of the FTL pulse [4], an excellent agreement between simulated and recorded ACF trace is reached (Fig. 1b). The corresponding pulses exhibit a FWHM pulse duration of 2.5 ps, with an estimated energy content in the main peak of >78%. This translates into a record high peak power of 14 GW for ps 2-µm CPA systems. The emitted 50 mJ pulses in the 1 kHz train are further distinguished by an excellent beam quality (M^2 <1.2) and pulse-to-pulse stability of <0.3% rms (Fig. 1a). This source is successfully applied for generation of few-cycle pulses around 5-µm with multi-millijoule energies [5], and further promising applications are under investigation.

References

[1] M. Hemmer, D. Sánchez, M. Jelínek, V. Smirnov, H. Jelinkova, V. Kubeček, J. Biegert, *Optics Letters* **40**, 451 (2015).
[2] L. von Grafenstein, M. Bock, D. Ueberschaer, U. Griebner, T. Elsaesser, *Optics Letters* **41**, 4668 (2016).
[3] L. von Grafenstein, M. Bock, U. Griebner, *IEEE Journal of Selected Topics in Quantum Electronics* **24**, (2018).
[4] D. N. Schimpf, J. Limpert, A. Tünnermann, *Optics Express* **15**, 16945 (2007).
[5] M. Bock, L. von Grafenstein, U. Griebner, T. Elsaesser, *JOSA* B **35**, C18 (2018).

Femtosecond Inscription of Fiber Bragg Gratings – Wavelength Tuning, and Phase Shifted Gratings

A. Halstuch, A. A. Ishaaya
Ben-Gurion University of the Negev, Beer-Sheva 84105, Israel

Femtosecond (fs) laser material processing, micromachining and induced refractive index change in transparent materials have become important tools for processing a variety of materials in the last two decades [1]. The advantage of using fs laser pulses is that they deliver energy into materials before thermal diffusion occurs, resulting in high precision processing and minimal collateral damage. Many devices and applications such as waveguides, couplers, and fiber Bragg gratings (FBGs) were reported [2]. NIR fs inscriptions of FBGs have been widely explored, as well as grating inscriptions in different types of fibers and with various focusing conditions have been demonstrated. FBGs are usually inscribed mainly by two techniques; the point-by-point (PbP) technique [3] and the line-by-line (LbL) technique [4] in which grating planes are formed one by one, and by the phase-mask (PM) technique, where the full grating length is inscribed as a whole [5]. Inscribing FBGs in an optical fiber using NIR fs laser radiation and a PM has been proven a fast and effective technique [6]. However, grating inscriptions using the PM technique are less flexible compared to PbP inscriptions because the Bragg wavelength is pre-determined by the PM period. In this talk, we show that by applying strain to the fiber, or by an additional defocusing lens and PM movement, or by applying various post treatments, we can tune the Bragg wavelength and inscribe phase shifted gratings (PSG). The experimental setup is shown in Fig. 1a. A PSG with two transmission dips and one peak can be seen in Fig. 1b. Tuning the Bragg wavelength with a wavelength shift of ~2 nm between each inscription with a defocusing lens and PM movement can be achieved as shown in Fig. 1c.

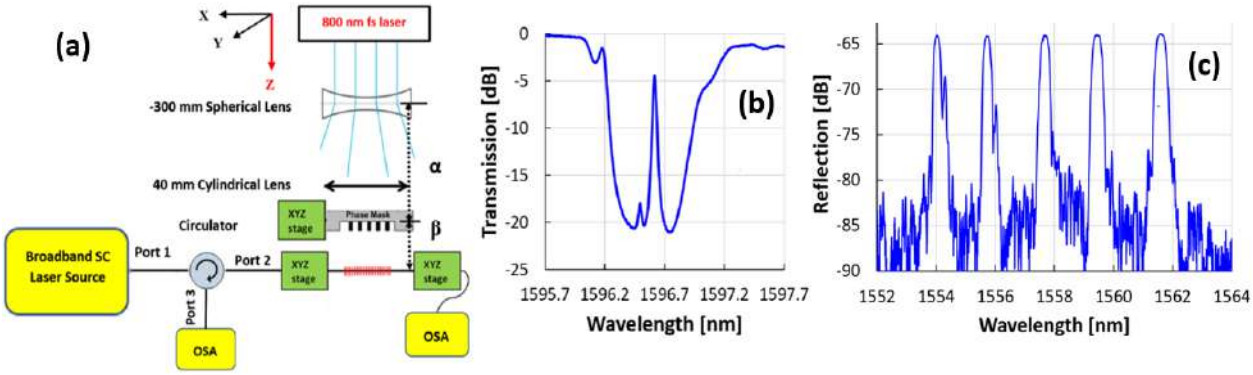

Fig. 1. *(**a**) Experimental setup. The defocusing lens is located at a distance α in front of the PM, which is located β in front of the fiber. (**b**) Inscription of a PSG with a single uniform PM. (**c**) Wavelength tuning of ~2 nm between each FBG is achieved with PM movement.*

Our experimental setup consists of an amplified 800 nm Ti-sapphire laser system (Coherent Legend Elite) producing 3.5 mJ, 35 fs pulses at a 1 kHz repetition rate. The Gaussian beam diameter is ~8 mm and is focused on the fiber core through the PM by a cylinder lens with a focal length of 40 mm. The fiber is held in two grooves, each on a three-axis stage and under controlled tension, which provide high repeatability of the system. We show that we can tune the Bragg wavelength with pre-strain. To fabricate PSGs, we inscribed two gratings, with and without strain, over the same section of the fiber, so they would overlay each other. The overlay grating structure acts as a PSG [7]. Another technique to achieve and control the wavelength tuning is to introduce a defocusing lens in front of the PM. By moving the PM to the fiber or away from the fiber we can red-shift and blue-shift the Bragg wavelength. Here we show that it is possible to inscribe FBG arrays with the same single uniform PM and PSGs as well, by simply inscribing two gratings on the same spot while tuning the Bragg wavelength between the two inscriptions with PM movement [8].

References

[1] R. R. Gattass, E. Mazur, *Nature Photonics* **2**, 219 (2008).
[2] G. Della Valle, et al., *Journal of Optics A: Pure and Applied Optics* **11**, 013001 (2009).
[3] A. Martinez, et al., *Electronics Letters* **40**, 1170 (2004).
[4] K. Zhou, et al., *IEEE Photonics Technology Letters* **22**, 1190 (2010).
[5] J. Thomas, et al., *Laser Photonics Review* **6**, 709 (2012).
[6] S. J. Mihailov, et al., *Optical Materials Express* **1**, 754 (2011).
[7] A. Halstuch, A. A. Ishaaya, *Optics Letters* **16**, 3893 (2018).
[8] A. Halstuch, A. A. Ishaaya, *Optical Fiber Technology* **67**, 102689 (2021).

High-power THz Sources based on Ultrafast Thin-Disk Lasers

F. Meyer, T. Vogel, N. Hekmat, S. Ahmed, A. Omar, Y. Wang, M. Hoffmann, C. Saraceno
Ruhr-Universität Bochum, 44801Bohum, Germany

Terahertz time domain spectroscopy (THz-TDS) has been one of the cornerstones of Terahertz science for several decades, enabling many breakthroughs both in fundamental science and applied technology. In the last decades, many impressive advancements have been achieved in laser-driven THz sources for TDS in terms of pulse energy, bandwidth and tunability. However, one crucial limitation is still the very low average power achieved (typically in the µW range), which limits many experiments due to low signal-to-noise ratios (SNR) and/or impractically long measurement times. One possible path to increase the average power of current ultrafast laser-driven THz sources is to adopt novel ultrafast solid-state lasers based on Yb as driving sources, which can nowadays provide kilowatt average powers. Despite this potential, this path has so far remained widely unexplored. To the best of our knowledge, high average power excitation >20W remained so far unexplored.

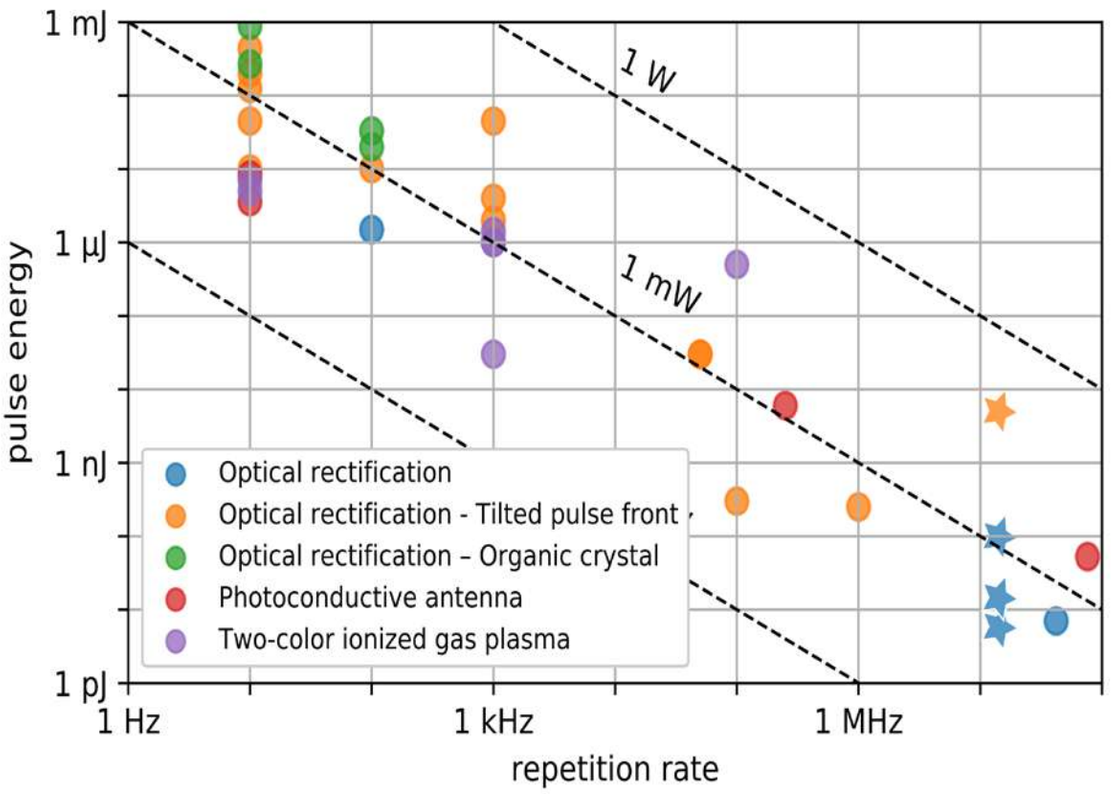

***Fig. 1**. Overview of the current state of the art THz sources. Star symbols represent our results.*

We will review here latest results of THz generation using multi-100W ultrafast laser systems. We will particularly focus our attention on recent results based on the TPF method in LN, driven by a mode-locked thin-disk oscillator with >100 W average power and operating at 13.3 MHz repetition rate. Our source reaches 66 mW of average power in optimized conditions. To the best of our knowledge this is the highest average power ever reported from a few-cycle THz source so far, reaching record high-power at 4 orders of magnitude higher repetition rate than previously reported for similar experiments. We identify the main limiting mechanisms in terms of conversion efficiency in this unusual excitation regime (MHz repetition rates and pump pulse energies around 10 µJ) and discuss possibilities for further upscaling. We believe that the watt level is within close reach, paving the way for linear and nonlinear THz-TDS experiments with unprecedented SNR at MHz repetition rates.

References

[1]. F. Meyer, et al., and C. J. Saraceno, *Optics Express* **27**, 30340 (2019).
[2]. J. Hebling, K.-L. Yeh, M. C. Hoffmann, B. Bartal, K. A. Nelson, *Journal of Optical Society of America* B **25**, B6 (2008).
[3]. S.-W. Huang, E. Granados, W. R. Huang, K.-H. Hong, L. E. Zapata, F. X. Kärtner, *Optics Letters* **38**, 796 (2013).
[4]. C. J. Saraceno, et al., and U. Keller, *IEEE Journal of. Selected Topics in. Quantum Electronics* **21**, 106–123 (2015).

Ultrafast Mid-IR Lasers: Making a Difference in Science and Industry

I. T. Sorokina[1], N. Tolstik[2], R. A. Richter[1], V. L. Kalashnikov[1], A. Rudenkov[1], E. Sorokin[3]
[1]*Norwegian University of Science and Technology, 7034 Trondheim, Norway*
[2]*ATLA lasers AS, 7034 Trondheim Norway*
[3]*TU Wien, A-1040 Vienna, Austria*

Development of ultrashort-pulsed sources in the 2–6 μm spectral bands is driven by several applications including spectroscopy, remote sensing, environmental monitoring and fine material processing. There exist several ways to reach this wavelength region, that include direct laser oscillators and amplifiers in selected mid-infrared regions, Raman frequency shifting, parametric and difference-frequency converters. The exceedingly demanding requirements set by the modern industrial applications such as fine material processing call for controlling the light generation to its extremes. The talk reviews our recent break-throughs in development and applications of a new class of industrial grade fiber/waveguide based ultrafast mid-IR lasers and frequency combs. The finely tunable operation of femto- and picosecond lasers between 2.1 microns and 3 microns, with down to few optical cycle pulse durations and up to multi-mJ pulse energies provide a new dimension, for the first time enabling *single-shot sub-wavelength and sub-surface micro-processing of semiconductors* with industrially relevant processing speeds.In this talk we review the state-of-the art in the field with a particular emphasis on our recent advances in high energy ultra-short pulsed generation and nonlinear self-frequency conversion in LMA Tm-fiber and Ho-fiber based MOPAs and their industrial applications.Direct ultrafast laser sources with wavelength beyond 2 μm are currently represented by solid-state oscillators based on Cr^{2+}-doped II-VI crystals at 2.3–2.4 μm [1], Ho-doped silica fiber lasers at 2.07–2.14 μm [2], and by fluoride fiber-based oscillators doped with Er around 2.8 μm [3] and with Ho,Pr around 2.9 μm [4]. Of these sources, the Cr^{2+}:II-VI-based lasers have shown the broadest range of parameters, from <10 MHz to GHz repetition rate, <30 fs to ps pulse duration. They also operate as a full-rep-rate 50 nJ MOPA and mJ-class kHz CPA system with 10 GW peak power [5]. Directly from the oscillator, we have demonstrated up to 100 nJ pulses using the dissipative soliton approach. The fiber-based sources are less suitable for generating high-energy pulses, but offer a possibility of easy wavelength shifting by using the Raman soliton generation in fiber amplifiers with anomalous dispersion, which is the case for silica and fluoride fibers in the mid-IR. Using this approach, Tm-fiber pulses could be shifted from 1.9 μm up to 2.4 μm [6], and Er-fiber pulses from 2.8 to 3.6 μm [3], with up to 60% of energy converted to Raman soliton. Their particular property is a possibility to finely tune the wavelength (Fig. 1, left), which is an important factor for applications [7]. Recently we could extend this technique to LMA Tm-fiber amplifier, opening the path to energy scaling [8] (Fig.1).

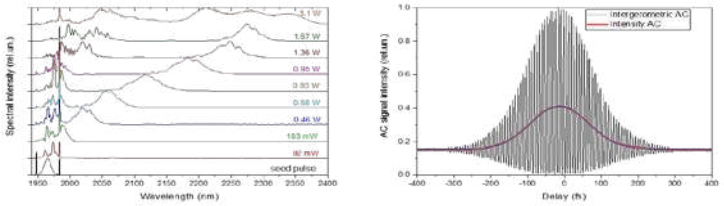

Fig. 1*. Spectral development of Raman solitons and formation of Raman soliton-induced supercontinuum in LMA Tm-fiber amplifier (**left**); autocorrelation trace of a Raman soliton at 0.95 W output power (**right**).*

Finally, the nonlinear-optical conversion, based on second-order optical nonlinearity, allows covering the wavelength gaps between the direct mid-IR sources and advancing further to longer wavelength. Such techniques as ultrafast optical parametric oscillators, amplifiers (OPAs and OPCPAs), difference-frequency and supercontinuum generation have been shown at virtually any wavelength and down to single-cycle pulse durations [9], and three optical cycle pulses with 50% absolute conversion efficiency using a periodically patterned GaP [10].

Sub-wavelength single pulse 3-D Si processing with 2.1 μm ultra-short pulsed laser. Recently, the mid-IR ultrashort pulses have been applied to fine processing of semiconductors, most notably silicon, where advancing to the mid-IR played a crucial role. Matching the wavelength to the Si "soft spot" at 2.1 μm [7,11] (Fig. 2a), we have been able for the first time to demonstrate single-pulse subsurface modification of Si with sub-wavelength resolution (down to 0.7 μm defect size (Fig. 2b) using μJ pulses at up to 50 kHz repetition rate. We were able to write single points, lines, layers, and waveguides (Fig. 2c) at 40–400 μm depths, and exfoliate 50-μm thin layers of Si along the written layer.

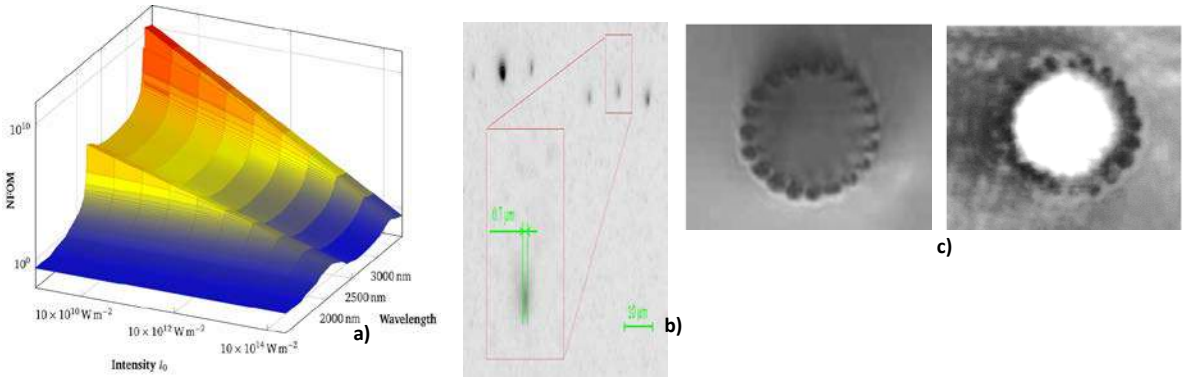

Fig. 2. *Nonlinear figure of merit (NFOM) in silicon* ***(a)****; IR transmission microscope images of subsurface sub-micron structures in silicon: top view of single-pulse defects* ***(b)****, and cross-section view of a waveguide structure at 1.55 µm* ***(c)****.*

We used the same laser for other materials, for example, for composites in Li-batteries (Fig. 3b), or for Gorilla glass, where we could realize smooth cutting with <10 µm chip and crack defect size (Fig. 3 c). Energy scaling this unique fiber based ultra-short pulsed Ho-MOPA to several mJ level opened up high throughput fine material processing.

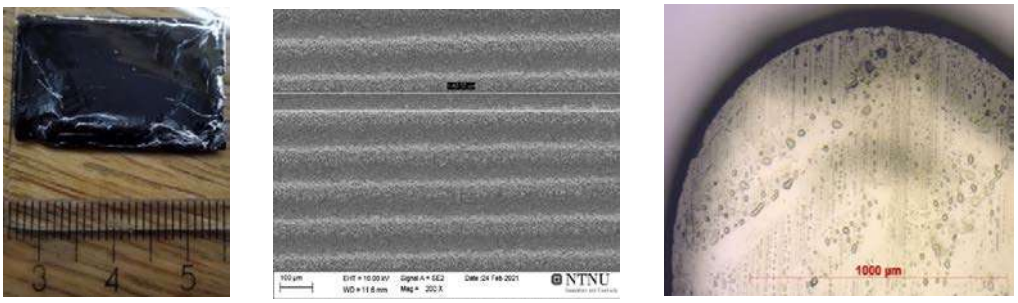

Fig. 3*. Exfoliated thin layer of silicon after inducing a defect layer by 2 um laser* ***(a)****; SEM image of laser-microprocessed electrode of lithium battery* ***(b)****, microscope image of laser-cut Gorilla glass* ***(c)****.*

This break-through in fine processing of semiconductors became possible not only due to the advancements in mid-IR ultrafast laser technology, but due to a deeper understanding and careful analysis of the nonlinear optical phenomena in its complexity. The developed theory [11] applicable to sub-surface processing of any semiconductor material not only allowed finding an optimum laser wavelength as well as optimum set of laser parameters, enabling for the first time sub-surface 3D structuring and stealth dicing of silicon with sub-wavelength spatial resolution. It laid the foundations for the next generation industrial laser processing tools acting like a *3D printer*, freely setting the point modifications at different depths pulse by pulse, potentially at up to MHz repetition rates.

References

[1] S. B. Mirov et al, *IEEE Journal of Selected Topics in Quantum Electronics* **21**, 1601719 (2015);
[2] N. Tolstik et al, *CLEO/Europe-EQEC*, (2017).
[3] S. Duval et al, *Optics Letters* **41**, 5294 (2016)
[4] S. Antipov at al, *Optica* **3,** 1373 (2016).
[5] V. Smolski et al, *Applied Physics* B **124,** 101 (2018);
[6] I. T. Sorokina et al, *IEEE Journal of Selected Topics in Quantum Electronics* **20,** 0903412 (2014);
[7] R. A. Richter et al, JOSA B **37,** 2543 (2020).
[8] R. A. Richter et al, *Optics Express* **30**, 3329 (2022).
[9] U. Elu et al, *Optica* **4**, 1024 (2017).
[10] E. Sorokin et al, *Optics Express* **26**, 9963-9971 (2018).
[11] R. A. Richter et al, Physical Review Research, submitted (2022).

Acknowledgments: NT, RR, and ITS acknowledge support by ATLA Lasers AS, the projects Energix N225003/E20 & UNLOCK N303347 & MIR N326503, VK the ERC Adv. Grant N740355 (STEMS), Marie-Curie Grant N713694 (MULTIPLY).

CEP-stable Cr:ZnS Lasers for Ultra-broadband Mid-infrared Generation

A. Weigel[1], M. Kowalczyk[1], N. Nagl[1], P. Steinleitner[1], S. Qu[1], A. Sebesta[1], A. Paudel[1]
A. Głuszek[2], J. Sotor[2], K. F. Mak[1], F. Krausz[1]
[1]*Max Planck Institute of Quantum Optics, 85748 Garching, Germany*
[2]*Wrocław University of Science and Technology, 50-370 Wrocław, Poland*

Broadband coherent mid-infrared (MIR) radiation gives access to the vibrational response of chemical bonds and is thus highly sensitive to the molecular composition of a complex biological sample. Field-resolved detection allows to record directly the response emitted upon MIR excitation, opening up new applications in life science and biology [1]. The information content accessible from such measurements depends crucially on the spectral coverage, brightness, as well as on the intensity and waveform stability of the MIR pulses. Cr:ZnS/ZnSe lasers directly produce few-optical-cycle pulses in the 2-3 μm spectral region [2-4], making them ideal sources to drive efficient mid-infrared generation by intra-pulse difference frequency generation in suitable nonlinear crystals [5-8]. Our group has developed directly diode-pumped Kerr-lens mode-locked femtosecond Cr:ZnS/ZnSe oscillators providing sub-50-fs pulses with extremely low intensity noise [8,9]. We are now able to control also the output waveform of the pulses by stabilizing their carrier-envelope phase (CEP). The corresponding setup, shown in Fig. 1a, is based on a diode-pumped 23-MHz Cr:ZnS oscillator, providing compressed 28-fs-long pulses, centered at 2.3 μm. The output is subsequently broadened by self-phase modulation (SPM) in a single TiO_2 bulk plate. The resulting output spectrum covers more than an octave between 1.17 and 3.12 μm at -20 dB (Fig. 1b). Two reflections from a beam splitter (BS) are used for CEP stabilization and *out-of-loop* CEP characterization, while the main part of the output is compressed, providing 225 mW for the experiment. The spectral bandwidth of the output pulses directly enables common-path *f*-2*f* interferometry to efficiently generate a feedback signal for CEP stabilization, which then modulates the power of one of the pump diodes. Figure 1c presents the measured CEP noise power spectral density with an exceptionally low residual integrated phase jitter of 8.6 mrad over the range from 0.2 Hz to 11.4 MHz ($f_{rep}/2$). Frequency mixing of the CEP-stable output pulses in a $ZnGeP_2$ (ZGP) crystal generates ultrabroadband MIR radiation, which spectrally overlaps with the driving pulses. Altogether, the resulting polarized supercontinuum spectrum covers more than three optical octaves from 24 THz (12.5 μm) to 270 THz (1.11 μm) at the -20- dB-level (Fig. 1 d).In order to increase the brightness of our coherent MIR source, we also developed a directly diode-pumped Cr:ZnS amplifier [10]. Using a non-collinear multi-pass geometry, we were able to boost the output of a few-cycle Cr:ZnS oscillator to the > 2 W level, with minimum increase in intensity noise.

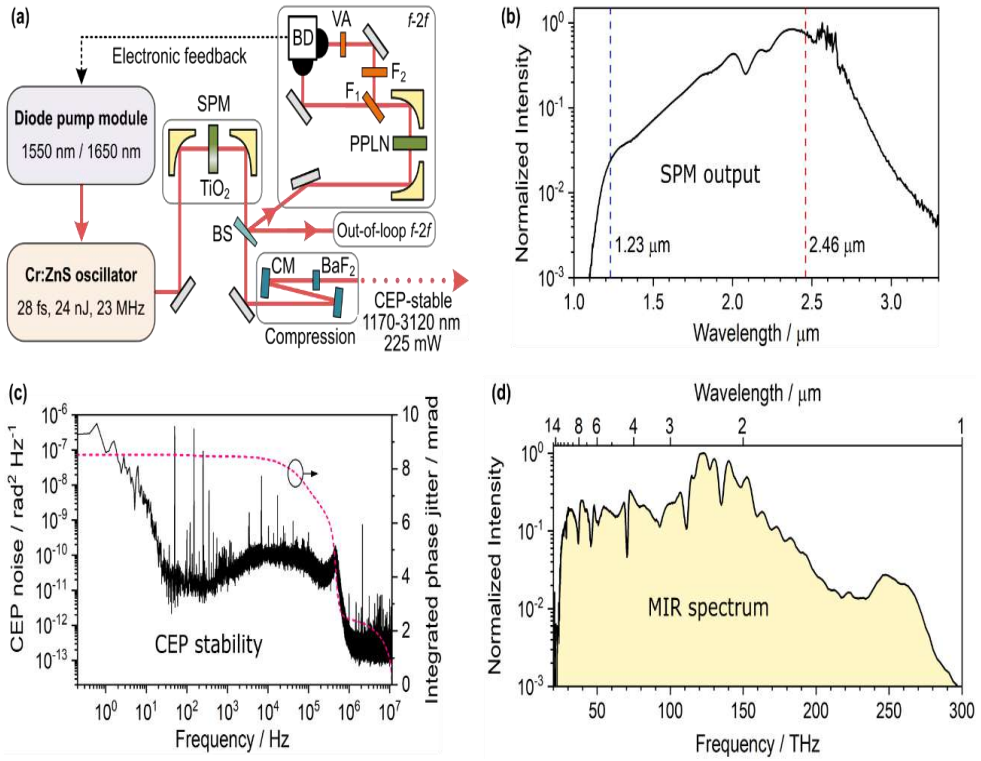

Fig.1 ***(a)*** *Schematic of the carrier-envelope (CEP) stabilized Cr:ZnS oscillator, including spectral broadening by self-phase modulation (SPM). $F_{1,2}$ – spectral filters; VA – variable attenuator; BD – balanced photodetector; BS – beamsplitter; CM – chirped mirror.*
(b) *Optical spectrum after spectral broadening in TiO_2; the positions of f* ***(red)*** *and 2f* ***(blue)*** *spectral components are marked with dashed lines.*
(c) *Carrier-envelope phase noise measured out-of-loop in the range from 0.2 Hz to 11.4 MHz and the corresponding integrated phase jitter.*
(d) *Spectrum of the polarized infrared supercontinuum generated in a $ZnGeP_2$ (ZGP) crystal.*

In conclusion, we demonstrate a coherent mid-infrared source with more than three octaves spectral coverage, based on a directly diode-pumped Cr:ZnS oscillator with ultra-low intensity noise and exceptional CEP stabilization. Diode-pumped amplifiers provide the possibility to power-scale the frontend. Combined with field-resolved detection and dual-oscillator scanning techniques [11], we expect to reach new levels in sensitivity and specificity for infrared-based biosensing and life science applications.

References

[1] I. Pupeza *et al*, *Nature* **577**, 52 (2020).
[2] I. T. Sorokina, E. Sorokin, *IEE Journal of Selected Topics in Quantum Electronics* **21**, 273 (2015).
[3] S. Vasilyev *et al.*, *Optics Letters* **40**, 5054 (2015).
[4] S. B. Mirov *et al*., *IEEE Journal of Selected Topics in Quantum Electronics* **24**, 1 (2018).
[5] S. Vasilyev *et al.*, *Optica* **6**, 111 (2019).
[6] Q. Wang *et al*., *Optics Letters* **44**, 2566 (2019).
[7] J. Zhang *et al*., *Optics Express* **28**, 27903 (2020).
[8] N. Nagl *et al*., *OSA Technical Digest*, CLEO/Europe – EQEC (2021).
[9] N. Nagl *et al*., *Optics Express* **27**, 24445 (2019).
[10] S. Qu *et al*., *OSA Technical Digest* , CLEO/Europe -EQEC (2021).
[11] A. Weigel *et al*., *OSA Technical Digest*, CLEO/Europe -EQEC (2021).

Nonlinear Optics in Multi-pass Cells

O. Pronin[1], V. Hariton[2], K. Fritsch[1]
[1] *Helmut-Schmidt-University, D-22043 Hamburg, Germany*
[2] *Universidade de Lisboa, 1049-001 Lisbon, Portugal*

Over decades solid- and hollow-core fibers (waveguides) were used as a nonlinear platform for many nonlinear effects, and they enabled multiple breakthroughs in the research and industry. Recently, multi-pass cells (quasi-waveguides) demonstrated superior performance to fibers when related to nonlinear spectral broadening and compression in the high-energy and high-average power range. A multi-pass cell is a free-space quasi-waveguide. In contrast to fiber, it can accommodate substantial beam sizes and get customized dispersion profiles, thanks to dispersive multilayer mirrors.
Here we would like to review the progress in nonlinear optical experiments that have been assisted by multi-pass cells over the last several years. This technology became a well-established approach for spectral broadening and pulse compression in high average power and ultrashort pulse duration systems [1,2]. Moreover, multi-pass cells have been widely employed to realize other nonlinear effects. They have recently found uses in Raman frequency shifting and Raman-enhanced spectral broadening [4], and even nonlinear polarization rotation [5] for pulse cleaning applications. Spectral broadening and pulse compression with the multi-pass cells was demonstrated not only around 1030 nm but also in green, 515 nm, in near-infrared 1.5 µm and 2 µm wavelengths. Extension towards UV and longer wavelengths is also feasible. Impressive energy scalability of this technology was demonstrated approaching 100 mJ range [6]. Nearly one octave spectra and pulse compression down to 7 fs were demonstrated too [7].

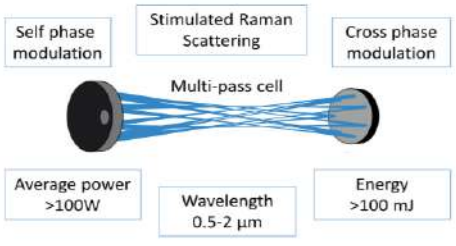

Fig.1 *Schematic representation of different nonlinear effects realized in multi-pass cells.*

The robustness and misalignment insensitivity of the multi-pass cells makes this technology a perfect choice for a combination with well-established industrial-grade Yb-based sub-picosecond lasers. Many technologies limited by the laboratory environment become feasible. Deep UV and XUV sources based on high harmonic generation in gases require short pulses with <10 fs pulse duration. Plasma accelerators, particle, THz and X-ray sources are driven by high-energy Yb-based systems and would also benefit from the short pulse duration <100 fs. More applications facilitated by nonlinear optics in multi-pass will appear next years.

References

[1] J. Schulte, et al, *Optics Letters* **41**, 4511(2016).
[2] K. Fritsch, et al, *Optics Letters* **43**, 4643(2018).
[4] N. Daher, X. et al, *Optics Letters* **46**, 3380 (2021).
[5] V. Pajer, M. Kalashnikov, *Laser Physics Letters* **18**, 65401 (2021).
[6] M. Kaumanns, et al, *Optics Letters* **46**, 929 (2021).
[7] M. Müller, et al, *Optics Letters* **46**, 2678 (2021).

MILESTONES 2016-2023

Ultrafast Dynamics and Metastability Ultrafast Bandgap Photonics

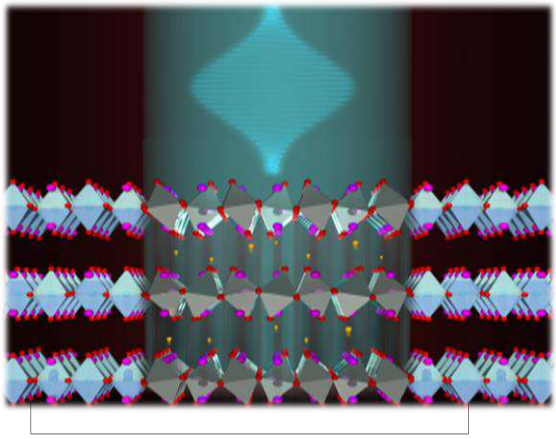

Physica Scripta – 2017

Focus: Ultrafast Bandgap Photonics
Guest Editors: Michael K. Rafailov and Luca Perfetti, 2017
http://iopscience.iop.org/journal/1402-4896/page/Focus-issue-on-Ultrafast-Bandgap-Photonics

Ultrafast Bandgap Photonics

Baltimore, 2016
http://spie.org/Publications/Proceedings/Volume/9835
Anaheim, 2017
http://spie.org/Publications/Proceedings/Volume/10193
Orlando, 2018
https://spie.org/Publications/Proceedings/Volume/10638

Ultrafast Dynamics and Metastability 2017
Washington, DC, 2018
https://sites.google.com/a/georgetown.edu/ultrafast-dynamics-and-metastability-archive-2017/

Ultrafast Dynamics and Metastability & Ultrafast Bandgap Photonics 2019
V International Conference,Washington, DC, April 2019
https://drive.google.com/file/d/1ralJMOMw21VEjbKVYq1c45Hir0dQXo4z/view

Ultrafast Bandgap Photonics: Dynamics and Metastability of Transient States 2019
VI International Conference,St. Petersburg, 2019
http://www.ioffe.ru/optics/UBGP2019/committees.html

Ultrafast Dynamics and Metastability & Ultrafast Bandgap Photonics 2021
VIII International Conference Washington, DC, November 2021
https://drive.google.com/file/d/1sh4dbWixbfFrk8yfs2oDqGROffTYyusw/view

Ultrafast Bandgap Photonics: Dynamics and Metastability of Transient States 2022
VII International Symposium, Hersonissos, Crete, Greece June 2022
https://udm-ubp20.physics.uoc.gr/

Ultrafast Dynamics and Metastability & Ultrafast Bandgap Photonics 2022

IX International Workshop, November 2022

Ultrafast Bandgap Photonics: Dynamics and Metastability of Transient States 2023
X International Symposium, May-June 2023